Spatial and Temporal Distribution of Bacterial Indicators and Microbial-Source Tracking within Tumacácori National Historical Park and the Upper Santa Cruz River, Southern Arizona and Northern Mexico, 2015–2016

Scientific Investigations Report 2019–5108

U.S. Department of the Interior
U.S. Geological Survey

Spatial and Temporal Distribution of Bacterial Indicators and Microbial-Source Tracking within Tumacácori National Historical Park and the Upper Santa Cruz River, Southern Arizona and Northern Mexico, 2015–2016

By Nicholas V. Paretti, Christopher M. Kephart, Thomas J. Porter, Edyth Hermosillo, Jay R. Cederberg, Justine P. Mayo, Bruce Gungle, Alissa L. Coes, Rachel S. Tucci, and Laura M. Norman

Scientific Investigations Report 2019–5108

U.S. Department of the Interior
U.S. Geological Survey

U.S. Department of the Interior
DAVID BERNHARDT, Secretary

U.S. Geological Survey
James F. Reilly II, Director

U.S. Geological Survey, Reston, Virginia: 2019

Acknowledgments

Contents

Figures

Tables

[Tables 2, 3, 5, and 6 are available as separate files for download at https://doi.org/10.3133/sir20195108]

Conversion Factors

U.S. customary units to International System of Units

Multiply	By	To obtain
Length		
inch (in.)	2.54	centimeter (cm)
inch (in.)	25.4	millimeter (mm)
foot (ft)	0.3048	meter (m)
mile (mi)	1.609	kilometer (km)
Area		
acre	4,047	square meter (m^2)
acre	0.4047	hectare (ha)
acre	0.4047	square hectometer (hm^2)
acre	0.004047	square kilometer (km^2)
square mile (mi^2)	259.0	hectare (ha)
square mile (mi^2)	2.590	square kilometer (km^2)
Volume		
gallon (gal)	3.785	liter (L)
gallon (gal)	0.003785	cubic meter (m^3)
cubic foot (ft^3)	0.02832	cubic meter (m^3)
acre-foot (acre-ft)	1,233	cubic meter (m^3)
acre-foot (acre-ft)	0.001233	cubic hectometer (hm^3)
Flow rate		
acre-foot per year (acre-ft/yr)	1,233	cubic meter per year (m^3/yr)
acre-foot per year (acre-ft/yr)	0.001233	cubic hectometer per year (hm^3/yr)
foot per second (ft/s)	0.3048	meter per second (m/s)
cubic foot per second (ft^3/s)	0.02832	cubic meter per second (m^3/s)
cubic foot per day (ft^3/d)	0.02832	cubic meter per day (m^3/d)
Mass		
ton, short (2,000 lb)	0.9072	metric ton (t)
ton, long (2,240 lb)	1.016	metric ton (t)

Temperature in degrees Celsius (°C) may be converted to degrees Fahrenheit (°F) as

$$°F = (1.8 \times °C) + 32.$$

Temperature in degrees Fahrenheit (°F) may be converted to degrees Celsius (°C) as

$$°C = (°F - 32) / 1.8.$$

International System of Units to U.S. customary units

Multiply	By	To obtain
Volume		
liter (L)	0.2642	gallon (gal)
milliliter (mL)	0.0002642	gallon (gal)
Mass		
gram (g)	0.03527	ounce, avoirdupois (oz)
kilogram (kg)	2.205	pound avoirdupois (lb)
metric ton (t)	1.102	ton, short [2,000 lb]
metric ton (t)	0.9842	ton, long [2,240 lb]

Temperature in degrees Celsius (°C) may be converted to degrees Fahrenheit (°F) as

$$°F = (1.8 \times °C) + 32.$$

Temperature in degrees Fahrenheit (°F) may be converted to degrees Celsius (°C) as

$$°C = (°F - 32) / 1.8.$$

Datum

Vertical coordinate information is referenced to the [insert datum name (and abbreviation) here; for example, North American Vertical Datum of 1988 (NAVD 88)].

Horizontal coordinate information is referenced to the [insert datum name (and abbreviation) here; for example, North American Datum of 1983 (NAD 83)].

Altitude, as used in this report, refers to distance above the vertical datum.

Supplemental Information

Specific conductance is given in microsiemens per centimeter at 25 degrees Celsius (µS/cm at 25 °C).

Concentrations of chemical constituents in water are given in either milligrams per liter (mg/L).

Abbreviations

ADEQ	Arizona Department of Environmental Quality
ALERT	Automated Local Evaluation in Real Time
AWS	Arizona warm-water aquatic wildlife standard
AZPDES	Arizona Pollutant Discharge Elimination System
AZWSC	USGS Arizona Water Science Center
BacCan	canine microbial-source tracking marker
BIC	Bayesian information criterion
CowM2	cattle microbial-source tracking marker
E. coli	*Escherichia coli*
EFASC	Environmental Flow Allocation and Statistics Calculator
EPA	U.S. Environmental Protection Agency
FBC	full-body contact
FNU	formazine turbidity units
FOSCR	Friends of the Santa Cruz River
GenBac	general-bacteria microbial-source tracking marker
GIS	geographic information system
HF183	human microbial-source tracking marker
HPyV	human-polyomavirus microbial-source tracking marker
IBWC	International Boundary and Water Commission
IOI	International Outfall Interceptor
MPN	most probable number
MST	microbial-source tracking
NADA	Nondetects and Data Analysis for Environmental Data
NIWTP	Nogales International Wastewater Treatment Plant
NMDS	nonmetric multidimensional scaling
PBC	partial-body contact
Rum2BAC	ruminant-animal microbial-source tracking marker
SCCFCD	Sant Cruz County Flood Control District
SWAT	soil and water assessment tool
TUMA	Tumacácori National Historical Park
USGS	U.S. Geological Survey
WD	watershed division
WD1	watershed division1—upper Santa Cruz River west of San Lázaro, Sonora, to the Nogales International Wastewater Treatment Plant
WD2	watershed division2—Nogales Wash to Santa Cruz River confluence
WD3	watershed division3—Nogales International Wastewater Treatment Plant to Santa Cruz River at the Palo Parado Bridge, plus tributaries Peck Canyon Wash, Agua Fria Canyon Wash, Sonoita Creek and Josephine Canyon Wash
WD4	watershed division4—Santa Cruz River TUMA southern boundary to Chavez Siding
WQS	water-quality standard

Spatial and Temporal Distribution of Bacterial Indicators and Microbial-Source Tracking within Tumacácori National Historical Park and the Upper Santa Cruz River, Southern Arizona and Northern Mexico, 2015–2016

By Nicholas V. Paretti, Christopher M. Kephart, Thomas J. Porter, Edyth Hermosillo, Jay R. Cederberg, Justine P. Mayo, Bruce Gungle, Alissa L. Coes, Rachel S. Tucci, and Laura M. Norman

Abstract

Tumacácori National Historical Park (TUMA) in southern Arizona protects the culturally important Mission San José de Tumacácori, while also managing a part of the ecologically diverse riparian corridor of the Santa Cruz River. The quality of the water flowing through depends solely on upstream watershed activities, and among the water-quality issues concerning TUMA is the microbiological pathogens in the river introduced by human and animal sources that pose a significant human health risk to employees and visitors. The U.S. Geological Survey (USGS) conducted a 3-year study to understand the sources, timing, and distribution of the fecal-indicator bacteria *Escherichia coli* (*E. coli*) within TUMA and the upstream watershed. The Upper Santa Cruz River Watershed was divided into four smaller subwatersheds based on surface-water source, land use, and anthropogenic activities, which are referred to as watershed divisions (WD). The four WDs were distinguished by river segments and are the following—(1) the upper Santa Cruz River west of San Lázaro, Sonora (Mexico), to the Nogales International Wastewater Treatment Plant (WD1), (2) Nogales Wash to Santa Cruz River confluence (WD2), (3) the Nogales International Wastewater Treatment Plant to Santa Cruz River at the Palo Parado Bridge, plus tributaries Peck Canyon Wash, Agua Fria Canyon Wash, Sonoita Creek, and Josephine Canyon Wash (WD3), and (4) the Santa Cruz River TUMA southern boundary to Chavez Siding (WD4). *E. coli*, microbial-source-tracking (MST) markers, suspended sediment, water-quality parameters, and water-stage data were collected at 20 locations in these WDs and at various temporal scales to understand the quality of water flowing through the park year round. More than 1,000 samples were collected by the USGS, and existing data collected by various agencies were also compiled and analyzed in relation to the new data set.

Overall the Upper Santa Cruz River Watershed *E. coli* levels were found to be highly variable both spatially and temporally, highlighting the importance of sample-collection timing and the potential effects this may have on data analysis and interpretation of the results. The 24-hour base flow collections done in multiple WDs showed a several fold to an order of magnitude change within the span of 24 hours, and at times the *E. coli* contents exceeded water-quality standards. Waters influenced by any amount of runoff were multiple orders of magnitude greater in both *E. coli* and suspended sediment compared to levels observed during base-flow conditions. After any rainfall event in the urbanized Nogales Wash Watershed (WD2), the runoff was rapid and the flood peak traveled downstream within hours of the precipitation event. The highest *E. coli* concentrations and suspended-sediment peaks were usually correlated with the rise of the flood peak, and average travel times of floods were 8 hours from the USGS Nogales Wash streamgage (09481000) to the Santa Cruz River Tubac streamgage (09481740). This timing was dependent on seasonal patterns, watershed characteristics, and hydrologic conditions. During the study, WD2 most frequently connected with the main Santa Cruz River, sending elevated levels of *E. coli* and suspended sediment several orders of magnitude above the State of Arizona's water-quality standards downstream to TUMA. The mean concentrations, flux, and yields of *E. coli* and suspended sediment were also highest from WD2 compared to any other WD. The ephemeral Santa Cruz River WD1 rarely contributed to the waters flowing downstream to TUMA, but during widespread precipitation events there were measured instances of connection to the perennial section of the Santa Cruz River. The *E. coli* and suspended sediment of those waters were highly elevated, and based on land use and MST markers, the *E. coli* were likely related to cattle grazing and other agricultural related activities. The WD3 included the Nogales International Wastewater Treatment Plant (NIWTP) and ephemeral tributary drainages but also represented a mixture of waters from the upstream sources contributed by WD1 and WD2 during periods of flooding. The NIWTP contributed mostly nondetectable levels of *E. coli* at the outfall, but concentrations increased with downstream distance and this increase was in part likely related to nearby streambank grazing activities and the resuspension of fine sediments, which act as a reservoir for *E. coli*. Because major tributaries are ephemeral, the levels of *E. coli* and suspended sediment in the tributary drainages were solely a result of flooding, and these events were infrequent during the study. The *E. coli* concentrations from tributaries were proportionally small compared

to the levels from WD2 during runoff events, although MST inputs were different, with more detections of ruminant sources rather than human or canine sources.

WD4 included TUMA and downstream parts of the Santa Cruz River below the section of the river that included the Santa Cruz River at Tubac streamgage. For more than half of the year, water quality in the park was primarily a function of the treated effluent discharged by the NIWTP and the nonpoint source activities in between the NIWTP and TUMA (for example, cattle entering the stream channel). Except during times of wetter seasonal conditions and increased runoff, WD1 and WD2 were mostly disconnected from perennial streamflow sustained by the NIWTP discharge. About 15 to 20 percent of the yearly floodwaters or seasonal flow connected with the perennial section of the river, and as a result elevated *E. coli* and suspended-sediment concentration, several orders of magnitude above the water-quality standards, flowed through TUMA during these periods.

The median *E. coli* and suspended-sediment concentrations between WDs were roughly similar or decreased slightly from upstream to downstream. Not until floods were separated from base-flow samples did the results show a significantly higher concentration of *E. coli* and suspended-sediment concentrations coming from upstream in WD2. Overall the flux and yield of *E. coli* and suspended sediment was 4 to 6 orders greater during flooding compared to base flow conditions. During floods, WD2 had the greatest contribution of suspended sediment per area, which corresponded with the greatest *E. coli* yields of all the WDs. Despite the infrequent surface-water connection, the mean annual mass of suspended sediment transported downstream from WD2 could be several hundred to several thousand tons (in this report, ton is always in reference to short tons, 2,000 pounds) depending on the flow of the water year (a water year begins on October 1 of the previous year; for example, water year 2015 covers October 1, 2014, to October 1, 2015), whereas the WD3 and WD4 were several orders of magnitude less.

The MST results showed that WD2 had the greatest concentrations of the human marker, whereas WD4 had the greatest concentrations of the ruminant marker. The multivariate analysis showed a gradient by concentration and marker type. The endpoints were bounded by a Nogales Wash chlorinated sample (low in *E. coli* concentration) and the NIWTP influent sample (high in *E. coli* concentration). The tributaries graphically clustered together, but Peck Canyon Wash samples had higher human- and canine-marker concentrations, whereas Josephine Canyon Wash and Sonoita Creek had higher cattle- and ruminant-marker concentrations. The WD2 samples clustered primarily along the human-canine side of the gradient, whereas the Santa Cruz River location samples had more variability and appeared to be related to

timing in the year. June, July, and September samples plotted more with the human and canine sources in the analysis, whereas July samples appeared to be more related to cattle and ruminant sources. WD4 had a high proportion of detections for all markers, likely a result of the mixture of waters from upstream.

Regional regression models using data from all WDs were developed to predict *E. coli*, suspended-sediment concentrations, and flux. Of all the explanatory variable combinations used in the model development, suspended sediment alone explained more than 80 percent of the variation in *E. coli* concentrations; however, turbidity serves as an inexpensive proxy for suspended-sediment concentrations, and the measure is relatively easy to collect. The final models using turbidity and other seasonal and hydrologic variables to predict *E. coli* explained between 80 and 90 percent of the variation in *E. coli* concentration. The suspended-sediment models used many of the same variables, and the model explained about 87 to 90 percent of the variation.

Subsurface or hyporheic samples were collected at a few locations to better understand *E. coli* persisting in the interstitial wetted sediments below the dry stream channel, acting as reservoir for microorganisms and an additional source when floods resuspended fines in the water column. At a location in the downstream part of WD2, 1 to 2 feet (ft) below the dry active channel, the *E. coli* concentrations were two-fold greater than the upstream or adjacent flowing surface-water source. These concentrations were also an order of magnitude greater than downstream subsurface samples collected at WD4.

The information provided in this investigation is a result of a comprehensive approach to quantify the spatial and temporal variability of *E. coli* and suspended sediment in the Upper Santa Cruz River Watershed. Several types of flow were sampled from base flow to flood flow and at high frequency intervals (rise, peak, and recession) to determine daily variability, as well as seasonal variability. Hydrologic data collection and estimation techniques were used to establish a hydrologic relation with *E. coli* and suspended sediment. Furthermore, source tracking was used to describe the potential sources of *E. coli*. Models were developed that are expected to be useful for predicting *E. coli* concentrations to help TUMA managers understand instantaneous conditions to keep the public and staff informed about potentially harmful water-quality conditions. In addition, the concentration, flux, and source information will provide more accurate data for other surface-water modeling and can be useful in the development of total maximum daily load standards. This will help TUMA describe the water-quality conditions at the park and waters flowing through the park, as well as prioritize and help carry out future best-management actions to address these issues.
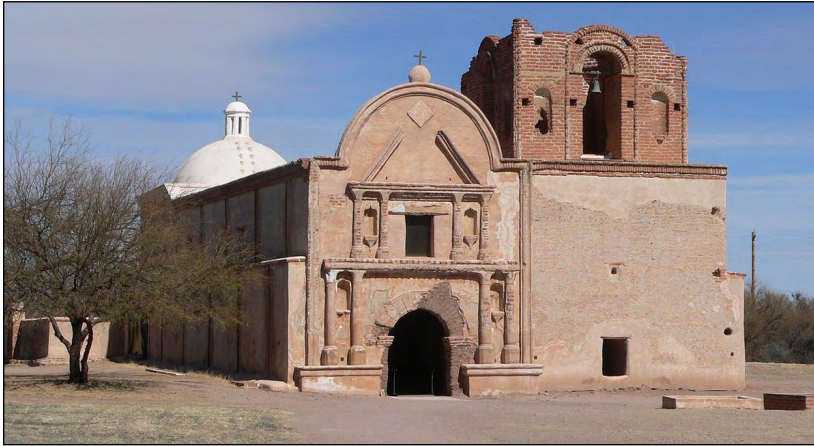
Mission San José de Tumacácori, seen from the south, February 2012 (photograph from Wikimedia Commons, the free media repository, https://commons.wikimedia.org/wiki/File:Tumacacori_NHP_church_1.JPG).

Introduction

Tumacácori National Historical Park (TUMA) was established in 1908 to protect, preserve, and communicate the history of the old Spanish and Tohono O'odham mission church of San José de Tumacácori. In 2002, Congress passed the Tumacácori National Historical Park Boundary Revision Act of 2002 (Public Law 107–218), expanding the park's purpose and mission and increasing park area by 300 acres. This expansion reunited the church grounds with historical mission property and included more than 1 mile of the Santa Cruz River and its associated riparian area (fig. 1). Congress' stated reason for the expansion was to protect and improve the riparian habitat and provide visitors with a complete picture of mission life, which revolved around riverine resources (National Park Service, 2016).

The Santa Cruz River originates as perennial flow in southern Arizona above Lochiel, flows south into Sonora, Mexico, and then curves back north—returning to Arizona east of Nogales—as an intermittent stream (fig. 2). Base flow in the perennial reach of the river within TUMA is maintained by treated effluent discharged from the International Boundary and Water Commission-Nogales International Wastewater Treatment Plant (NIWTP), located approximately 10 miles upstream (south) of TUMA. The NIWTP upgraded its treatment facilities in 2009 to an advanced biological treatment that uses ultraviolet disinfection to remove harmful microorganisms. This upgrade significantly improved water-quality conditions, specifically decreasing nutrients—primarily un-ionized ammonia—and *Escherichia coli* (*E. coli*) (Sonoran Institute, 2016; Sanders and others, 2013; Tetra Tech, 2014).

The river, adjacent riparian area, and flood plain sustain a diverse ecosystem (Powell and others, 2005) that serves as an economic driver for the local community through tourism, agriculture, ranching, and recreation (Norman and others, 2013; Graham, 2011). Because of the importance of the river and the associated riparian area to the community, the quality of the water and condition of the watershed are very important to TUMA, local stakeholders, and other State and Federal agencies managing these resources. Although the NIWTP mostly reports nondetectable to low-level *E. coli* concentrations in the effluent discharged from the outfall into the Santa Cruz River, elevated levels of *E. coli* continue to be an issue in downstream reaches of the Santa Cruz River, including the section within TUMA. The National Park Service (NPS), Arizona Department of Environmental Quality (ADEQ), and other agencies regularly monitor the *E. coli* because it is a bacterium that is commonly found in the lower intestine of warm-blooded organisms and serves as an indicator of other pathogenic microorganisms. Indicator organisms are relatively harmless, easy to collect, and less expensive to analyze compared to the multitude of pathogenic microbes. Since 2010, ADEQ has listed the TUMA reach of the Santa Cruz River as impaired for *E. coli* exceedances (Arizona Department of Environmental Quality, 2015). Because the treated effluent from NIWTP is a minor contributor to the *E. coli* concentrations found within the watershed, a majority of *E. coli* loading must be from additional sources contributing to the river.

Although work has been done to quantify *E. coli* and identify sources of bacteria in the river (Sanders and others, 2013; McOmber, 2014), significant information gaps remain with regard to the distribution, variability, timing, loading, and source(s) of bacteria. Additionally, *E. coli* levels measured in the watershed can vary several orders of magnitude depending on flow conditions and season, suggesting a lack of information about the watershed response and hydrologic function driving the variability of both concentration and source. Samples previously collected along various reaches of the river have been spatially and temporally inconsistent, and nonexistent in contributing ephemeral tributary washes. This investigation provides additional information needed to understand the spatial and temporal variability of *E. coli* with the goal of providing TUMA a watershed-scale perspective on the water-quality issues that affect park resources. TUMA staff can use this additional information and interpretation to guide management strategies for safeguarding visitor health and improving ecological conditions.
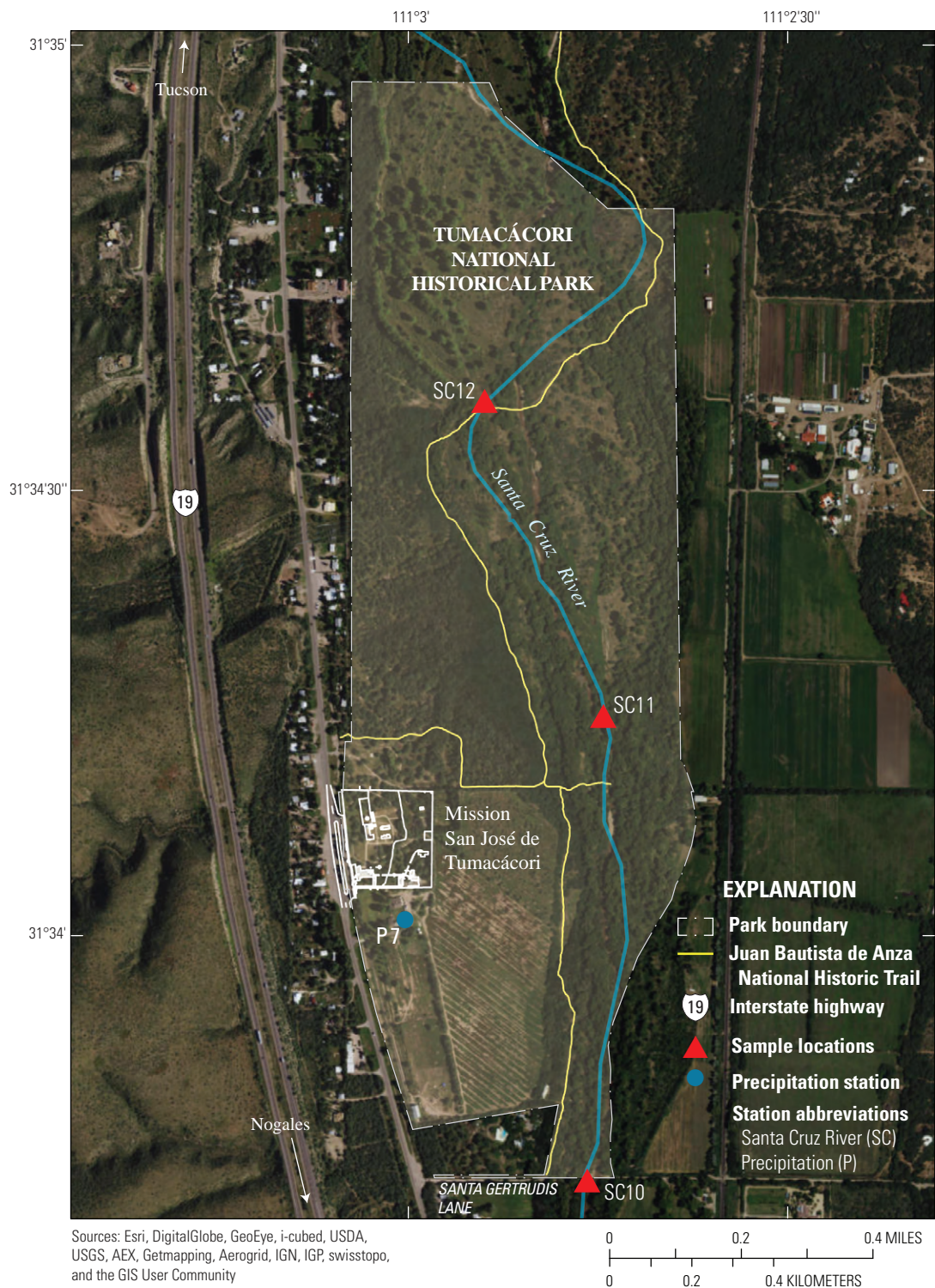
Figure 1.   Map of Tumacácori National Historical Park (TUMA) in southern Arizona. Precipitation stations and stations at which samples were collected are shown—SC, Santa Cruz River; P, precipitation. For detailed descriptions of stations/sample locations, see table 1.
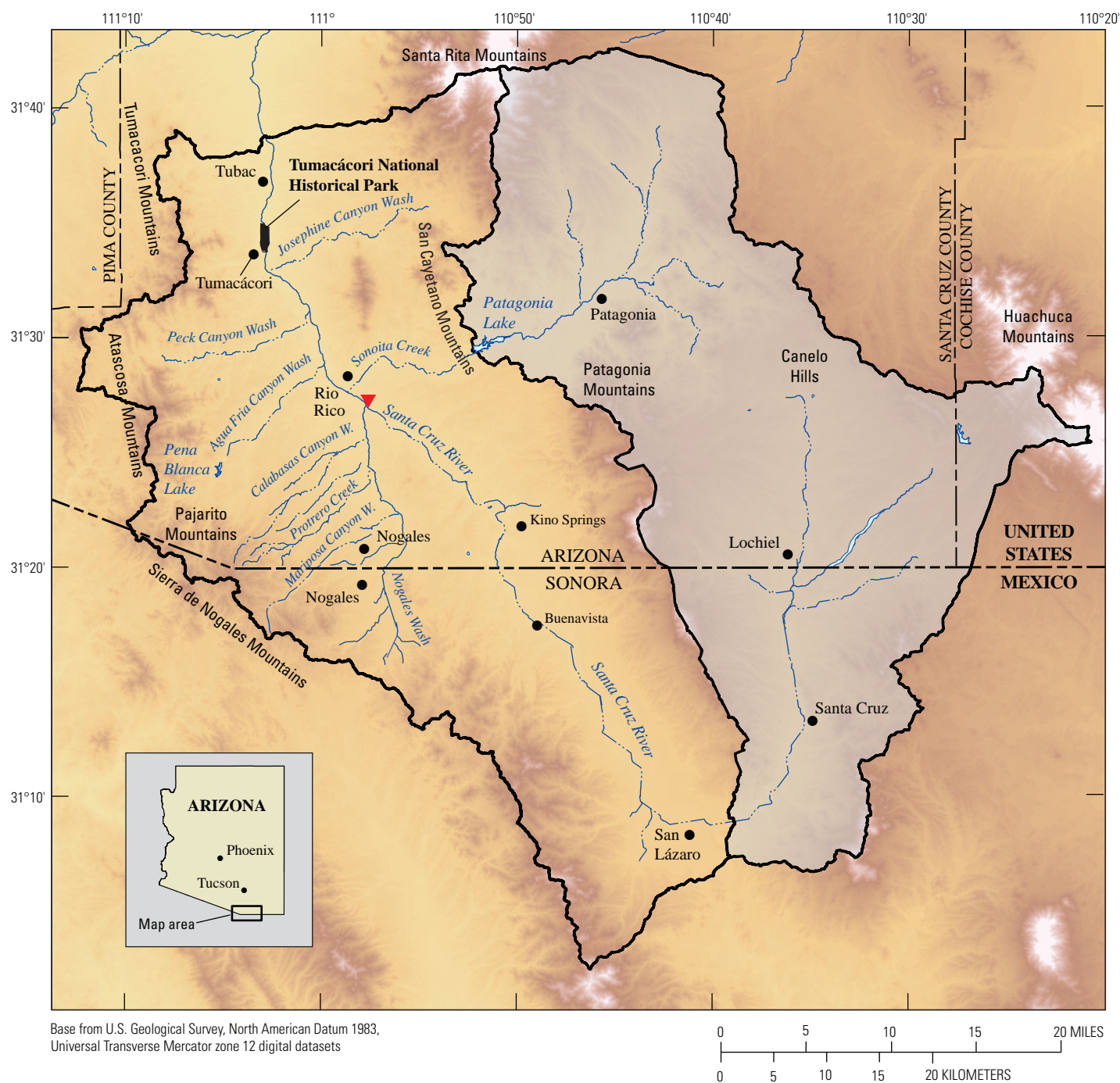
Figure 2. Map of the study area in southern Arizona and northern Mexico, including Tumacácori National Historical Park, Nogales International Wastewater Treatment Plant, and the Upper Santa Cruz River Watershed.

Purpose and Scope

The purpose of this report is to describe the spatial and temporal variability of *E. coli* and to describe sources of *E. coli* in the Upper Santa Cruz River Subbasin. This information is needed by landowners, advocacy groups, and managers of the river to help develop total maximum daily load standards and to determine if risks to human health exist within the perennial reach of the Santa Cruz River. If risks to human health do exist within the park, then TUMA can work with local, State, and Federal agencies and other organizations to implement best management strategies for remediation.

This investigation assesses existing data sources and determines the 2015–2016 status of water quality of the upper Santa Cruz River and major tributaries upstream of TUMA by quantifying *E. coli* density, *E. coli* sources (using microbial-source tracking), suspended sediment, and other general water-quality parameters, and relating these measurements to surface-water hydrology and precipitation to characterize diel, seasonal, and flooding induced variability of *E. coli*. This information has important implications for subsequent monitoring, nonpoint assessments, and remediation of affected water resources. To accomplish this task, roughly 850 water samples were collected by the USGS during water years 2015 and 2016, and more than 2,300 additional samples were collected by various agencies from 2007 to 2015. Existing data were compiled and analyzed within a historical context and presented with a current understanding of the hydrologic system. Timing (event and season), duration, variability, magnitude, and spatial analyses were conducted in the Upper Santa Cruz River Watershed and related to the river reach managed by the park.

Description of Study Area

The Upper Santa Cruz River Watershed accounts for 60 percent of the land area within Santa Cruz County, Arizona. The study area is composed of several subbasins within the Upper Santa Cruz River Watershed (fig. 2). The study area begins on the watershed boundary north of Tubac, Arizona, and extends south of Nogales, Sonora (Mexico), to include the Nogales Wash Watershed. The upper part of the study area includes parts of the watershed in the State of Sonora, areas south of Buenavista, Sonora, and east of San Lázaro, Sonora. The watershed drainage areas upstream of Patagonia Lake Dam and east of San Lázaro, Sonora, were excluded from the analysis to maintain focus on the receiving surface waters of TUMA and to minimize the noncontributing or infrequently contributing drainage area. This minimally contributing area accounts for about 575 square miles (mi^2) or 45 percent of the larger watershed area and most of it is east of the Patagonia Mountains.

The population within the study area is about 250,000 residents and includes the cities of Nogales, Arizona, and Nogales, Sonora, known collectively as Ambos Nogales ("ambos" is Spanish for "both" and used hereafter). Nogales, Arizona, is the largest metropolitan region in the study area, and together the Ambos Nogales cities accounted for 234,000 residents in

the most recent censuses (Instituto Nacional de Estadística y Geografía, 2010; U.S. Census Bureau, 2012). The unincorporated town of Rio Rico, along the Santa Cruz River upstream of TUMA just north of Nogales, Arizona, had a population of about 19,000 persons in 2010. The unincorporated town of Tubac, Arizona, on the Santa Cruz River but downstream of TUMA, had a population of about 1,200 in 2010. Population throughout the rest of the surrounding subwatersheds are generally dispersed with a slightly higher concentration along the Santa Cruz River valley.

Watershed Characterization

The headwaters of the Santa Cruz River are found in the Canelo Hills and southwest facing slopes of the Huachuca Mountains of southeastern Arizona. The river initially flows south, crossing the international boundary with Mexico at Lochiel and then loops around to the west and then north and crosses back into Arizona about 5.5 miles east of Ambos Nogales (fig. 2) at an elevation of about 3,750 ft. Once the Santa Cruz River heads north of the international boundary, it flows through a relatively narrow fault block basin bounded to the west by the Mount Benedict horst block and the Pajarito, Atascosa, and Tumacácori Mountains and to the east by the San Cayetano Mountains and Grosvenor Hills near Rio Rico. The Mount Benedict horst block separates the Nogales Wash (west) and Santa Cruz River (east) in the southern part of the subbasin. Further north on the eastern side of the valley (northeastern corner of the study area) are the 9,450-ft Santa Rita Mountains. The river passes out of the Upper Santa Cruz River Subbasin about 9 miles north of Tubac, at an elevation of about 3,050 ft. For most of its length through the subbasin, the Santa Cruz River follows the Mount Benedict Fault.

The largest actively contributing tributary in the subbasin is Nogales Wash, which is the principal drainage channel for Ambos Nogales and flows perennially into Arizona from Mexico. About 5 miles north of the international boundary, Nogales Wash joins Potrero Creek and 3 miles later flows into the Santa Cruz River south of Rio Rico, Arizona. In recent years, the entire reach from the confluence of Nogales Wash with Potrero Creek to the Santa Cruz River has been referred to as "Nogales Wash," and this report maintains the use of "Nogales Wash" for this entire reach. The NIWTP is located just below the confluence of Nogales Wash and the Santa Cruz River.

Other major tributaries in the Upper Santa Cruz River Subbasin include Sonoita Creek and Josephine Canyon Wash on the east, and Agua Fria and Peck Canyon Wash on the west. All of these tributary streams are ephemeral at their confluences with the Santa Cruz River. Sonoita Creek was dammed midway between its source and mouth in the late 1960s to form 250-acre Patagonia Lake. Sonoita Creek State Natural Area is also found there. On the west side of the subbasin, 45-acre Peña Blanca Lake, created in 1957, is impounded on Pajarito Wash. In 2008–2009 Pena Blanca Lake was closed and dredged in an unsuccessful attempt to reduce mercury levels in the lake (Woodhouse, 2015). Pajarito Wash joins Agua Fria Wash below Peña Blanca Lake, and Agua Fria Wash then

enters the Santa Cruz River about 1.5 miles north of Sonoita Creek. There is a large sand and gravel operation in Agua Fria Wash about 1.5 miles above the confluence with the Santa Cruz River (U.S. Fish and Wildlife Service, 2011). Smaller sand and gravel operations in Mariposa and Calabasas Canyon Washes are about 1 to 2 miles from the confluence with the Santa Cruz River.

About half of the study area located within the United States is public land (0.02 percent Bureau of Land Management, 44.2 percent Coronado National Forest, and 5.7 percent State Trust Land), whereas the other half is private land. The primary vegetation types can be classified as Apacherian-chihuahuan mesquite upland scrub (44.6 percent), Madrean encinal (27.0 percent), and the Apacherian-Chihuahan piedmont semi-desert grassland (8.7 percent) (Wallace and others, 2011).

A relatively small amount of agricultural-related activities occurs on land in the study area (about 5,300 acres), but proportionally agricultural water use is higher than other water needs in the watershed (Arizona Department of Water Resources, 2017). Cattle grazing occurs in both the Sonora and Arizona parts of the Upper Santa Cruz River Subbasin. Fifteen grazing allotments covering 185 mi^2 (118,400 acres) are within the Arizona part of the study area. This accounts for 25 percent of the area within the Upper Santa Cruz River Watershed. In 2012, 21,177 cattle and calves were counted in Santa Cruz County (U.S. Department of Agriculture, 2012), or about 17 head per mi^2. There were an additional 1,526 horses, ponies, and alpacas in the county. Livestock quantity in the Sonoran part of the subbasin is more difficult to quantify, although Nabhan and Holdsworth (1998) show cattle density in the region as 26 to 36 head per mi^2 in the 1990s.

About 5 percent of the study area is developed or urbanized with a majority of this occurring in Ambos Nogales. Many people living in unincorporated communities in Nogales, Sonora, are lacking in clean-water or wastewater infrastructure (Norman and others, 2012), conditions that affect water quality in the downstream watershed. According to the Asociación de Maquiladoras de Sonora (2013) there were between 92 and 110 factories (maquiladoras) in Nogales, Sonora, in 2013. This industrial activity can contribute to poor water quality, because waste disposal by maquiladoras is largely unregulated (Norman and others, 2012). Little largescale mining currently takes place in the Upper Santa Cruz River Subbasin, although major unmined metal deposits do exist in this region on both sides of the international boundary (Broch, 2012; Hudson Institute of Minerology, 2017).

Climate

Precipitation in southern Arizona is bimodal and falls primarily in the higher elevations (fig. 3*A*). More than half of the annual precipitation in the subwatershed falls from late June through September during the North American monsoon (Adams and Comrie, 1997; hereafter referred to as monsoon). May and June are typically quite dry, as can be October and November. However, occasionally tropical weather systems off the coast of Baja, California (Mexico), can be a source of increased moisture moving northeast, causing widespread precipitation events in late September and October. Average annual precipitation (1981–2010) is about 20 inches, with about 60 percent of that falling during the four summer monsoon months and 20 percent falling during the three winter months. May is the driest month with 0.25 inch of rain on average, and July and August are the wettest months, averaging more than 4 inches each. Precipitation has on average been decreasing since 1980 (fig. 3*B*), while average temperature has increased slightly. Average temperatures are more moderate than in the lower parts of the watershed and range from about 47 to 65 Fahrenheit (°F). January is the coldest month, averaging 46 °F and July is the hottest month, averaging 77.5 °F. Regional climate trends are similar to those observed in other parts of the Southwest. Southern Arizona has been experiencing patterns of decreased precipitation coupled with increases in temperature since the early 1980s. In the context of the study period, seasonal average precipitation amounts were less than the long-term 30-year average, although July, August, and September (monsoon) had more than average amounts compared to the long-term average. Aquatic and riparian forest ecosystems that rely on surface waters are particularly vulnerable to these climate shifts and the synergistic effects from other stressors, such as contaminants, invasive species, and urbanization, will likely intensify the effects on these ecosystems in the Upper Santa Cruz River Watershed (Shamir and others, 2015; National Invasive Species Council, 2015; National Park Service, 2013).

Hydrology

The Santa Cruz River aquifer supplies about half of the potable water to Ambos Nogales (Sprouse, 2005), but pumping in the subbasin has reduced water levels and surface flows in the transboundary watershed. Hydraulically, the Santa Cruz River is considered a losing system and, beginning in 2010, the number of no-flow days on the Santa Cruz River increased significantly. More than 300 days of no-flow were observed at Santa Cruz streamgage near Nogales for each of the water years 2011, 2012, and 2013. These patterns have also been visible in the State groundwater monitoring, and water-level measurements from wells upstream of the NIWTP are trending downward, although a few wells near TUMA receiving Santa Cruz River effluent have been static or trending upward (Arizona Department of Water Resources, 2017). Treated wastewater effluent has been seen as a management option to address both aquifer and river issues (Treese and others, 2009). Currently, the treated effluent supplements the aquifer, but Sonora has expressed interest in keeping a part of the treated effluent that is coming from the Los Alisos Basin, Nogales, Sonora. If treated effluent was retained by Sonora, then this would likely have negative effects on the downstream groundwater and the TUMA riparian and aquatic ecosystems that rely on the current flow regime.

Regional climatological shifts and changes in the surface-water patterns will be a primary factor in understanding the

A

Universal Transverse Mercator zone 12 digital datasets, North American datum 1983, base from U.S.
Geological Survey. Data modified and interpolated from Callegary and others (2016). Data were
orginally retrieved from World Clim (WorldClim.org)

B
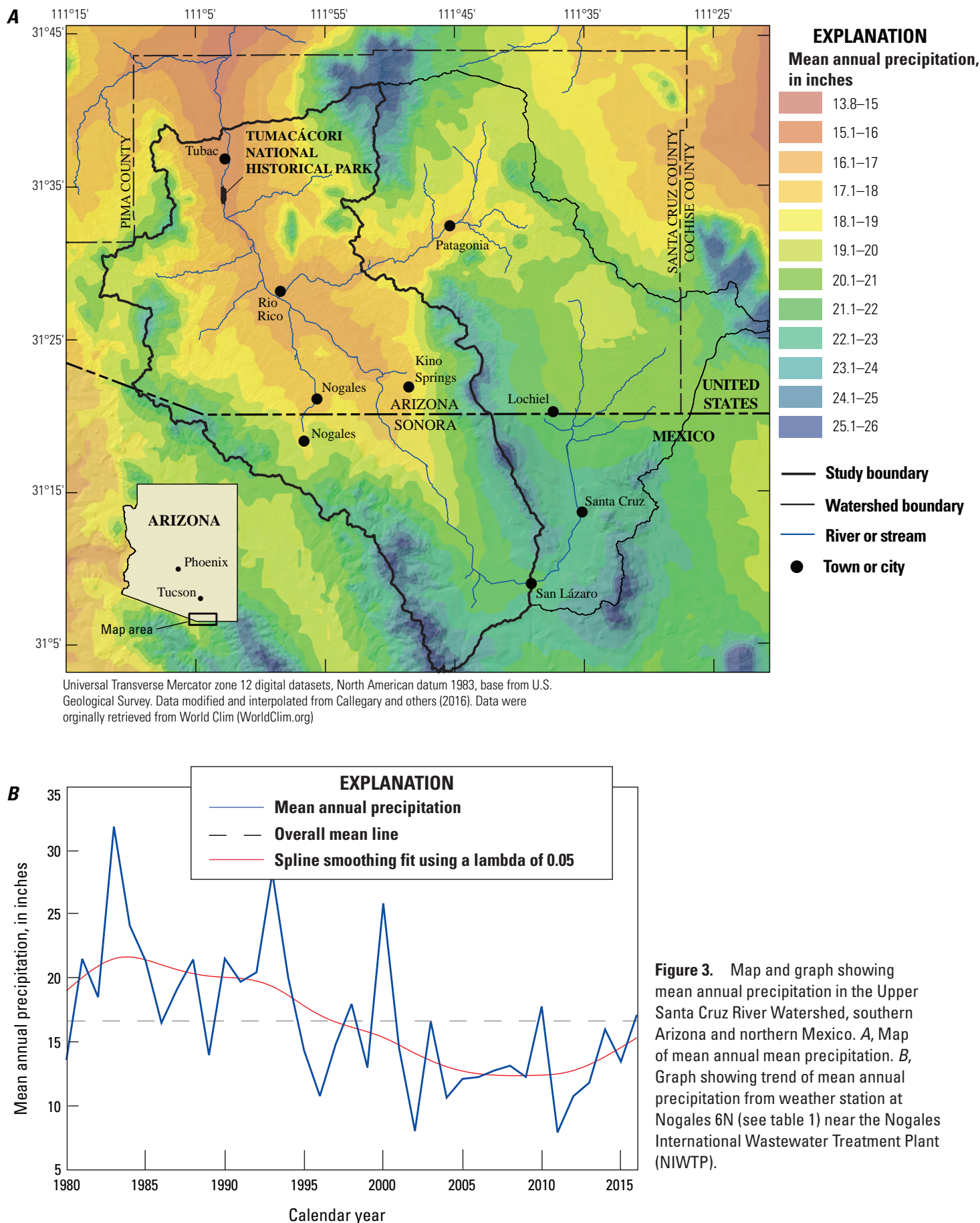
Figure 3. Map and graph showing
mean annual precipitation in the Upper
Santa Cruz River Watershed, southern
Arizona and northern Mexico. *A*, Map
of mean annual mean precipitation. *B*,
Graph showing trend of mean annual
precipitation from weather station at
Nogales 6N (see table 1) near the Nogales
International Wastewater Treatment Plant
(NIWTP).

levels of microbial contamination in the watershed. As such, a continued understanding of the hydrologic relation to the concentrations and loading of *E. coli* is key in predicting how a changing streamflow regime will affect the quality of waters flowing through TUMA. The Santa Cruz River streamgage near Nogales (SC1, 09480500) has more than 100 years of historical record, whereas the Nogales Wash (NW4, 09471000) and NIWTP (SC6) streamgages and the Santa Cruz River streamgage at Tubac (SC14, 09481740) have 9, 7, and 21 years of record, respectively. Median discharge is relatively low compared to other streams in the central region of Arizona, but flooding discharge in the Upper Santa Cruz River Watershed can be several orders magnitude higher than many streams in the State. This extreme and highly variable streamflow regime is typical of desert streams. During the study period, median discharge ranged between 1 and 15 cubic feet per second (ft^3/s) (lowest at SC1 and highest at SC6), and maximum daily discharges were several hundred cubic feet per second at each location except for SC6 where no flooding occurs. Instantaneous peak discharges exceeded 5,000 ft^3/s at NW4 and 1,000 ft^3/s at SC14 during the study period, but maximum peaks on record have exceeded 6,000 ft^3/s and 10,000 ft^3/s, respectively.

Each of the four streamgages in the upper part of the watershed represents a unique hydrologic system within the study region. The SC1 streamgage is mostly in a natural, wide, and sandy channel that has been trending towards more no-flow days, as well as lower mean daily flows for all months of the year, whereas the Nogales Wash streamgage is in a highly urbanized setting with channelized geometry, and human inputs augment and alter the hydrograph for most nonflooding discharge. The discharge from the wastewater treatment plant outfall is gaged at SC6 and measures the effluent discharged into the dry Santa Cruz River channel, establishing flow that remains perennial to TUMA. The SC14 streamgage is downstream of TUMA and measures the culmination of all of the upstream streamflow contributions with very little additional natural and agricultural subsurface inputs (losing reach). The discharge resembles a more natural desert-stream flow regime even with the enhanced base flow from the NIWTP contributions.

Discharge in conjunction with a contaminant concentration provides an estimate of contaminant loading. The total volume of contaminated water discharged downstream during a rain event is crucial for quantifying the effects of remediation strategies or best management practices. Available records showed that SC6 outfall consistently discharges about 10,000 acre-feet/year (acre-ft/yr) into the Santa Cruz River and the downstream SC14 location had a median volume of about 8,400 acre-feet/yr between 2013 and 2016 (period in common between the 4 streamgages). The SC1 and NW4 streamgages measured about 2,300 and 5,700 acre-ft/yr, respectively. During the study, total-discharge volumes at NW4 and SC6 were near or above the median volume for the period of record, although NW4 and SC6 streamflow records were shorter than the Santa Cruz streamgage records. The NW4 base flow is maintained by anthropogenic inputs (leaking infrastructure and effluent

discharge), and unless flooding occurred these inputs kept cumulative volumes constant and consistent between years (Norman, Huth, and others, 2010). During the study, the Santa Cruz streamgages (SC1 and SC14) were below the median volumes for the respective period of streamflow record. Streamflow variability was greatest at the SC locations because of the more natural flow regime where volume fluctuations were more influenced by large runoff events. The water volume can be used to estimate the contaminant loading of water transferring between subwatersheds (yields).

The three upstream streamgages (SC1, NW4, and SC6) represent a majority of the upstream inputs of streamflow volume that flow downstream to TUMA and the SC14 streamgage. During base- and low-flow conditions, much the water infiltrates and undergoes evapotranspiration before reaching SC14 downstream of TUMA. During the study, monthly volumes measured at SC14 were between 30 and 85 percent less than the combined monthly volumes measured at the upper three streamgages. During winter and spring periods, when evapotranspiration is minimal, volume differences between upstream and downstream were still reduced by 30 to 65 percent during the study. This suggests that infiltrating waters with elevated levels of contaminants and microorganisms, not flowing out of the basin, can concentrate or reside in streambed substrates, potentially contaminating local resources or resuspending during high-flow events (Kiefer and others, 2012; Garzio-Hadzick and others, 2010). Specifically, the limited connection between the surface-water flow between NW4 and SC6 indicates that contaminated waters from NW8 are infiltrated into the dry streambed channel just upstream of where the NIWTP discharges into the Santa Cruz River near SC6. Understanding viability of pathogenic microorganisms depositing in this hyporheic zone, as well as the extent of accumulation and loading magnitude, is necessary for quantifying the amount of contaminants flowing downstream during floods. Fecal contaminants in bed sediments are typically ignored and need to be considered because of their potential to increase pathogen loadings during high flows that produce bed-load transport (Bradshaw and others, 2014).

Regional climatological changes, a shift in hydrologic patterns (decreased average flow and increased magnitude flow), and an increase in urbanization along with population growth are likely to affect the *E. coli* levels, sources, and timing of elevated concentrations flowing through TUMA. Increased rainfall intensity with increased percentage of impervious surfaces will result in greater storm-water runoff and greater microbial contamination and loading during rain events. In addition, longer periods of no rain and lower flow can allow fecal sources to accumulate on the landscape or concentrate in streambed sediments. The resulting extremes of hydrologic conditions can promote unfavorable microbial communities, some of which could be pathogenic (Constantin de Magny and Colwell, 2009; Patz and others, 2005). A fundamental understanding of the hydrologic system is necessary for determining *E. coli* sources, transport routes, magnitude, and timing of loads flowing from the upper watershed to TUMA.

Previous Monitoring and Studies

Fecal coliform and *E. coli* bacteria densities in the upper Santa Cruz River and tributaries above the NIWTP have been monitored by different agencies and studied by many researchers. Monitoring and data collection has mostly been conducted by the ADEQ, U.S. International Boundary and Water Commission (IBWC), the Friends of the Santa Cruz River (FOSCR), and TUMA. Each entity collected data with different objectives, over different lengths of time, and at different frequencies. The types of fecal-indicator bacteria most often collected were fecal coliforms, *E. coli*, and total coliforms. More detailed information about the monitoring and methods used by ADEQ, IBWC, and FOSCR can be found in Paretti and others (2018).

Previously collected data have been compiled and analyzed by researchers associated with U.S. Environmental Protection Agency (EPA) projects (Tetra Tech, 2014; Sanders and others, 2013) in an effort to describe river reaches in or out of compliance with State and Federal water-quality standards (WQS; standards for both full- and partial-human body contact with water). Sanders and others (2013) were the first to publish these summarized data and perform an analysis of fecal coliform and *E. coli* concentrations in the Upper and Lower Santa Cruz River Watersheds. Their analysis period (2008–2011) spanned the upgrade of the NIWTP in 2009, but they did not design the analysis to distinguish between pre-upgrade and postupgrade. Reports have shown that since the upgrade in late 2009 the NIWTP has effectively reduced daily *E. coli* concentrations to below the detection limit for most samples (Sonoran Institute, 2016; Tetra Tech, 2014). Sanders showed that Nogales Wash had a higher *E. coli* geometric mean concentration than any of the in-stream Santa Cruz grab samples, but the percentage of full-body-contact WQS exceedances were similar to several of the sites within TUMA. The analysis did not determine a clear downstream pattern, but it did appear that downstream of the NIWTP there was an increasing trend in both the geometric mean and percentage of full-body-contact WQS exceedances (Sanders and others, 2013). Discharge and rainfall data were analyzed in relation to fecal-indicator bacteria concentrations but in a limited capacity using one streamgage and one precipitation station. Nonetheless, elevated fecal-coliform and *E. coli* concentrations were positively correlated with periods of increased streamflow from rainfall. Sanders and others (2013) concluded that bacteria concentrations were highly variable and suggested future assessments consider ecological factors such as interaction with sediment, fecal-bacteria regrowth, and source tracking (Sanders and others, 2013).

Tetra Tech (2014) compiled existing data and used a similar WQS exceedance approach for an EPA Watershed Implementation Plan for the upper Santa Cruz River. The intent was to build tools to estimate bacteria and suspended-sediment loading such as a soil and water assessment tool (SWAT) model. The Tetra Tech (2014) SWAT model was modified from the Niraula and others (2012) model and was used to simulate bacteria and suspended-sediment loading. Tetra Tech (2014) also reported highly variable *E. coli* concentrations before and after NIWTP upgrades, although there was still a notable decrease in *E. coli* exceedances when compared with preupgrade samples taken from the Santa Cruz River, specifically in the reach from Josephine Canyon Wash to the Tubac bridge. Five reaches exceeded the full-body-contact WQS in more than 30 percent of the samples. A two-station (Nogales Wash and Santa Cruz at the southern edge of TUMA) assessment incorporated season and hydrology and observed some changes of *E. coli* concentrations with season and flow conditions. Similar to other studies, Tetra Tech (2014) showed a relation between timing of flow and bacteria concentrations. Nogales Wash was shown to have increasing bacteria concentrations beginning in May, before the monsoon, peaking in July soon after the onset of the monsoon when sources of storm-water runoff increase.

University of Arizona research was conducted by McOmber (2014) to better understand the sources of *E. coli* in the Upper Santa Cruz River Watershed. The study area included reaches of the Santa Cruz River near the U.S.-Mexico border, at the NIWTP, and near Tubac, as well as reaches of Nogales Wash and Potrero Creek. McOmber (2014) used microbial-source tracking (MST), a technique in which host-specific markers are used to detect fecal contamination from different animals and discriminate between sources of *E. coli.*

Results from the McOmber (2014) study showed greater incidence and concentrations of a human MST marker in Nogales Wash. Additionally, from below the NIWTP, downstream to the most northern site at Tubac, a cattle MST marker was more frequently detected and at higher concentrations than at other sites, suggesting greater cattle influence in this region of the study area. Although the NIWTP is the primary source of surface flow upstream of Rio Rico and the human MST marker was detected at significant concentrations in the effluent discharge from the treatment plant, the magnitude of the *E. coli* concentrations in the effluent were nonetheless very low to nondetectable. In contrast to other findings in Nogales Wash, McOmber (2014) suggested that increased discharge may not be the primary variable explaining the increased pollutant levels observed, and further indicated that pollutant surges at Nogales Wash observed during the monsoon may be due to variables other than discharge alone. However, this finding was not clearly supported by results because few or no samples were collected during monsoon flooding events.

These and other studies have quantified concentrations and identified sources of bacteria in the Santa Cruz River (Sanders and others, 2013; McOmber, 2014), but significant information gaps remain with regard to the distribution, variability, timing, loading, source of bacteria, and *E. coli* levels. Additionally, there is a lack of information relating the hydrologic function and suspended sediment driving the variability of both concentration and source of *E. coli*. Data collection in previous studies has been limited both spatially and temporally and nonexistent in contributing ephemeral tributary washes. This investigation aims to provide additional information needed to quantify the spatial and temporal variability of *E. coli* and suspended sediment.

Methods

The methods used for the collection and processing of water samples during the 3-year investigation at TUMA and in the Upper Santa Cruz River Watershed can be found in Paretti and others (2018). The following methods describe the statistical methods and hydrological estimation procedures used in the analysis as well as criteria used to characterize the past and present status of water quality in the Upper Santa Cruz River Watershed.

Collection, Processing, and Quality Control

The data collection methods used in this study followed the procedures and protocols published by the USGS in Wilde (2003), Anderson (1998), U.S. Geological Survey (2006), Wagner and others (2006), Myers and others (2007), and EPA (U.S. Environmental Protection Agency, 2000, 2012). Water and sediment samples were collected on the Santa Cruz River and nearby tributaries at a frequency that captures the entire hydrograph on both a diel and a seasonal scale. Samples were analyzed for suspended sediment, *E. coli* concentrations, and MST markers as a method for characterizing sources of fecal contamination. Host-associated markers have been identified from different groups of fecal-origin bacteria, often from the genus *Bacteroides*, bacteria abundant in the gut of warm-blooded animals, and these can be used to identify and quantify bacterial indicators. Detailed data collection, processing, analysis, and quality assessment descriptions can be found in Paretti and others (2018).

Data Sources

The USGS water-quality and continuous-stage discharge and turbidity data were retrieved from the USGS National Water Information System (NWIS) database (see https://nwis.waterdata.usgs.gov/). *E. coli* data collected by the National Park Service and Friends of the Santa Cruz have also been stored in NWIS (Paretti and others, 2018). Water-stage data were collected by the USGS using pressure transducers (Mayo, 2017). Stage data were not referenced to an elevation and were used for the purpose of understanding timing and relative magnitude of flow hydrographs. In a few instances this resulted in negative water-stage values. Additional water-quality data collected by the ADEQ were retrieved from the EPA Water Quality Data (WQX) data portal (see https://www.epa.gov/waterdata/water-quality-data-wqx). Precipitation, water-stage, and volume data were retrieved from the Water Resources Climate Assessment Tool developed for the Santa Cruz Active Management Area (Shamir and others, 2016). The mean-daily datasets are assembled from sources provided by the IBWC, the National Weather Service, USGS, and the Santa Cruz County Flood Control District ALERT (Automated

Local Evaluation in Real Time) system. Higher resolution data for individual precipitation and flow events were retrieved from the Santa Cruz County Flood Control District ALERT flood-warning system (see https://santacruz.jefulleralert.com/jefmap/), which is maintained by a private hydrological consulting firm in cooperation with the USGS Geology, Minerals, Energy, and Geophysics Science Center. They maintain and serve data for a series of precipitation gages, stream-stage sensors (pressure transducer or radar), and weather stations spanning the Upper Santa Cruz River Watershed (United States and Mexico) as part of a flood alert network for the Santa Cruz Flood Control District and Arizona Department of Water Resources (table 1).

Land-use data were retrieved from the USGS StreamStats portal (see https://water.usgs.gov/osw/streamstats/), which is an integrated web-based geographic information system (GIS) application. Data sources and processing procedures can be found in Paretti and others (2014). Other land-use and land-cover data were retrieved from sources and GIS processes found in Villarreal and others (2011), Norman and others (2010), and Wallace and others (2011). Land-use and land-cover metrics for the sample locations are given in table 2 (available as a separate file for download at https://doi.org/10.3133/sir20195108).

Flux (sometimes referred to as the load) of a river-borne constituent, such as suspended sediment, is the amount (mass) that passes a given point on a river over a given period of time. The yield of that same constituent is the flux per unit drainage area. Data for the Upper Santa Cruz River Watershed are available in Mayo and Paretti (2018).

E. coli flux and yield for the Upper Santa Cruz River Watershed were computed as follows:

$$Q_{E.coli} = C_{E.coli} \times K \ , \tag{1}$$

where

$Q_{E.\ coli}$ is *E. coli* discharge, in most probable number (MPN) per day,

$C_{E.\ coli}$ is the concentration of *E. coli* in MPN per 100 milliliters (MPN/100 mL), and

K is a units-conversion constant (2.45×10^7) for concentrations in MPN/100 mL to convert instantaneous *E. coli* discharge to an equivalent daily *E. coli* discharge (for instantaneous *E. coli* discharge the units-conversion constant is 287.17).

$$Y_{E.coli} = Q_{E.coli} \ / \ DA \ , \tag{2}$$

where

$Y_{E.\ coli}$ is *E. coli* yield, in MPN per square mile

DA is the drainage area upstream of the sampling location.

Suspended sediment flux was calculated using:

$$Q_{ss} = C_{ss} \times K ,$$ (3)

where

Q_{ss}	is suspended-sediment discharge, in tons per day,
C_{ss}	is the concentration of suspended sediment in milligrams per liter, and
K	is a units-conversion constant (0.0027 for concentrations in milligrams per liter) to convert instantaneous suspended sediment discharge to an equivalent daily suspended-sediment discharge (for instantaneous suspended sediment discharge the units-conversion constant is 3.12×10^{-8}).

Suspended-sediment yield was calculated using:

$$Y_{ss} = Q_{ss} / DA ,$$ (4)

where

Y_{ss}	is suspended-sediment yield, in tons per square mile and
DA	is the drainage area upstream of the sampling location.

Table 1. Station/sample location descriptions for the Upper Santa Cruz River Watershed, southern Arizona and northern Mexico.

[SCCFCD, Santa Cruz County Flood Control District; USGS, U.S. Geological Survey; NPS, National Park Service; FOSCR, Friends of the Santa Cruz; IBWC, International Boundary Water Commission; NOAA, National Oceanic Atmospheric Administration; CILA, Comisión Internacional de Límites y Aguas; NAD83, North American Datum of 1983; NA, not applicable]

Station/ sample location abbreviation[1]	Water-shed division	Collecting agency	Station number	Station name	Instrumentation	Latitude, in decimal degrees (NAD83)	Longitude, in decimal degrees (NAD83)	Drainage area, in square miles
NW1	2	USGS /consultant	2524 and 2527	Chiminea Arroyo	Precipitation gage and stage sensor	31.30925	−110.9438	12.5
NW2	2	USGS/ consultant	2540 and 2543	Las Canoas Wash	Precipitation gage and stage sensor	31.33306	−110.96611	4.79
NW3	2	USGS/ consultant	2510 and 2513	Ephraim Wash	Precipitation gage and stage sensor	31.33944	−110.95472	5.23
NW4	2	USGS	09481000	Nogales Wash at Nogales, Arizona	Streamgage	31.34327	−110.93167	29.7
NW5	2	SCCFCD	2530 and 2533	Portrero Canyon Wash	Precipitation gage and stage sensor	31.35305	−111.01472	5.36
NW6	2	SCCFCD	2550 and 2553	Nogales Wash	Precipitation gage and stage sensor	31.35583	−110.92888	44.1
NW7	2	USGS	312536110573401	Nogales Wash Near Old Tucson Highway	Single discrete sample	31.42658	−110.95935	NA
NW8	2	USGS, FOSCR	312551110573901	Nogales Wash at Ruby Road	Stage sensor, automatic sampler, turbidity sensor	31.43075	−110.96083	94.5
INFLUENT	NA	USGS	312640110575101	Nogales International Wastewater Treatment Plant inflow	Treatment plant inflow (IBWC)	31.44457	−110.96410	NA

Table 1. Station/sample location descriptions for the Upper Santa Cruz River Watershed, southern Arizona and northern Mexico.—Continued

[SCCFCD, Santa Cruz County Flood Control District; USGS, U.S. Geological Survey; NPS, National Park Service; FOSCR, Friends of the Santa Cruz; IBWC, International Boundary Water Commission; NOAA, National Oceanic Atmospheric Administration; CILA, Comisión Internacional de Límites y Aguas; NAD83, North American Datum of 1983; NA, not applicable]

Station/ sample location abbrevia- tion[1]	Water- shed division	Collecting agency	Station number	Station name	Instrumentation	Latitude, in decimal degrees (NAD83)	Longitude, in decimal degrees (NAD83)	Drainage area, in square miles
SC1	1	USGS, FOSCR	09480500	Santa Cruz River near Nogales, Arizona	Streamgage	31.34454	−110.85147	532
SC2	1	SCCFCD	2549 and 2552	Santa Cruz River at State Route 82	Precipitation gage and radar	31.38694	−110.87472	573
SC3	1	USGS	312654110573201	Santa Cruz River above Nogales Wash	Stage sensor	31.44836	−110.95897	628
SC4	2	USGS	312710110574201	Santa Cruz River below confluence of Nogales Wash	Discrete samples	31.45275	−110.96163	726
SC5	3	USGS	312733110581401	Santa Cruz River near Nogales International Wastewater Treatment Plant upstream of railroad trestle	Stage sensor	31.45913	−110.97052	728
SC6	3	USGS	312724110580501	Nogales International Wastewater Treatment Plant at outfall	Treatment plant effluent discharge (IBWC)	31.45669	−110.96811	NA
SC7	3	USGS	312730110581301	Nogales International Wastewater Treatment Plant downstream of outfall	None	31.45838	−110.97014	NA
SC8	3	USGS, FOSCR	312809110592801	Santa Cruz River near Rio Rico, Arizona	Stage sensor (temporary)	31.46926	−110.99175	1,000
SC8	3	USGS	09481710	Santa Cruz River at Rio Rico, Arizona	None	31.47037	−110.99231	1,000
SC9	3	SCCFCD	2541 and 2544	Santa Cruz River at Palo Parado bridge	Precipitation gage and radar	31.53	−111.02027	1,116
SC9	3	USGS	313148111011101	Santa Cruz River at Palo Parado bridge	Stage sensor (temporary)	31.53002	−111.01969	1,116

Table 1. Station/sample location descriptions for the Upper Santa Cruz River Watershed, southern Arizona and northern Mexico.—
Continued

[SCCFCD, Santa Cruz County Flood Control District; USGS, U.S. Geological Survey; NPS, National Park Service; FOSCR, Friends of the Santa Cruz; IBWC, International Boundary Water Commission; NOAA, National Oceanic Atmospheric Administration; CILA, Comisión Internacional de Límites y Aguas; NAD83, North American Datum of 1983; NA, not applicable]

Station/ sample location abbrevia- tion[1]	Water- shed division	Collecting agency	Station number	Station name	Instrumentation	Latitude, in decimal degrees (NAD83)	Longitude, in decimal degrees (NAD83)	Drainage area, in square miles
SC10	4	USGS, FOSCR, NPS	313343110024701	Santa Cruz River at Santa Ger- trudis Lane	Stage sensor	31.56203	−111.04703	1,180
SC11	4	USGS, NPS	313413111024400	Santa Cruz River at Tumacacori downstream site	Stage sensor (temporary)	31.57036	−111.04569	1,190
SC12	4	USGS, NPS	313436111025101	Santa Cruz River at Anza trail crossing	Stage sensor	31.57658	−111.04758	1,190
SC13	4	USGS, FOSCR	313542111025801	Santa Cruz River at Clark cross- ing	None	31.595	−111.04944	1,190
SC14	4	USGS	09481740	Santa Cruz River at Tu- bac, Arizona	Streamgage, automatic sampler, tur- bidity sensor, precipitation gage	31.61286	−111.04147	1,210
SC15	4	FOSCR	313854111025701	Santa Cruz River at Chavez Sid- ing	None	31.64833	−111.04916	1,250
SON1	3	SCCFCD	2556 and 2557	Patagonia Lake	Precipitation gage and stage sensor	31.49194	−110.86944	228
SON2	3	USGS	312750110582801	Sonoita Creek Canyon near Rio Rico, Arizona	Stage sensor	31.46380	−110.97452	31
AF1	3	SCCFCD	2502 and 2505	Pena Blanca	Precipitation gage and stage sensor	31.40916	−111.085	13.8
AF2	3	USGS	312843111000201	Miscellaneous Agua Fria Canyon Wash near Rio Rico, Arizona	Stage sensor	31.47870	−111.00119	40.2

Table 1. Station/sample location descriptions for the Upper Santa Cruz River Watershed, southern Arizona and northern Mexico.— Continued

[SCCFCD, Santa Cruz County Flood Control District; USGS, U.S. Geological Survey; NPS, National Park Service; FOSCR, Friends of the Santa Cruz; IBWC, International Boundary Water Commission; NOAA, National Oceanic Atmospheric Administration; CILA, Comisión Internacional de Límites y Aguas; NAD83, North American Datum of 1983; NA, not applicable]

Station/ sample location abbrevia-tion[1]	Water-shed division	Collecting agency	Station number	Station name	Instrumentation	Latitude, in decimal degrees (NAD83)	Longitude, in decimal degrees (NAD83)	Drainage area, in square miles
PC1	3	USGS	313040111004601	Miscellaneous Peck Canyon Wash near Nogales, Arizona	Stage sensor	31.51120	−111.01342	47.8
JC1	3	USGS	313307111020201	Josephine Canyon Wash near Tumacacori, Arizona	Stage sensor	31.552	−111.03383	48.6
P1	2	SCCFCD	2570	Cobach College	Precipitation gage	31.246	−110.938	NA
P2	2	SCCFCD	2560	San Fernando Hill	Precipitation gage	31.28888	−110.9925	NA
P3	2	SCCFCD	2531	CILA Nogales, Sonora	Precipitation gage	31.29305	−110.94638	NA
P4	2	SCCFCD	2537	Calabasas Canyon Wash	Precipitation gage	31.34305	−111.07083	NA
P5	1	NOAA	US1AZSC0003	Nogales 8.9 NNE	Precipitation gage	31.4519	−110.855	NA
P6	1	NOAA	USW00003196	Nogales International airport	Precipitation gage	31.4208	−110.846	NA
P7	4	NOAA	USC00028865	Tumacacori	Precipitation gage	31.56667	−111.05	NA
P8	4	NOAA	US1AZSC0010	Tubac 2.9 SW	Precipitation gage	31.5883	−111.0876	NA
P9	4	SCCFCD	6080	Santa Cruz River at Tubac	Precipitation gage	31.61286	−111.04147	NA
P10	4	NOAA	US1AZSC0011	Tubac 0.7 S	Precipitation gage	31.6019	−111.0458	NA
P11	3	NOAA	US1AZSC0007	Rio Rico 3.6 E	Precipitation gage	31.4677	−110.915	NA
P12	3	NOAA	US1AZSC0013	Rio Rico 4.4 WSW	Precipitation gage	31.437	−111.04	NA
P13	3	SCCFCD	2561	Peck Canyon Wash	Precipitation gage	31.49361111	−111.08138	NA
PNIWTP	3	NOAA	USC00025924	Nogales 6N	Precipitation gage	31.4554	−110.968	NA

[1]Station abbreviations: NW, Nogales Wash; INFLUENT, Nogales International Wastewater Treatment Plant inflow; SC, Santa Cruz River; SON, Sonoita Creek; AF, Agua Fria Canyon Wash; PC, Peck Canyon Wash; JC, Josephine Canyon Wash; P, precipitation gage; PNIWTP, Nogales International Wastewater Treatment Plant precipitation gage.

Statistical Analysis

The data were statistically summarized using general descriptive statistics and graphed representations of the distributions and relations using box plots, ordinary least-squares regression, correlation, and trend analysis in JMP® version 12 software (SAS Institute, Inc., 2007). Contour plots were generated using a nonparametric bivariate density surface created with a smoothing function, and interpolation (represented by color variables) contours were computed using Delaunay triangulation. Hydrologic metrics were computing using the Environmental Flow Allocation and Statistics Calculator (EFASC; Konrad, 2011). A subset of the EFASC hydrologic metrics were selected to define general flow periods that could then be used to categorize samples collected in river reaches associated with that respective streamgage. These metrics consisted of streamflow quantiles, meaning streamflow values that were equaled or exceeded a percent of the period of analysis. In addition, exceedance probabilities, commonly used in hydrology to examine streamflow duration curves, were used to describe *E. coli* and suspended-sediment concentrations.

Microbial-source tracking (MST) and other *E. coli* concentration data were examined using censored statistical methods to properly quantify and represent *E. coli* concentration data that was below or above the method detection limit. Reporting limit procedures for the MST analysis can be accessed in Paretti and others (2018). Censored box-plot analyses using the "cenboxplot" function and robust-regression on order statistics using the "cenros" function from the Nondetects and Data Analysis for Environmental Data (NADA; Helsel, 2012) package in R (Lee, 2015) was used to calculate the median, mean, and standard deviation for comparison using the "cendiff" function from the NADA package in R (Lee, 2015). The "cendiff" function uses the Peto-Prentice test (Helsel and Lee, 2006) to determine whether there were significant differences between the groups for elements with censored data.

MST data were also analyzed using a robust nonmetric multidimensional scaling (NMDS) multivariate-analysis procedure (Clarke and Gorley, 2006). The NMDS analysis was performed on a Bray-Curtis similarity matrix and plotted in two-dimensional space to aid interpretation of multivariate patterns. A Bray-Curtis similarity matrix is well suited for MST data because of the flexibility to include censored information into the matrix, effectively capturing the information of one or more censored data pairs. A measure of stress is provided from the NMDS analysis as a diagnostic to determine how well the data are fitting the NMDS ordination. Lower stress values are desired, and stress values below 0.20 generally indicate that the NMDS plot is providing an accurate representation of the data in multivariate space. A multivariate centroid analysis was used to further simplify the visualization of the NMDS structure (Anderson and others, 2008). This procedure essentially sums the distances of each observation (sample MST composition) relative to the observations within a group (within group sum of squares) and compares the distances to all other observations in all other groups (total sum of squares), and the measure of central location for the group constitutes a centroid location for that group, which can then be used in group comparisons.

Vector overlays were added to NMDS graphical outputs as an additional exploratory tool to visualize potential linear or monotonic relations between the MST concentrations and the ordination axes. Spearman rank correlations were restricted to a vector length of ±0.50 or greater, with ±1.0 indicating complete correlation. The length and direction of each vector indicates the strength and sign, respectively, of the relation between the MST marker type and the NMDS axes (Anderson and others, 2008).

A time series analysis (SAS Institute, Inc., 2007) was used to determine the lag or period between discharge recorded at a streamgage and a pressure transducer downstream or upstream of the gage. The sample cross-correlation function was used for identifying this lag between streamgage height and stream stage at the pressure transducer. This lag shift was applied to high flows, and statistical relations between discharge and pressure transducer stream-stage height were examined for potential discharge estimation at the pressure-transducer location. Discharge was estimated at locations near USGS streamgages using the upstream and downstream relations between stage height and discharge. This was only computed for high flows, which generally ensured elevated velocities and discharge between locations and effectively reduced the lag time caused by channel characteristics. The lag time obtained from the time series analysis was used to adjust downstream or upstream data and once adjusted, an ordinary least-squares regression or locally weighted scatter-plot-smoothing-regression relation was developed to estimate discharge from stage height at the downstream or upstream location.

Multiple linear regression was used to develop predictive models for *E. coli* and suspended sediment. Explanatory variables were evaluated in a forward stepwise regression procedure. Significant parameters that most improved the model were selected by using the minimum Bayesian information criterion (BIC) as a stopping rule to choose the best model. The BIC criterion introduces a penalty term for the number of parameters in the model; the penalty term is larger in BIC than in Akaike information criterion (Schwarz, 1978). Several diagnostics described in Rasmussen and others (2009) were used to evaluate models. The variance inflation factor was evaluated to avoid multicollinearity in the explanatory variable selection process. It measures the degree to which the variance of the coefficient of determination for a particular variable is increased because of correlation between that variable and other variables selected in the model. The Durbin-Watson (Durbin and Watson, 1950) statistic was used to test whether the errors have first-order autocorrelation. It is useful for time-series data when errors are correlated across time.

After model selection and development, other regression statistics are used to evaluate model performance. The coefficient of determination (R^2) describes how much of the

variability is explained in the model. The root-mean-square error indicates the range in uncertainty associated with each regression equation. The *p*-values indicate significant variables based on the *t*-statistics, and determine variable importance for final inclusion in the model. Plots of the observed versus the predicted values from the model were visually assessed, as well as the variance of the residuals plotted against the model predicted values. These plots can help to identify issues with normality and transformations made to the data sets prior to regression analysis.

The variables had to be logarithmically (base 10) transformed to adjust sample distributions to normal. After the models were developed the regression estimates had to be retransformed to the original units, a step that introduces a bias in the computed values. The bias arises because regression estimates are the mean of *y* given *x* in log units, and retransformation of these estimates is not equal to the mean of *y* given *x* in linear space (Rasmussen and others, 2009). To correct for this retransformation bias, Duan (1983) introduced a nonparametric bias correction factor called the "smearing" estimator (Helsel and Hirsch, 2002). The residuals from the model are retransformed into the original units and averaged. This value is multiplied with the predicted values to adjust them for the bias introduced during retransformation.

Hydrological Characterization

Characterizing the hydrology with respect to the water quality provides context for relating the physical mechanism to the concentration, timing, and loading of *E. coli* and suspended sediment in the Upper Santa Cruz River Watershed. The hydrology was analyzed for two temporal scales to examine the variability of *E. coli* and suspended-sediment at different resolutions of discharge data. Streamgages provide a 15-minute resolution (hereafter referred to as instantaneous), but water-quality data are frequently analyzed on a daily, monthly, or annual basis to better relate them to historical data and look at trends or patterns. Water quality is commonly collected as a single sample, and results are translated into daily estimates for monitoring and reporting purposes. As a result, both variability and magnitude information are reduced as the data are effectively averaged or smoothed for the time period of interest. To quantify the concentration variability, water-quality samples were collected and analyzed on both a daily and an instantaneous timescale. Furthermore, the hydrographs of each timescale were divided and assigned factors to assess differences in *E. coli* and suspended-sediment classifications.

Instantaneous discharge and stage-height data were used to classify samples by when they were collected during a daily or flood hydrograph, meaning that samples were identified as rise, peak, or recession (fig. 4*A*). Measurements of suspended sediment and *E. coli* at different points along a hydrograph will have varying concentrations and when analyzed as a relation with discharge will, in certain streams, produce nonlinear

relations that loop, a pattern known as hysteresis (Miller and Orbock Miller, 2007; Nistor and Church, 2005; Williams, 1989; Hickin, 1989). The most common pattern is a concentration peak arriving before the streamflow peak occurs and causing a clockwise hysteresis loop. If suspended sediment is delayed or easily erodible sediments have runoff in previous events, then the hysteresis loop will go counter clockwise. Several other hysteresis patterns are described or have been classified (Nistor and Church, 2005; Williams, 1989). Base-flow hydrograph classifications were possible because of the anthropogenic influences on discharge at the Nogales Wash (NW4) and the NIWTP (SC6) locations. These influences produce a pronounced daily hydrograph with a distinct rise, peak, and trough that occurs roughly 6 to 10 hours later at the downstream Santa Cruz River streamgage (SC14). Several floods were sampled over the hydrograph, and instantaneous concentrations and loads were analyzed to better understand the timing, magnitude, and duration of *E. coli* and suspended sediment in the watershed.

Discharge data were also summarized in the form of mean-daily values and classified to test the effects from different flow conditions as well as monthly and seasonal influences. The distinction between flooding and nonflooding provides little information about the discharge relation and the quantity of flow necessary to elevate *E. coli* concentrations. A finer distinction in discharge information was used to group samples by flow thresholds developed from long-term daily streamgage data, hereafter referred to flow-condition classes. Samples collected with or near a discharge measurement were assigned one of six flow-condition classes. These flow-condition classes were developed using hydrologic metrics, such as the 90-percent or 10-percent exceedance discharge, and then used to generalize discharge thresholds for the analysis of *E. coli* and suspended sediment (figs. 4*B*, *C*; table 3, available as a separate file for download at https://doi.org/10.3133/sir20195108). The quantitatively determined flow condition classes were given general names (very low flow, low flow, medium flow, high flow, and very high flow) to more easily distinguish between classes for purposes of group comparison. Season was also an important factor for samples collected below a low-flow threshold. Specifically, summer samples were statistically different from other samples, and a separate group, summer low flow, was created to investigate this low-flow seasonal influence.

E. coli and suspended-sediment data were analyzed as concentrations and as flux in this study. Stream mass flux, often referred to as load, is the mass of a contaminant such as *E. coli* or suspended sediment transported at a point in a stream or the actual measurement for a specified amount of time (in seconds for instantaneous measurements or days for daily average). Mass flux is the product of constituent concentration and discharge integrated over time (Aulenbach and others, 2007). Yields are the flux divided by the watershed area and reported as a mass flux per square mile.

A. Rising limb

B. NW4

C. SC14

EXPLANATION

Flow conditions
- ○ Very low flow
- ○ Low flow
- ○ Summer Low flow
- ○ Medium flow
- ○ High flow
- ○ Very high flow

Stream abbreviations
Nogales International Wastewater Treatment Plant (NIWTP)
Santa Cruz River (SC)
Nogales Wash (NW)

Q_{90} Streamflow equaled or exceeded 90 percent of the period of analysis

Q_{50} Streamflow equaled or exceeded 50 percent of the period of analysis

Q_{25} streamflow equaled or exceeded 25 percent of the period of analysis

$Q_{MAX/Q50}$ Median annual maximum daily streamflow (Qmax) divided by median streamflow (Q50)

Figure 4. (page 18)   Hydrographs showing the two temporal hydrologic classifications used for the Upper Santa Cruz River Watershed, southern Arizona and northern Mexico. *A*, Fifteen-minute hydrograph classified by flood event and daily diel signal from the Nogales International Wastewater Treatment Plant (NIWTP). *B* and *C*, Multiyear daily mean hydrographs for Nogales Wash (NW4) and Santa Cruz River at Tubac (SC14), respectively, classified by the following metrics—streamflow equaled or exceeded 90, 50, 25, and 10 percent of the time (QXX) and median annual maximum daily streamflow (QMAX) divided by median streamflow (Q50). Daily values are color coded as very low flow (less than Q90), low flow (Q90–Q50, months September to April), summer low flow (Q90–Q50, months May to August), medium flow (Q50–Q25), high flow (Q25–Q10 or QMAX/Q50 for NW4), and very high flow (greater than Q10 or QMAX/Q50 for NW4).

Water-Quality Standards

As part of the Clean Water Act (Federal Water Pollution Control Act Amendments of 1972; Public Law 92–500 and related statutes), WQS are used to establish numeric and narrative standards necessary to protect and ensure that beneficial uses of the Nation's water, such as drinking water, fishing, aquatic and wildlife habitat, recreation, agriculture, and irrigation, are attained. A surface water may have more than one designated use assigned to it and more than one standard for a given pollutant that applies based on the designated uses. Examples of designated uses include full-body contact, partial-body contact, domestic water source, fish consumption, and aquatic and wildlife. WQS are provisions of State or Federal law approved by the EPA that describe the desired condition of a waterbody or the level of protection or mandate how the desired condition will be expressed or established for such waters in the future.

The ADEQ uses the federally established standards for the *E. coli* full-body-contact and partial-body-contact WQS (table 4). *E. coli* are expressed in colony forming units per 100 milliliters of water (CFU/100 mL) or as MPN/100 mL. Other Arizona warm-water aquatic wildlife standards for pH, dissolved oxygen, and suspended sediment are used in the report to provide reference for the concentrations observed during the study.

Study Area and Watershed Characterization

For the purposes of this investigation, the upper Santa Cruz River and watershed references a study area boundary which begins in the intermittent part of the upper Santa Cruz River south of the Mexico border near San Lázaro, Sonora, and extends west to include the Nogales Wash Watershed spanning Ambos Nogales. The northern or downstream boundary is downstream of Tubac near where Chavez Siding Road crosses the Santa Cruz River (SC15). The Upper Santa Cruz River Watershed was divided into four subwatersheds or watershed divisions based on unique hydrology, land-use, and water quality resulting from the landscape characteristics. The four watershed divisions are (1) the upper Santa Cruz River between San Lázaro, Sonora (Mexico), to the start of perennial flow at the NIWTP (WD1); (2) the Nogales Wash, beginning in Sonora, to the confluence with the upper Santa Cruz River just south of the NIWTP (WD2); (3) the NIWTP outfall to the southern TUMA boundary near Santa Gertrudis Lane, including major contributing watersheds of Agua Fria Canyon Wash, Sonoita Creek, Peck Canyon Wash, and Josephine Canyon Wash (WD3); and (4) the southern TUMA Boundary to Chavez Siding Road crossing, downstream of the USGS streamgage at Tubac (WD4; fig. 5). Descriptive statistics for each WD can be found in table 5 (available as a separate file for download at https://doi.org/10.3133/sir201908).

Table 4. Arizona Department of Environmental Quality water-quality standards (Arizona Department of Environmental Quality, 2009; U.S. Environmental Protection Agency, 2012).

[NA, not applicable]

Parameter	Designated use	Minimum	Maximum	Geometric mean	Units
Escherichia coli	Full-body contact	NA	235	126	Most probable number per 100 milliliters
Escherichia coli	Partial-body contact	NA	575	126	Most probable number per 100 milliliters
pH	Aquatic and wildlife—warm water	6.5	9	NA	Standard units
Dissolved oxygen	Aquatic and wildlife—warm water	6.0	NA	NA	Milligrams per liter
Suspended sediment	Aquatic and wildlife—warm water	80	NA	NA	Milligrams per liter

Watershed Division 1 (WD1)—Upper Santa Cruz River West of San Lázaro, Sonora, to the Nogales International Wastewater Treatment Plant

WD1 focuses on the area west of San Lázaro, Sonora. Historically, perennial segments occurred along several parts of the Santa Cruz River from Lochiel, Arizona, south into Mexico, and back north into the United States (Condes de la Torre, 1970; Sprouse, 2005). However, currently, with the exception of flooding, the upstream intermittent and perennial sections of the river between the towns of Santa Cruz and San Lázaro, Sonora, do not continuously flow back into the United States, as documented with aerial imagery and the high proportion of zero-flow days at SC1. The groundwater system in this subwatershed is complex, with sediment and sedimentary rock that are affected by many factors, including particle size distribution, fracturing, aquifer-storage capacity, pumping, evapotranspiration, bank storage, and runoff infiltration (Nelson and Erwin, 2001). Increased groundwater pumping, effluent allocation, and shifts in regional weather patterns have lowered groundwater levels and reduced or eliminated base flow in once perennial segments of the river (Arizona Department of Water Resources, 2017; Prichard and Scott, 2014; McAndrew, 2011; Nelson and Erwin, 2001; Treese and others, 2009). In some reaches, highly permeable bed sediments allow rapid infiltration of large flood events, which attenuates surface flows and raises near-stream groundwater-levels (Corkhill and Dubas, 2007; Wood and others, 1999). The Santa Cruz River near Nogales, Arizona, USGS streamgaging station 09480500 (SC1) is located less than a mile north of the international border (fig. 6*A*). Nearby are two ADEQ/FOSCR sampling locations where water-quality data were collected intermittently for about 17 years (1994–2011; fig. 6*B*). Roughly 5 miles downstream of SC1, State Route 82 crosses the Santa Cruz River; the Flood Control District of Santa Cruz County, in cooperation with a consultant, has established a flood-warning-stage sensor and precipitation gage at this location (SC2, fig. 6*C*). The National Weather Service has maintained several weather stations in the vicinity, two of which are referenced here in relation to the ephemeral Santa Cruz River reach (P5 and P6; fig. 6*A*). For the purposes of this study, the USGS deployed two pressure transducers as water-stage sensors upstream of the NIWTP, one above (SC3, fig. 5*D*) and the other below (SC5; figs. 6*F*, *G*) the confluence of Nogales Wash and the Santa Cruz River. As a result, the timing and relative magnitude of water discharging from the ephemeral Santa Cruz River could be distinguished from that of the contributing Nogales Wash Watershed to the west. The SC5 sensor was used to determine the frequency of connectivity between Nogales Wash and the ephemeral Santa Cruz River near the start to the perennial part of the Santa Cruz River that initiates with the NIWTP outfall.

The WD1 area is mostly rangelands and agricultural lands with very little impervious surface area and low population density. A third of the area of WD1 is composed of highly permeable alluvial deposits resulting in a wide sandy channel that no longer has base flow because of a lowered groundwater

table. Of the four WDs included in this analysis, WD1 is the least developed. More than 90 percent of the land cover is shrub, grassland, and mixed forest, whereas agriculture only accounts for a little more than 1 percent of the land used. The river flood plain, the primary focus, is mostly used for this agricultural activity, which concentrates much of the effects within the active channel. Grazing is also very prominent in floodplain and accelerates erosion and causes elevated suspended sediment during periods of flooding (McOmber, 2014). For rivers in general, grazing and animal feeding pens introduce a majority of the inputs of animal waste, *E. coli*, and other potential pathogenic organisms (Pandey and Soupir, 2014; Garzio-Hadzick and others, 2010; Wilkes and others, 2013).

Water Quality

A limited number of water-quality samples were collected from WD1 primarily because of the ephemeral and intermittent characteristics of this section of river. When flow does occur, it is generally low-flow or flooding that is short in duration coupled with a high rate of infiltration and evaporation. These characteristics create challenges for collecting water-quality samples in a timely manner. When the river reach flowed, FOSCR monitored two locations just upstream of SC1 between 1995 and 2011.

The ADEQ lists this section of river as having exceedances in *E. coli* concentrations for the WQS for full-body contact (FBC WQS; 235 MPN/100 mL; Arizona Department of Environmental Quality, 2015). Of the 25 samples collected by ADEQ, roughly 30 percent of the samples exceeded either the partial-body contact (PBC WQS; 575 MPN/100 mL) or FBC WQS. In 2013, four samples collected by McOmber (2014) had a geometric mean of 114 MPN/100 mL. General parameters (temperature, dissolved oxygen, specific conductance, and pH; fig. 7*A*, table 5) trend with season and flow conditions; dissolved oxygen and specific conductance were greater during cooler and low-flow periods. Increased flow during the monsoon reduced specific conductance, and warmer temperatures reduced dissolved oxygen in the summer. The pH remained mostly stable throughout the year between 7.50 and 8.25 pH units. Turbidity, suspended sediment, and *E. coli* fluctuated an order of magnitude or more in the summer and fall months in response to fluctuations in discharge common during the monsoon (fig. 7*B*). Bacteria have an affinity for inorganic particles, such as suspended sediment, and many factors affect this adsorption process, such as pH, mineralogy, and charge of particles (Liang and others, 2016; Hipsey and others, 2006). *E. coli* was positively correlated to the concentrations of suspended sediment, likely due to the fact that microorganisms transport with fine sediments that are put into suspension by streamflow (Jamieson and others, 2005). Turbidity is the measure of relative clarity of a liquid and can be used as a surrogate for suspended sediment because they are correlative. In WD1, *E. coli* was significantly correlated to turbidity and temperature but showed a weaker and not significant relation to increasing discharge and suspended sediment (fig. 8).
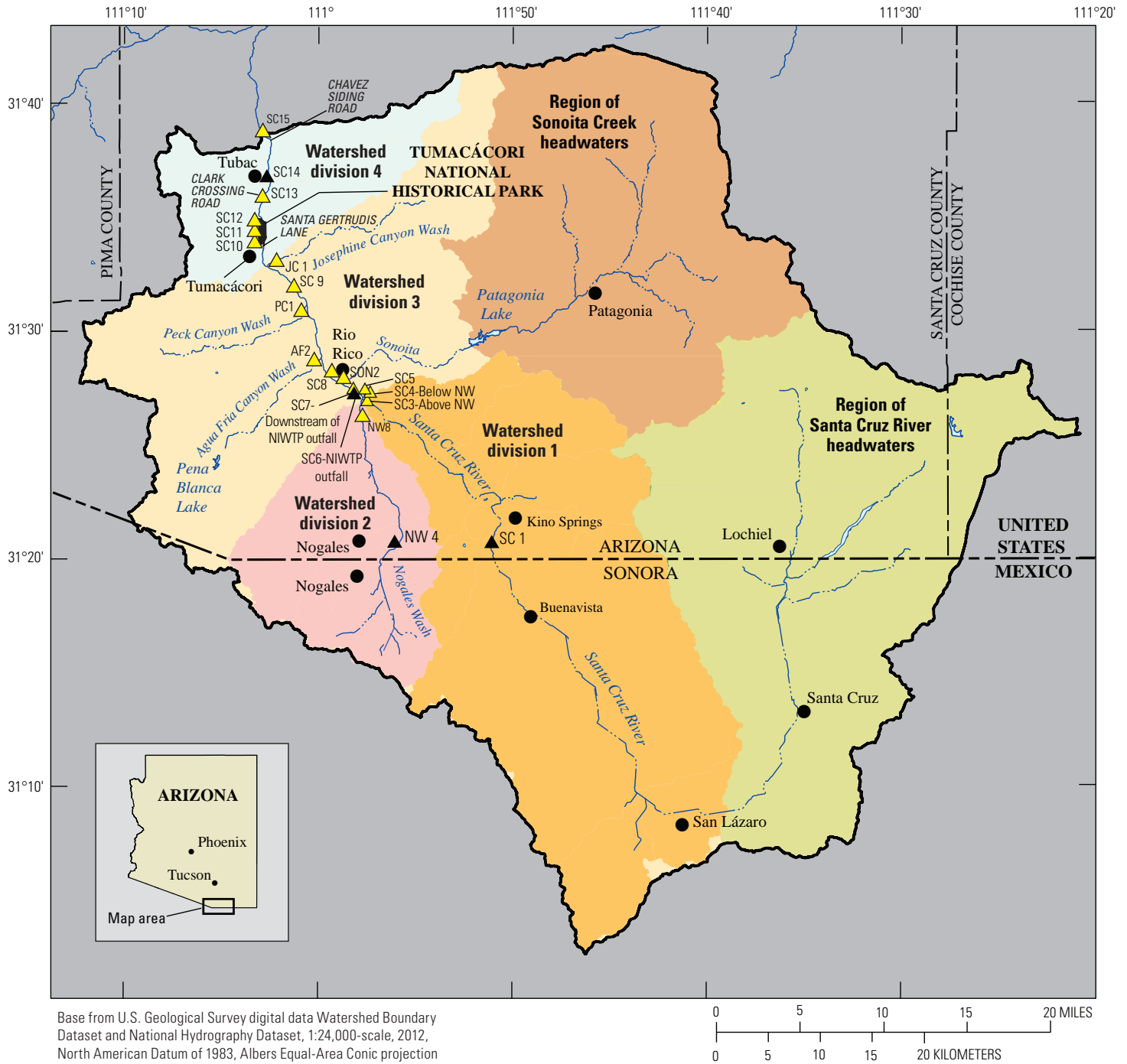
Figure 5.   Map of the study area in southern Arizona and northern Mexico, including watershed divisions, Tumacácori National Historical Park, Nogales International Wastewater Treatment Plant (NIWTP), and the Upper Santa Cruz River Watershed. Surface water in the region of Santa Cruz River headwaters only infrequently contributes to the western part of the river. Sample locations and other hydrologic sites are shown. For detailed descriptions of station/sample locations (for example, SC1) see table 1.
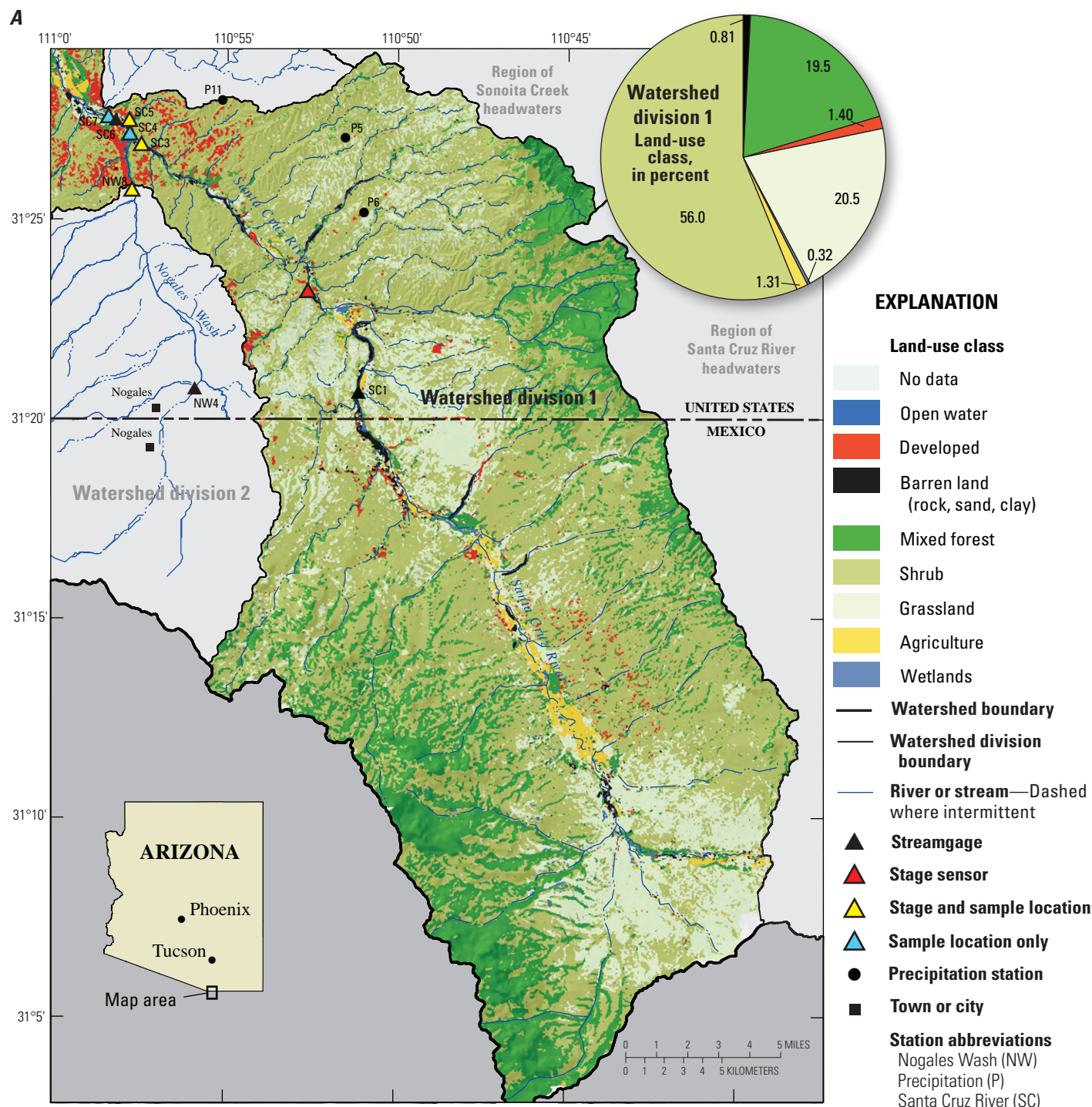
Figure 6. (pages 22–23)   Map and photographs of watershed division 1 of the Upper Santa Cruz River Watershed, southern Arizona and northern Mexico. *A*, Map showing watershed division 1 and station/sample locations (for detailed descriptions of station/sample locations see table 1). Land-use classes are shown in percent in the pie chart; sample locations and other hydrologic sites are annotated; SC, Santa Cruz River; P, precipitation stations; NW, Nogales Wash. *B–F*, Photographs of watershed division 1 and station/sample locations. *B*, SC1 base flow looking north and downstream (March 3, 2016); *C*, SC2 flooding looking east and downstream (July 29, 2007); *D*, SC3 looking downstream and northwest (November 29, 2015); *E*, SC4 flow from Nogales Wash looking upstream and southwest (April 3, 2015); *F*, SC5 flooding looking west (July 1, 2015); *G*, SC5 looking upstream and south (May 15, 2015) (U.S. Geological Survey photographs).
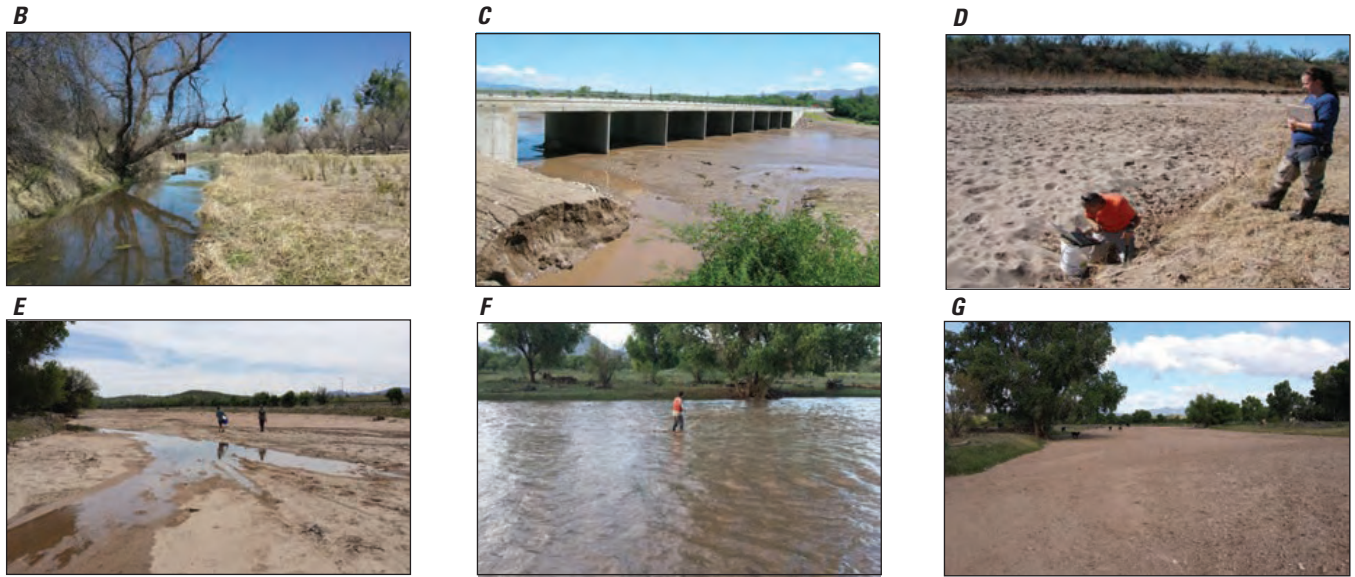
Figure 6. (pages 22–23)   —Continued
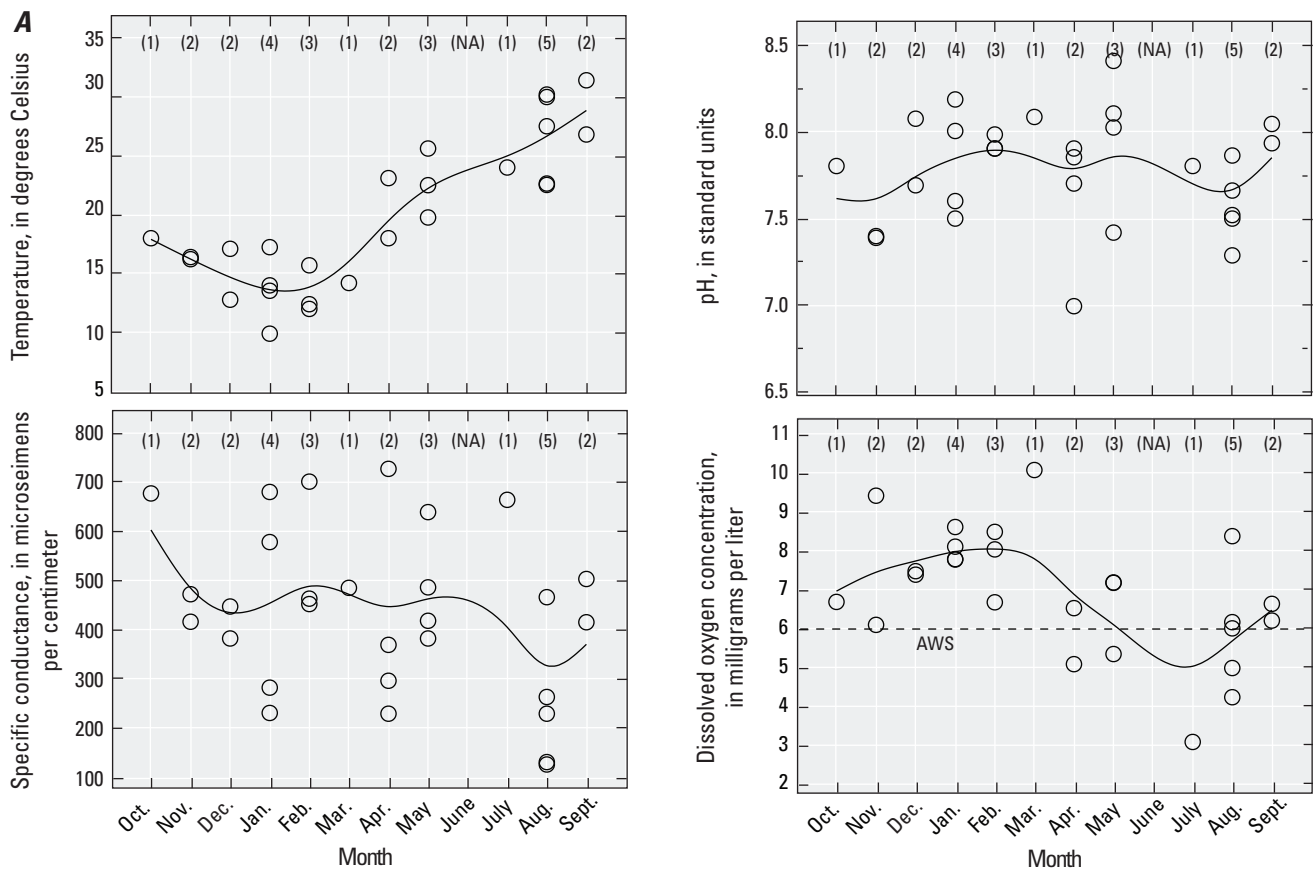
Figure 7. (pages 23-24)   Graphs showing water-quality parameters and *Escherichia coli* concentrations and related sediment parameters by month (water years 1994–2016) for watershed division 1 of the Upper Santa Cruz River Watershed, southern Arizona and northern Mexico. *A*, General water-quality parameters; *B*, *Escherichia coli* concentration (in most probable number per 100 milliliters), suspended sediment, and turbidity. Line of fit used instead of boxplot due to limited dataset; the fit is a cubic spline (lambda of 0.05). Number of values are shown in parentheses (NA, not applicable). FBC WQS, full-body-contact water-quality standard; PBC WQS, partial-body-contact water-quality standard; AWS, Arizona warm-water aquatic wildlife standard.

Figure 7. (pages 23-24)   —Continued

Figure 8.   Graphs showing relations of *Escherichia coli* to discharge, suspended sediment, temperature, and turbidity for watershed division 1 of the Upper Santa Cruz River Watershed, southern Arizona and northern Mexico. Kendall's tau and probability (p) are presented for significant relations. Due to limited dataset a cubic spline was fit to data (lambda of 0.05).

EXPLANATION

△ Discharge estimated
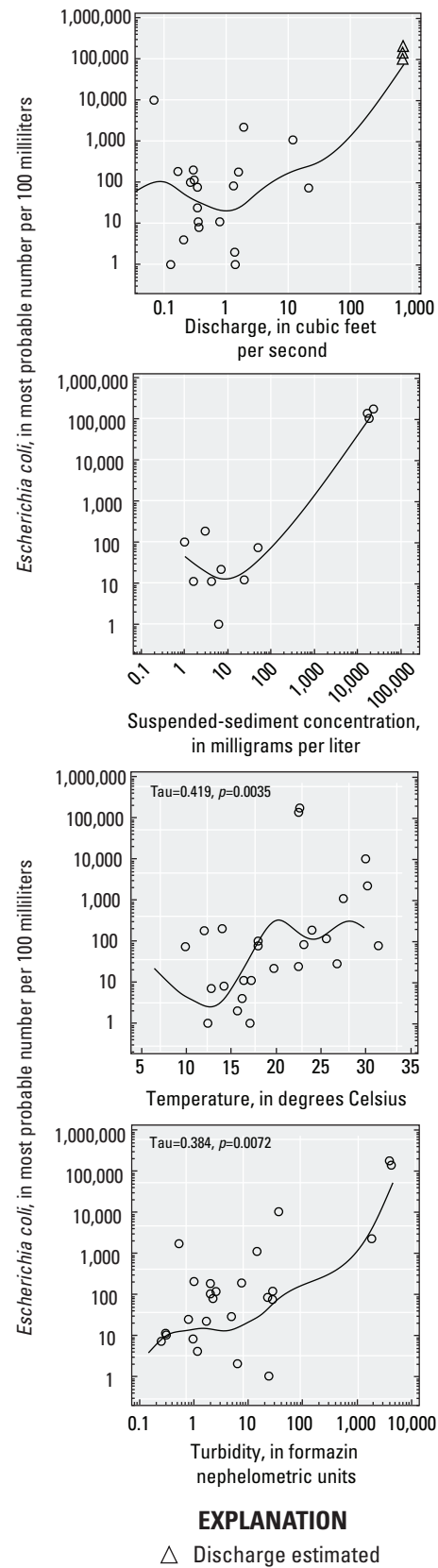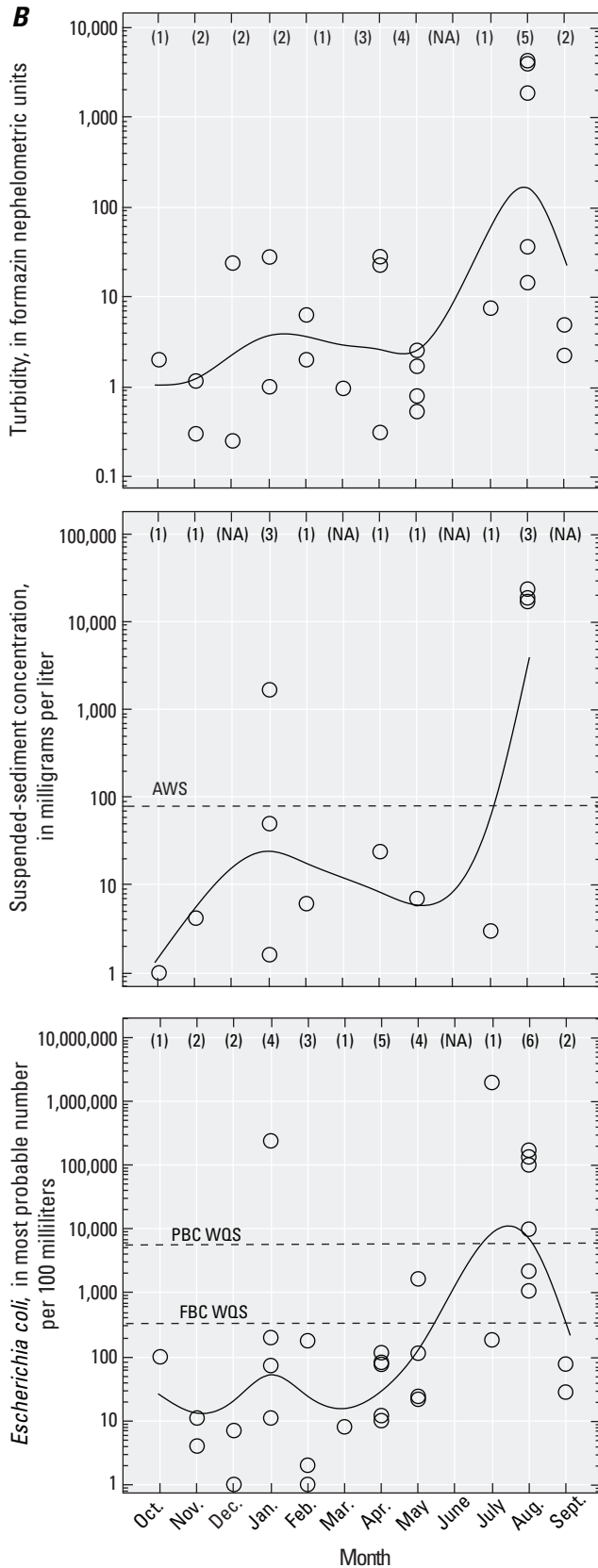
Hydrologic Characterization of *E. coli* and Suspended Sediment

During the 2 years of this study, the water-stage and discharge data indicated that the flow measured at SC1 connected to the perennial section of the Santa Cruz River near the NIWTP outfall at least four times (fig. 9). Connection between SC1 and the perennial reach was likely more frequent in the past when there were more perennial sections of the Santa Cruz River. Although only one event was sampled at SC3, it represented the first large flow for water year 2016 and the largest flow since September of 2014. This event was the result of widespread heavy precipitation over multiple days in early August 2016. The peak, which occurred at 5:00 p.m. on August 3, 2016, was rapid and samples were collected on the rise, peak, and fall (fig. 10*A*). Travel time between sensors increased downstream because of the dry, wide, and sandy channel conditions. The stage sensor failed at SC3, and the transducer temperature and visual markers of stage were used to assess the flood progression. Concentrations of *E. coli* and suspended sediment were greatest on the rising limb of the peak (170,000 MPN/100 mL and 23,400 milligrams per liter, mg/L, respectively), and concentrations decreased by about 20 to 40 percent through the event sampling. The time of arrival from SC1 to SC3 was approximately 3 hours over a distance of 14 miles (fig. 10*A*).

The MST samples were collected on the rise, peak, and fall of the August 3 event (fig. 10*B*). The greatest concentration of *E. coli* and suspended sediment was on the rising limb of the hydrograph, as was the greatest concentration for both the ruminant-animal (Rum2Bac; 1,220,000, in copies per 100 mL) and cattle (CowM2; 22,500, in copies per 100 mL) MST markers. The rise of the peak represents a first seasonal flush of the channel and likely the inputs from all the grazing activity upstream. The general-bacteria (GenBac), human (HF183), and canine (BacCan) markers increased by roughly 26 to 58 percent as the flood progressed, possibly indicating other runoff inputs from residences after the first significant runoff event of the year or the first flush of the watershed.

E. coli and Suspended-Sediment Flux

There was no stage-discharge relation at SC3 where the samples were collected, so computing sediment and *E. coli* flux was not possible. However, a discharge estimate was made on the basis of channel characteristics and flood timing, as well as referencing documentation on channel losses for floods on the Santa Cruz River. The Santa Cruz River channel is wide, low-gradient, and primarily has a sandy substrate that increases infiltration and attenuates flood peaks due to subsurface channel losses during flooding (Wood and others, 1999). This is supported by the responsiveness of water levels observed in shallow wells near the streambank (Nelson and Erwin, 2001). Flooding magnitude and timing in this region are also affected by the rate and volume of precipitation, spatial coverage, time of year, and antecedent wetting conditions.

At SC1, the USGS has historically measured mean velocities between 2.5 and 5.5 feet per second (ft/s) for discharges computed between 500 and 1,800 ft³/s. There was a peak discharge of 1,190 ft³/s observed on August 6, 2016. If flow measurement relations (velocity, width, and depth) were assumed similar at SC3 as SC1, then using an approximated flooding cross-sectional width and mean depth of 75 ft and 2.5 ft, respectively, provides an estimate of 450 to 800 ft³/s for the August 2016 peak flow. This approach assumes no reduction in velocity and no loss from infiltration along the 13-mile reach.

Previous investigations in this region noted a 40- to 80-percent reduction in discharge over an 80-mile section in the upper Santa Cruz River, and other studies done on the Santa Cruz and Gila Rivers indicated discharge loss from subsurface attenuation of about 30 to 50 percent, depending on the channel conditions and distance (Condes De La Torre, 1970; Burkham, 1970, 1976; Wood and others, 1999). There were antecedent wetting conditions from at least three previous precipitation events, each approximately 0.5 in per event. Incorporating a 30 to 50 percent attenuation of the 1,190 ft³/s peak discharge based on August flow and channel conditions, discharge was estimated to be between 600 and 800 ft³/s. This simplified estimate was similar to the cross-sectional estimate and supports the rough approximation of discharge for this event peak. Applying this discharge range to the average *E. coli* and suspended-sediment concentrations provides instantaneous-flux estimates ranging from 1.93×10^{10} to 3.09×10^{10} most probable number per second (MPN/s) and 3.06×10^{-1} to 4.90×10^{-1} tons per second (ton/s), respectively.

Summary

Watershed Division 1 focused on the area west of San Lázaro. Historically, this section of the Santa Cruz River was perennial, but in the past 10 years the stream has become more intermittent, and the lower sections are ephemeral. This trend has become more apparent from the increasing number of zero-flow days measured at the SC1 streamgage. The area is mostly range and agricultural lands with very little impervious surface area and a low population density. Existing data and the data collected showed that *E. coli* was positively correlated to turbidity and temperature. During the 2 years of this study, the water-stage and discharge data indicated that the flow measured at SC1 connected to the perennial section of the Santa Cruz River near the NIWTP outfall at least four times. The largest event during the study period (a peak discharge of 1,190 ft³/s at SC1) was sampled, and the highest concentrations of *E. coli* and suspended sediment were on the rising limb of the flood peak. The MST marker concentrations also changed during the flood peak and showed elevated concentrations for all markers, but the ruminant and cattle markers were among the highest measured during the entire study. The estimated flux of this event was several billion MPN/s for *E. coli* and less than a half of a ton per second for the instantaneous suspended-sediment estimates. Although the *E. coli* and suspended sediment originating from this region of the upper watershed was very high during flow events, the low frequency, short duration, and limited connection of these events suggests the overall contributions flowing through TUMA are likely minimal relative to the contributions from other WDs in the greater watershed.

Figure 9. Graphs showing times series of instantaneous discharge and stage height for the Santa Cruz River (SC), southern Arizona and northern Mexico. Graphs show discharge at station SC1 and stage height at stations SC2 (including daily mean precipitation at SC2 and precipitation stations P5 and P6) and SC3, as well as stage height at SC5 east of the Nogales International Wastewater Treatment Plant. For detailed descriptions of station/sample locations see table 1.

Figure 10.   Graphs showing times series of the August 3, 2016, flood of the Santa Cruz River (SC), southern Arizona and northern Mexico. *A*, stage height of at stations SC1, SC2, SC3 (includes *Escherichia coli* and suspended sediment concentration; see scale at right of graph), and SC5. *B*, Concentrations at SC3 of suspended sediment, *Escherichia coli*, and microbial-source-tracking markers (Rum2Bac, ruminant animal; CowM2, cattle; BacCan, canine; GenBac, general bacteria). *E. coli, Escherichia coli*; MPN/100 mL, most probable number per 100 milliliters. For detailed descriptions of station/sample locations see table 1.

Watershed Division 2 (WD2)—Nogales Wash to the Santa Cruz River Confluence

WD2 focuses on the area from Nogales Wash to the Santa Cruz River confluence. At 95 mi², Nogales Wash is perhaps the best known and the largest tributary in the Upper Santa Cruz River Watershed and is the principal drainage channel for Ambos Nogales. It flows through a concrete channel for about 2 miles south and north of the international boundary, much of that in a tunnel (fig. 11A). Base flow in Nogales Wash is augmented by contributions from perched groundwater, as well as leaking potable water and wastewater infrastructure in Nogales, Sonora (Norman, Huth, and others, 2010). There is a USGS streamgaging station on Nogales Wash (station identification 09481000; NW4, figs. 11C, D), located less than a mile north of the international boundary.

About 5 miles north of the international boundary, Nogales Wash meets Potrero Creek; 3 miles downstream it flows into the Santa Cruz River south of the unincorporated town of Rio Rico, Arizona. As previously mentioned, this report maintains the name "Nogales Wash" for this reach. The NIWTP is found at the confluence of Nogales Wash and the Santa Cruz River, about 8.5 miles north of the international boundary and on the southern edge of Rio Rico, Arizona. The NIWTP provides sewage treatment for Ambos Nogales. Sewage is piped to the NIWTP by way of the International Outfall Interceptor (IOI), a 30-inch pipe that is mostly adjacent to Nogales Wash but runs about 3 ft beneath Nogales Wash for a little less than a mile, from south of the Morley Avenue bridge to near the City of Nogales Public Works Building at North Detention Road (Huth, 2011). Numerous occurrences of flooding between 2007 and 2015 resulted in repeated failure of the IOI and the direct input of untreated sewage into Nogales Wash. The resulting fecal contamination from the 2015 failure was immense, causing some of the highest *E. coli* concentrations observed in the current study. Years of flooding and scouring have compromised the pipe, and in August 2007, severe flooding caused the concrete bottom of the channel of Nogales Wash to break up. The channel-bottom damages were very near the IOI alignment (Huth, 2011). Between June and October 2015, there were chronic sanitary sewer overflows near the border that affected Nogales Wash and its tributaries. In addition, there are number of locations downstream of the border where exposed sewer line in the stream channel can be damaged and contaminate Nogales Wash (fig. 11F).

The Nogales Wash Watershed is the most urbanized part of the Upper Santa Cruz River Watershed, with 19 percent of the watershed classified as having high-, medium-, or low-intensity urbanization. In addition, there are large residential areas, referred to as colonias, along the border, often on devegetated and unprotected slopes that lack infrastructure such as potable water and sewer systems (Norman, 2007). Households lacking connections to a sewer system use latrines or open pits for the disposal of human waste, which can be transported with eroded sediments by surface runoff in heavy rainstorms into the Nogales Wash (Norman, Huth, and others, 2010). Herbaceous scrub and mixed forest account for the other large parts of land cover in the Nogales Wash Watershed (55 and 17 percent, respectively); these areas experience grazing activities and are susceptible to additional erosion, manure, and suspended-sediment issues.

Because of the rapid hydrological responsiveness of the watershed, the USGS has worked with several partners to establish a flood warning project in Nogales, Sonora (the network of five water-stage and nine precipitation stations used in this study can currently be accessed along with the other Santa Cruz County Flood Control District's flood-warning stations at http://jefullerdata.com/Nogales/Nogales.html). Instrumented waterways include Chiminea Arroyo (NW1, fig. 11B), Las Canoas Wash (NW2), Ephraim Wash (NW3), Portrero Canyon Wash (NW5, fig. 11E), and Nogales Wash (NW6; table 2). The Ruby Road location (NW8, fig. 11G) was established as a primary sampling location for this study because of its close proximity to the Santa Cruz River and ease of access. An automatic sampler and stage sensor were deployed at this location, and more details can be found in Paretti and others (2018). In addition, a water-stage sensor (SC5; mentioned previously in WD1) was established downstream of the confluence of Nogales Wash and the Santa Cruz River to quantify the frequency of surface-water connection and loading from Nogales Wash into the perennial Santa Cruz River.

Water Quality

Nogales Wash flows through a tunnel until it exits the Morely Tunnel conduit in Nogales, Arizona, and it is here where it enters the open concrete-lined channel just upstream of NW4 (fig. 11C). The direct addition of chlorine to the water in this section is frequently used as a disinfection method, but as far as the authors understand there is no standard operating procedure for chlorinating the wash and during site visits the chlorine odor was very strong. McOmber (2014) observed chlorine concentrations 25 times greater than the acute ADEQ WQS. For this study, concentrations of *E. coli* at NW4 were measured less than 1 MPN/100 mL, which is a likely result of the chlorination. Repeated failures of the IOI and the direct input of untreated sewage into Nogales Wash are often referred to as "fugitive flows." On June 12, 2015, samples were collected at NW8 during base flow, and average concentrations of *E. coli* were 7.27×10^6 MPN/100 mL. A major breach of the IOI occurred in late July 2017, and samples were collected at NW7. The *E. coli* was measured at a concentration of 3.26×10^6 MPN/100 mL, among the highest concentrations observed during the study, and was similar in concentration to the influent sample.

Since 1993, FOSCR, in cooperation with ADEQ, has monitored several locations on Nogales Wash (NW4, NW6, NW7, and NW8), and FOSCR currently monitors NW8 on a monthly basis. ADEQ lists the upper part of the Nogales Wash as impaired for *E. coli*, chlorine, ammonia, and copper
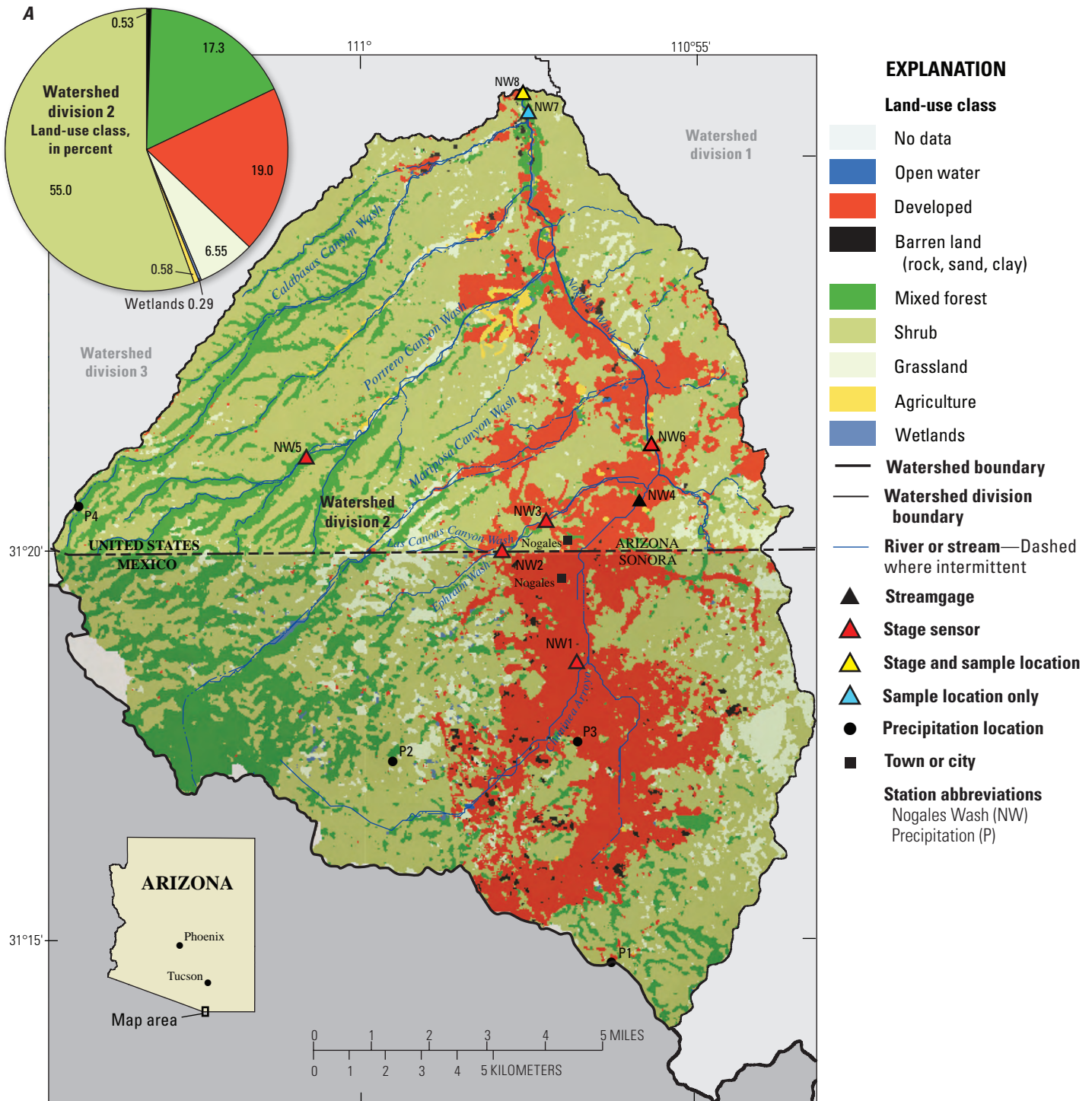
Figure 11. (pages 29–30)   Map and photographs of watershed division 2 of the Upper Santa Cruz River Watershed, southern Arizona and northern Mexico. *A*, Map showing watershed division 2 and station/sample locations (for detailed descriptions of station/sample locations see table 1). Land-use classes are shown in percent in the pie chart; sample locations and other hydrologic sites are annotated; P, precipitation station; NW, Nogales Wash. *B–G*, Photographs of watershed division 2 and station/sample locations. *B*, NW1 looking upstream (photograph from U.S. Army Corps of Engineers, 2004); *C*, NW4 looking upstream and south towards the tunnel where NW daylights (U.S. Geological Survey, USGS, November 11, 2009); *D*, NW4 flooding looking west (Arizona Department of Water Quality photograph, July 3, 2018); *E*, NW5 looking downstream and southeast (USGS photograph, January 21, 2015); *F*, NW7 looking east showing International Outfall Interceptor contributions to Nogales Wash (Arizona Departerment of Water Quality photograph, July 26, 2017); *G*, NW8 base flow looking east (USGS photograph, March 1, 2016).

Breach discharging

Figure 11. (pages 29–30) —Continued

(Arizona Department of Environment, 2015). The lower part at NW8 is also listed as impaired for exceedances of *E. coli* concentrations for the FBC WQS standard (235 MPN/100 mL), chlorine, and dissolved oxygen standards (fig. 12*A*) (less than 6 mg/L for Arizona warm-water aquatic wildlife standards, AWS; Arizona Department of Environmental Quality, 2015). Past and current results support that flooding conditions result in concentrations that typically exceed the PBC WQS (575 MPN/100 mL; AWS of 80 mg/L for sediment; Tetra Tech, 2014). Data summaries reported by Tetra Tech (2014) reported a geometric mean of 251 MPN/100 mL for *E. coli* (2005–2012). During this study the geometric mean of *E. coli* concentrations were more than double those reported by Tetra Tech, and maximum concentrations an order of magnitude greater than the maximum reported by Tetra Tech, although their reported maximum was the upper reporting level of the analysis method with a 100 mL dilution, 2,420 MPN/100 mL (fig. 12*B*; table 3). Median *E. coli* and suspended sediment was below the WQS standards for the months between October and May, and the median turbidity was below 10 formazine turbidity units (FNUs), supporting the inference that exceedances are mostly occurring during monsoon flooding. The median pH and specific conductance were more stable than in WD1, likely because of

the consistent base flow, but parameters were more variable during low-flow and monsoon-season months (fig. 12*A*).

Samples collected on 63 days (235 samples) between September 2014 and December 2016 and analyzed for *E. coli* showed that mean daily concentrations for 58 percent of the samples exceeded the FBC WQS, and 48 percent exceeded the PBC WQS (fig. 13*A*). In comparison to historical exceedances this was approximately 10 and 15 percent greater, which was likely related to the differences in timing of sampling and increased number of samples collected during flood events. All samples collected during flood conditions exceeded the PBC and FBC standards, whereas about 20 percent exceeded the PBC standard during base flow (fig. 13*B*). Most suspended-sediment concentrations were collected during flood events, and the mean concentration was 3,890 mg/L. All but one mean daily concentration exceeded the AWS criteria threshold of 80 mg/L.

In WD2, *E. coli* was correlated with suspended sediment (Kendall's tau=0.578, *p*-value=0.0001) and moderately with turbidity (Kendall's tau=0.333, *p*-value=0.0001). Although the relation was not linear or without variability, *E. coli* mostly increased as suspended sediment increased (fig. 14). The turbidity and the *E. coli* relation was highly variable between 1 and 10 FNUs, and within this range *E. coli* concentrations

Figure 12. (page 31)   Boxplots showing water-quality parameters and *Escherichia coli* concentrations and related sediment parameters by month (water years 1994–2017) for watershed division 2 of the Upper Santa Cruz River Watershed, southern Arizona and northern Mexico. *A*, General water-quality parameters—temperature, specific conductance, pH, and dissolved oxygen; *B*, *Escherichia coli* concentration, suspended sediment, and turbidity. FBC WQS, full-body-contact water-quality standard; PBC WQS, partial-body-contact water-quality standard; AWS, Arizona warm-water aquatic wildlife standard.

A

Temperature, in degrees Celsius

(9) (9) (10) (15) (9) (11) (13) (9) (9) (13) (7) (12)

Specific conductance, in microseimens per centimeter

(11) (11) (10) (20) (9) (12) (14) (11) (16) (7) (14)

pH, in standard units

(11) (11) (10) (20) (8) (14) (12) (11) (9) (16) (7) (14)

AWS

Dissolved oxygen, in milligrams per liter

(9) (9) (10) (15) (9) (11) (13) (9) (9) (13) (7) (12)

AWS

Oct. Nov. Dec. Jan. Feb. Mar. Apr. May June July Aug. Sept.

Month

B

Turbidity, in formazin nephelometric units

(10) (9) (9) (19) (7) (10) (12) (11) (8) (15) (6) (13)

Suspended-sediment concentration, in milligrams per liter

(2) (2) (6) (2) (3) (2) (8) (4) (3)

AWS

Escherichia coli, in most probable number per 100 milliliters

(12) (10) (10) (20) (11) (13) (15) (11) (8) (28) (11) (16)

FBC WQS

PBC WQS

Oct. Nov. Dec. Jan. Feb. Mar. Apr. May June July Aug. Sept.

Month

EXPLANATION

(4) **Number of values**

○   **Outside value**—Value is >1.5 and <3 times the interquartile range beyond either end of the box

Largest value within 1.5 times interquartile range above 75th percentile

75th percentile
50th percentile (median) } **Interquartile range**
25th percentile

Smallest value within 1.5 times interquartile range below 25th percentile

A

B

Percentage of *Escherichia coli* samples equaled or exceeded

Figure 13.   Graphs showing the percentage of *Escherichia coli* concentrations that were equaled or exceeded in watershed division 2 of the Upper Santa Cruz River Watershed, southern Arizona and northern Mexico. *A*, Graph for previous monitoring and this current U.S. Geological Survey study; *B*, Graph for flooding and baseflow conditions. FBC WQS, full-body-contact water-quality standard; PBC WQS, partial-body-contact water-quality standard. Boxes indicate concentrations greater than the Colilert method reporting limit of 2,420 most probable number per 100 milliliters. *n*, sample size.
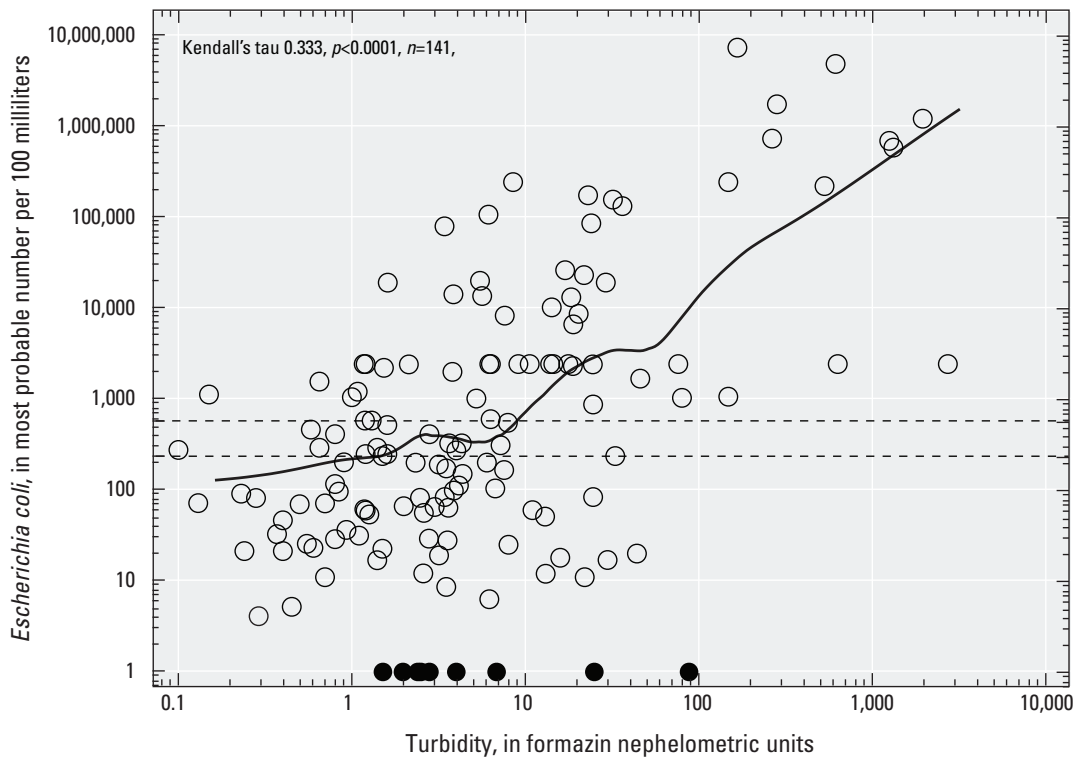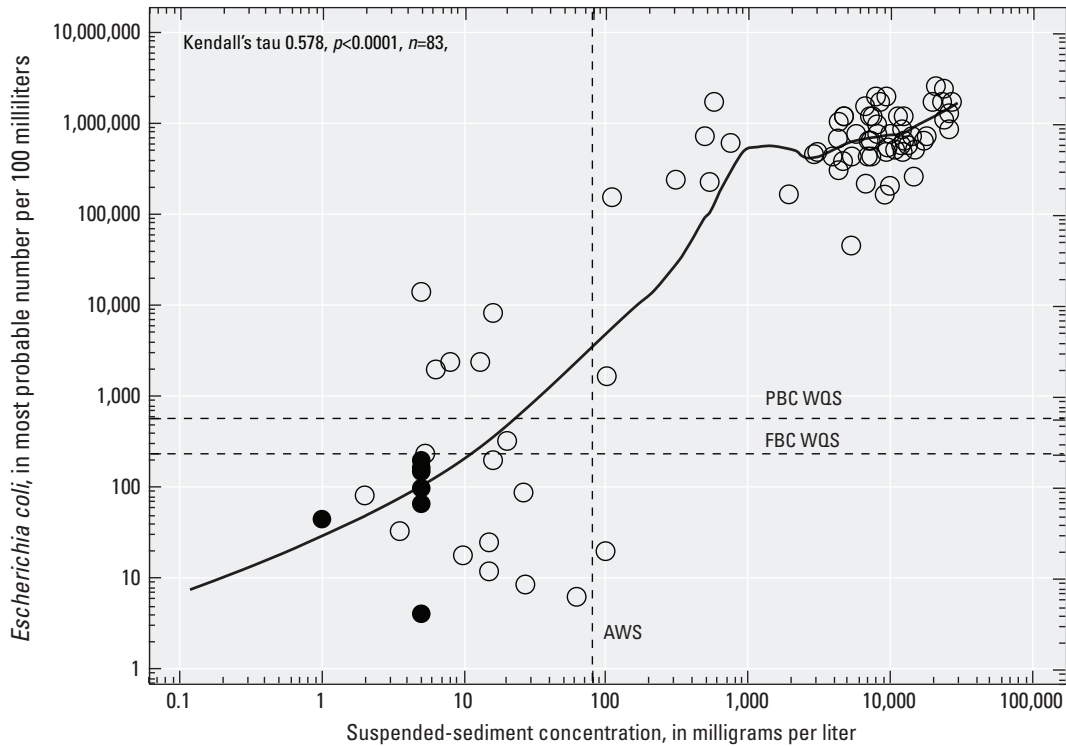
Figure 14. Graphs showing relations of *Escherichia coli* to suspended sediment and turbidity for watershed division 2 of the Upper Santa Cruz River Watershed, southern Arizona and northern Mexico. A locally weighted scatterplot smoothing (LOWESS) was used to fit the relations and Kendall's tau and probability (p) are presented for significant relations. n, sample size. FBC WQS, full-body-contact water-quality standard; PBC WQS, partial-body-contact water-quality standard; AWS, Arizona warm-water aquatic wildlife standard.

EXPLANATION

●   Below the laboratory minimum dectection limit, suspended sediment on the top and *E. coli* on the bottom

———   LOWESS smoothing fit, coefficient of determination=0.83 (top) and 0.35 (bottom)
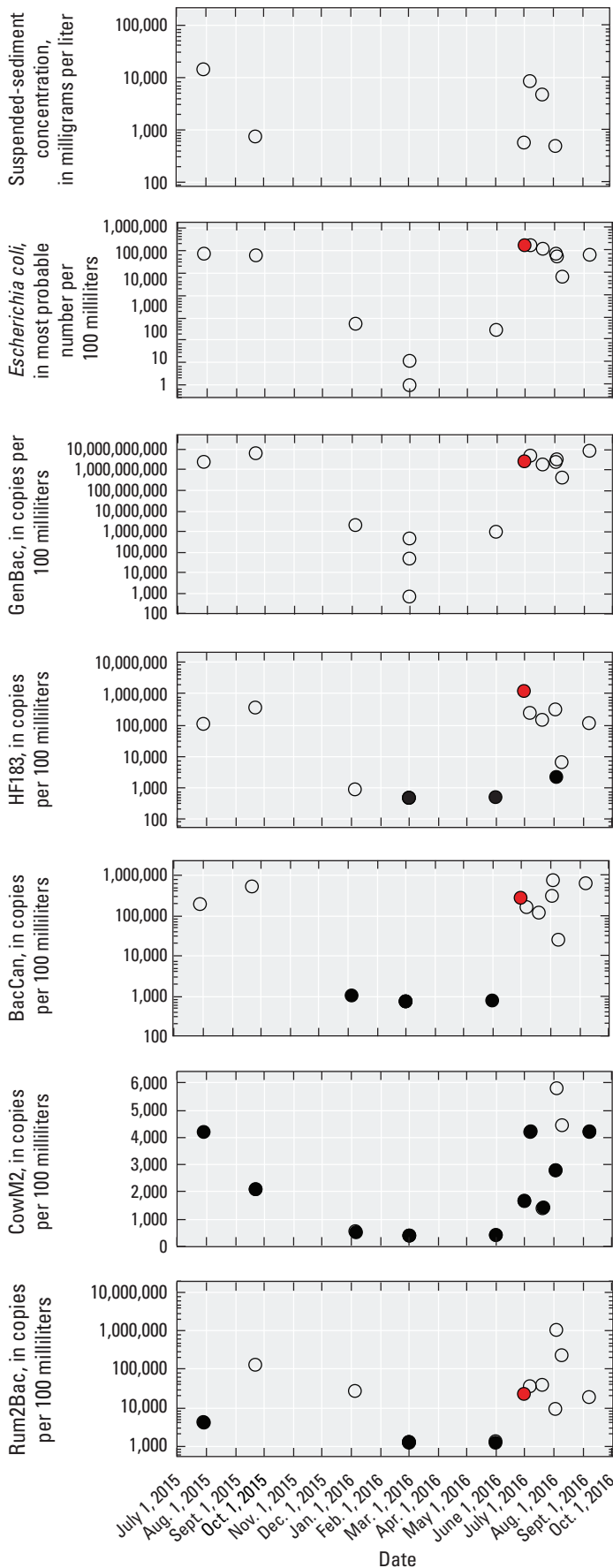
varied as much as four orders of magnitude, suggesting that other variables factor into this relation. Factors may include, but are not limited to, leaking septic tanks, sewer pipes, and latrines with limited containment of human waste (Norman and others, 2012).

The MST marker concentrations in WD2 followed patterns similar to those characterized by seasonal flow conditions described previously (fig. 15), and flooding samples have marker concentrations several fold to several orders of magnitude greater than base-flow samples. Samples collected between years were similar, although different flow conditions were sampled during the 2016 monsoon as compared to 2015 monsoon. The first large flood of the 2016 season (June 30) had the only surface-water detection of the human polyomavirus marker, a marker for human sewage. This was likely related to the first seasonal flush of the drainage and the potential accumulation of contaminants from the winter and spring. The human marker (HF183) was more frequently detected above the reporting limit than the cattle marker (CowM2), although the ruminant marker (Rum2Bac) was detected as frequently. These results indicate multiple sources of fecal contamination influencing water quality in WD2.

EXPLANATION

● Sample below the minimum reporting limit

● Only surface water-sample with a human polyomavirus detection
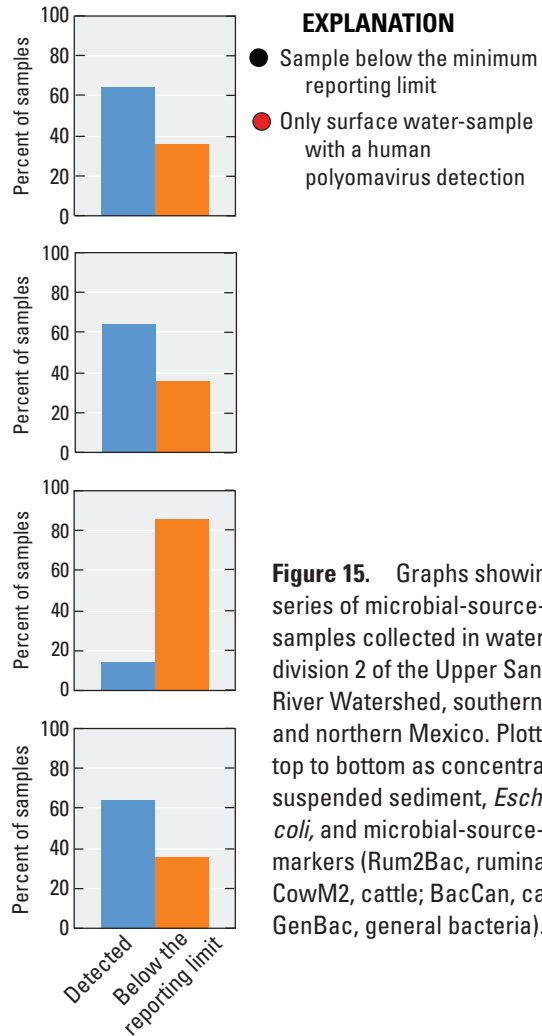
Figure 15.   Graphs showing times series of microbial-source-tracking samples collected in watershed division 2 of the Upper Santa Cruz River Watershed, southern Arizona and northern Mexico. Plotted from top to bottom as concentrations of suspended sediment, *Escherichia coli,* and microbial-source-tracking markers (Rum2Bac, ruminant animal; CowM2, cattle; BacCan, canine; GenBac, general bacteria).

Hydrologic Characterization of *E. coli* and Suspended Sediment

During flooding, sediment-associated bacteria are suspended into the water column, elevating *E. coli* concentrations in the flow. *E. coli* adsorption to fine sediments and increasing relation to suspended sediment is well documented and generally explained or modeled using measurements of turbidity as a proxy for suspended sediment, because of ease and low-cost of collection (Pandey and Soupir, 2014; Murphy and others, 2016; Lawrence, 2012; Rasmussen and others, 2008; Rasmussen and others, 2005). The fate of *E. coli* in surface-water systems is governed by multiple physical, chemical, and biological factors. Often the relations between *E. coli* and suspended sediment, discharge, and turbidity can be explained as a linear function, but in many circumstances these relations are far more complex and require multiple water-quality parameters or more sophisticated modeling techniques.

The WD2 *E. coli* and discharge relation was similar to the *E. coli* and suspended-sediment relation. Below 10 ft³/s the relation was highly variable, and at higher discharge the suspended-sediment and *E. coli* levels plateaued, meaning a slope break occurred about 100 ft³/s (fig. 16). This pattern is in part related to hysteresis, meaning that much of the variability

in the discharge-concentration relation was caused by instantaneous measures collected on the rising and recession limbs of the hydrograph. Hysteresis can manifest in several relation types and typically loop in a clockwise, counter clockwise, or crossover loop depending if the peak of the concentration leads or lags the peak of the discharge hydrograph (Miller and Orbock Miller; 2007; Nistor and Church, 2005; Williams, 1989; Hickin, 1989).

To better define the response of *E. coli* and suspended-sediment levels to different hydrologic conditions, several base-flow and flooding events were sampled at higher frequency and measured at multiple points during the event (figs. 17*A*, *B*, *C*, and *D*). Results from these sampling events revealed the peak maximum and the rate of change from low to high concentrations during the event duration. During the three 24-hour base-flow conditions, *E. coli* concentrations varied one to two orders of magnitude depending on the season and stage, although season and stage did not appear to always explain the randomness in the *E. coli* concentration magnitude (fig. 17*A*). Several flooding events were sampled in July, August, and September (figs. 17*B*, *C*, and *D*). The duration of the July and August events was generally a few hours, whereas the duration of the September floods was about 12 hours. During the rapid rise of the hydrograph, an hour or less, there was

EXPLANATION

△ Discharge estimated

● Sample below the laboratory minimum reporting limit

— LOWESS smoothing fit, coefficient of determination=0.78
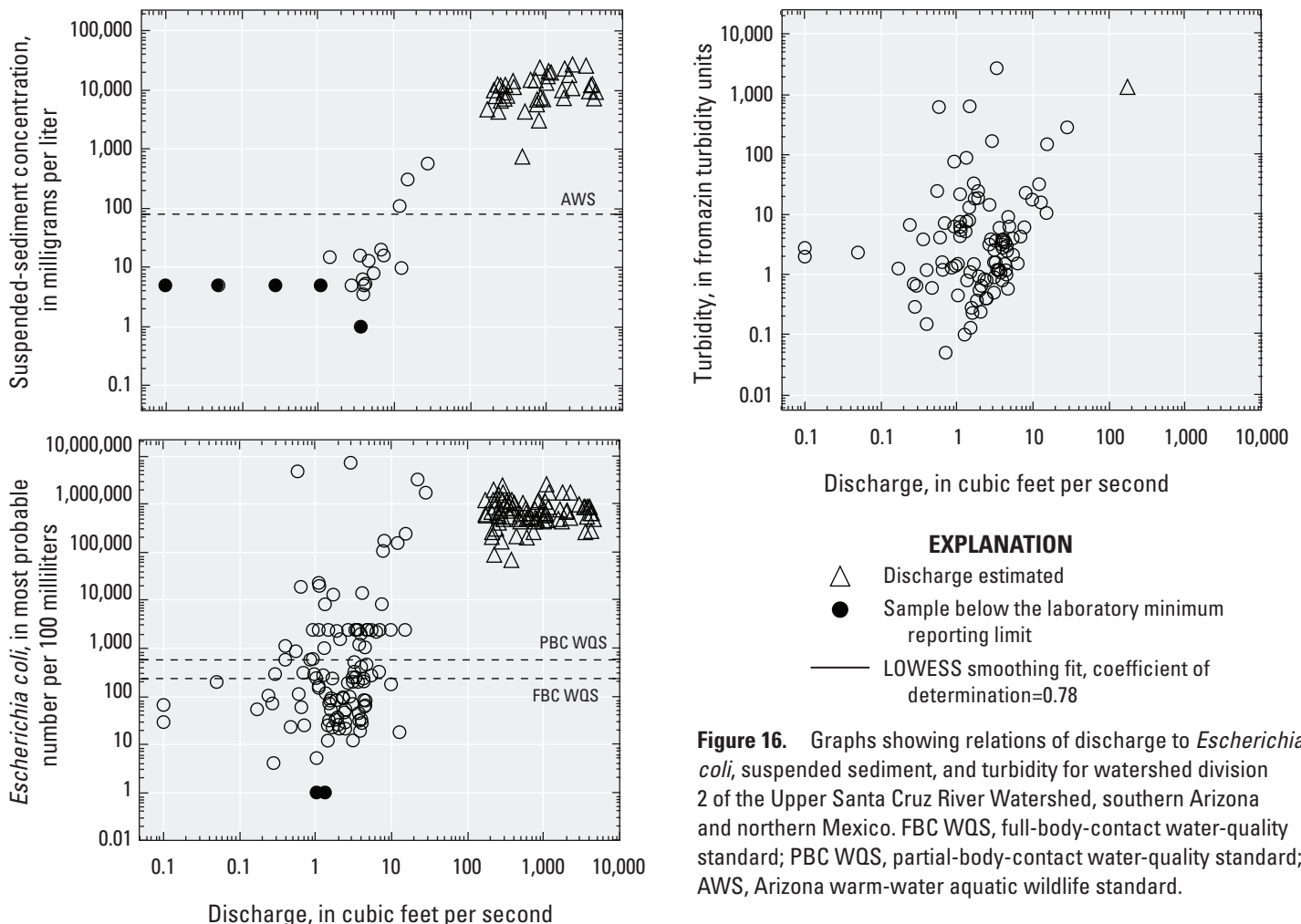
Figure 16. Graphs showing relations of discharge to *Escherichia coli*, suspended sediment, and turbidity for watershed division 2 of the Upper Santa Cruz River Watershed, southern Arizona and northern Mexico. FBC WQS, full-body-contact water-quality standard; PBC WQS, partial-body-contact water-quality standard; AWS, Arizona warm-water aquatic wildlife standard.
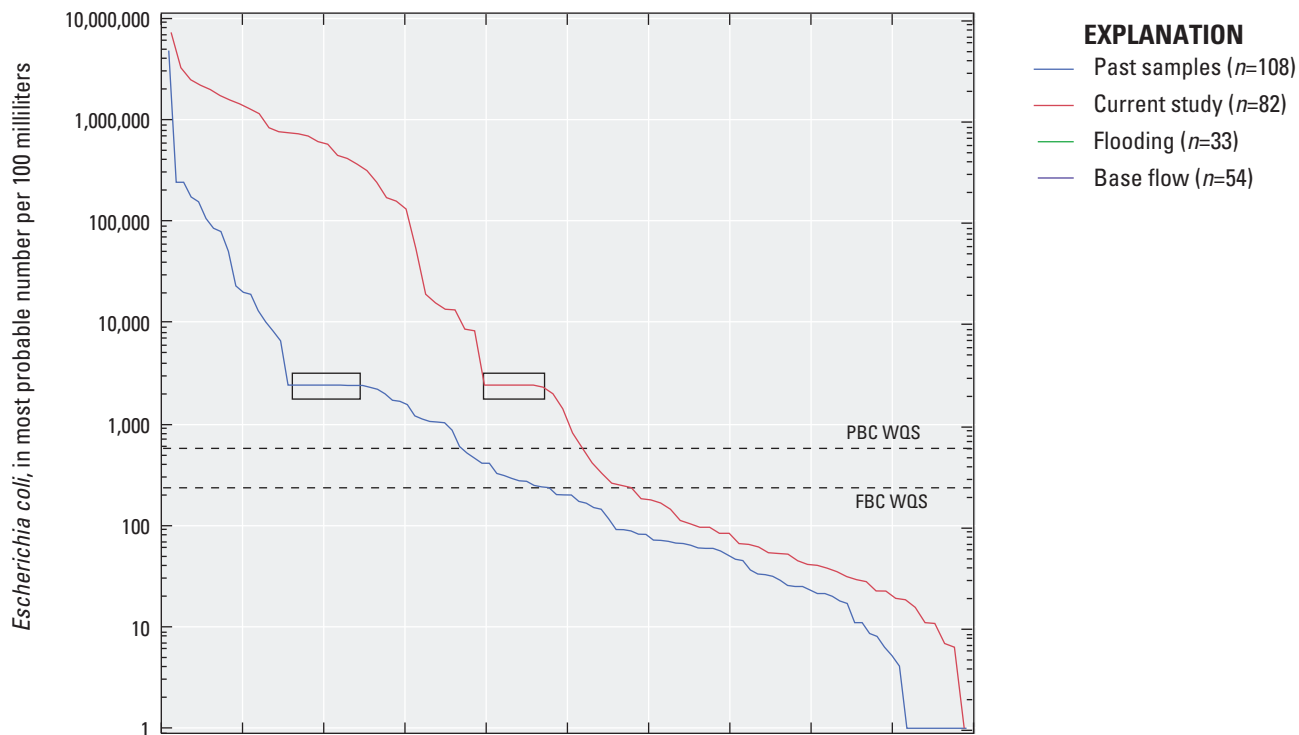
Figure 17. (pages 36–38) Hydrographs of stage plotted with *Escherichia coli* and suspended sediment as 15-minute data for Nogales Wash (NW 8) in watershed division 2 of the Upper Santa Cruz River Watershed, southern Arizona and northern Mexico. Identical reference graphs are provided showing the time period of the study and annotating each graph in *A–D* by number. *A,* Reference graph for *A* and *B* and graphs for 24-hour automatic sampler collections for 2016 spring, summer, and winter (1, 2, and 3). *B,* Graphs for July (4, 5, and 6). *C,* Reference graph for *C* and *D* and graphs for the August monsoon for 2015 and 2016 (7, 8, and 9). *D,* Graphs for the September monsoon for 2015 and 2016 (10 and 11). For detailed explanation of stations NW4 and NW8 see table 1. FBC WQS, full-body-contact water-quality standard; PBC WQS, partial-body-contact water-quality standard.

Figure 17. (pages 36–38)   —Continued

Figure 17.(pages 36–38) Hydrographs of stage plotted with *Escherichia coli* and suspended sediment as 15-minute data for Nogales Wash (NW 8) in watershed division 2 of the Upper Santa Cruz River Watershed, southern Arizona and northern Mexico. Identical reference graphs are provided showing the time period of the study and annotating each graph in *A*–*D* by number. *A*, Reference graph for *A* and *B* and graphs for 24-hour automatic sampler collections for 2016 spring, summer, and winter (1, 2, and 3); *B*, Graphs for July (4, 5, and 6), *C*, Reference graph for *C* and *D* and graphs for the August monsoon for 2015 and 2016 (7, 8, and 9); *D*, Graphs for the September monsoon for 2015 and 2016 (10 and 11). For detailed explanation of stations NW4 and NW8 see table 1. FBC WQS, full-body-contact water-quality standard; PBC WQS, partial-body-contact water-quality standard.—Continued

an increase of as much as an order of magnitude for both *E. coli* and suspended sediment. The concentration recession was also rapid, often at a rate similar to the rise. The inconsistent timing of the arrival of the peak *E. coli* concentration likely contributed to the hysteresis pattern observed in the *E. coli* and discharge relation. Consecutive floods in August 2016 showed the peak of concentration leading the flood peak. However, the peak concentration shifted closer in time to the flood peak during subsequent flood pulses during a season. The September 2015 and 2016 precipitation events caused widespread runoff resulting in multiple discharge peaks at the streamgage. The *E. coli* concentration peaks appeared to lead many of the discharge peaks, whereas suspended sediment appeared to slightly lag the discharge peak. During the September events, *E. coli* and suspended-sediment concentrations did not directly correlate with the discharge hydrograph, and peak concentrations occurred at times outside of the flood peak, possibly indicating additional inputs from tributary sources that had previously not flowed yet in the season.

Using the most general of classifications—base flow versus flooding—we found that significantly greater concentrations of *E. coli* and turbidity occurred during flooding conditions (fig. 18*A*). Flooding levels were several orders of magnitude greater than base-flow levels for *E. coli*, suspended sediment, and turbidity. The distinction between flooding and base flow provides little information about the discharge relation and the quantity of flow necessary to elevate *E. coli* concentrations. Discharge information was used to group samples by flow thresholds developed from long-term daily streamgage data, hereafter referred to flow-condition classes (table 3, available for download at https://doi.org/10.3133/sir20195108; fig. 4; see "Hydrological Characterization" in the "Methods" section). Samples collected with or near a discharge measurement were assigned one of six flow condition classes. The quantitively determined flow condition classes were given general names (very low flow, low flow, medium flow, high flow, and very high flow) to more easily distinguish between classes. Season was also an important factor for samples collected during flows below 4 ft^3/s; specifically, summer samples were statistically different from other samples and a separate group (summer low flow) was created to investigate this seasonal low-flow hydrology further.

There were several differences in flow-condition classes for *E. coli,* suspended sediment, and turbidity. Similar to the flooding and baseflow comparison, samples grouped in the two highest classes (greater than 75 ft^3/s and 75–9.5 ft^3/s, respectively) were similar and both significantly greater than the medium (3.9 to 9.1 ft^3/s), low-flow (2.2 to 3.9 ft^3/s), and very low-flow classes (less than 2.2 ft^3/s). The medium-flow class appeared to represent an important threshold range for when discharge between 4 and 10 ft^3/s might exceed the *E. coli* WQS values. The summer low-flow class was significantly greater than the undifferentiated low-flow class, and the median concentration was greater than the medium-flow class. Similar to the medium-flow condition class, this summer low-flow class is an important range of seasonal discharges which require additional investigation, as it also highlights the importance of considering both season and hydrology when analyzing patterns of *E. coli* concentrations.

The event-hydrograph instantaneous-discharge classifications (rise, peak, and recession) showed that during flooding the rise of the peak and the peak itself have the greatest concentrations of *E. coli* and suspended sediment (fig. 18*B*). Also, the flooding rise, peak, and recession had less variability (lower interquartile range) of *E. coli* sample distribution compared to the base-flow samples. Defining the event-hydrograph features of a base flow was not as straightforward as a flood peak and likely contributed to the variability. Defining the rise and recession of the base-flow hydrograph was generally more straightforward than identifying the peak because of the inconsistent upstream flow contributions. The recession was significantly greater in *E. coli* concentrations than that of the rise of the hydrograph.

E. coli and Suspended-Sediment Flux

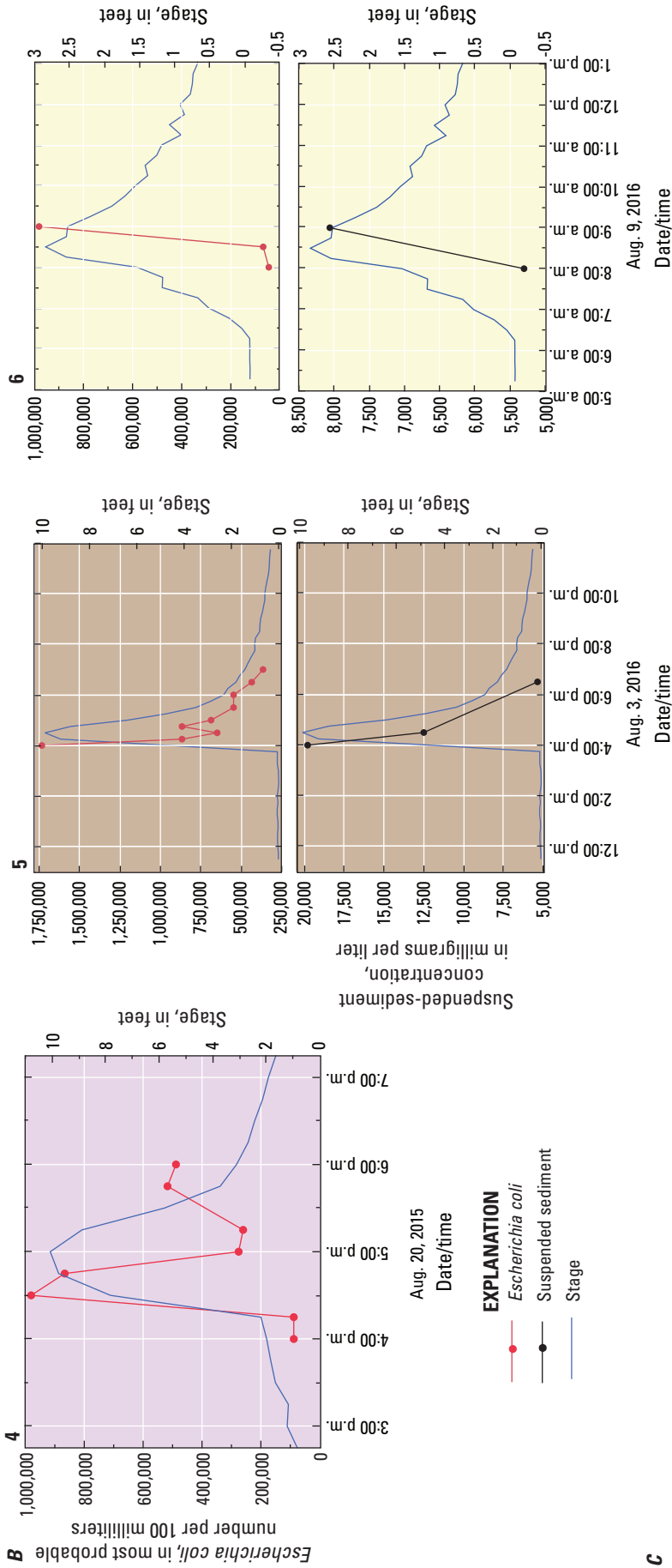The distance between the streamgage at NW4 and the stage sensor at NW8 is about 7 miles, and the channel has been straightened and armored in sections of this reach. At NW4, the USGS has measured average velocities between 8 and 9 ft/s and computed discharges between 300 and 400 ft^3/s for this velocity range. The high velocities in these channel conditions during flooding minimize channel losses to infiltration, and velocities are generally maintained throughout this stream section. This was observed during the study where a time series lag of 1 to 2 hours was computed for most flow events between NW4 and NW8. For discharges above 200 ft^3/s, the lag time was consistently 1 hour.

Note that several tributaries enter Nogales Wash between NW4 and NW8. The four largest contributing watersheds are Las Canoas-Ephraim Wash (6.3 mi^2), Mariposa Canyon Wash (13.2 mi^2), Portrero Canyon Wash (14.0 mi^2), and Calabasas Canyon Wash (7.5 mi^2). Some of these tributaries have wetlands and gravel pits that may attenuate part or most of the volume of water depending on the precipitation and type of runoff. There are stage and precipitation sensors located on Las Canoas-Ephraim Wash and Portrero Creek Wash, as well as in Calabasas Canyon Wash. These tributaries are a recognized source of uncertainty not quantified in the following approach to estimate discharge for flooding events at NW8. However, the data from the sensors in these tributaries listed above, as well as sensors on nearby downstream tributaries, suggest that the west-side tributaries of the drainage flowed infrequently during the study period.

Streamgage NW4 is located in a trapezoidal concrete-lined channel, and both NW4 and NW8 locations have bridges and embankments providing a stable control for discharge. As a means to estimate loading, the discharge was estimated for stage that exceeded 2 ft at NW8 (fig. 19*A*). This stage reflects a bank-to-bank depth and correlated well with flow greater
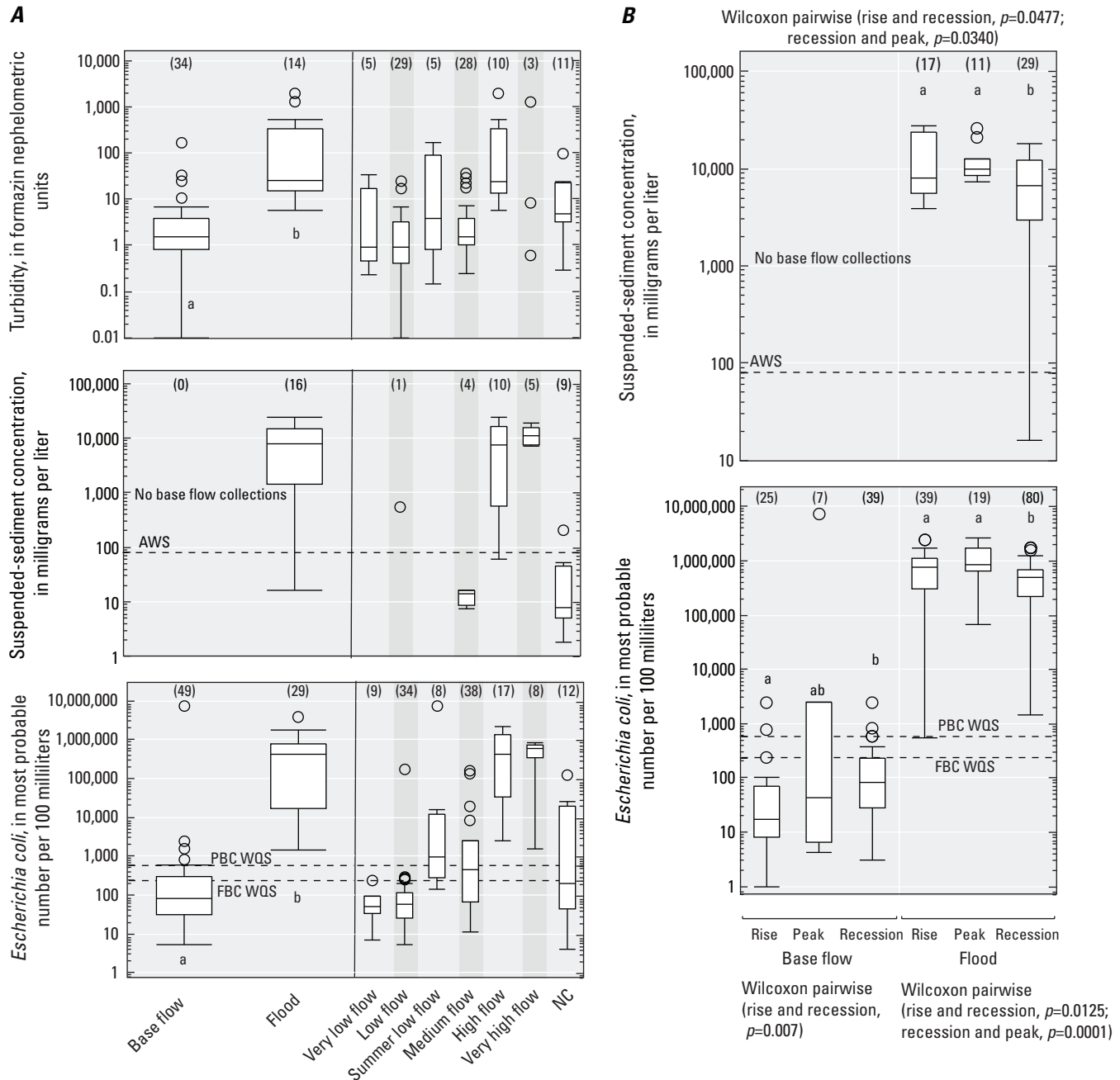
A

B

EXPLANATION

(4)   **Number of values**

Outside value—Value is >1.5 and <3 times the interquartile range beyond either end of the box

Largest value within 1.5 times interquartile range above 75th percentile
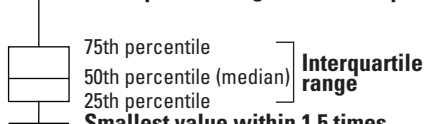
75th percentile
50th percentile (median)   **Interquartile range**
25th percentile
Smallest value within 1.5 times interquartile range below 25th percentile

△   Discharge estimated

●   Below the minimum reporting limit

a, b, or ab denotes statistical difference; when letters are the same, groups are not significantly different

Figure 18.   Boxplots of water-quality parameters and *Escherichia coli* concentrations and related sediment parameters for watershed division 2 of the Upper Santa Cruz River Watershed, southern Arizona and northern Mexico. *A*, Boxplots of daily mean *Escherichia coli*, suspended sediment, and turbidity plotted by base flow and flood conditions (left) and by flow-condition categories (right). *B*, Boxplots of 15-minute turbidity, *Escherichia coli,* and suspended sediment plotted by hydrograph classification grouped by base flow and flood conditions. Significant Wilcoxon pairwise tests are labeled with letters indicating significant differences between hydrologic condition distributions. FBC WQS, full-body-contact water-quality standard; PBC WQS, partial-body-contact water-quality standard; AWS, Arizona warm-water aquatic wildlife standard; NC, not counted.
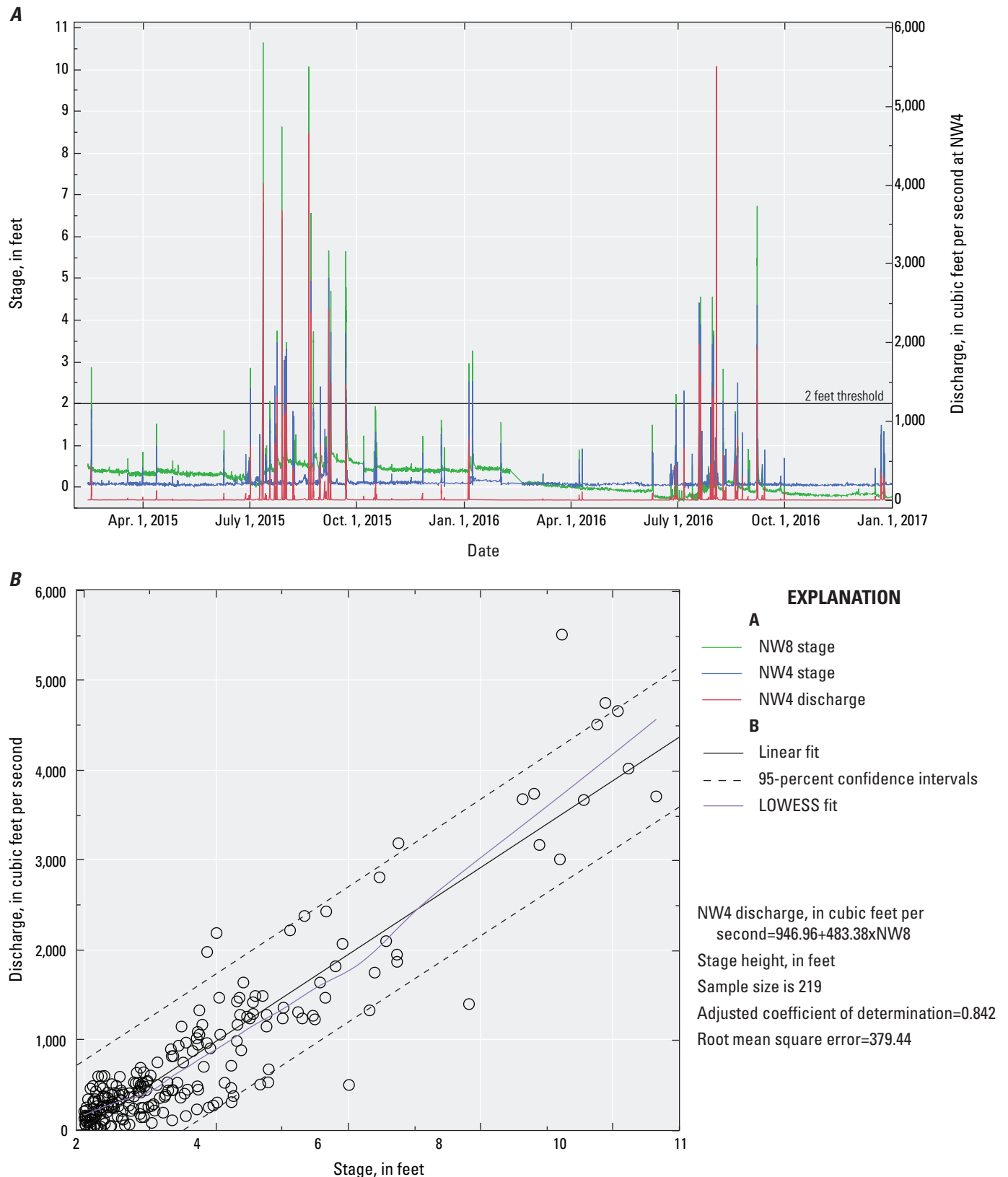
Figure 19.   Graphs showing time series of stream discharge and water stage for Nogales Wash (NW) in watershed division 2 of the Upper Santa Cruz River Watershed, southern Arizona and northern Mexico. *A*, Times series of streamgage NW4 discharge, 1-hour time-lag adjusted NW4 water stage, and 1-hour time-lag adjusted NW8 water stage; a water stage threshold is labeled at 2 feet. *B*, Ordinary least squares regression analysis between water 1-hour time-lag adjusted NW8 water stage and NW4 discharge. For detailed descriptions of station/sample locations see table 1.

than 200 ft³/s at NW4. Hysteresis effects between sensors were also minimized. Stage was adjusted using the 1-hour lag time computed in a time series analysis. In a few instances, the upstream and downstream hydrographs did not exactly match due to the application of a constant lag to unit-value data (15 minute). For example, the increase of the hydrograph may have occurred over two 15-minute recordings upstream, whereas downstream three 15-minute recordings represented the same unit of increased discharge that was measured upstream. This lag mismatch in the relation did introduce a few erroneous data pair points into the stage-discharge model between gages. A locally weighted scatterplot smoothing (LOWESS) model was developed to estimate discharge at NW8 because the nonlinear fit of the LOWESS better fit the observed data (fig. 19B). Although the ordinary least squares regression provided similar results, the LOWESS model provided a slightly better fit at the low and high end of the regression fit and this equation was used to estimate the discharges at NW8.

Concentrations at all locations that had associated discharge measurements were converted into flux (figs. 20A, B). The instantaneous discharge used mass-flux calculations converted to a daily equivalent because mean daily discharge was not available for most samples (that is, very few samples were collected at NW4). Except for the increased flood sampling during the study, similar patterns were observed for most of the study period. Flood samples were about 3 to 5 orders of magnitude greater in E. coli and suspended sediment. E. coli flux estimates were similar to sewer contamination related to IOI releases. This could indicate that inputs from the IOI often occur during flooding, because damage to sewer infrastructure is frequently documented during flooding. In late June of 2016 and late July of 2017, base flow was contaminated by a nonregulated release from the IOI inflow pipe, and the measured discharge along with the high concentrations resulted in daily flux estimates comparable to flooding events. The ADEQ monitored the July 2017 IOI breach for several days, but the one measured discharge equaled an E. coli flux of 2.03×10^{10} MPN/s, and with the breach lasting multiple days, the volume of contaminated water introduced to the upper part of the watershed was immense.

Summary

Nogales Wash is the largest actively contributing tributary in the Upper Santa Cruz River Watershed, and it is the principle drainage channel for the area of Ambos Nogales. Most precipitation events resulted in intense runoff due to the highly urbanized and impervious area in WD2. Multiple large flooding events during the study caused damage to infrastructure and resulted in repeated failures of the IOI. This allowed the direct input of untreated sewage into Nogales Wash, and water concentrations of E. coli were the highest measured during the study, in the millions of MPN/100 mL. On average, E. coli samples exceeded the FBC WQS 58 percent of the time and the PBC WQS 48 percent of the time, although all samples collected during flooding conditions exceeded both WQS thresholds. E. coli concentrations were correlated with suspended sediment and turbidity, but regression relations were highly variable and the variance may be related to E. coli sources unrelated to increased flow, such as leaking septic tanks or failing sewer infrastructure. The MST human marker was more frequently detected than the cattle marker and at the highest concentrations observed during the study. The ruminant marker was also detected frequently, but more often at lower concentrations than those observed in other WDs. Overall the multiple marker detection suggests several different sources of E. coli, and the contributions of different markers are likely affected by season. The summer season was also shown to influence E. coli by elevating concentrations above WQS thresholds for samples collected during low flow. The concentrations in the medium flow-condition class were also elevated and appeared to represent a range of flow conditions that would have a greater likelihood of E. coli WQS exceedances. These lower discharge flow-condition classes potentially represent an important hydrologic threshold and highlight the importance of considering both season and hydrology when investigating the timing of E. coli exceedances. Classifying samples by discharge provides more descriptive information and, depending on the monitoring design, a more objective approach to quantifying exceedances.

The high frequency of sampling at multiple points along the hydrograph of multiple floods demonstrated that within hours of the flood initiation there was an increase of several orders of magnitude in the concentrations of E. coli and suspended sediment. Samples collected on the rise of the peak and the peak itself have the greatest concentrations of E. coli and suspended sediment compared to the recession. The rising limb of the peak was shown to represent a potential maximum of the contaminant transported downstream, and it might be best for future studies to consider collection timing in terms of characterizing contaminant concentration and flux. During 24-hour base-flow collections, E. coli concentrations were quite variable, seemingly unrelated to discharge, and at times peaked above WQS thresholds. Again, this could potentially be related to leaking septic tanks or failing sewer infrastructure, and additional investigation would be needed to identify these sources.

Discharge and flux were estimated for high flows at NW8 using a relation developed from the upstream NW4 streamgage. The flux estimates determined for multiple flood samples in WD2 were the largest for the period of record. However, additional on-site discharge measurements need to be collected to verify the magnitude of these of E. coli and suspended-sediment flux estimates reported in this study. The intensity and rapidness of runoff in WD2 makes it logistically difficult to assemble resources necessary to measure floods in the urban setting, and the use of more streamgages and alternative estimation techniques for quantifying the contaminants moving downstream might best be considered. Overall, the frequency of flooding during certain periods of the year and connection to the main Santa Cruz River allow for large volumes of E. coli and suspended sediment to flow downstream through TUMA.
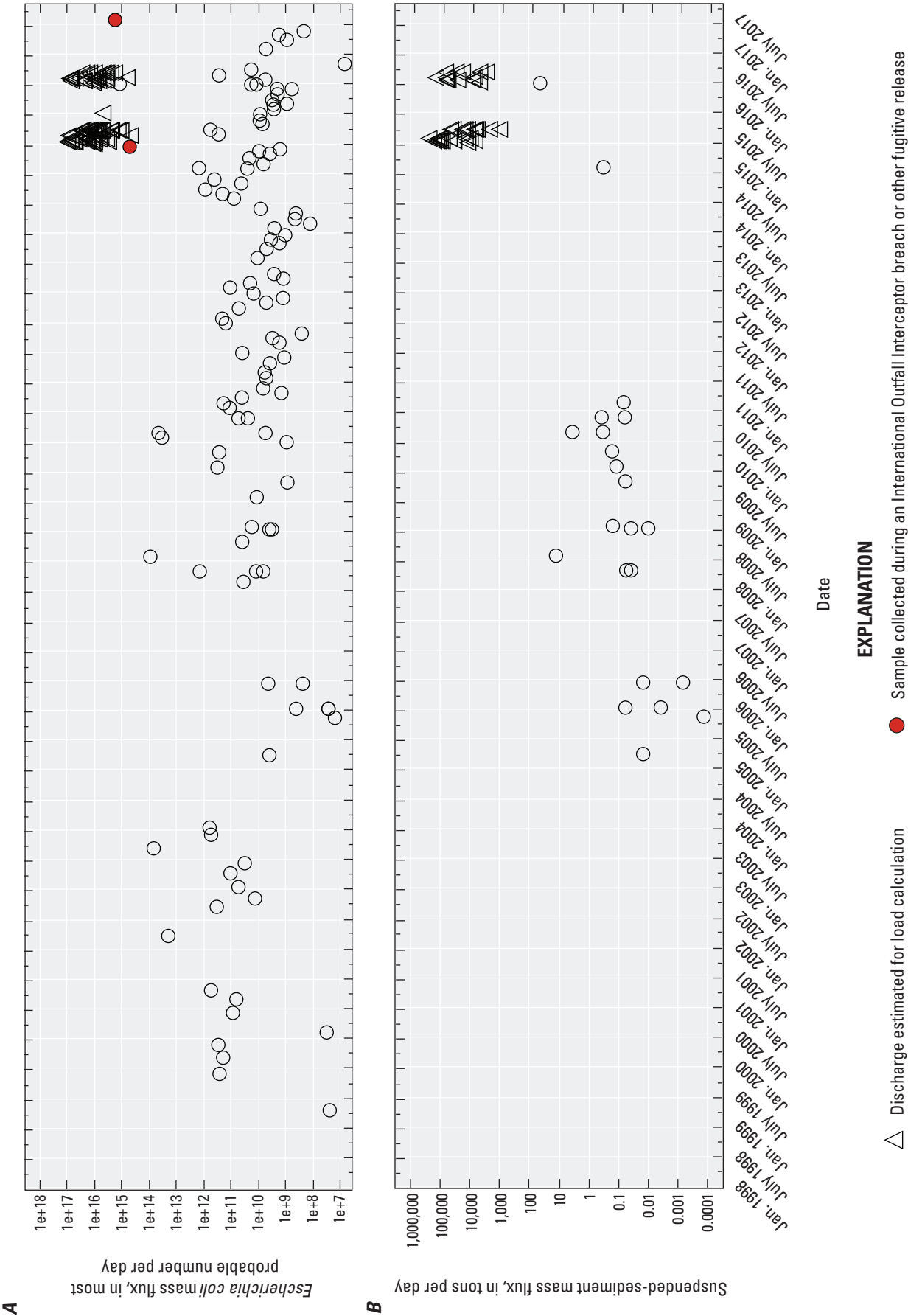
Figure 20. Graphs showing mean daily mass-flux time series over the entire period of record for watershed division 2 of the Upper Santa Cruz River Watershed, southern Arizona and northern Mexico. *A*, *Escherichia coli*; *B*, suspended sediment.

Watershed Division 3 (WD3)—Nogales International Wastewater Treatment Plant to Santa Cruz River at Palo Parado Bridge, As Well As the Tributaries of Peck Canyon Wash, Agua Fria Canyon Wash, Sonoita Creek, and Josephine Canyon Wash

WD3 is defined as the area from the NIWTP to Santa Cruz River at Palo Parado Bridge, as well as the tributaries of Peck Canyon Wash, Agua Fria Canyon Wash, Sonoita Creek, and Josephine Canyon Wash (fig. 21). The NIWTP provides sewage treatment for 14.74 million gallons of wastewater per day for Ambos Nogales. Nogales, Sonora, provides about 70 percent of the flow and load to the plant (Stantec, 2017). Different standards for regulating industrial discharges on both sides of the border create operational, maintenance, and regulatory challenges for IBWC, particularly with respect to its Arizona Pollutant Discharge Elimination System permit and management of biosolids (Huth, 2015). The ADEQ lists this reach of the river for exceedances in *E. coli* and cadmium, but in previous assessments ammonia, low dissolved oxygen, and other metals were listed (Arizona Department of Environmental Quality, 2015). Because the treatment facilities at NIWTP were upgraded in 2009, there was reduction in nutrient concentrations—most significantly for un-ionized ammonia—in the Santa Cruz River. Reductions in chlorine and a microbial clogging layer or "schmutzdecke" on the surface of the streambed were also observed along with increases in dissolved oxygen and fish abundances (Sonoran Institute, 2016; Tetra Tech, 2013; Treese and others, 2009). Once the upgrade was fully implemented, *E. coli* concentrations were consistently measured below the detection limit near the outfall.

Upstream and adjacent to the NIWTP outfall, the active Santa Cruz River channel is dry (fig. 21*A*). The NIWTP outfall, where the perennial source of water for the Santa Cruz River begins, is located slightly west of this dry active channel (fig. 21*B*). The treated perennial wastewater joins a branch of the active Santa Cruz River channel about 1,100 ft northwest of the NIWTP outfall, shortly after passing under a railroad bridge. Discussed previously in the WD1 section, the USGS established a stage sensor (SC5) in the dry channel just upstream of the railroad bridge to understand the frequency of connection from the upper Santa Cruz and Nogales Wash to WD3. WD3 is more complex than the other three divisions because of several major ephemeral tributaries that enter the Santa Cruz River here. In addition, concentrated within the historical floodplain are urbanization and grazing activities, all of which contribute to the variability in water quality.

Water-stage sensors were deployed or already existed at Sonoita Creek (SON1 and SON2, figs. 27*C*, *D*), Agua Fria Canyon Wash (AF1, fig. 27*J*, and AF2, figs. 27*H*, *I*), Peck Canyon Wash (PC1, figs. 27*K*, *L*), and Josephine Canyon Wash (JC1, figs. 27*O*, *P*). The Flood Control District of Santa Cruz County operates a radar sensor and precipitation gage at the Palo Parado Bridge crossing of the Santa Cruz River (SC9, figs. 27*M*, *N*). Other sample locations include the NIWTP outfall (SC6), just downstream of the outfall (SC7), and the Santa Cruz River at the Rio Rico Bridge (SC8, figs. 27*F*, *G*). Five rain gages are located in this watershed division—P10, P11, P12, P13, and PNIWTP (table 2, available for download at https://doi.org/10.3133/sir20195108). Josephine Canyon Wash experienced a large flood on September 21, 2015, and it was sampled for *E. coli* and suspended sediment; however, discharge was not measured. On September 30, 2015, the high watermarks were identified and the channel was surveyed. An indirect measure was computed using methods described in Bradley (2012). The estimated peak discharge for that event was 1,050 ft^3/s.

Grazing activities are prominent in WD3, and cattle have direct access to the Santa Cruz River from above the NIWTP outfall to areas near the Palo Parado Bridge crossing. Agricultural land-use activity is about 3.5 percent, which is the greatest of all the WDs, and the developed area is about 6 percent. The contributing ephemeral watersheds have less than 1 percent of agricultural land use, but Sonoita Creek and Agua Fria Canyon Wash have developed land-use densities of about 2.5 and 3.0 percent, respectively.

Figure 21 (pages 45–48).   Maps and photographs of watershed division 3 of the Upper Santa Cruz River Watershed, southern Arizona and northern Mexico. *A*, Map showing the Sonoita Creek, Josephine Canyon Wash, and Middle Santa Cruz River Watersheds and sample locations in watershed division 3 (for detailed descriptions of station/sample locations see table 1). Land-use classes are shown in percent in the pie charts; sample locations and other hydrologic sites are annotated—SC, Santa Cruz River; P, precipitation stations; NW, Nogales Wash; AF, Agua Fria; SON, Sonoita Creek; JC, Josephine Canyon Wash. *B–I*, Photographs of this part of watershed division 3 and station/sample locations. *B*, SC6, Nogales International Wastewater Treatment Plant Outfall, NIWTPO, looking southeast (U.S. Geological Survey, USGS photograph, December 9, 2016); *C*, NIWTPO looking south (USGS, December 9, 2016); *D*, SON2 looking west and downstream (USGS, April 4, 2017); *E*, SON2 flooding looking northwest and downstream (USGS, August 9, 2016); *F*, SC8 base flow upstream of Rio Rico Bridge looking east (USGS, January 20, 2015); *G*, SC8 recent flood looking upstream and south, downstream of bridge (USGS, February 2, 2015); *H*, AF2, under the bridge looking downstream and east (USGS, April 4, 2017); *I*, AF2 flooding is moving left and downstream looking south (USGS, September 9, 2016). *J*, Map showing Agua Fria and Peck Canyon Wash Watersheds in watershed division 3. *K–P*, Photographs of this part of watershed division 3 and station/sample locations. *K*, PC1 looking north downstream of bridge (USGS, January 20, 2015); *L*, PC1 flood looking north and downstream of bridge (USGS, July 1, 2015); *M*, SC9 base flow looking northwest (USGS, February 12, 2015); *N*, SC9 flooding looking west (USGS, August 9, 2016); *O*, JC1 looking northeast (USGS January 20, 2015); *P*, JC1 flood looking northwest (USGS, September 21, 2015).

A

EXPLANATION

Land-use class

- No data
- Open water
- Developed
- Barren land (rock, sand, clay)
- Mixed forest
- Shrub
- Grassland
- Agriculture
- Wetlands

▲ **Streamgage**

▲ **Stage sensor**

▲ **Stage and sample location**

▲ **Sample location only**

● **Precipitation location**

── **Watershed boundary**

── **Watershed division boundary**

── **River**—Except for the Santa Cruz River, all stream channels are ephemeral or intermittent

Station abbreviations
Nogales Wash (NW)
Precipitation (P)
Santa Cruz River (SC)

Sources: Esri, DigitalGlobe, GeoEye, i-cubed, USDA, USGS, AEX, Getmapping, Aerogrid, IGN, IGP, swisstopo, and the GIS User Community
Land-use cover adapted from Norman, Villareal, and others, 2010

B

C

D

E

F

G

H

I

Figure 21 (pages 45–48).   Maps and photographs of watershed division 3 of the Upper Santa Cruz River Watershed, southern Arizona and northern Mexico. *A*, Map showing the Sonoita Creek, Josephine Canyon Wash, and Middle Santa Cruz River Watersheds and sample locations in watershed division 3 (for detailed descriptions of station/sample locations see table 1). Land-use classes are shown in percent in the pie charts; sample locations and other hydrologic sites are annotated—SC, Santa Cruz River; P, precipitation stations; NW, Nogales Wash; AF, Agua Fria; SON, Sonoita Creek; JC, Josephine Canyon Wash. *B–I*, Photographs of this part of watershed division 3 and station/sample locations. *B*, SC6, Nogales International Wastewater Treatment Plant Outfall, NIWTPO, looking southeast (U.S. Geological Survey, USGS photograph, December 9, 2016); *C*, NIWTPO looking south (USGS, December 9, 2016); *D*, SON2 looking west and downstream (USGS, April 4, 2017); *E*, SON2 flooding looking northwest and downstream (USGS, August 9, 2016); *F*, SC8 base flow upstream of Rio Rico Bridge looking east (USGS, January 20, 2015); *G*, SC8 recent flood looking upstream and south, downstream of bridge (USGS, February 2, 2015); *H*, AF2, under the bridge looking downstream and east (USGS, April 4, 2017); *I*, AF2 flooding is moving left and downstream looking south (USGS, September 9, 2016). *J*, Map showing Agua Fria and Peck Canyon Wash Watersheds in watershed division 3. *K–P*, Photographs of this part of watershed division 3 and station/sample locations. *K*, PC1 looking north downstream of bridge (USGS, January 20, 2015); *L*, PC1 flood looking north and downstream of bridge (USGS, July 1, 2015); *M*, SC9 base flow looking northwest (USGS, February 12, 2015); *N*, SC9 flooding looking west (USGS, August 9, 2016); *O*, JC1 looking northeast (USGS January 20, 2015); *P*, JC1 flood looking northwest (USGS, September 21, 2015).—Continued.

J

EXPLANATION

Land-use class

No data

Open water

Developed

Barren land
(rock, sand, clay)

Mixed forest

Shrub

Grassland

Agriculture

Wetlands

▲ **Streamgage**

▲ **Stage sensor**

▲ **Stage and sample location**

▲ **Sample location only**

● **Precipitation location**

━━ **Watershed boundary**

━━ **Watershed division
boundary**

━━ **River**—Except for the
Santa Cruz River, all
stream channels are
ephemeral
or intermittent

Station abbreviations
Nogales Wash (NW)
Precipitation (P)
Santa Cruz River (SC)

Peck Canyon Wash Watershed
Land-use class, in percent

Barren land 0.30
25.5
0.85
64.9
8.50
0.10 Agriculture

Agua Fria Canyon Wash Watershed
Land-use class, in percent

0.88
23.8
2.97
64.6
7.47
0.06 Agriculture

Watershed division 4

Peck Canyon Wash Watershed

Agua Fria Canyon Wash Watershed

Pena Blanca Lake

Infrequently contributing area upstream of Peña Blanca Lake

UNITED STATES
MEXICO

ARIZONA

● Phoenix

Tucson ●

■ Map area

Sources: Esri, DigitalGlobe, GeoEye, i-cubed, USDA, USGS, AEX, Getmapping,
Aerogrid, IGN, IGP, swisstopo, and the GIS User Community
Land-use cover adapted from Norman, Villareal, and others, 2010

0 1 2 3 4 5 MILES
0 1 2 3 4 5 KILOMETERS

Figure 21. (pages 45–48)   —Continued

K

L

M

N

O

P

Figure 21. (pages 45–48)   Maps and photographs of watershed division 3 of the Upper Santa Cruz River Watershed, southern Arizona and northern Mexico. *A*, Map showing the Sonoita Creek, Josephine Canyon Wash, and Middle Santa Cruz River Watersheds and sample locations in watershed division 3 (for detailed descriptions of station/sample locations see table 1). Land-use classes are shown in percent in the pie charts; sample locations and other hydrologic sites are annotated—SC, Santa Cruz River; P, precipitation stations; NW, Nogales Wash; AF, Agua Fria; SON, Sonoita Creek; JC, Josephine Canyon Wash. *B–I*, Photographs of this part of watershed division 3 and station/sample locations. *B*, SC6, Nogales International Wastewater Treatment Plant Outfall, NIWTPO, looking southeast (U.S. Geological Survey, USGS photograph, December 9, 2016); *C*, NIWTPO looking south (USGS, December 9, 2016); *D*, SON2 looking west and downstream (USGS, April 4, 2017); *E*, SON2 flooding looking northwest and downstream (USGS, August 9, 2016); *F*, SC8 base flow upstream of Rio Rico Bridge looking east (USGS, January 20, 2015); *G*, SC8 recent flood looking upstream and south, downstream of bridge (USGS, February 2, 2015); *H*, AF2, under the bridge looking downstream and east (USGS, April 4, 2017); *I*, AF2 flooding is moving left and downstream looking south (USGS, September 9, 2016). *J*, Map showing Agua Fria and Peck Canyon Wash Watersheds in watershed division 3. *K–P*, Photographs of this part of watershed division 3 and station/sample locations. *K*, PC1 looking north downstream of bridge (USGS, January 20, 2015); *L*, PC1 flood looking north and downstream of bridge (USGS, July 1, 2015); *M*, SC9 base flow looking northwest (USGS, February 12, 2015); *N*, SC9 flooding looking west (USGS, August 9, 2016); *O*, JC1 looking northeast (USGS January 20, 2015); *P*, JC1 flood looking northwest (USGS, September 21, 2015).—Continued
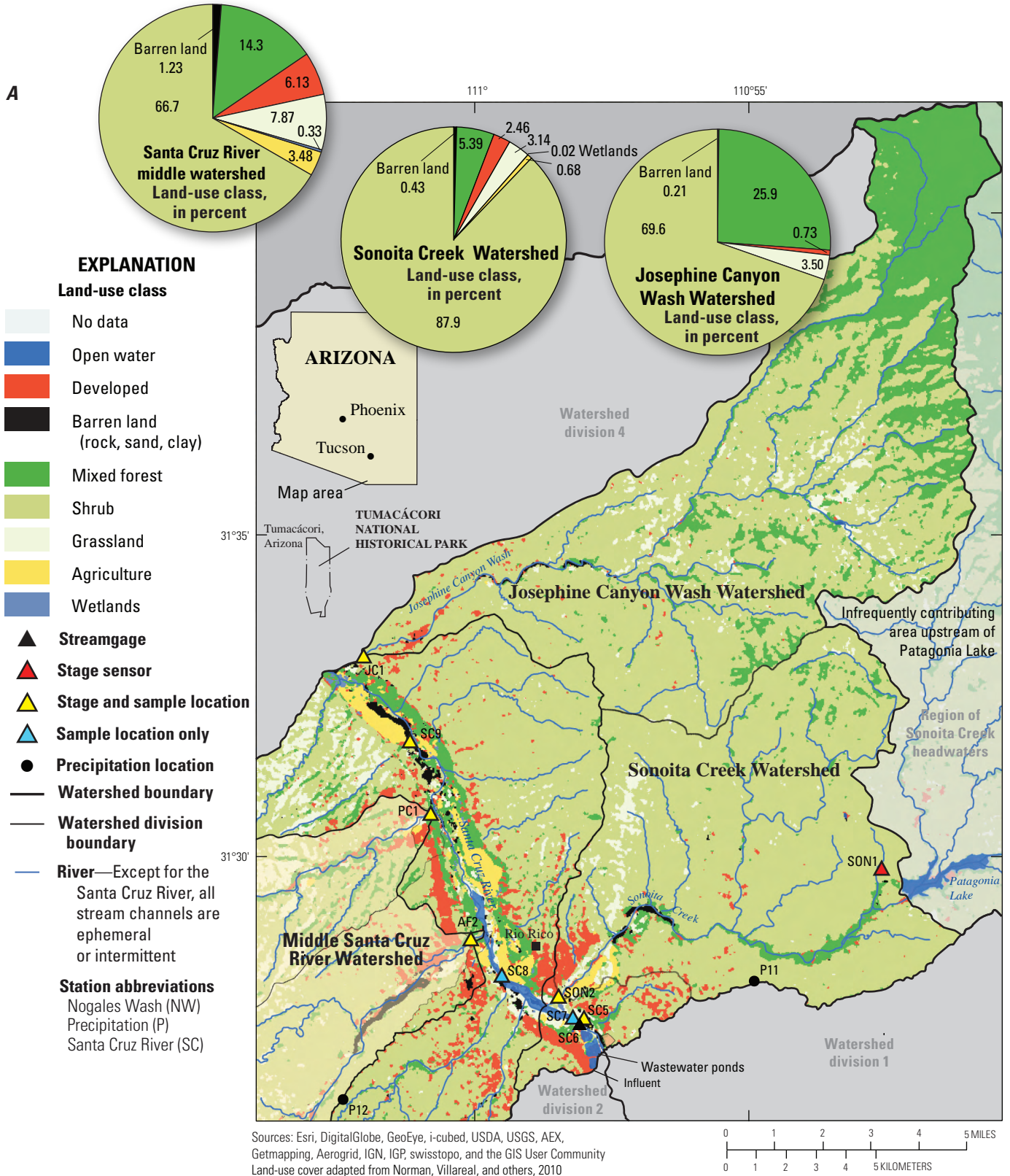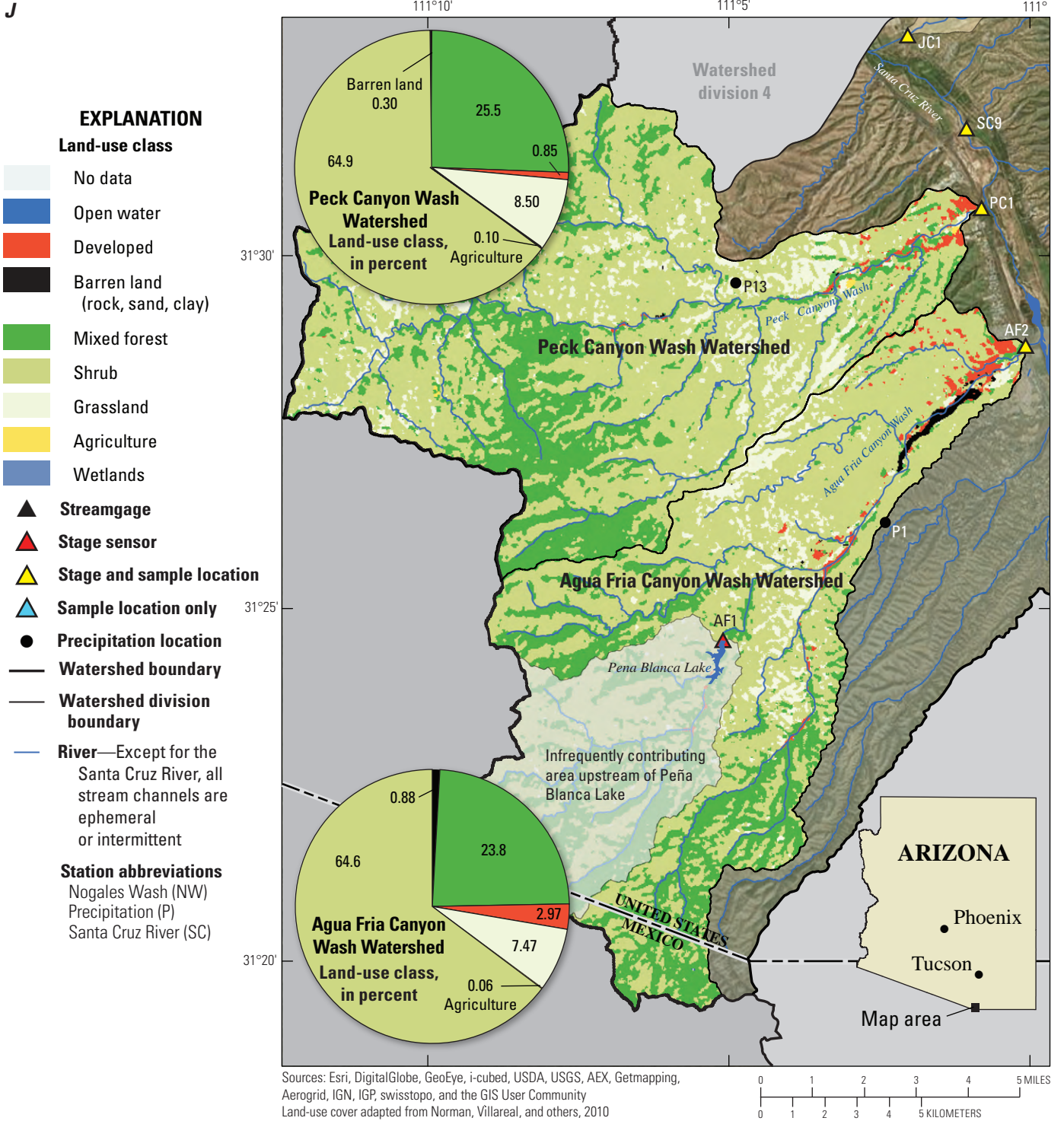
Water Quality

The perennial flow maintained by the NIWTP determines the water quality of the Santa Cruz River for a majority of the year. General water-quality parameters of the effluent are most influenced by the groundwater pumped to the south in Ambos Nogales, which supplies residents and industry on both sides of the international boundary and is ultimately treated at the NIWTP. The consistent discharge of this effluent reduces the seasonal variability in water-quality parameters compared to upstream and downstream watershed divisions (fig. 22A). The uniform flow regime, stable temperatures, increased organics, and lower dissolved oxygen associated with treated effluent (Westerhoff and Anning, 2000; Sonoran Institute, 2016) may also contribute to conditions that support nonnative species, such as mosquito fish and bullfrogs (anecdotally observed in

large quantities). The specific conductance was on average more than 100 microsiemens per centimeter (µS/cm) greater, and pH on average was lower than other divisions. This is consistent with other treated effluent sources in southern Arizona, and generally no additional processes are used to reduce inputs of dissolved solids contributed by residential, industrial, and commercial sources (Anning, 2003). Regional groundwater characteristics maintain water pH at slightly basic for most of the year, and no major exceedances have been observed (Nelson and Erwin, 2001). Median dissolved-oxygen concentrations increased two to three fold after the NIWTP facility upgrade and mostly fluctuate between 5.0 and 7.5 mg/L, with lowest concentrations occurring during the hottest months of June and July. This division has the greatest number of dissolved oxygen exceedances for the AWS criteria of less than 6.0 mg/L. Significant changes in water chemistry are
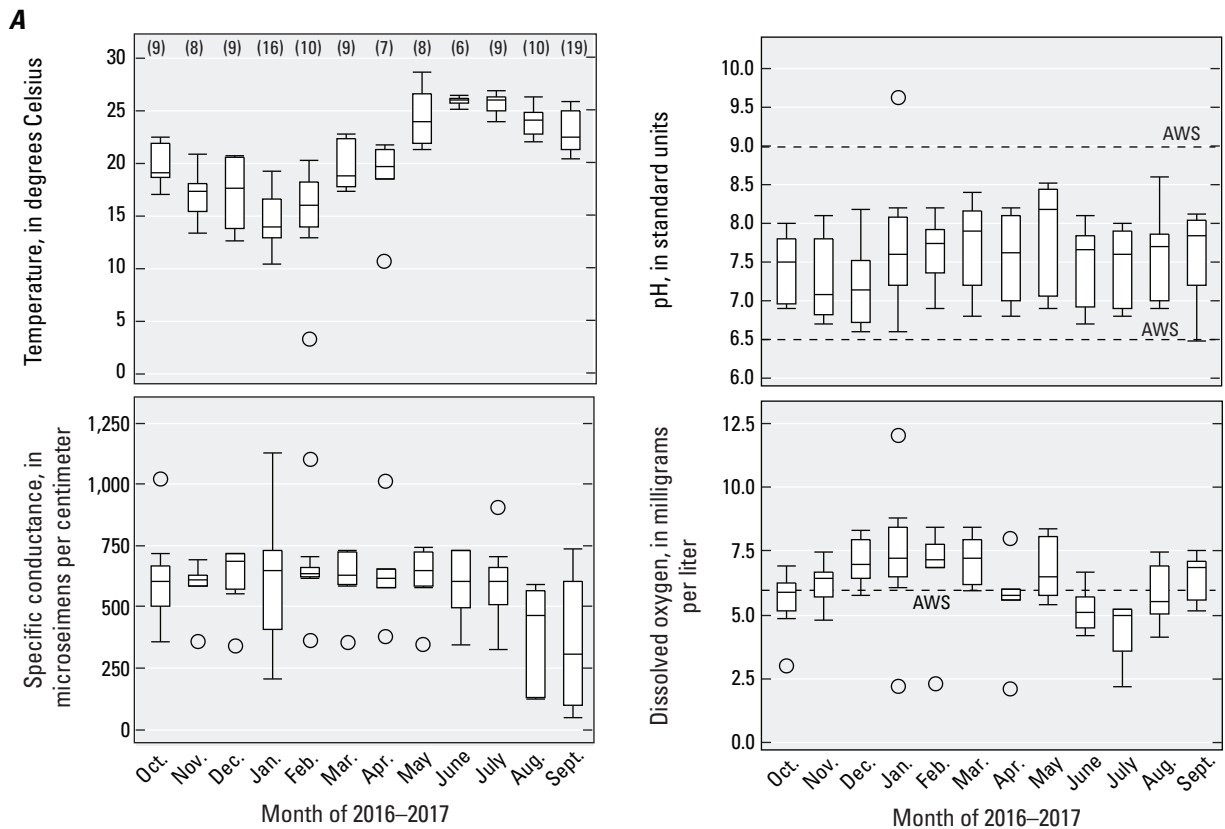
Figure 22. (page 49-50) Box plots showing *Escherichia coli* concentrations and water-quality parameters and related sediment parameters by month (water years 2006–2017) for watershed division 3 of the Upper Santa Cruz River Watershed, southern Arizona and northern Mexico. *A*, General water-quality parameters—temperature, specific conductance, pH, and dissolved oxygen. *B*, *Escherichia coli* concentration, suspended sediment, and turbidity; *Escherichia coli* concentration for the Nogales International Wastewater Treatment Plant (NIWTP) was plotted separately (bottom). FBC WQS, full-body-contact water-quality standard; PBC WQS, partial-body-contact water-quality standard; AWS, Arizona warm-water aquatic wildlife standard.

EXPLANATION

(4) **Number of values**

○ **Outside value**—Value is >1.5 and <3 times the interquartile range beyond either end of the box

⊤ **Largest value within 1.5 times interquartile range above 75th percentile**

75th percentile
50th percentile (median)   **Interquartile range**
25th percentile
⊥ **Smallest value within 1.5 times interquartile range below 25th percentile**

generally observed during periods of flooding and the water quality is dominated by runoff from upstream and tributary flow. The overall monthly *E. coli*, suspended-sediment, and turbidity concentrations all follow a seasonal trend similar to other divisions where concentrations are elevated and exceed WQS during the months associated with monsoon flooding (fig. 22*B*). This also in part due to the mixing with upstream waters during flooding. Between June and September levels of suspended sediment and *E. coli* can get above 1,000 mg/L and 100,000 MPN/100 mL, respectively. The SC6 *E. coli* levels were historically low for all months except June and July, when concentrations have ranged between 10 and 250 MPN/100 mL, albeit rarely in the context of the entire period of record. These infrequent increases may have been related to operational maintenance issues or seasonal rainfall runoff overloading treatment-plant capacity as pass throughs.

The land-use activities downstream of the NIWTP are a secondary influence on water quality and these are dominated by grazing activities that include animal access along parts of the Santa Cruz River. Effects from grazing are observed almost immediately downstream of the outfall (SC7), where *E. coli* concentrations become elevated just downstream of the outfall (fig. 23). When the ephemeral tributaries flow, *E. coli* is generally between 1,000 and 30,000 MPN/100 mL, and this flow contributes to the downstream elevated concentrations of *E. coli* at SC8 and SC9. Overall *E. coli* levels increased in the Santa Cruz River with downstream distance.

There was a strong increasing association between *E. coli* and suspended sediment and *E. coli* and turbidity (Kendall's tau=0.658 and 0.498, respectively; fig. 24). Similar to other WD relations, visual slope breaks occurred in the linear relations. There was not an automatic sampler in WD3,
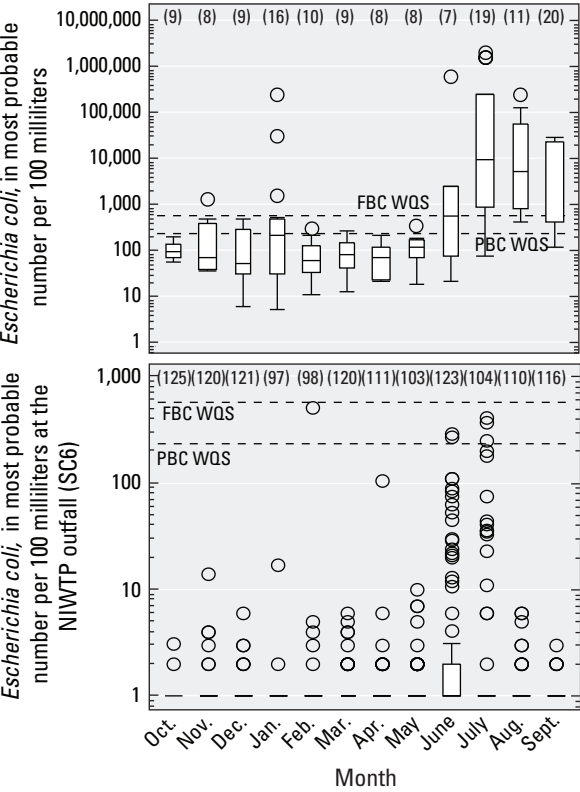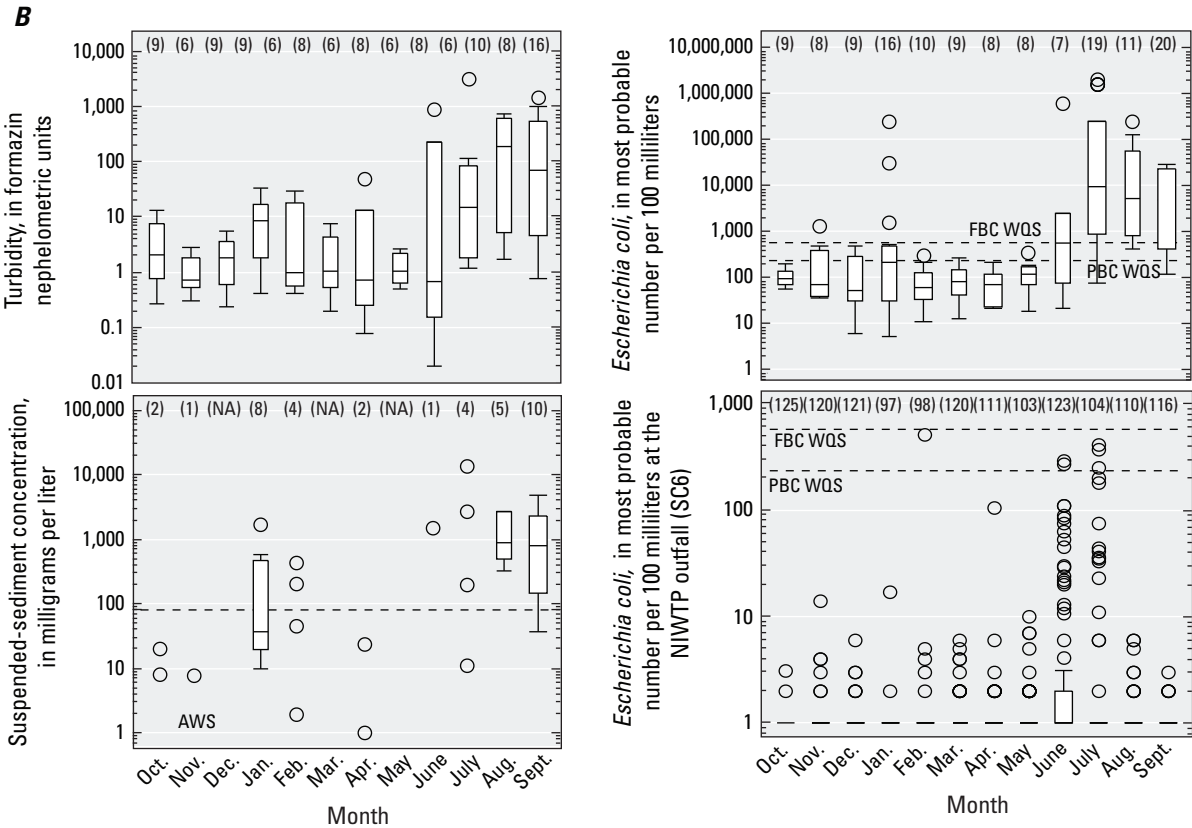
Figure 22. (page 49-50)   —Continued

EXPLANATION

(4)   **Number of values**

○   **Outside value**—Value is >1.5 and <3 times the interquartile range beyond either end of the box

⊤   **Largest value within 1.5 times interquartile range above 75th percentile**

▭   75th percentile
50th percentile (median)   } **Interquartile range**
25th percentile
⊥   **Smallest value within 1.5 times interquartile range below 25th percentile**
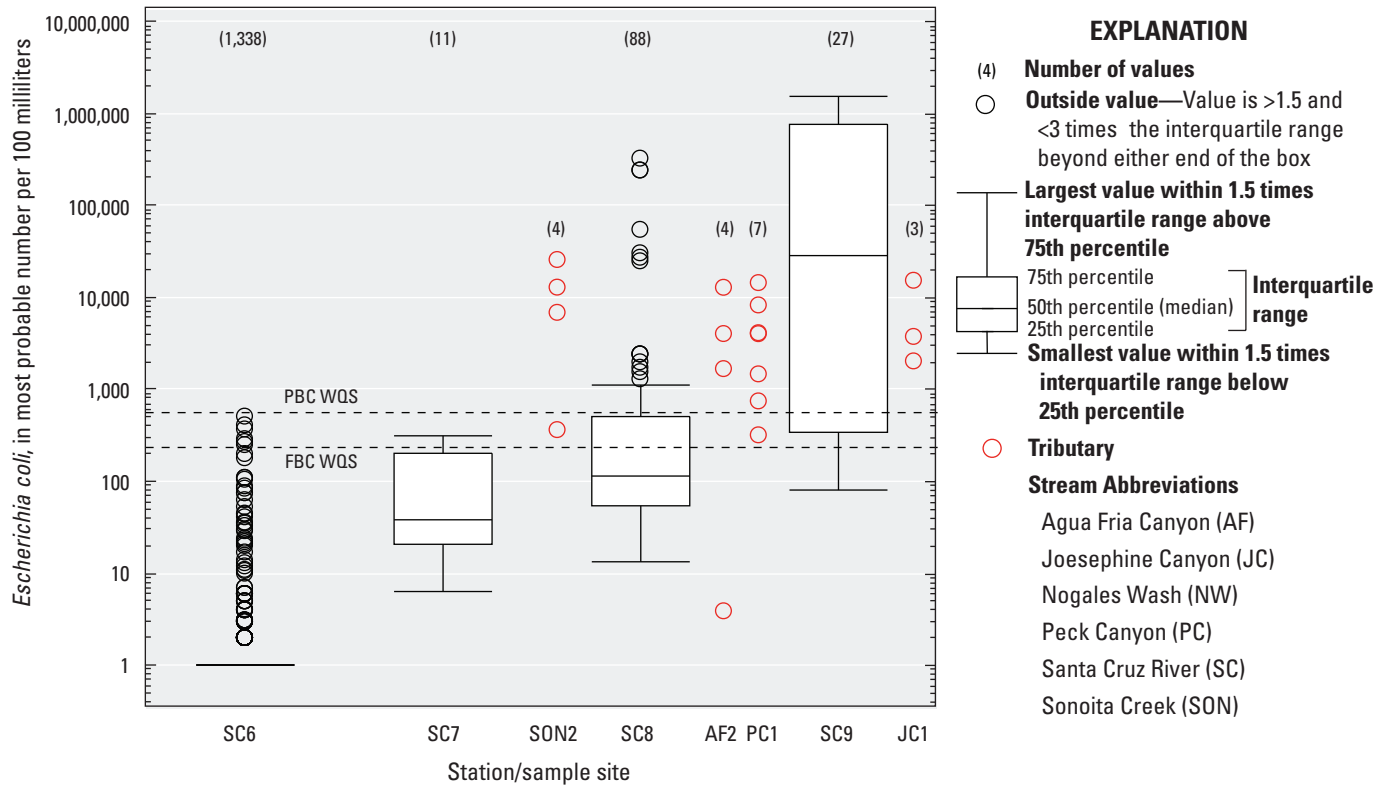
Figure 23. Boxplot of *Escherichia coli* concentration for watershed division 3 of the Upper Santa Cruz River Watershed, southern Arizona and northern Mexico. Boxplot shows station/sample locations (for detailed descriptions of station/sample locations see table 1) from the main Santa Cruz River beginning from SC6 down to SC9, as well as for the major contributing tributaries. FBC WQS, full-body-contact water-quality standard; PBC WQS, partial-body-contact water-quality standard; AWS, Arizona warm-water aquatic wildlife standard.

Figure 24. Graphs showing relations of *Escherichia coli* to suspended sediment and turbidity for watershed division 3 of the Upper Santa Cruz River Watershed, southern Arizona and northern Mexico. A locally weighted scatterplot smoothing (LOWESS) was used to fit the relations, and Kendall's tau and probability (p) are presented for significant relations. n, sample size. FBC WQS, full-body-contact water-quality standard; PBC WQS, partial-body-contact water-quality standard; AWS, Arizona warm-water aquatic wildlife standard.
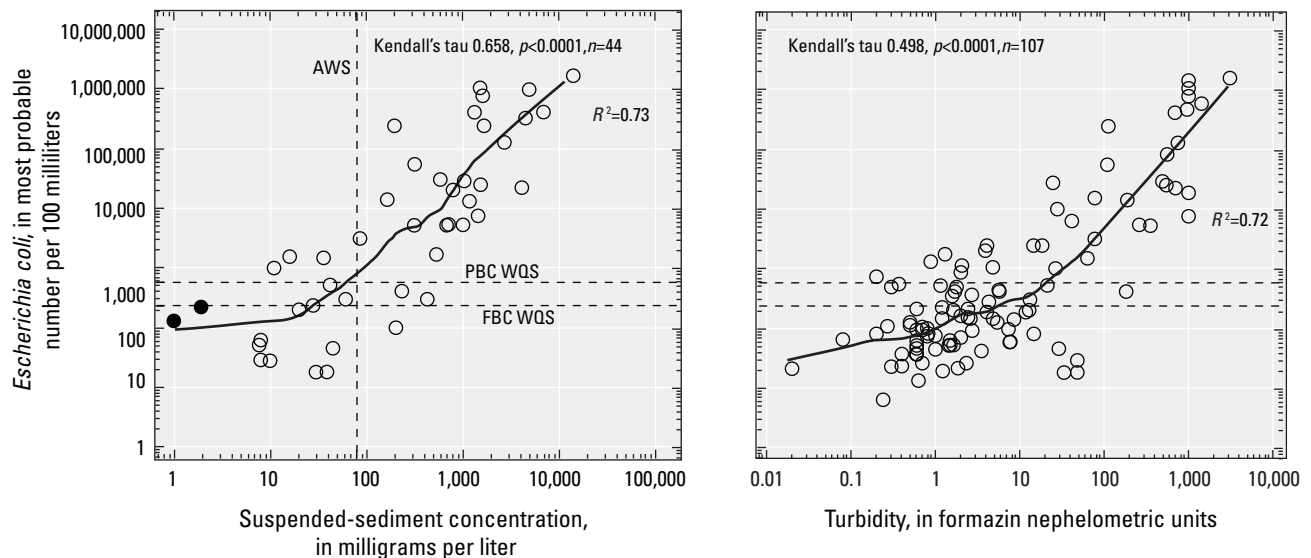
and fewer samples were collected at various times during individual flood events, which minimized hysteresis patterns. The lower slope break may represent a lag related to fluvial processes such as shear stress or the stream power to transport sediment particles. Measured turbidity between 200 and 600 FNUs roughly equated to 10,000 and 100,000 MPN/100 mL of *E. coli* in this WD.

Before the full implementation of the NIWTP upgrade in 2009, *E. coli* exceedances occurred primarily in June and July. This pattern may have coincided with capacity issues (pass throughs) during elevated storm-water inputs from Ambos Nogales. The *E. coli* patterns and median concentrations were similar to WD2. The percent of daily samples exceeding WQS standards ranged from about 30 to 50 percent (fig 25*A*). The NIWTP contributed very little to exceedances, most of which were caused by flooding contributions from upstream and tributary watersheds (fig. 25*B*).

The MST marker concentrations were greatest in the summer and fall months, and concentrations of the human (HF183) and canine (BacCan) markers were higher at the Santa Cruz River locations and more frequently above the reporting limit than marker concentrations in the tributaries (fig. 26). The ruminant and cattle markers (Rum2Bac and CowM2) were the only two markers detected in the tributaries. The influent sample collected at NIWTP was used to define a human and wastewater influence endpoint. The human polyomavirus (HPyV) marker was two orders of magnitude greater than the only detection observed in watershed division 2. HPyV was analyzed as an additional human fecal molecular marker, but it can be more associated with untreated sewage. The influent sample had the greatest concentrations of the human (HF183) and canine (BacCan) markers and no cattle (CowM2) or ruminant (Rum2Bac) marker was detected above the reporting limit.
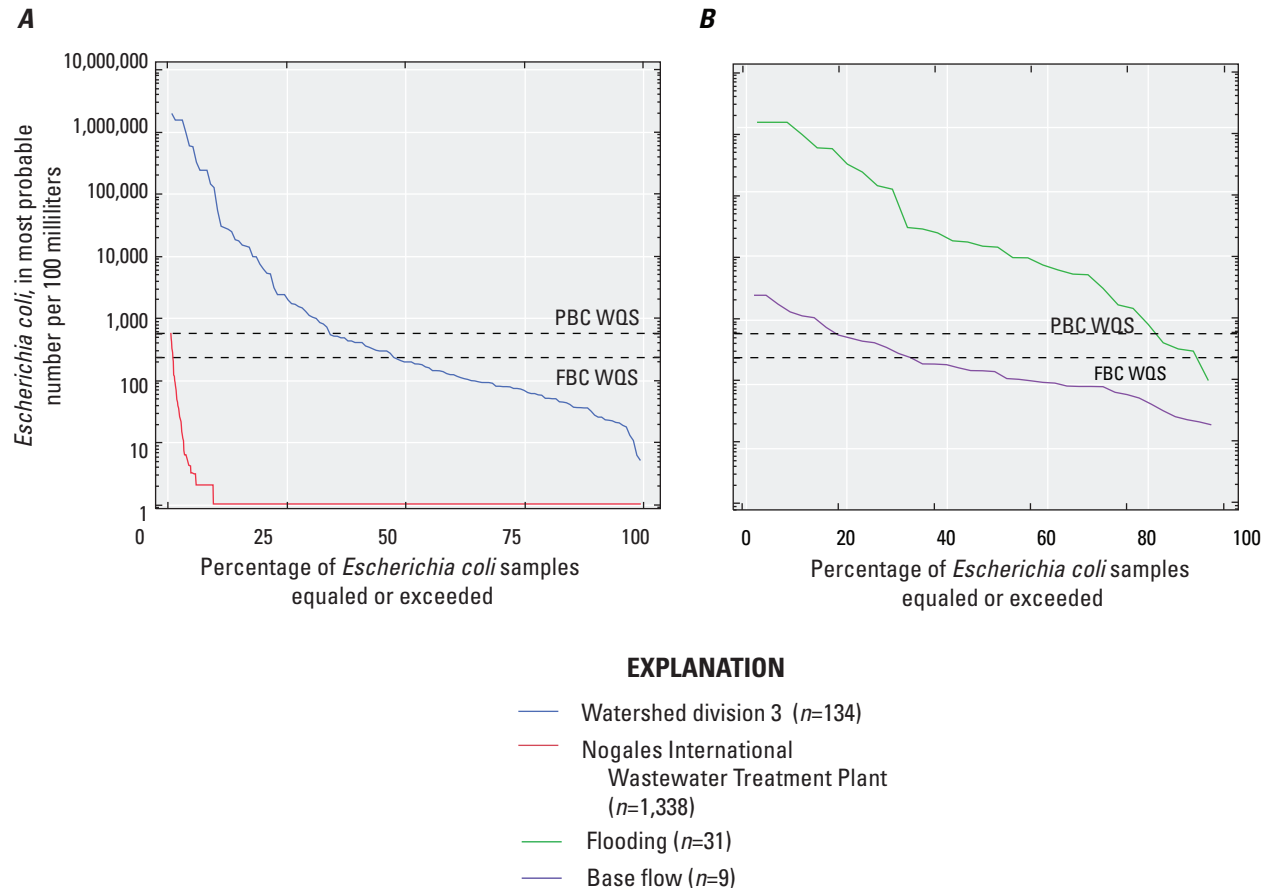
Figure 25.   Graphs showing the percentage of *Escherichia coli* concentrations that were equaled or exceeded in watershed division 3 of the Upper Santa Cruz River Watershed, southern Arizona and northern Mexico. *A*, Graph for Nogales International Wastewater Treatment Plant; *B*, graph for the remaining watershed division 3 samples. n, sample size; FBC WQS, full-body-contact water-quality standard; PBC WQS, partial-body-contact water-quality standard.

EXPLANATION
- ○ Santa Cruz River Stations
- △ Tributary Stations
- ○ Nogales International Wastewater Treatment Plant Influent

Opaque symbols are below the minimum laboratory reporting limit

Figure 26. Graphs showing time series of microbial-source-tracking samples collected in watershed division 3 of the Upper Santa Cruz River Watershed, southern Arizona and northern Mexico. Plotted from top to bottom as concentrations of suspended sediment, *Escherichia coli*, and microbial-source-tracking markers (Rum2Bac, ruminant animal; CowM2, cattle; BacCan, canine; GenBac, general bacteria).

Hydrologic Characterization of *E. coli* and Suspended Sediment

Mean discharge between 2009 and 2016 has been consistently maintained between 13 and 16 ft^3/s at the NIWTP outfall, and since the upgrade in 2009, there has been a significant reduction in the levels of *E. coli* to the level of detection limit (fig. 27). During the study, concentrations were observed at or near the detection limit, supporting that inputs upstream and downstream of the NIWTP are primary sources of *E. coli* affecting WD3. The ephemeral tributary flow in this WD was infrequent but when it did occur, tributary flow contributed waters with elevated *E. coli* coupled with higher incidence of cattle (CowM2) and ruminant (Rum2Bac) MST marker detection. During the study, tributary flow to the Santa Cruz River likely occurred four to five times on Sonoita Creek and Peck Canyon Wash, and three to four times on Agua Fria Canyon Wash and Josephine Canyon Wash (fig. 28). Patagonia and Pena Blanca Lakes (reservoirs) infrequently contributed surface-water flow to the Santa Cruz River. However, during large storm events, excess water from these reservoirs spilled over into Sonoita Creek and Agua Fria Canyon Wash, respectively. The contribution of reservoir water changed the water chemistry and likely diluted the *E. coli* concentrations when samples were collected.

Discharge was infrequently measured in this reach of the Santa Cruz River or the major tributaries entering this reach, because of the difficulties related to access and the short duration of ephemeral flows. Correlations did exist between discharge and suspended sediment (Kendall's tau=0.544, *p*-value=0.0003), and turbidity (Kendall's tau=0.278, *p*-value=0.0003), but not *E. coli*. Overall the linear relation with discharge was very weak or nonexistent for all three. Flood samples were two to three orders of magnitude greater than base-flow samples for *E. coli* and turbidity (fig. 29*A*). During flood events, the *E. coli* and turbidity levels were greatest along the peak of the hydrograph, whereas suspended sediment tended to be greatest on the rise and the peak of the hydrograph (fig. 29*B*). Rising concentrations were most similar to recession concentrations for *E. coli*, suspended sediment, and turbidity.

EXPLANATION

○ *Escherichia coli*   ——— Nogales International WastewaterTreatment Plant (NIWTP)   ——— NIWTP upgrade
                                      mean daily discharge
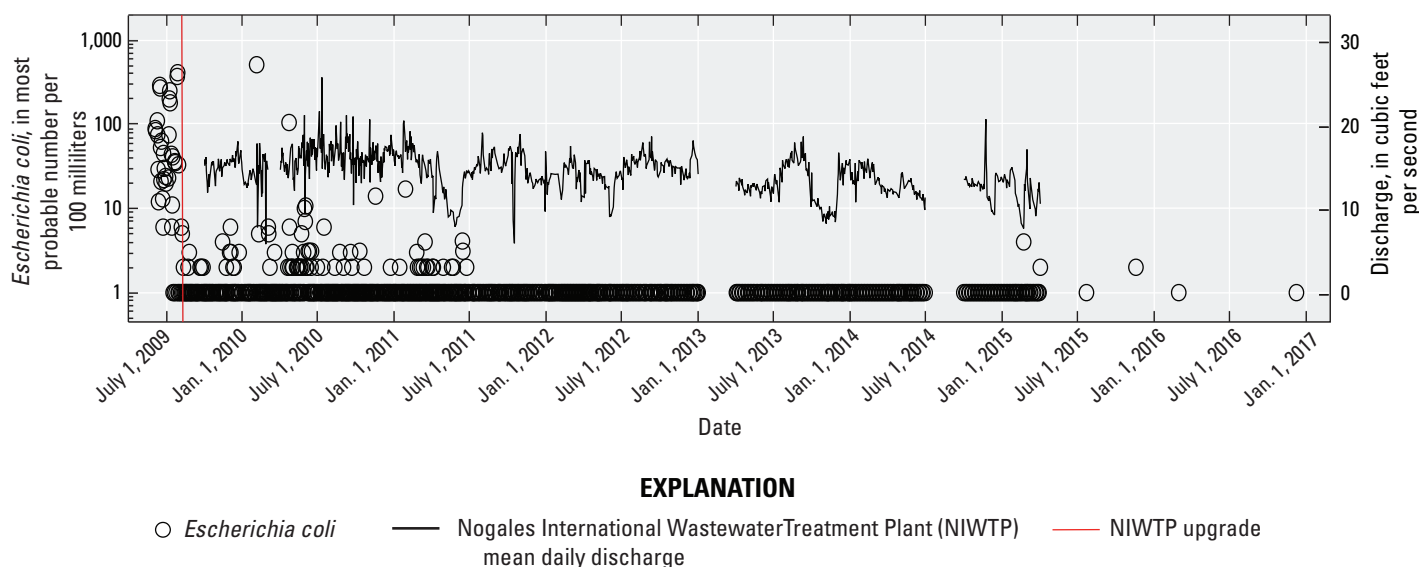
Figure 27.   Graph showing time series of *Escherichia coli* and daily mean discharge at the Nogales International Wastewater Treatment Plant outfall (SC6; see table 1) in watershed division 3 of the Upper Santa Cruz River Watershed, southern Arizona and northern Mexico.

Figure 28. (page 55)   Graphs showing time series of instantaneous stage height and daily mean precipitation in watershed division 3 of the Upper Santa Cruz River Watershed, southern Arizona and northern Mexico. Data from stations SON1, SON2, AF1, AF2, PC1, JC1, SC9, and SC10 (for detailed descriptions of station/sample locations see table 1). Stream abbreviations—SON, Sonoita Creek; AF, Agua Fria Canyon Wash; JC, Josephine Canyon Wash; PC, Peck Canyon Wash; SC, Santa Cruz River; precipitation stations (P); and precipitation at Nogales International Wastewater Treatment Plant (PNIWTP). Stage height was not referenced to an elevation; the magnitude is relative and may be negative in the unadjusted form.

EXPLANATION

(4)   **Number of values**

○   **Outside value**—Value is >1.5 and
     <3 times the interquartile range
     beyond either end of the box

───   **Largest value within 1.5 times
       interquartile range above 75th percentile**

     75th percentile   **Interquartile**
     50th percentile (median) **range**
     25th percentile
───   **Smallest value within 1.5 times interquartile range
       below 25th percentile**

     a, b, or ab denotes statistical difference;
     when letters are the same, groups are
     not significantly different

Figure 29.   Boxplots of *Escherichia coli* concentrations and
related sediment parameters for watershed division 3 of the
Upper Santa Cruz River Watershed, southern Arizona and
northern Mexico. *A*, boxplots of daily mean *Escherichia coli*
and turbidity plotted by general flow condition. *B*, Boxplots of
15-minute turbidity, *Escherichia coli*, and suspended sediment
plotted by hydrograph classification grouped for flood conditions
only. Significant Wilcoxon pairwise tests are labeled with letters
indicating significant differences between hydrologic condition
distributions. FBC WQS, full-body-contact water-quality standard;
PBC WQS, partial-body-contact water-quality standard; AWS,
Arizona warm-water aquatic wildlife standard.

E. coli and Suspended-Sediment Flux

Because discharge was infrequently measured during
flooding, the flux estimates for WD3 were based mostly on
base-flow instantaneous measurements instead of daily means,
and flux estimates were converted to a daily equivalent based
on the instantaneous discharge (fig. 30). The base-flow flux
of both *E. coli* and suspended sediment were similar to WD2,
with most samples ranging between 1×10^9 and 1×10^{12} MPN/day
for *E. coli* and 0.01 to 10 tons per day for suspended sediment.
The flooding samples in terms of flux for *E. coli* and suspended
sediment were several orders of magnitude lower than WD2,
but this could also be related to the limited number of flood
samples collected with an associated discharge. At Josephine
Canyon Wash, using the indirect peak flow approximation
and the assumption that the sample collected represented this
peak, a computed flux of 5.5×10^9 MPN/s was estimated for the
September 2015 flood.
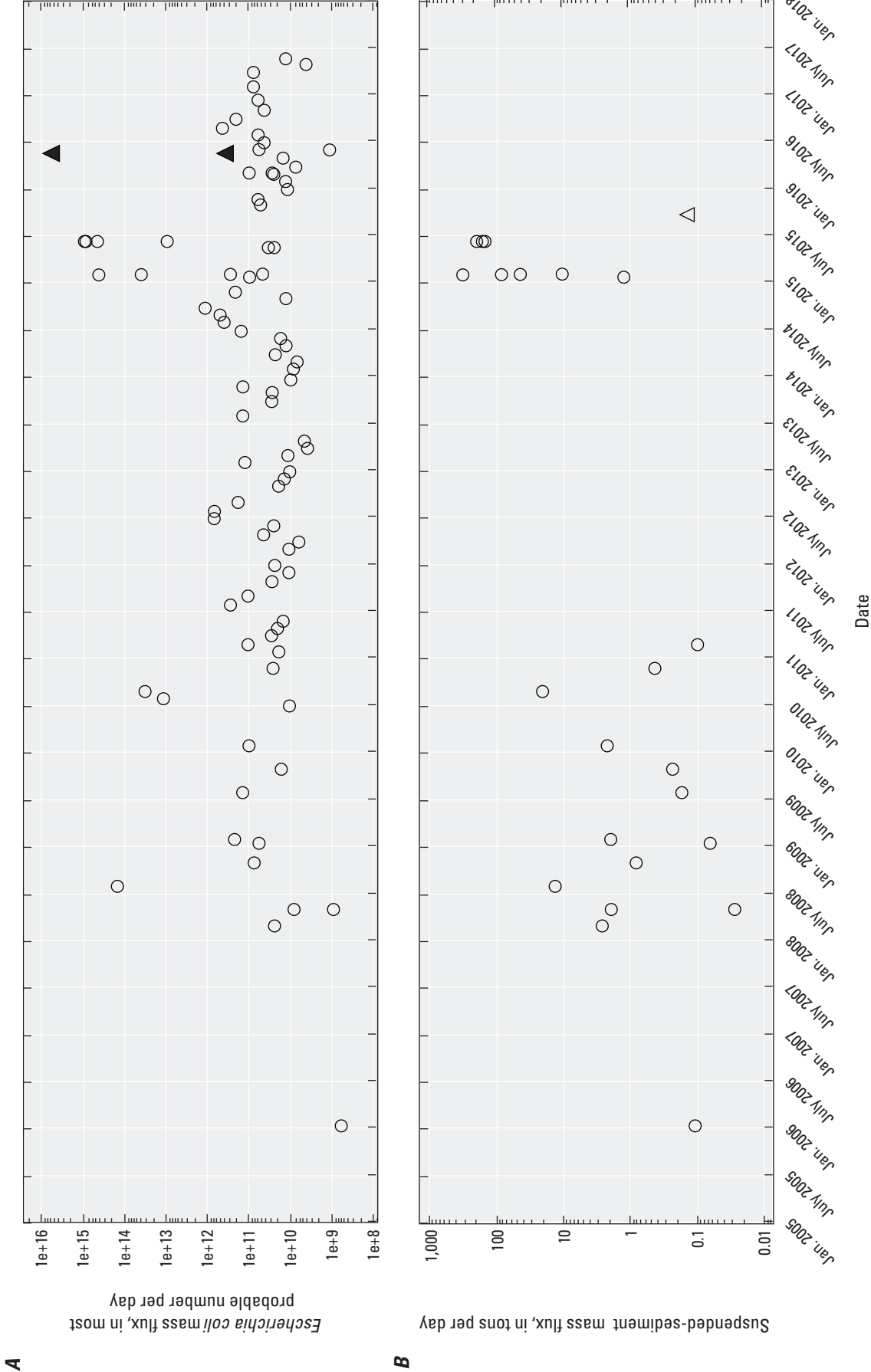
Figure 30. Graphs showing mean daily flux time series for over the entire period of record for watershed division 3 of the Upper Santa Cruz River Watershed, southern Arizona and northern Mexico. *A, Escherichia coli; B,* suspended sediment. Instantaneous flux concentrations are converted to a daily mass flux estimates for comparison to other watershed divisions.

EXPLANATION

△ Tributary—opaque indicates an indirect discharge measurement in flux calculation

○ Santa Cruz River locations

NIWTP data were not included

Summary

The NIWTP discharges the water that sustains perennial flow in the Santa Cruz River, and since the NIWTP upgrade in 2009, the *E. coli* concentrations were consistently measured below the detection limit near the outfall. Grazing activities are prominent in WD3, and cattle have direct access to the Santa Cruz River near the NIWTP outfall, as well as to downstream areas and as far as the Palo Parado Bridge crossing. Agriculture is the primary land-use activity, about 3.5 percent, which is the greatest of all the WDs. General water-quality parameters are consistent throughout the main Santa Cruz River and resemble the groundwater delivered to residents and commercial properties in Ambos Nogales, which ultimately enters the sewer system for treatment and discharge from the NIWTP. During months associated with monsoon activity, the median levels of *E. coli* were measured above 10,000 MPN/100 mL on the main Santa Cruz River. When the ephemeral tributaries flowed, which was infrequent, *E. coli* was generally between 1,000 and 30,000 MPN/100 mL. Tributary flow mixes with the Santa Cruz River, often contributing to concentration measurements in the main river exceeding 100,000 MPN/100 mL. Similar to other WD relations, there was a strong increasing association between *E. coli* and suspended sediment and turbidity. Flood samples were 2 to 3 orders of magnitude greater than base-flow samples for *E. coli* and turbidity; during flood events, the *E. coli* and turbidity levels were greatest during the peak of the flood, whereas suspended sediment tended to be greatest on the rise and the peak of the hydrograph.

The MST marker concentrations were greatest in the summer and fall months, and concentrations of the human (HF183) and canine (BacCan) markers were only detected at the Santa Cruz River locations and not in the tributaries. Ruminant and cattle markers (Rum2Bac and CowM2) were the only markers detected in the tributaries. During the study, tributary flooding to the Santa Cruz River likely occurred four to five times on Sonoita Creek and Peck Canyon Wash, and three to four times on Agua Fria Canyon Wash and Josephine Canyon Wash. During flooding, all concentrations of *E. coli* were several orders of magnitude above the WQS thresholds. Discharge was less frequently measured in WD3, because there was no streamgage on the main river and the logistical difficulties related to access and the short duration of ephemeral flows in the tributaries. This limited the ability to calculate flux for many of the samples collected. Where discharge was measured, generally during base flow, correlations existed between discharge and suspended sediment, but not with *E. coli*. The base-flow flux of both *E. coli* and suspended sediment were similar to WD2, but the flood-sample flux for *E. coli* and suspended sediment were several orders of magnitude lower than WD2.

Watershed Division 4 (WD4)—Santa Cruz River at the TUMA Southern Boundary to Chavez Siding Road

WD4 is the area from the Santa Cruz River at the TUMA southern boundary to Chavez Siding Road (fig. 31*A*). The southern boundary of TUMA is located at the Santa Gertrudis Lane road crossing (fig. 1). This length of river is small relative to the other WDs, but the riparian corridor is ecologically intact because the 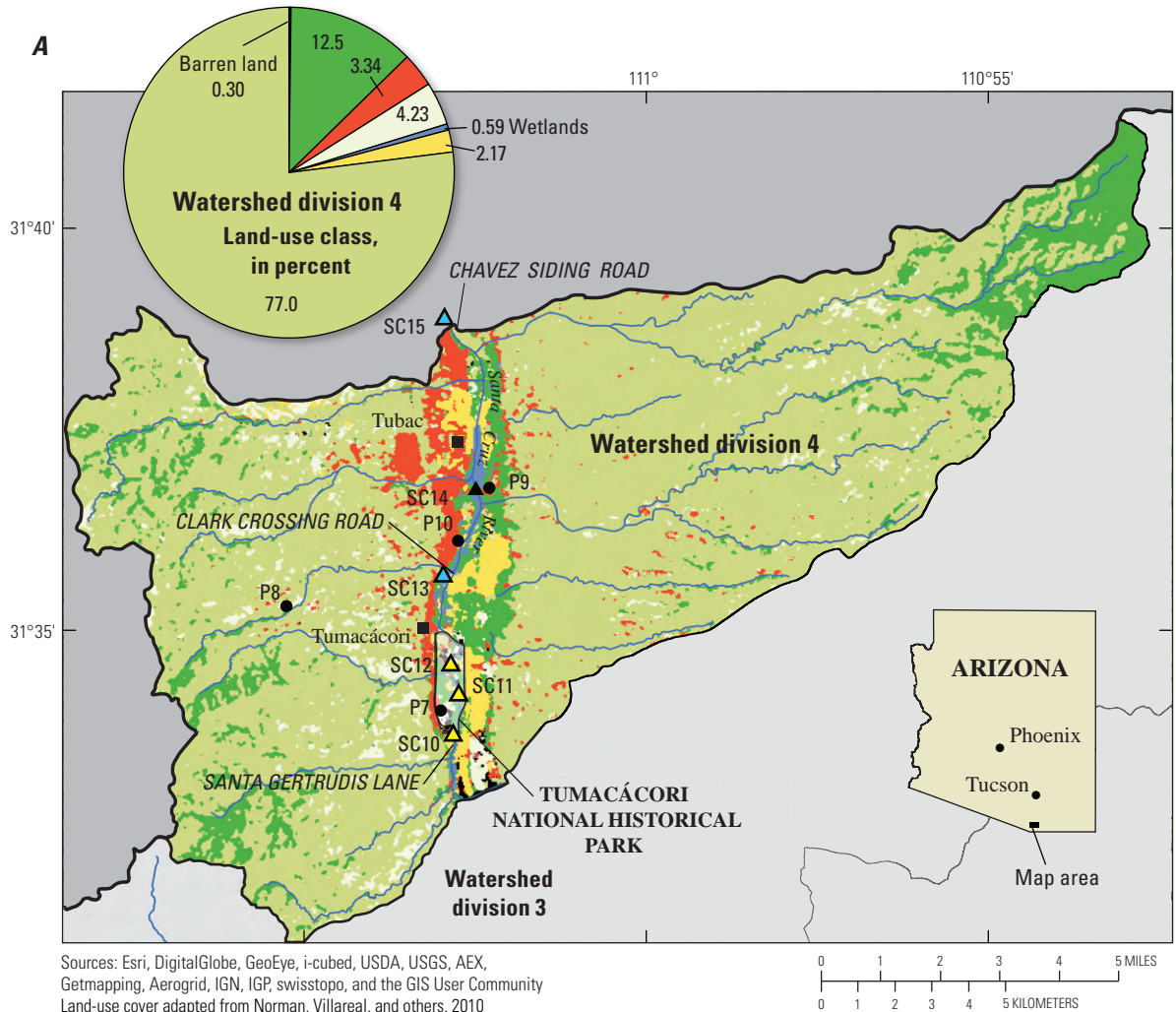park maintains fences, removes trash, manages nonnative plants, and monitors water quality (Gwilliam and others, 2014, 2016; Powell and others, 2005). Historically, this reach of Santa Cruz River has been extensively studied by the NPS, USGS, ADEQ, University of Arizona, FOSCR, U.S. Fish and Wildlife Service, Arizona Game and Fish Department, and EPA for ecological, archeological, and hydrological purposes (Gwilliam and others, 2016; Powell and others, 2005; Graham, 2011; Coes and others, 2014; Tetra Tech, 2014; LaBrie, 2016; King and others, 1999; Sonoran Institute, 2016). There are three frequently monitored locations within the park (SC10, figs. 31*A*–*C*; SC11, fig. 31*A*; and SC12, figs. 31 *A*, *D*), but SC10 has been the long-term index sampling location for both TUMA and FOSCR. At the three locations, pressure transducers were deployed for various periods during the study to understand the timing of a flood moving through the park. There is a wide and losing reach in the northern part of the park that reduces water velocity and can increase the lag time of a flood wave arrival at the Tubac streamgage (SC14; fig. 31*A*). Floods can be completely attenuated before reaching SC14 during dry periods of the year. Although SC14 is perennial, the dry and hot periods of June can result in northern sections in the park drying back as far as SC12. Less than a mile downstream of the park is an old stream crossing (Clark Crossing) that was sampled in the past by FOSCR; this location was only visited during periods of flooding for this study (SC13, figs. 31*A*, *E*). North of the TUMA boundary, the USGS streamgage at Tubac was instrumented with a continuous turbidity sensor and an automatic sampler (SC14, figs. 31 *A*, *F*, and *G*).

There are agricultural and grazing activities along the west side of the river and these activities likely affect the water quality in WD4. Developed and agricultural land-use account for about 3 and 2 percent of the watershed area in WD4, respectively. Outside of the floodplain, most of the land is shrub, grassland, and forest land cover. The ADEQ lists this reach of river as having WQS exceedances for ammonia and *E. coli*, which are likely related to grazing activities around and upstream of TUMA.

A

Barren land
0.30

12.5

3.34

4.23

0.59 Wetlands

2.17

Watershed division 4
Land-use class,
in percent

77.0

CHAVEZ SIDING ROAD

SC15

Tubac

Watershed division 4

SC14   P9

CLARK CROSSING ROAD   P10

P8   SC13

Tumacácori

SC12

SC11

P7

SC10

SANTA GERTRUDIS LANE

TUMACÁCORI
NATIONAL HISTORICAL
PARK

Watershed
division 3

111°   110°55'

31°40'

31°35'

Santa Cruz River

ARIZONA

Phoenix

Tucson

Map area

Sources: Esri, DigitalGlobe, GeoEye, i-cubed, USDA, USGS, AEX,
Getmapping, Aerogrid, IGN, IGP, swisstopo, and the GIS User Community
Land-use cover adapted from Norman, Villareal, and others, 2010

0   1   2   3   4   5 MILES

0   1   2   3   4   5 KILOMETERS

EXPLANATION

Land-use class

No data

Open water

Developed

Barren land
(rock, sand, clay)

Mixed forest

Shrub

Grassland

Agriculture

Wetlands

▲ **Streamgage**

▲ **Stage sensor**

▲ **Stage and sample location**

▲ **Sample location only**

● **Precipitation location**

— **Watershed boundary**

— **Watershed division**
    boundary

— **River**—Except for the
    Santa Cruz River, all
    stream channels are
    ephemeral
    or intermittent

Station abbreviations
Nogales Wash (NW)
Precipitation (P)
Santa Cruz River (SC)

Figure 31. (pages 59–60)   Map and photographs of watershed division 4 of the Upper Santa Cruz River
Watershed, southern Arizona and northern Mexico. *A*, Map showing watershed division 4 and sample
locations (for detailed descriptions of station/sample locations see table 1). Land-use classes are shown in
percent in the pie chart; sample locations and other hydrologic sites are annotated—SC, Santa Cruz River; P,
precipitation stations; NW, Nogales Wash; AF, Agua Fria; SON, Sonoita Creek; JC, Josephine Canyon Wash.
B–G, Photographs of watershed division 4. *B*, SC10 base flow looking downstream (U.S. Geological Survey,
USGS photograph, March 3, 2016); *C*, SC10 flood looking southeast (USGS, January 30, 2015); *D*, SC12 base flow
looking downstream (USGS, April 4, 2017); *E*, SC13 looking downstream (USGS, August 9, 2016); *F*, SC14 base
flow (USGS, April 14, 2017); *G*, SC14 flood looking east (USGS, July 17, 2017).
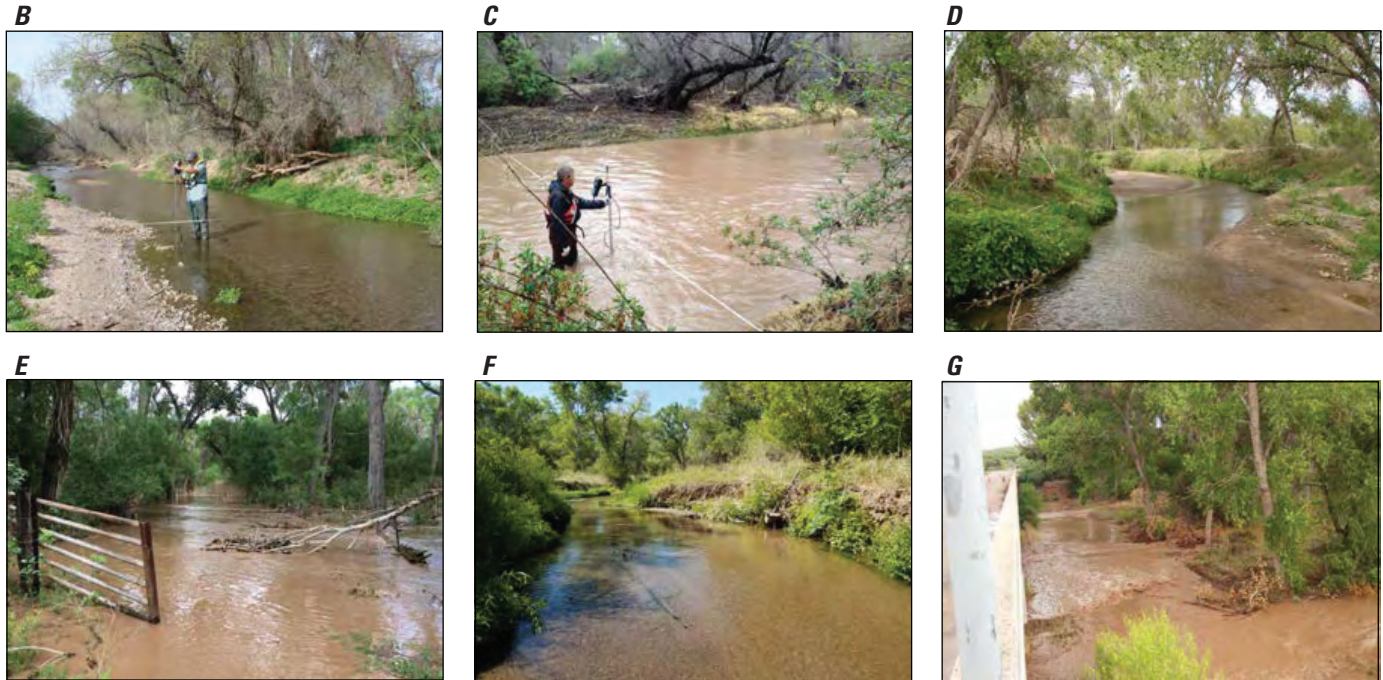
Figure 31. (page 59–60) —Continued

Water Quality

Perennial base flow is sustained by the NIWTP, base flow that would otherwise not be there most of the year because of a decreasing elevation of the regional groundwater. Water-quality parameters were similar to those in the WD3 (fig. 32*A*), but chemistry does change between the NIWTP and the park. Organic compounds and nutrients tend to decrease, whereas physical parameters such as temperature and dissolved oxygen will cycle with discharge and mostly vary with season and distance downstream, as it takes 6 to 10 hours for water to flow from the NIWTP to TUMA (Anning, 2003; Coes and others, 2014; Westerhoff and Anning, 2000). Dissolved-oxygen levels increase and the fish abundance is visibly higher in this river reach than in upstream sections of the river. Specific conductance and pH varied more than in WD3, likely from some additional local infiltration from nearby mountainous relief or bank storage during wet periods of the year. During the monsoon, the *E. coli* and suspended sediment in WD4 were almost an order of magnitude greater than WD3 for median concentrations (fig. 32*B*). Although increases downstream were likely related to additional inputs from surrounding land-use activities, more flood samples were collected in this WD, which may bias the analysis of the monthly sample distributions. Concentrations of *E. coli*, suspended sediment, and turbidity were overall lower within TUMA as compared to downstream (fig. 33). Specifically, where study efforts were focused, SC14 was significantly greater for *E. coli*, suspended sediment, and turbidity than SC10 (by an order of magnitude or more).

Agricultural activities downstream of the park were likely contributing to these differences over the 2-mile distance from SC10 to SC14.

At the beginning of the study, a 24-hour data collection was done at SC10 (TUMA southern boundary) in March 2015 to assess the variability of sampling methods and base-flow conditions (Paretti and others, 2018). March was selected to minimize variability that might be caused by evapotranspiration and because that time of year is when *E. coli* concentrations are typically lowest. Water-quality parameters, *E. coli*, and suspended sediment were collected every hour between March 11 and 12, 2015 (fig. 34*A*). The measurements and samples collected follow a distinct discharge signature created by SC6 outfall. Discharge was a strong predictor of several parameters and *E. coli* (fig. 34*B*), providing supporting information that the NIWTP discharge affects the concentration and loading of base-flow constituents flowing through the park. Dissolved oxygen changed 2 mg/L over the 24-hr period, and was close to exceeding the AWS. The *E. coli* increased four to five fold over the 24-hr period and had strong positive relation to turbidity and suspended sediment. Although no WQS exceedances were observed in March, later 24-hr automatic sampler collections showed variability within the collection period, similar to what was observed in March, and concentrations frequently exceeded one or more of the *E. coli* WQS standards.

Similar to upstream WDs, WD4 showed a strong correlation and increasing relation between *E. coli* and suspended sediment (Kendall's tau=0.609, *p* <0.0001; coefficient of determination, R^2,=0.88, *p*<0.0001, respectively; fig. 35). The relation to turbidity was random between 0 and 10 FNUs, but the relation improved between 10 and 1,000 FNUs as variance decreased. This upward slope break was observed in other WDs and may be attributed to one or multiple factors with turbidity methods at the low range or effects from hysteresis. The statistical noise in the low range between 0 and 10 FNUs
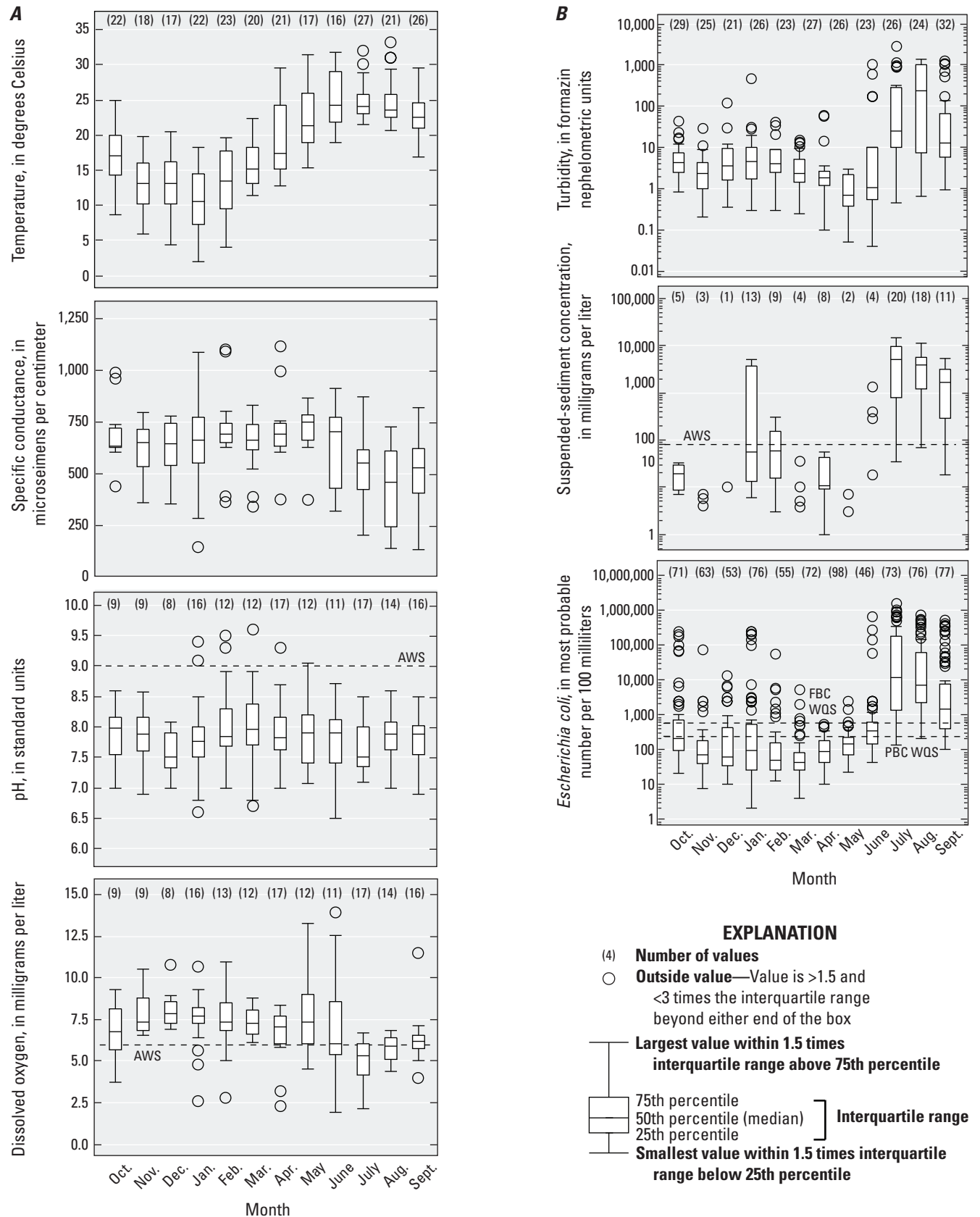
Figure 32.   Boxplots showing water-quality parameters and *Escherichia coli* concentrations and related sediment parameters by month (water years 2001–2017) for watershed division 4 of the Upper Santa Cruz River Watershed, southern Arizona and northern Mexico. *A,* Boxplots of general water-quality parameters including temperature, specific conductance, pH, and dissolved oxygen. *B,* Boxplots of *Escherichia coli* and suspended sediment, and turbidity. FBC WQS, full-body-contact water-quality standard; PBC WQS, partial-body-contact water-quality standard; AWS, Arizona warm-water aquatic wildlife standard.
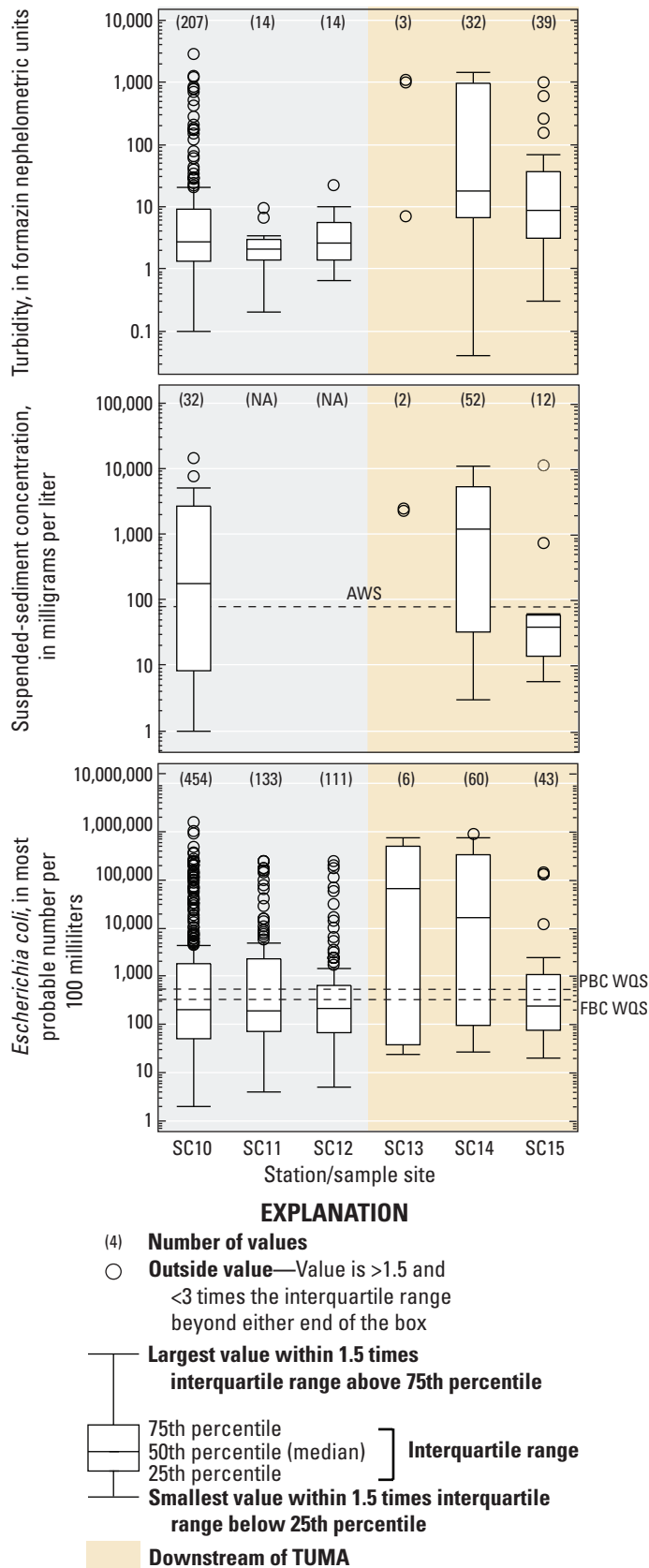
Figure 33. Boxplots showing *Escherichia coli* concentration, suspended sediment, and turbidity for watershed division 4 of the Upper Santa Cruz River Watershed, southern Arizona and northern Mexico. Station/sample locations SC10, 11, 12, 13, 14, 15 are shown (for detailed descriptions of station/sample locations see table 1). TUMA, Tumacácori National Historical Park; FBC WQS, full-body-contact water-quality standard; PBC WQS, partial-body-contact water-quality standard; AWS, Arizona warm-water aquatic wildlife standard.

is in part related to variability caused by sensor insensitivity to other light absorbing constituents like organics or algae.

E. coli exceedances of the PBC and FBC standards were similar between the current study and existing data collected in this section of river, suggesting that previous sampling conducted by FOSCR and NPS is representing the range of *E. coli* concentrations (fig. 36*A*). Over the entire period of record, 50 percent of the samples collected exceeded the FBC WQS and about 30 to 40 percent of the samples exceeded the PBC WQS. Flood sample WQS exceedances were more frequent than base flow exceedances (fig. 36*B*). A sample collected during flooding almost always exceeded both WQS standards, whereas 75 percent of base-flow samples did not exceed the FBC standard. These results indicate that any future flood sampling has a high probability of exceeding both thresholds.

The MST data in this WD, as with other WDs, was very correlated the suspended-sediment concentrations. MST concentrations were higher during flooding than during base-flow conditions. The percentage of human marker (HF183) detections was much greater than the cattle (CowM2) marker, but the ruminant animal (Rum2Bac) marker was similar to the human marker (fig. 37*A*). The cattle concentrations at SC10 and SC14 were the highest in the study area, indicating that cattle were a significant source of *E. coli* in TUMA during the study. Samples collected at the southern boundary were similar in percent detection and concentration of MST markers to samples collected downstream of the park, indicating that any new sources introduced are not significantly changing the source types measured from upstream to downstream. The canine (BacCan) marker was correlated with the human marker and these markers' concentrations were greatest during the months of June, July, and September, whereas the cattle and ruminant markers showed an overall decline between June and September (fig. 37*B*). The increase in the human and canine markers (HF183 and BacCan) during September flood events suggests additional or renewed upstream sources of human and canine *E. coli*, but the decline of ruminant and cattle (Rum2Bac and CowM2) contributions over the summer period of flooding is possibly related to a reduction in fecal material with viable *E. coli*. Summer temperatures will desiccate and reduce *E. coli* populations.

A
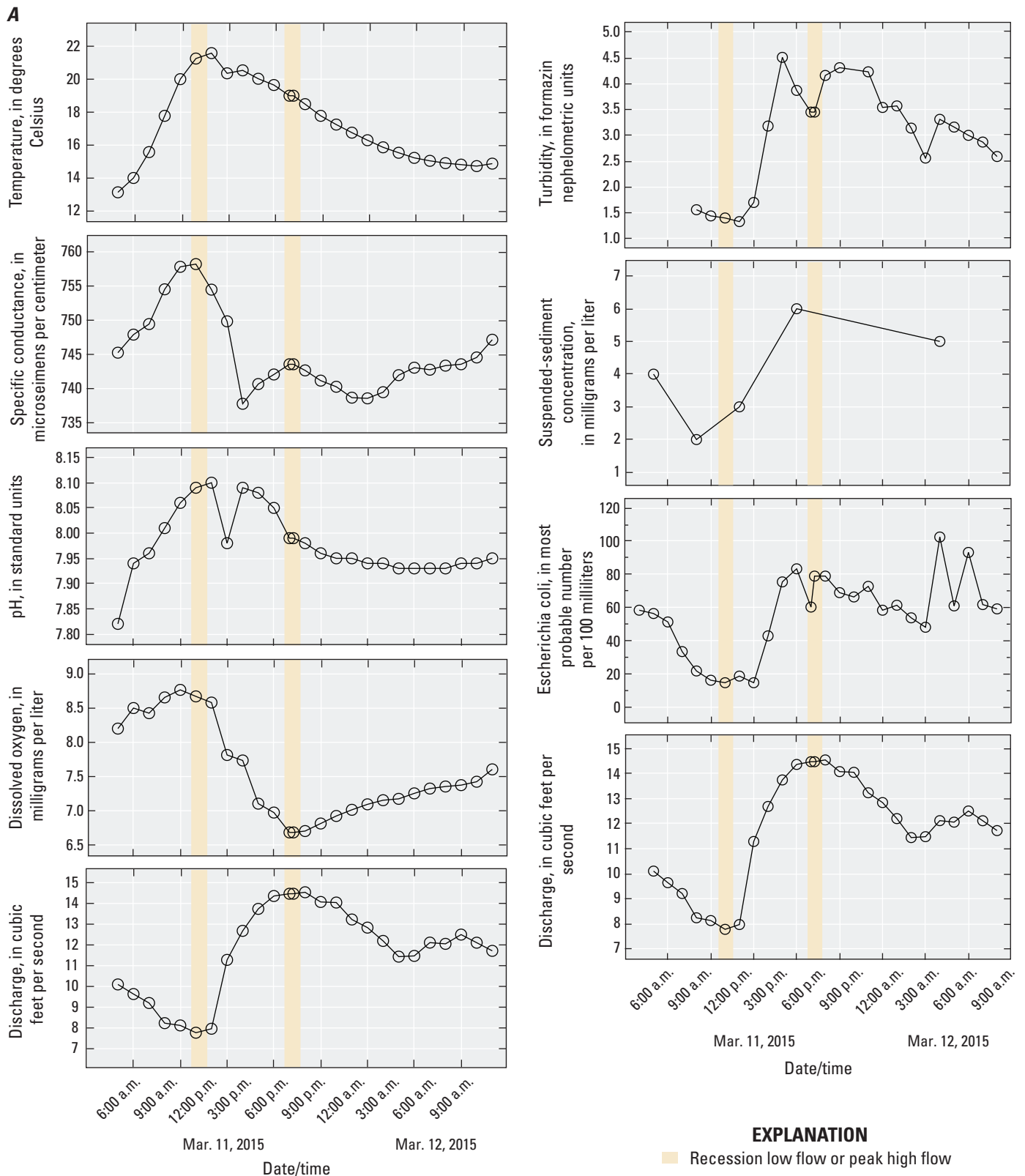
Figure 34. (pages 63–64)   Graphs showing a time series of a 24-hour study of *Escherichia coli* concentrations and related water-quality parameters at station SC10 in watershed division 4 of the Upper Santa Cruz River Watershed, southern Arizona and northern Mexico. *A*, Graphs of temperature, specific conductance, pH, dissolved oxygen, turbidity, discharge, *Escherichia coli*, and suspended sediment. *B*, Graphs showing significant and strong (greater than 0.5 coefficient of determination, R^2) linear relations between discharge and *E. coli,* suspended sediment, turbidity, dissolved oxygen, and specific conductance.

Figure 34. (pages 63–64) —Continued
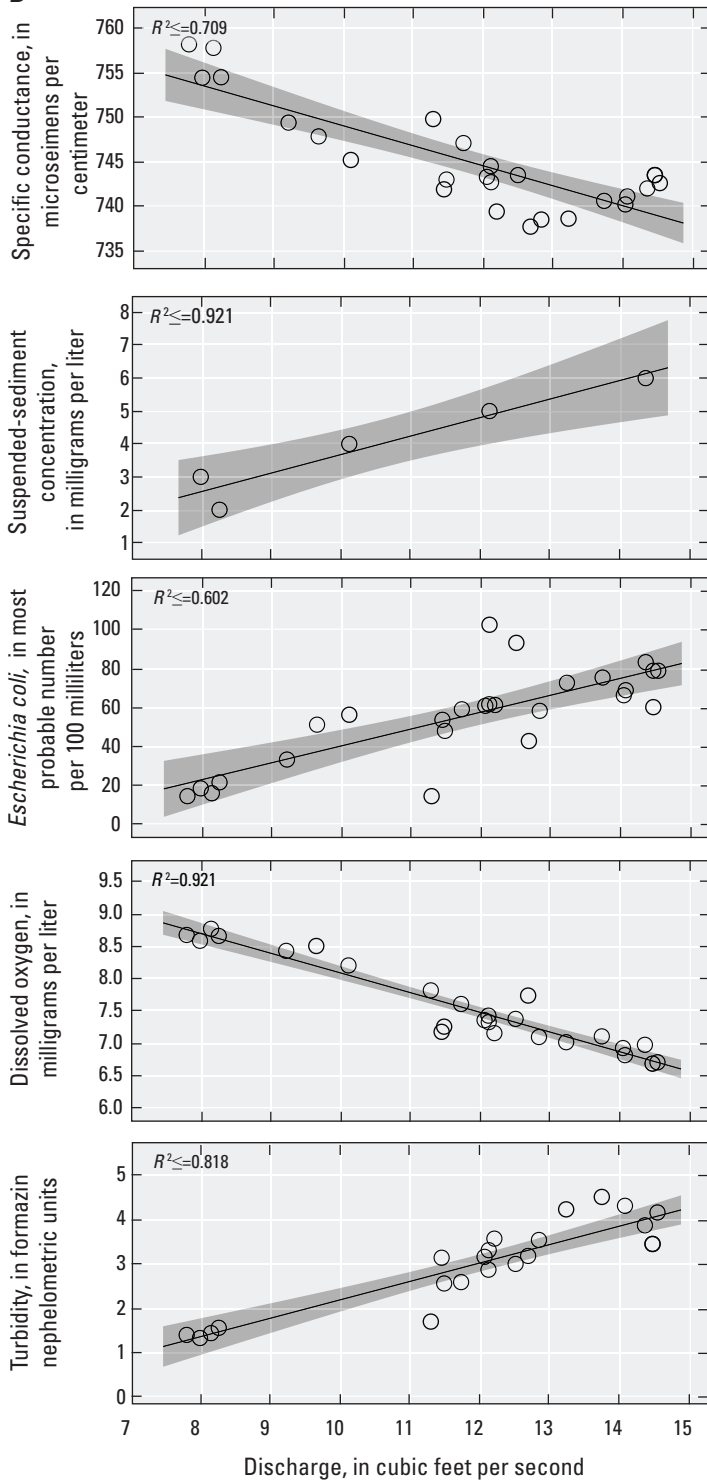
EXPLANATION

▬▬ Ordinary linear regression fit with 95-percent-confidence intervals
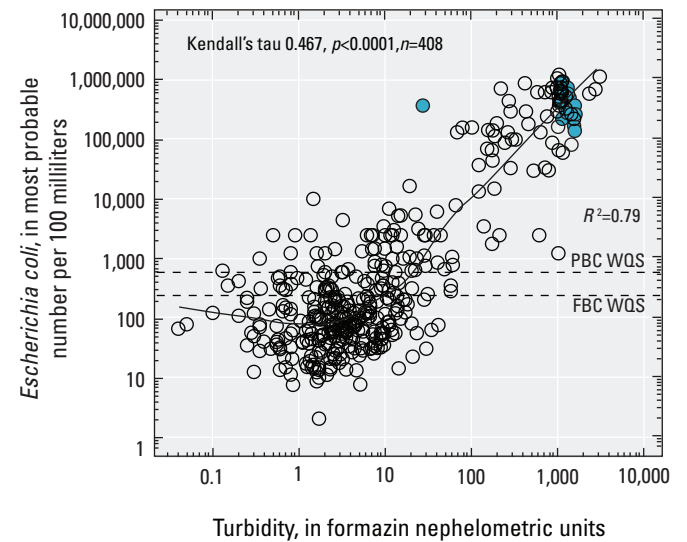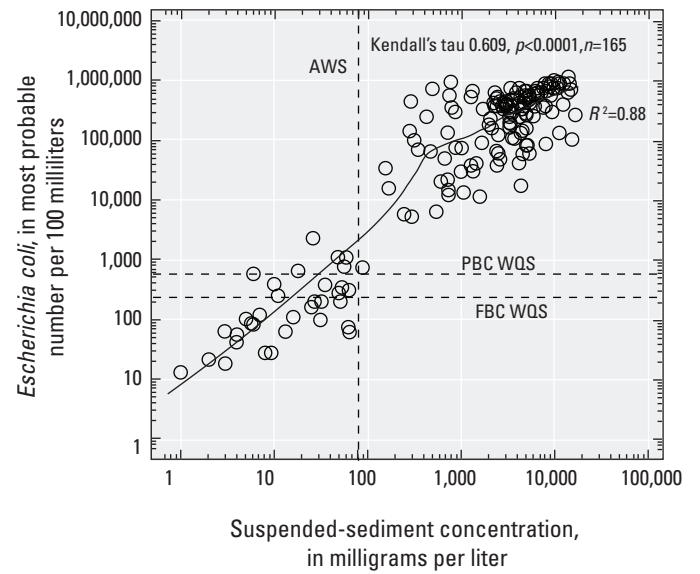
EXPLANATION

▬▬ LOWESS smoothing fit

🔵 21 backscatter measurements plotted using a relation between nephelometric units (in formazin backscatter units)

Figure 35. Graphs showing relations of *Escherichia coli* to suspended sediment and turbidity for watershed division 4 of the Upper Santa Cruz River Watershed, southern Arizona and northern Mexico. A locally weighted scatterplot smoothing (LOWESS) was used to fit the relations, and Kendall's tau and probability (p) are presented for significant relations. n, sample size; R²,coefficient of determination; FBC WQS, full-body-contact water-quality standard; PBC WQS, partial-body-contact water-quality standard; AWS, Arizona warm-water aquatic wildlife standard.

A

B

Figure 36. Graphs showing the percentage of *Escherichia coli* concentrations that were equaled or exceeded in watershed division 4 of the Upper Santa Cruz River Watershed, southern Arizona and northern Mexico. *A*, Graph for previous monitoring and this current U.S. Geological Survey study. *B*, Graph for flooding and baseflow conditions. FBC WQS, full-body-contact water-quality standard; PBC WQS, partial-body-contact water-quality standard. Boxes indicate concentrations greater than the Colilert method reporting limit of 2,420 most probable number per 100 milliliters. *n*, sample size.

Figure 37. (pages 66-67)   Graphs showing time series of microbial-source-tracking (MST) samples collected in watershed division 4 of the Upper Santa Cruz River Watershed, southern Arizona and northern Mexico. *A*, MST time-series graphs plotted from top to bottom as concentrations of suspended sediment, *Escherichia coli*, and MST markers (Rum2Bac, ruminant animal; CowM2, cattle; BacCan, canine; GenBac, general bacteria). *B*, Censored boxplots (generated using Nondetects and Data Analysis for Censored Environmental Data [NADA; Helsel, 2012] for data below the laboratory method detection limit) of MST markers for the monsoon months of June and July, August, and September.
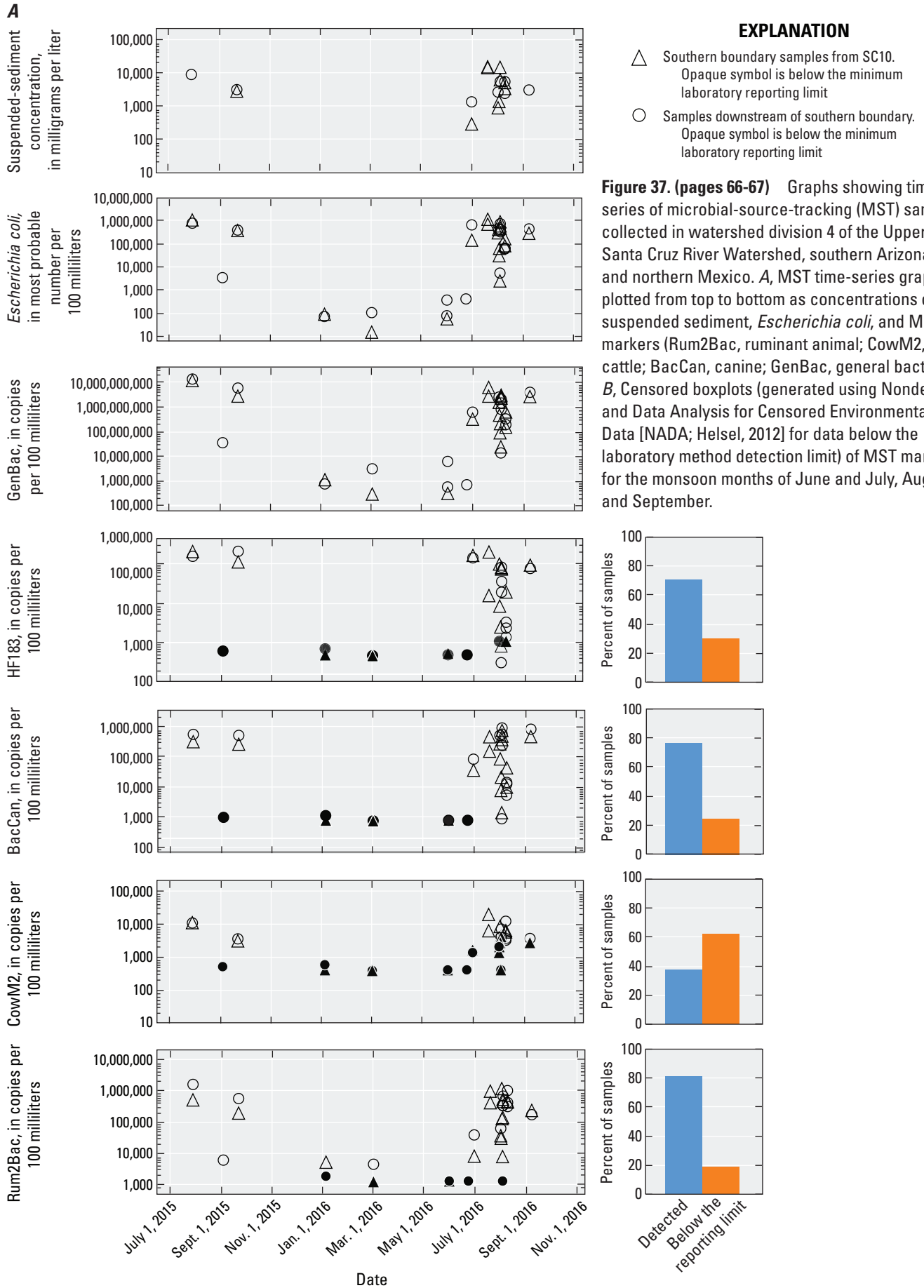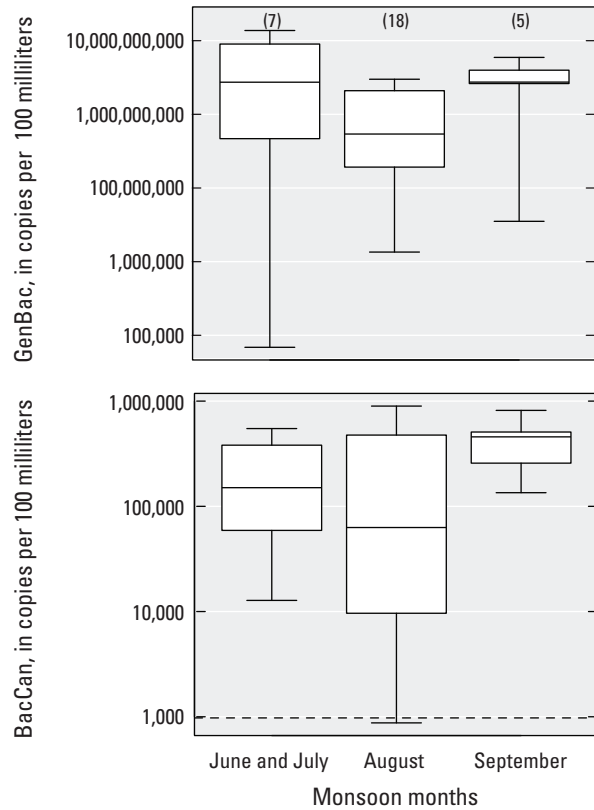
Figure 37. (pages 66-67)   —Continued

Hydrologic Characterization of *E. coli* and Suspended Sediment

Multiple 24-hour sampling events were conducted during different months to measure daily variability and seasonal effects in *E. coli* and suspended sediment concentrations. Automatic samplers were determined to be statistically similar to discrete sampling after collecting samples in March 2015 to test the variability of sampler methods (Paretti and others, 2018). Collections mostly occurred at SC10 and SC14. There was one other early-March 2015 sampler method testing before the mid-March variability study, and other collections were done in December and March of water year 2016, as well as one done at SC11 in June 2016.

Before the March 24-hour methods comparison study, a preliminary March 10-hour collection was done at SC10, and concentrations of *E. coli* exceeded the FBC WQS during the peak of the hydrograph and decreased in linear fashion with decreasing stage (fig. 38*A*). This same base-flow pattern was observed in water year 2016 during December and mid-March 24-hr collections; although discharge was about the same, the December *E. coli* concentrations were four- to five-fold greater than in March. This suggests that discharge is not the only factor explaining concentration, and other factors such as temperature, previous flooding, and subsurface loading might also contribute to seasonal patterns. During the 2016 24-hour collections at SC10, the downstream SC14 was also sampled for *E. coli* for the same duration. The March sampling event was much more variable than December, and the December hydrographs showed very little change in discharge and *E. coli* peak concentration from upstream to the downstream location. Concentrations and overall patterns remained similar between SC10 and SC14 throughout the sampling, indicating little to no loss of discharge or *E. coli* concentration.

The June low-flow 24-hour collection at SC11 was notable because of the extreme variability and random relation between *E. coli* and discharge. All samples exceeded the FBC WQS, and three exceeded the PBC WQS. Additional at-site and upstream samples collected close in time confirmed the high concentrations and supported influence from other sources unrelated to upstream activities. In this dry period, the river is receding during the day and expanding at night when evapotranspiration is reduced. This flow pattern creates a dynamic situation for available aquatic habitat, and pools were the only consistent habitat available, which had the effect of concentrating fish in high densities at certain times of the day. One stud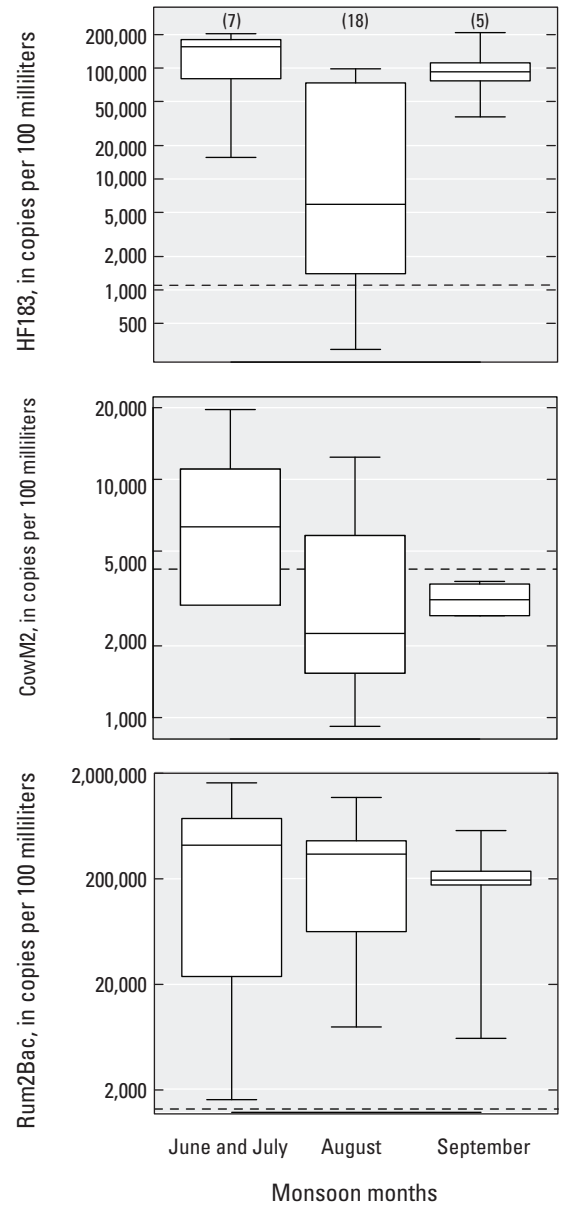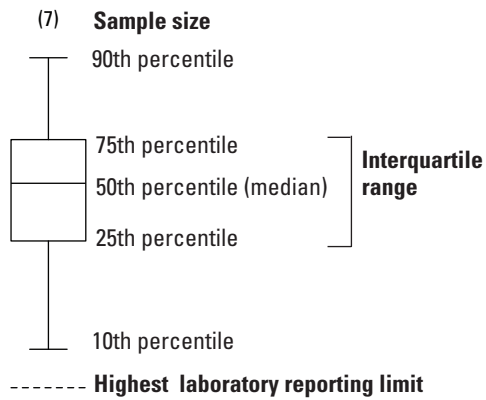y showed that fish are a source of indicator bacteria, and intestinal material from fish will elicit measurable concentrations using the Colilert method (Guillen and Wrast, 2010).

As a semiquantitative measure for the investigation, several western mosquito fish (*Gambusia affinis*) were collected, rinsed with deionized water, and brought back to the laboratory in groups or as individuals. Water that the fish were transported in was processed for *E. coli*, and the intestines of the fish were dissected and the intestinal contents were weighed and mixed with deionized water to be processed for *E. coli* testing. Intestines had average *E. coli* concentrations of 30 MPN/100

mL, and the transport water had *E. coli* concentrations of about 5 MPN/100 mL. This experiment was not designed in a way to test the effect of high fish densities on *E. coli* concentrations in the Santa Cruz River observed at SC11, but it could help to explain the high variability in the results, especially when hundreds to as many as thousands of mosquito fish were concentrating in the pools sampled.

Flooding events were sampled in July (fig. 38*B*), August (fig. 38*C*), September (fig. 38*B*), and once in January (fig. 38*A*). Suspended sediment was also collected at a higher frequency for several events sampled at SC14. During the July flood events, *E. coli* and suspended sediment tracked with discharge but peaked on the rising limb of the hydrograph rather than the peak. Peak concentrations at SC14 were about 900,000 to 1.2 million MPN/100 mL, whereas suspended sediment was generally between 10,000 and 14,000 mg/L. The July and August floods had the greatest concentrations, but the flood duration was less than the floods produced by the two September rainfall events, when flooding sustained longer periods of elevated suspended sediment and *E. coli*, ultimately resulting in a greater total load per event. The one January event sampled over the hydrograph had similar concentrations to the summer events. Like the December base-flow collection, the January *E. coli* concentrations remained consistent between the SC10 and SC14 locations. Consistency between locations during the winter event may be related to less intense, widespread rainfall and cooler temperatures which are characteristics of winter floods.

The discharge relation with turbidity, suspended sediment, and *E. coli* was not linear and had similar curvature and data-scatter issues as other WDs (fig. 39). Hysteresis patterns may be affecting these relations. The *E. coli* data had two primary clusters, one below 1,000 MPN/100 mL and one above that concentration. There was very little relation at discharges less than 25 ft^3/s, but between 20 and 30 ft^3/s an increase occurred of about one to two orders of magnitude. Variability in the *E. coli* precluded the fit of any continuous function with the discharge, but the hydrologic flow-condition classes showed a significant difference between flooding and base-flow samples. Similar to WD2, the summer low-flow condition class (1 to 12 ft^3/s) for *E. coli,* median levels were greater than the other two low-flow classes, reiterating the importance of distinguishing between seasons. There was an order of magnitude increase that occurred from medium flow to very high flow, but *E. coli* concentrations in the higher classes were significantly less than those same classes in WD2, yet discharge was almost three times as much at WD4. The PBC WQS for *E. coli* was commonly exceeded for median levels of the flow-condition classes above the low-flow class (fig. 40*A*). As for the event-based high-frequency sampling (rise, peak, and recession), no differences were observed in the samples collected at various points along the hydrograph during base flow (fig. 40*B*). Flood samples collected during the rise and peak of a flood hydrograph showed significantly greater concentrations of *E. coli* and suspended sediment when compared to samples collected along the recession. Compared to other WDs, the *E. coli* and suspended-sediment concentrations for both base flow and floods in WD4 were more consistent between similar types of flows during the sampling of individual events.
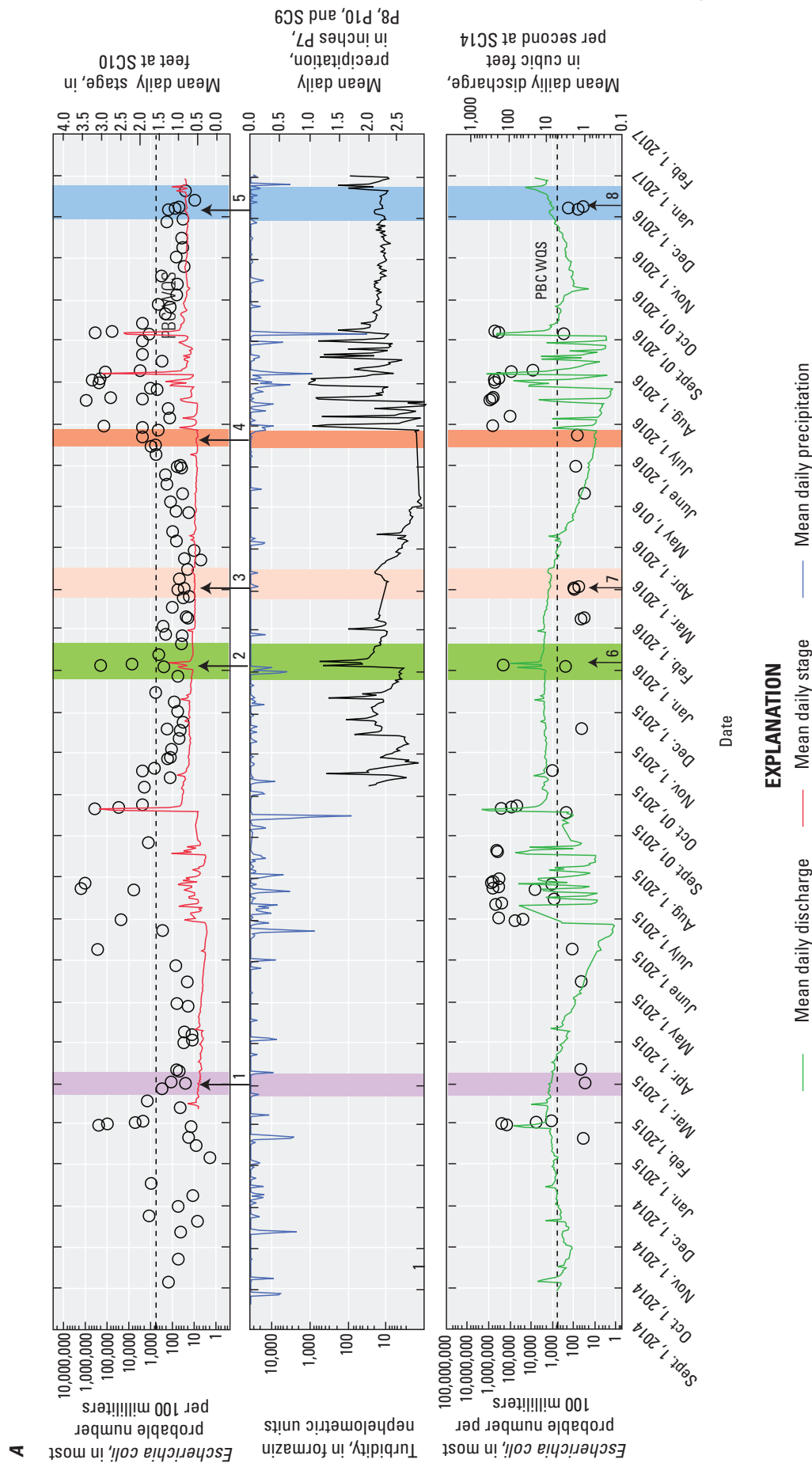
Figure 38. (pages 69–74) Hydrographs of stage plotted with *Escherichia coli* and suspended sediment as 15-minute data for Santa Cruz (SC) River stations in watershed division 4 of the Upper Santa Cruz River Watershed, southern Arizona and northern Mexico. Identical reference graphs are provided showing the time period of the study and annotating each graph in *A*–*C* by number. *A*, Reference graph and graphs for 24-hour automatic sampler collections for spring (1 and 3/7), summer (4), and winter (2/6 and 5/8) of 2016; *B*, Reference graph and graphs for July monsoon of 2015 (9 and 10) and 2016 (11); *C*, Reference graph and graphs for July, August, and September monsoon for 2015 (12 and 13) and 2016 (14/15 and 16). For detailed explanation of station/sample locations see table 1. P, precipitation; FBC WQS, full-body-contact water-quality standard; PBC WQS, partial-body-contact water-quality standard.

Figure 38. (pages 69–74) —Continued

Figure 38. (pages 69–74)   Graphs showing hydrographs of stage plotted with *Escherichia coli* and suspended sediment as 15-minute data for Santa Cruz (SC) River stations in watershed division 4 of the Upper Santa Cruz River Watershed, southern Arizona and northern Mexico. Identical reference graphs are provided showing the time period of the study and annotating each graph in *A*–*C* by number. *A*, Reference graph for graphs for 24-hour automatic sampler collections for spring (1 and 3/7), summer (4), and winter (2/6 and 5/8) of 2016; *B*, Reference graph for and graphs for July monsoon of 2015 (9 and 10) and 2016 (11); *C*, Reference graph and graphs for July, August, and September monsoon for 2015 (12 and 13) and 2016 (14/15 and 16). For detailed explanation of station/sample locations see table 1. P, precipitation; FBC WQS, full-body-contact water-quality standard; PBC WQS, partial-body-contact water-quality standard. —Continued

Figure 38. (pages 69–74) —Continued

Figure 38. (pages 69–74) Graphs showing hydrographs of stage plotted with *Escherichia coli* and suspended sediment as 15-minute data for Santa Cruz (SC) River stations in watershed division 4 of the Upper Santa Cruz River Watershed, southern Arizona and northern Mexico. Identical reference graphs are provided showing the time period of the study and annotating each graph in *A*–*C* by number. *A*, Reference graph for graphs for 24-hour automatic sampler collections for spring (1 and 3/7), summer (4), and winter (2/6 and 5/8) of 2016; *B*, Reference graph for and graphs for July monsoon of 2015 (9 and 10) and 2016 (11); *C*, Reference graph and graphs for July, August, and September monsoon for 2015 (12 and 13) and 2016 (14/15 and 16). For detailed explanation of station/sample locations see table 1. P, precipitation; FBC WQS, full-body-contact water-quality standard; PBC WQS, partial-body-contact water-quality standard.—Continued

Figure 38. (pages 69–74) —Continued

Figure 39. Graphs showing relations of discharge to *Escherichia coli*, suspended sediment, and turbidity for watershed division 4 of the Upper Santa Cruz River Watershed, southern Arizona and northern Mexico. FBC WQS, full-body-contact water-quality standard; PBC WQS, partial-body-contact water-quality standard; AWS, Arizona warm-water aquatic wildlife standard.

E. coli and Suspended-Sediment Flux

In past analyses, the downstream USGS streamgage at SC14 has been used as proxy for discharge in the TUMA (Gwilliam, 2016). Discharge at the southern boundary of TUMA (SC10) has g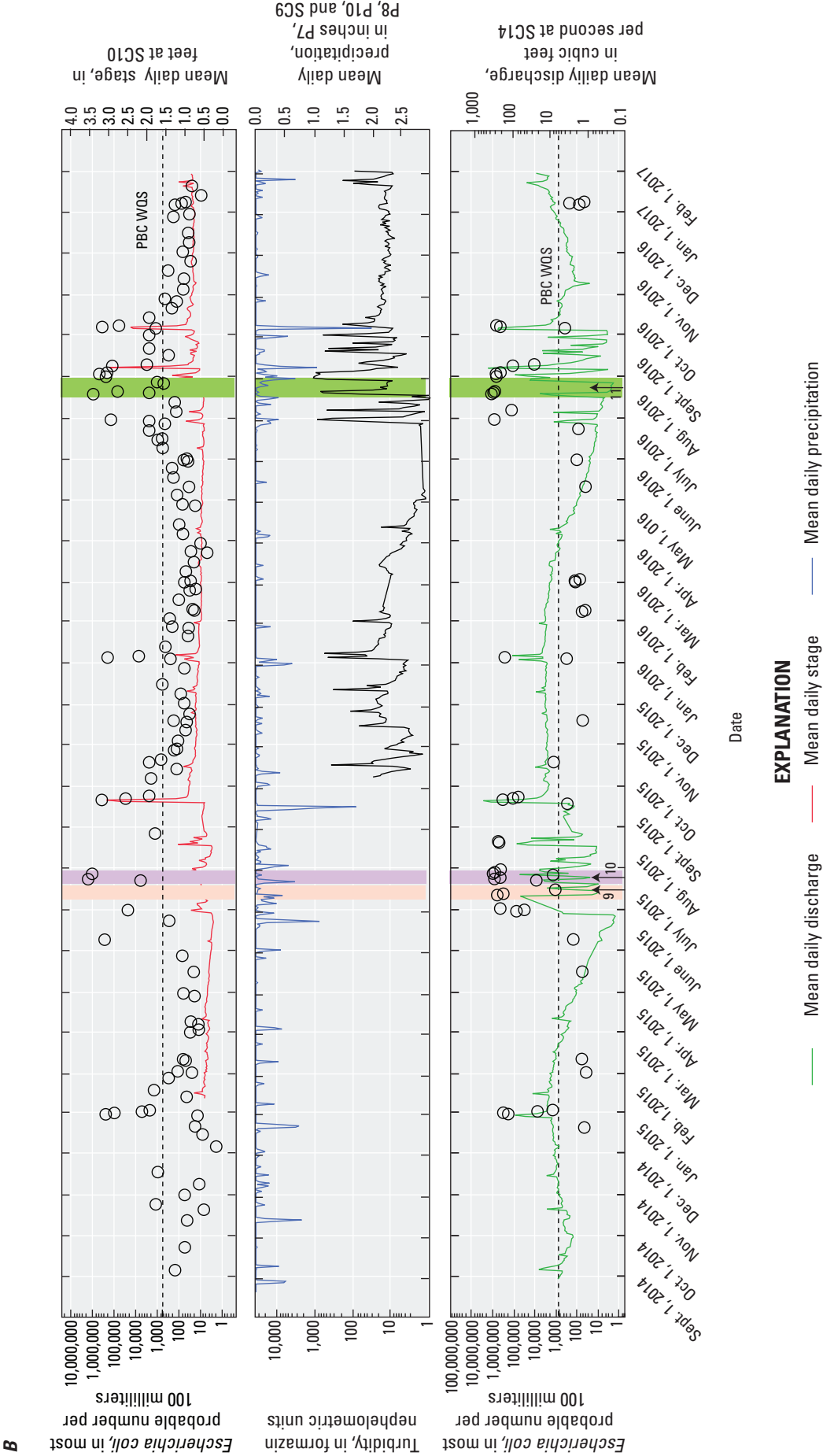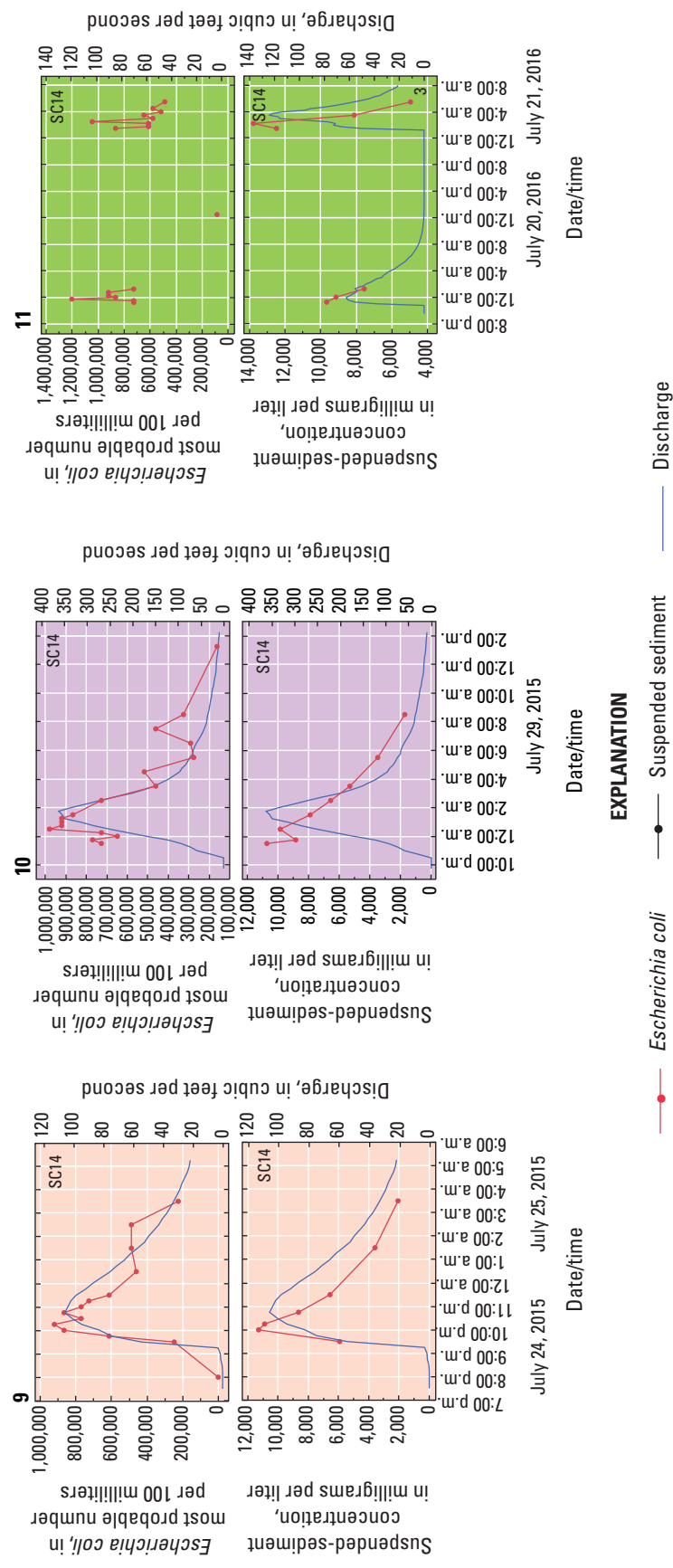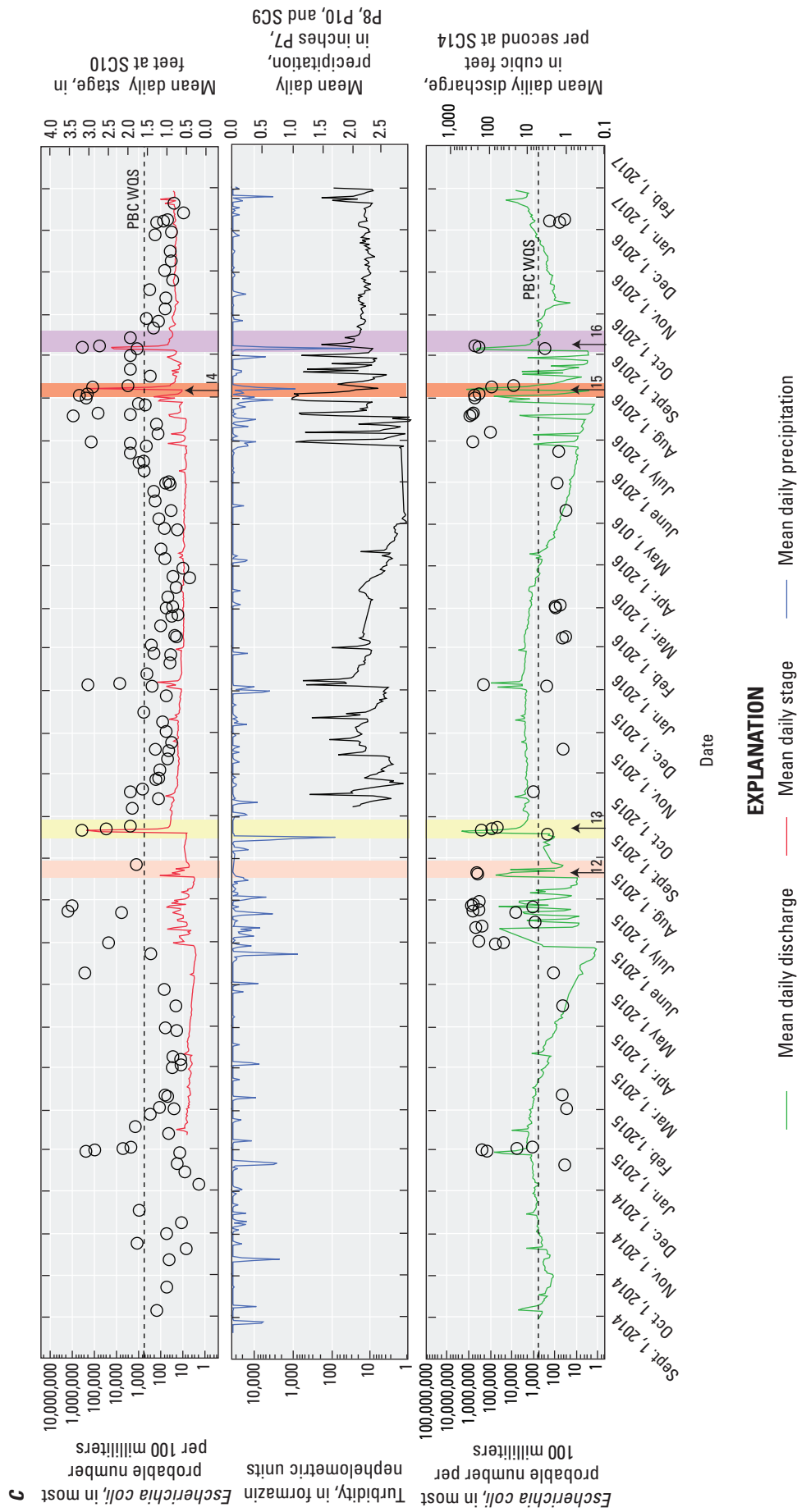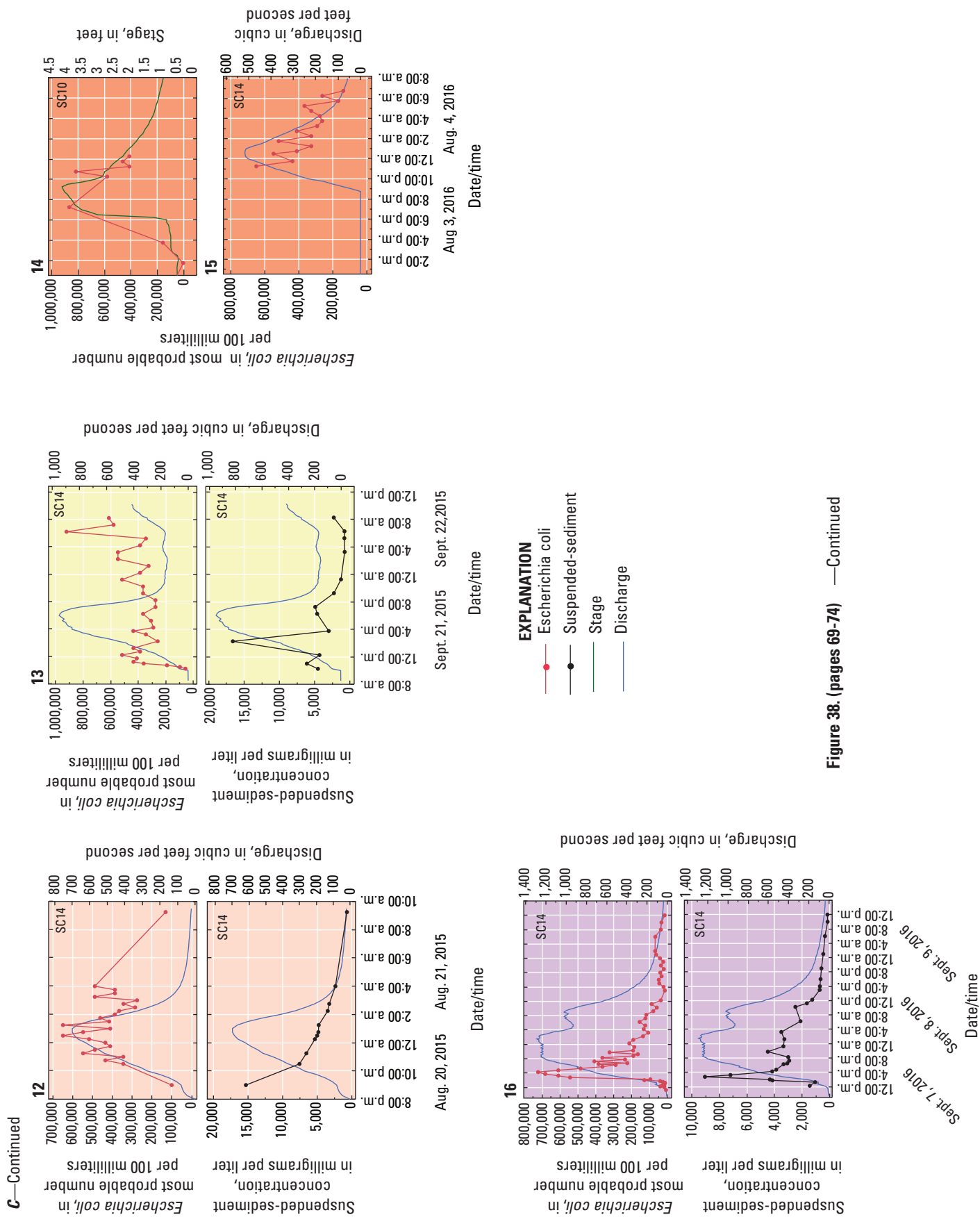enerally been described as a gaining section of the river (Treese and others, 2009). Less than a few miles downstream, the river becomes a losing section of river (Nelson and Erwin, 2001; Treese and others, 2009). This was the status prior to the NIWTP upgrade when water-quality conditions formed a clogging layer, reducing infiltration and extending streamflow further downstream (Treese and others, 2009). Currently, this reach has an active flood plain that is wide with no predominate stream channel, and the streambed substrate is mostly sand, all of which contributes to losing conditions and attenuation of floods, especially during dry conditions before the start of monsoon season. During the study, the attenuation of measured base flow varied greatest between May and August and less so during spring and winter months. Base-flow discharges measured at SC10 and compared to SC14 were on average attenuated by 0 to 25 percent between September and March. Between April and August, measured discharges were attenuated between 30 and 80 percent.

The losing reach within the TUMA affects the magnitude, duration, and shape of flood hydrographs depending on the time of year and antecedent wetting conditions. A time series analysis indicated the lag times between discharge at SC10 and SC14 were about 5 to 6 hours for base-flow conditions. By the middle to late monsoon season, after rainfall saturated the region, these antecedent wetting conditions increased runoff and reduced flood attenuation, and lag times were on average 3 hours between SC10 and SC14. At SC14, the discharge and hydrograph (shape and timing) relations were used to estimate discharge at SC10. For the purposes of estimation, a generalization of the flooding regime and percentage of attenuation was applied to discharge at SC14 to estimate the discharge at SC10. Attenuation was estimated as a ratio of the discharge or stage magnitude between sites. Other than May and June, flooding above 200 ft³/s was treated as non-attenuating with a lag time of about 3 hours between stations. Base-flow discharge between September and March was bounded by an attenuation factor of 5 to 25 percent with a 5-hour lag time. Base-flow discharge between April and August was bounded by an attenuation factor of 30 to 80 percent with a 6 hour lag time. Adjusting SC14 by these criteria and pairing samples with the discharge from the shifted hydrograph was the method used for estimating discharge at SC10 for the purposes of computing flux estimates.

Flux showed a significant increase in *E. coli* and suspended sediment over the period of record. However, this is likely an artifact of a limited number of flood samples collected in the past but also highlights the underrepresentation of flood samples in WD4. *E. coli* and suspended-sediment flux (figs. 41*A*, *B*) was similar between TUMA locations and downstream locations. For all flow conditions, median

A

Turbidity, in formazin nephelometric units

(104) (44) (73) (128) (21) (17) (9) (21) (40)

10,000
1,000
100
10
1
0.1
0.01

Suspended-sediment concentration, in milligrams per liter

(4) (48) (2) (22) (16) (9) (6) (25) (18)

100,000
10,000
1,000
100
10
1

AWS

Escherichia coli, in most probable number per 100 milliliters

(166) (83) (111)(247)(101) (69) (22) (61) (196)

10,000,000
1,000,000
100,000
10,000
1,000
100
10
1

PBC WQS
FBC WQS

Base flow   Flood   Very low flow   Low flow   Summer low flow   Medium-flow   High flow   Very high flow   NC

B

Turbidity, in formazin nephelometric units

(45) (9) (70) (17) (19) (51)

10,000
1,000
100
10
1
0.1

ac   bc   c

Wilcoxon pairwise (rise and peak, p=0.0031)

Suspended-sediment concentration, in milligrams per liter

(3) (4) (47) (23) (60)

100,000
10,000
1,000
100
10
1
0.1

a   a   b

AWS

Wilcoxon pairwise (rise and recession, p=0.0001; peak and recession, p=0.0004)

Escherichia coli, in most probable number per 100 milliliters

(79) (20) (132) (112) (50) (171)

10,000,000
1,000,000
100,000
10,000
1,000
100
10
1
0.1

a   a   b

PBC WQS
FBC WQS

Wilcoxon pairwise (rise and recession, p=0.0026; peak and recession, p=0.0329)

Rise   Peak   Recession   Rise   Peak   Recession

Base flow   Flood

EXPLANATION

(4)   **Number of values**

Outside value—Value is >1.5 and <3 times the interquartile range beyond either end of the box

Largest value within 1.5 times interquartile range above 75th percentile

75th percentile
50th percentile (median)   **Interquartile range**
25th percentile

Smallest value within 1.5 times interquartile range below 25th percentile

a, b, or ab denotes statistical difference; when letters are the same, groups are not significantly different

Figure 40. (page 76)   Boxplots of water-quality parameters and *Escherichia coli* concentrations and related sediment parameters for watershed division 4 of the Upper Santa Cruz River Watershed, southern Arizona and northern Mexico. *A,* Boxplots of daily mean *Escherichia coli,* suspended sediment, and turbidity plotted by general flow condition. *B,* Boxplots of 15-minute *Escherichia coli* and suspended sediment, and turbidity plotted by hydrograph classification grouped by base flow and flood conditions. Significant Wilcoxon pairwise tests are labeled with letters indicating significant differences between hydrologic condition distributions. FBC WQS, full-body-contact water-quality standard; PBC WQS, partial-body-contact water-quality standard; AWS, Arizona warm-water aquatic wildlife standard; NC, not counted.
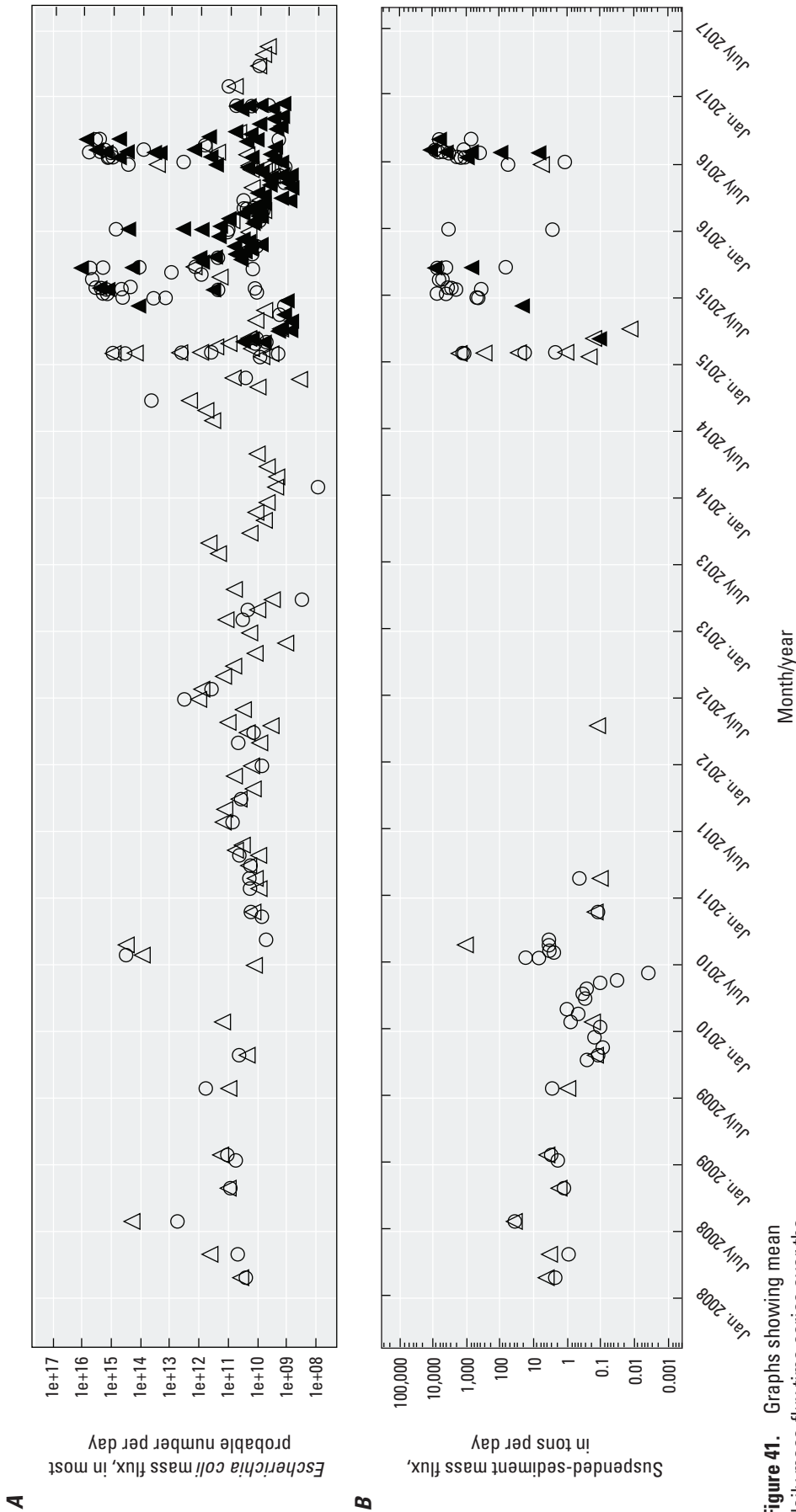
Figure 41.   Graphs showing mean daily mass-flux time series over the entire period of record for watershed division 4 of the Upper Santa Cruz River Watershed, southern Arizona and northern Mexico. A, *Escherichia coli;* B, suspended sediment. TUMA, Tumacácori National Historical Park; for detailed explanation of station/ sample locations see table 1.

EXPLANATION

△ TUMA—SC10, SC11, SC12 samples.

   Opaque shape indicates estimated discharge measurement in the flux calculation

○ Downstream of TUMA—C13, SC14, and SC15 samples

   These are instantaneous flux concentrations converted to a daily mass-flux estimates for comparison to other watershed divisions

concentrations of *E. coli* and suspended sediment were 2.63×10^{10} MPN/day and 7.07 tons/day, respectively. Flood samples were three orders or more of magnitude greater than base-flow flux for both *E. coli* and suspended sediment. The overall *E. coli* (base flow and flood) flux was similar to upstream flux at WD3 and WD2, but suspended sediment was an order of magnitude greater than in WD2. Although suspended sediment increased with downstream distance, the *E. coli* flux did not increase with downstream distance. Suspended sediment was more correlated to the cattle (CowM2) and ruminant (Rum2BAC) MST markers and this increase in suspended sediment with downstream distance may help to explain the increase in these MST marker detections. The WD4 flood samples were significantly lower for both *E. coli* and suspended-sediment flux compared to WD2.

Summary

The southern boundary of TUMA is located at the Santa Gertrudis Lane road crossing and the northern boundary is about 3 miles upstream of the streamgage at SC14 (fig. 1). The riparian corridor is a feature destination for park visitors and TUMA protects the river resources by keeping cattle out, removing trash, controlling nonnative plants, and monitoring water quality. Perennial base flow is sustained by the treated effluent discharged from the NIWTP, otherwise this section of river would be dry for extended periods of the year. As a result, water-quality parameters were similar to the treated effluent flowing from upstream in WD3. Median concentrations of *E. coli*, suspended sediment, and turbidity generally increased with downstream distance and the Tubac streamgage (SC14) had higher median concentrations of *E. coli*, suspended sediment, and turbidity than those measured at the southern park-boundary location (SC10). Agricultural activities downstream of the park likely contributed to these differences.

Several 24-hour base flow and flooding periods were sampled for *E. coli*, suspended sediment, and turbidity during the course of the study to determine the variability, timing, and discharge relation. The high-frequency sampling of base flow demonstrated that during a few sample periods *E. coli* increased several fold over a 24-hour period and exceeded WQS thresholds during hours not generally sampled, such as in the night or early morning. *E. coli* had strong positive relation to suspended sediment. Although relations with discharge and turbidity were less evident, patterns were similar during the high-frequency sampling during base flow and flood

events. The peak of *E. coli* and suspended-sediment concentration occurred in many instances on the rising limb of the flood peak, a factor which might best be considered when determining timing of sample collection during future monitoring. Of all flood samples collected, almost all exceeded both the FBS and PBC WQS standards for *E. coli*, whereas 75 percent of base-flow samples did not exceed the FBC standard. Overall, 50 percent of the samples collected exceeded the FBC WQS and about 30 to 40 percent of the samples exceeded the PBC WQS for *E. coli*. The percent of *E. coli* exceedances of the PBC and FBC standards were similar between the current study and past data collected, confirming that ongoing monitoring efforts were adequately representing WQS exceedances at TUMA, although future monitoring might best consider increasing efforts to collect additional samples and at a higher frequency during off-hours (night and early morning), as well as during floods and for an extended duration post flooding. This type of sampling would help to define the optimal timing of *E. coli* sample collection and the extent of time needed to quantify the duration that *E. coli* concentrations are exceeding WQS thresholds during the entirety of a flood event.

The MST samples collected at the southern park boundary were similar in marker types and concentration magnitude to samples collected downstream of TUMA, suggesting that no significantly new sources were being introduced in between the two river locations. In WD4, the percent detection for the ruminant animal marker was similar to the human marker. Although cattle markers were detected less frequently than other markers, the cattle concentrations at SC10 and SC14 were the highest in the study area, indicating that cattle were a significant source of *E. coli* in TUMA during the study.

The NPS has used the streamgage record at SC14 as a proxy for discharge in the park, but the losing reach within the park affects the magnitude, duration, and shape of flood hydrographs depending on the time of year and antecedent wetting conditions. An analysis of the timing of flood flows between SC10 and SC14 was done, and the approach was applied to estimate discharge of flood flows at SC10 using SC14 streamgage data. Flux was computed for floods using these estimated discharges. Results showed that both estimated and computed flux were the highest on record during the study period, highlighting the lack of historical samples collected during flooding. In the past, the volume of *E. coli* and suspended sediment flowing through the park was likely biased low because of the underrepresentation of flood samples. Future monitoring at SC10 might best include water-stage data and discharge measurements during flooding to further refine the hydrologic relation between SC10 and SC14.

Regional Analysis

To understand the quality of water in the Santa Cruz River flowing through TUMA, the dynamic and complex nature of the upstream area of the watershed must be considered in the context of regional influence on the localized conditions of the park. For more than half of a given water year, water quality in the TUMA river reach is primarily a function of the treated effluent discharged by the NIWTP and the nonpoint source activities between the NIWTP and TUMA, such as free-roaming cattle using the wetted stream channel. WD1 (Upper Santa Cruz River Watershed to NIWTP) and WD2 (Nogales Wash Watershed to Santa Cruz River confluence) streamflow and influences are mostly disconnected from perennial streamflow sustained by the NIWTP discharge at SC6 (WD3, NIWTP to Santa Cruz at Palo Parado Bridge; fig. 2). Depending on the amount and timing of rainfall for the water year, 15 to 20 percent of floodwaters or seasonal flow connect with the perennial section of the river, and these waters generally have high concentrations of *E. coli* and suspended sediment, often at concentrations several orders of magnitude above the WQS thresholds. Several climate and landscape factors affect the timing, duration, amount, and source of *E. coli* and suspended sediment in the flood waters passing through WD4 and TUMA (Santa Cruz River at TUMA southern boundary to Chavez Siding). The primary influence on contaminant mobility is the seasonal rainfall that can be intense and patchy or steady and widespread, causing the region to experience different runoff and erosional processes. Understanding these climatologic differences and the watershed response will help provide the information necessary for predicting the timing, flux, and sources of *E. coli* affecting TUMA.

Seasonal and Hydrologic Patterns

For most of the year, *E. coli* and suspended-sediment median concentrations were similar among the perennial WDs (WD 2, 3, and 4; fig. 42). Base-flow conditions outside of summer were slightly more elevated for *E. coli* in WD3, potentially indicating more nonpoint sources such as cattle in or near the stream. However, the overall median concentrations were about 100 MPN/mL, which is far below the FBC WQS. Seasonal summer flow conditions had the largest influence on *E. coli* during base flow and monsoon floods. Summer base-flow *E. coli* concentrations were an order of magnitude higher compared to other seasons. All WD summer *E. coli* and suspended-sediment concentrations were elevated compared to other seasons, and concentrations in WD2 were highest of all the WDs.

In WD2 and WD4, flow condition classes assigned to samples collected with discharge helped to distinguish important ranges of flow affecting *E. coli* concentrations. Most high-flow samples (flood) exceeded WQS thresholds; samples in the low-flow (summer) and medium-flow condition classes also exceeded WQS thresholds, and this classification

identified a range of nonflooding discharges associated with increasing *E. coli* concentrations. In TUMA, discharge between 12 and 32 ft³/s might best be monitored more frequently in order to validate exceedances in this discharge range and to determine what additional action is needed. This will also help stakeholders and ADEQ identify periods in need of increased monitoring and investigation into potential sources or causes. The largest component of *E. coli* and suspended sediment flowing through TUMA was shown to be predominantly related to flooding, not base flow, and specifically floods originating from WD2. Individual floods measured for *E. coli* at similar points on the rising limb of the same event at WD2 and WD4 showed an order of magnitude reduction in the *E. coli* concentration from upstream to downstream, and on the respective peaks of the hydrograph, less than half of the concentration measured at WD2 was observed at WD4. Although this additional flow was also highly elevated above the WQS for *E. coli* and suspended sediment, the overall reduction suggests that sources from base flow, overland flow, and tributary waters were diluting the contaminated water flowing from WD2, but the waters mixing with the flow coming from WD2 had different composition of MST marker concentrations. Relative to WD2, the proportion of markers detected in WD1 and WD3 was greater for cattle and other ruminants than the human and canine markers. During flooding, the median and maximum instantaneous detections for *E. coli* in tributaries (AF2, PC1, SON2, and JC1) were 5,340 and 22,240 MPN/100 mL, whereas the median concentrations for WD2 were 579,000 MPN/100 mL. Suspended sediment collected during flooding at WD2 was two-fold greater than WD4, and the tributary median instantaneous contribution was almost 700 mg/L, whereas WD2 was 8,070 mg/L. Although infrequent, the widespread flooding associated with winter or tropical storms caused *E. coli* levels in WD2 to be less than downstream WDs.

Season is integrated with several weather-related processes, such as rainfall and flooding, and these factors help to explain *E. coli* and suspended sediment concentrations. The rain intensity, rain duration, and geographical extent were factors that contributed to the differences in WD concentrations. Much of the flooding and water quality WD4 experienced during the study was a function of rainfall characteristics (duration, magnitude, and intensity) occurring in WD2, primarily because of the urbanization and issues with degrading wastewater infrastructure and lack of flooding retention. The relation of seasonal rainfall in WD2 to *E. coli* levels showed a strong relation to rainfall duration, magnitude, and intensity. Although the fall and summer concentrations were similar in magnitude, the duration of fall events were two to four times longer, a finding that has temporal implications for seasonal loading in the Upper Santa Cruz River Watershed. Intensity was more important during summer storms, when concentrations would frequently exceed 500,000 MPN/100 mL for short durations. Specific months were more affected by certain types of events; for example, January, June, and September rainfall events were dominated by longer duration storms, whereas July and August were affected mostly by intense and rapid rainfall
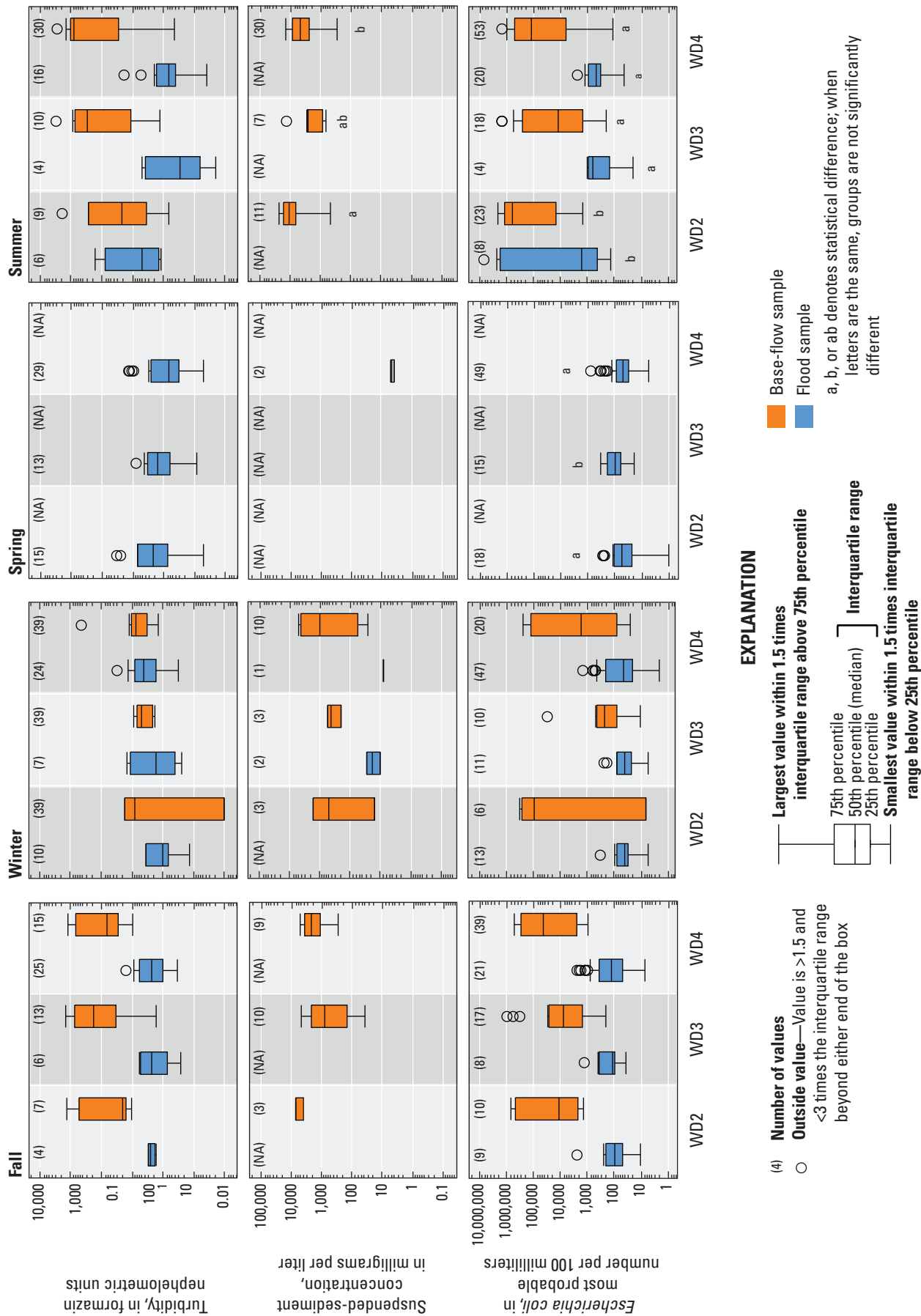
Figure 42. Boxplots of *Escherichia coli*, suspended sediment, and turbidity plotted by season, hydrologic condition, and watershed division (WD) of the Upper Santa Cruz River Watershed, southern Arizona and northern Mexico. WD2, Nogales Wash Watershed; WD3, Nogales International Wastewater Treatment Plant to Santa Cruz at Palo Parado Bridge; WD4, Santa Cruz River at Tumacácori National Historical Park southern boundary to Chavez Siding Road. NA, not applicable.

events. During the study, the fall and winter storms lasted multiple days and were geographically widespread, resulting in a longer flooding durations with wider flood-peak profiles that were multimodal (multiple peaks) in shape. In contrast, the summer convective storms produced short intense downpours often concentrated in a smaller area, and this resulted in short flooding periods with the hydrograph having one or two abrupt peaks.

The timing and progression of rainfall to runoff in the graph of a flood hydrograph profile is presented for three event sequences (rain and hydrograph)—September 2015 (figs. 43*A*, *B*), August 2016 (figs. 44*A*, *B*), and January, 2016 (figs. 45*A*, *B*). The timing and contributions of *E. coli* were tracked along the event progression from upstream to downstream locations. The 2015 and 2016 (not shown) September rainfall events were different in the geographical breadth and intensity compared to the more common monsoon-related July and August events. Remnant tropical moisture off the coast of Baja California can cycle north into already convective conditions and create widespread precipitation. Because September is late in the monsoon season, antecedent conditions from previous rainfall often saturates much of the landscape, creating less infiltration and increased runoff and additional erosion. During the 2015 September event, 1 to 3 inches of rainfall (fig. 43*B*) were observed in many parts of the watershed and over multiple days. This precipitation event translated into a multimodal flood hydrograph (fig. 43*A*), likely from a delayed flow response from the more natural landscape area in contributing drainages to the east and west of the watershed discharging slower than the rapid pulse of runoff from the more central urbanized areas. The *E. coli* levels spiked with the flood peak and the levels mostly correlated with flow magnitude, although there was a large spike later in the hydrograph that was proportionally greater than the rest of the *E. coli*-discharge relation. This *E. coli* peak was possibly related to a sewage source or an ephemeral tributary flowing. As the peak transitioned downstream and additional tributary flow entered the Santa Cruz River mainstem, the flood hydrograph widened and the *E. coli* concentrations decreased. The four elevated spikes of *E. coli* levels observed immediately following the peak at SC14 were likely related to tributary flow pulses from Agua Fria, Peck Canyon Wash, Sonoita Creek, and Josephine Canyon Wash, which all flowed during this event.

The August 2016 event represented a more common monsoon rainfall, although this particular event had greater than normal monsoon rainfall amounts in the major tributaries on the western and eastern sides of the watershed (fig. 45*B*). For tributary locations, AF2, PC1, SON2, and JC1, rainfall fell in amounts not always observed during the monsoon, but the rainfall was intense and localized, which is typical of an event during these months. By comparison, the primary volume of the flood flowed downstream from NW4 to SC14 in about half the time it took during the September event (fig. 45*A*). The *E. coli* levels again correlated with the flood changes in the hydrographs at NW8 and NW4, but the flood shape eventually transitioned from one primary peak to two peaks. This

was again likely related to tributary flow from the Agua Fria, Peck Canyon Wash, Sonoita Creek, and Josephine tributaries, plus reservoir spill over from Patagonia Lake. *E. coli* concentrations at SC14 peaked at a quarter of the concentration observed at NW8, but in the middle of the two discharge peaks of the hydrograph for SC14. This pattern was somewhat unique and could be related to the first yearly widespread runoff or first flush of other major tributaries.

Compared to the summer events, fewer winter events occurred, and as a result there were fewer individual flood-event hydrographs sampled. There was widespread precipitation in January 2016 (fig. 45*B*), but the discharge was less in magnitude and intensity than the September and August flow events. This caused differences in the *E. coli* concentration peak, and it lagged behind or followed the discharge hydrograph, which may be a characteristic of these types of precipitation events (fig. 45*A*). The August event had the concentration peak of *E. coli* occurring on the rising limb of the hydrograph. A common characteristic of NW4 runoff is one or more rapid water-stage spikes caused by intense rainfall in a small area and this will cause multiple feet of stage rise in minutes. These high-velocity floods lose energy quickly after flowing into the wider Santa Cruz River. Contributing flow from the tributaries mixes, and the spikes morph into smoother peaks as waters flowed downstream to SC10 and SC14.

These flood-event hydrographs were presented to demonstrate the timing and pattern of runoff caused by different types of precipitation events. These also convey the complexities of monitoring contaminants in the Upper Santa Cruz River Watershed. Additional monitoring stations would need to be created to fully quantify and characterize *E. coli* and suspended sediment in the watershed.

Trends and Regional Statistical Models

Long-term trends in the region were difficult to assess due to the inconsistent frequency of sampling during different hydrologic conditions. Regionally there did not appear to be a consistent trend over the period of record for *E. coli*, but suspended sediment did show an overall increase over time (Kendall's tau=0.38, *p*-value<0.0001). Splitting the analysis by WDs increased the strength of this trend at WD2 (Kendall's tau=0.54, *p*-value <0.0001), but it remained similar at WD4 (Kendall's tau=0.38, *p*-value<0.0001). Urbanization in WD2 affects erosion and sedimentation in the Upper Santa Cruz River Watershed (Norman and others, 2008, 2009), and urban area in the watershed is predicted to almost double by 2030 (using the 2002 estimate). This growth in urban area will increase landscape erosion, impervious area (such as parking lots and roads), and ultimately the delivery of sediment to stream channels (Norman and others, 2008). The observed trend supported this pattern of increasing suspended sediment with increasing population and urban growth.

Predictive estimation can be useful for multiple applications, such as identifying the potential for exceedances of
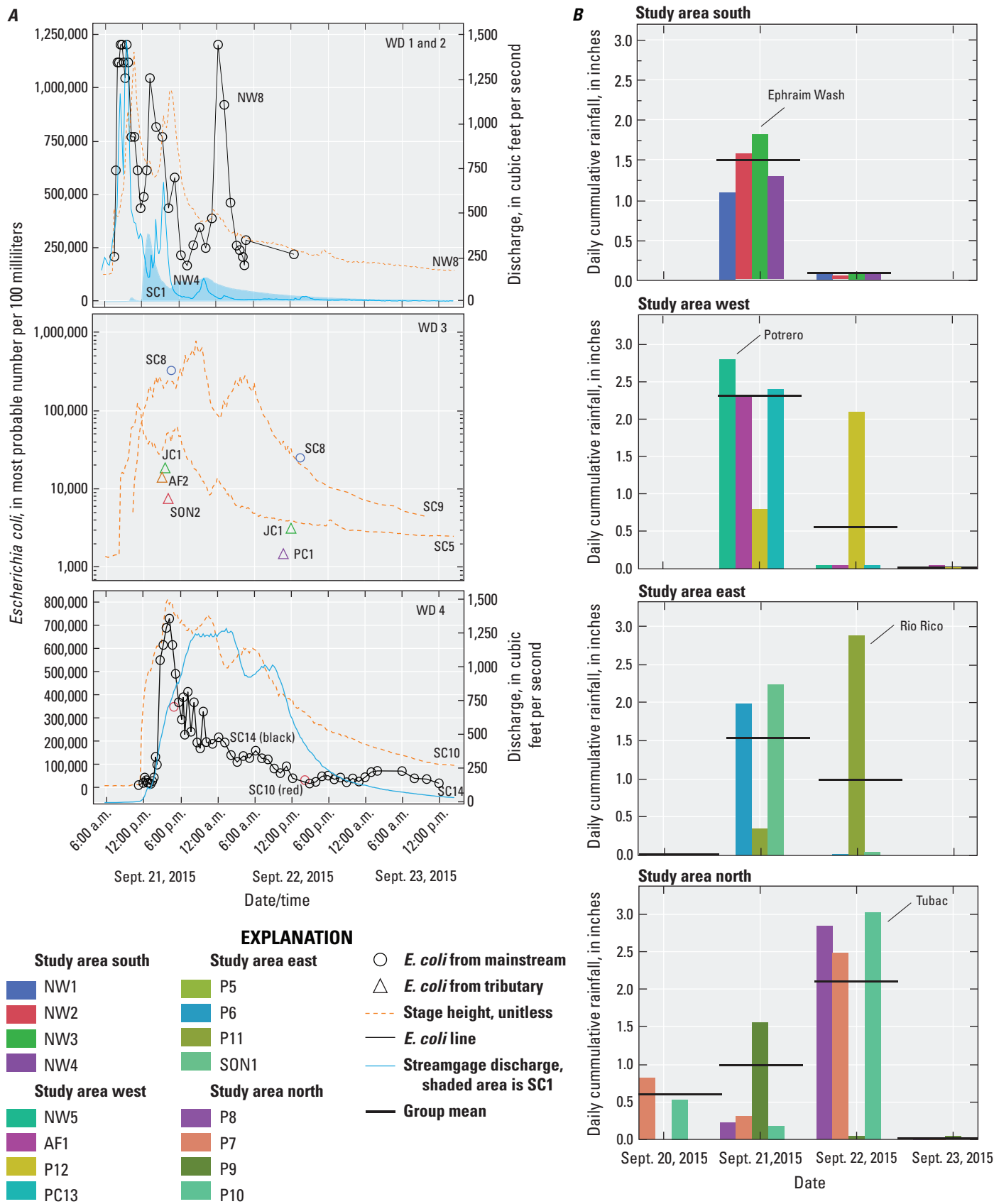
Figure 43.   Graphs showing September 2015 flood event hydrograph progression from upstream to downstream locations in the Upper Santa Cruz River Watershed, southern Arizona and northern Mexico. *A*, *Escherichia coli* (*E. coli*); *B*, rainfall. For detailed explanation of station/sample locations see table 1. WD, watershed division. Station abbreviations—SC, Santa Cruz River; NW, Nogales Wash; AF, Agua Fria Wash; SON; Sonoita Creek; P, precipitation.
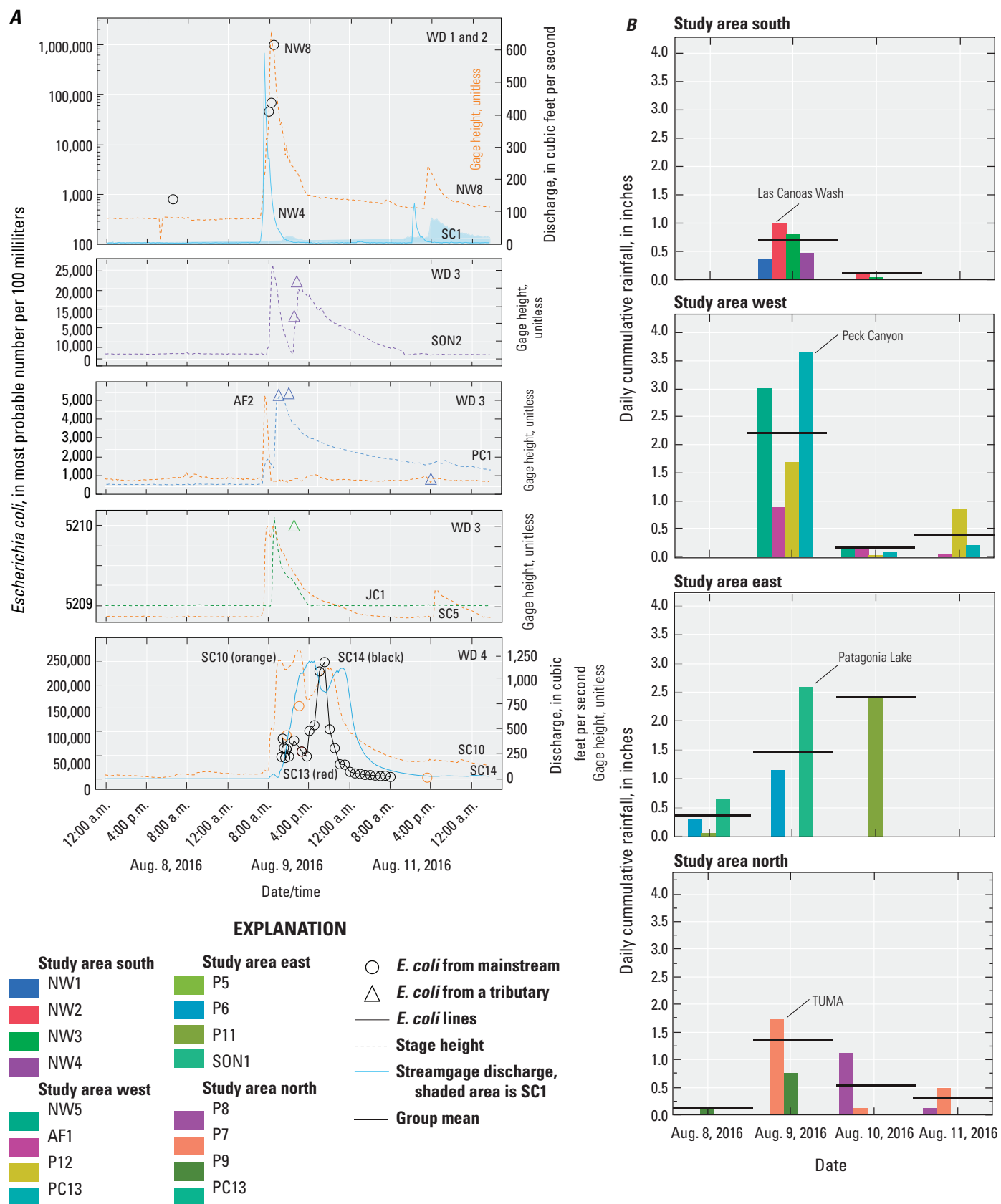
Figure 44. Graphs showing August 2016 flood event hydrograph progression from upstream to downstream locations in the Upper Santa Cruz River Watershed, southern Arizona and northern Mexico. *A, Escherichia coli (E. coli); B*, rainfall. For detailed explanation of station/sample locations see table 1. WD, watershed division; TUMA, Tumacácori National Historical Park. Station abbreviations—SC, Santa Cruz River; NW, Nogales Wash; AF, Agua Fria Wash; SON; Sonoita Creek; P, precipitation.

Figure 45.   Graphs showing January 2016 flood event hydrograph progression from upstream to downstream locations in the Upper Santa Cruz River Watershed, southern Arizona and northern Mexico. *A, Escherichia coli (E. coli); B*, rainfall. For detailed explanation of station/sample locations see table 1. WD, watershed division. Station abbreviations—SC, Santa Cruz River; NW, Nogales Wash; AF, Agua Fria Wash; SON; Sonoita Creek; P, precipitation.

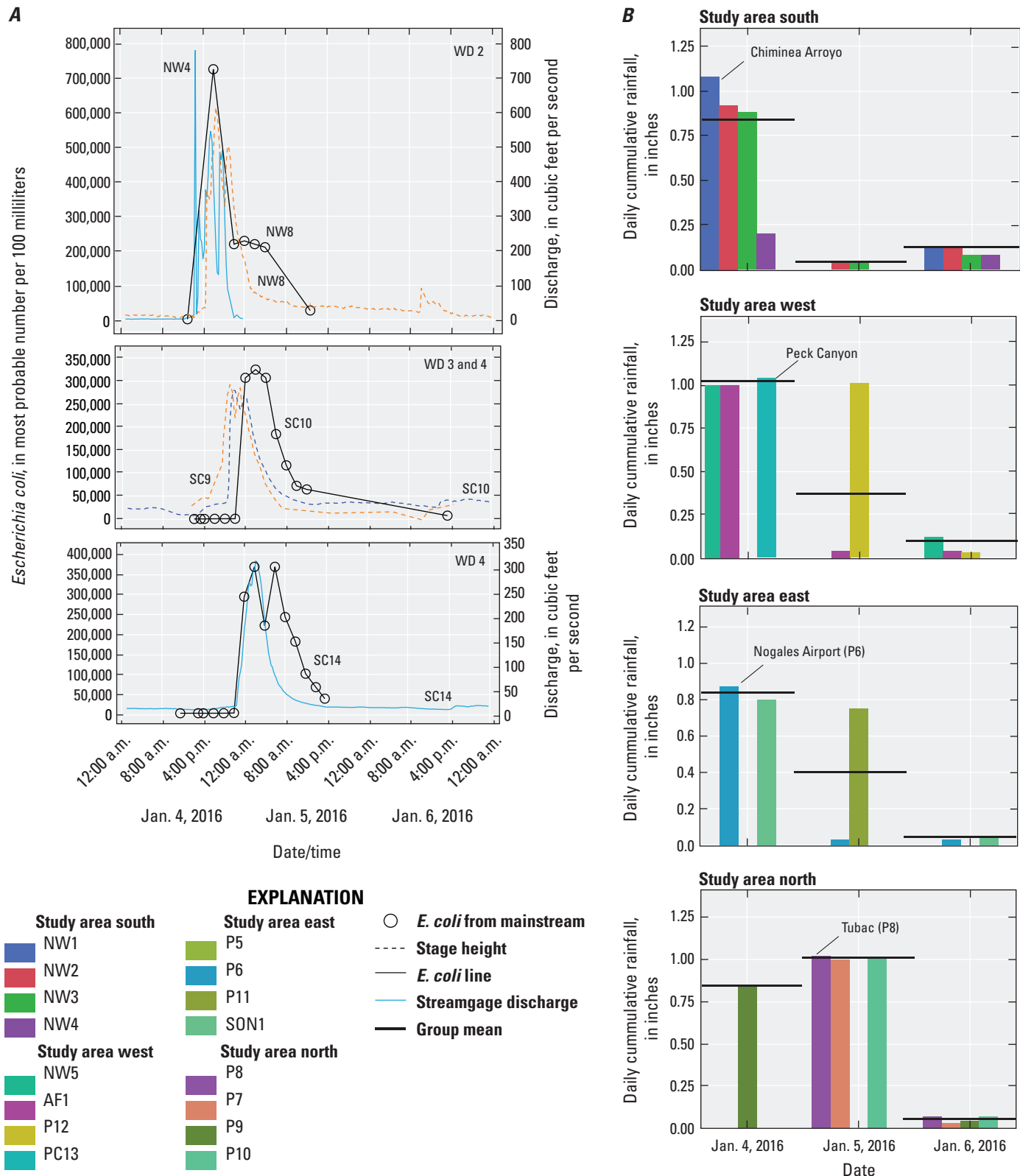health-standards for *E. coli*, improvement of the development of total maximum daily load (the maximum amount of a pollutant allowed in a waterbody) for *E. coli*, and adding to the overall understanding of *E. coli* transport in streams so that consistent methodologies can be applied to other regions of Arizona. Predictive regression models can also be used in real-time monitoring with a surrogate measure, such as turbidity, to predict instantaneous *E. coli* concentrations and loading that can be used to make faster management decisions or warn the public of potential risk. Linear and nonlinear relations were assessed for the individual WD analysis, but sample sizes were too small and variance in the individual WD relations was too high. Regional assessments can provide more robust estimates because of an increased sample size. The *E. coli* response in the WD regression relations were similar, which also suggests combining the data for each WD would lead to an improvement in the regression model.

The intent of this regression analysis was in part to test the potential of developing real-time *E. coli* monitoring at SC14 for the purposes of delivering instantaneous information to TUMA managers for visitor and employee safety. The analysis also serves as a straightforward approach for estimating *E. coli* and suspended sediment anywhere in the Upper Santa Cruz River Watershed. Agencies can use this as an approximation for quickly determining *E. coli* and suspended-sediment concentrations based on other measurements, such as turbidity and discharge, that are easy and cost efficient to collect. There are more sophisticated modeling approaches available, such as probabilistic neural networks and ensemble learning, as well as more continuous approaches such as a rating-curve method implemented in Load Estimator (Runkel and others, 2004) or weighted regressions on time, discharge and season (Hirsh and De Cicco, 2015) that can be used to estimate concentration continuously from daily data, thus enabling a direct calculation of mass flux. This level of model development was beyond the scope of the present study.

Data for the entire study area were compiled and several explanatory variables were explored using a step-wise multiple linear regression procedure for developing regional models to help predict *E. coli* and suspended-sediment concentrations and loads in the Upper Santa Cruz River Watershed, which supplies water to TUMA (table 6, available for download at https://doi.org/10.3133/sir20195108). In addition, seasonal and event-based concentrations were explored using indicator or dummy variables as a means to improve prediction accuracy for different temporal hydrologic conditions. Both mean-daily and instantaneous measurements were analyzed to identify hysteresis effects, and no added benefits were observed by using the mean-daily data. In addition, no obvious hysteresis effects were observed in the regional analysis when using the instantaneous data.

Equations to estimate *E. coli* and suspended sediment concentrations were developed for TUMA using downstream instantaneous USGS Tubac streamgage discharge as a tool for assisting the park in rapid estimation of elevated *E. coli* levels. Equations were also developed for the greater study area that did not include discharge and focused on turbidity as the primary explanatory variable as a way to provide a relatively easy and cost-effective way to estimate *E. coli* and suspended sediment concentrations when discharge data was not available.

In most of the explanatory variable combinations used in the predictive model development, the suspended sediment alone explained more than 80 percent of the variation in *E. coli* concentrations. Turbidity and discharge explained less of the variation in *E. coli* concentrations than suspended sediment and accounted for about 66 to 53 percent of the variation in *E. coli*; however, turbidity serves as an inexpensive proxy for suspended sediment, and the measure is relatively easy to collect. Turbidity models were significantly improved with the inclusion of a hydrologic condition variable (a binary variable: flooding or not flooding). Other variables useful in the prediction of *E. coli* levels were seasonal and hydrologic condition variables that distinguished the summer season and flooding conditions, although those explained much less of the variation compared to suspended sediment or turbidity. Seasonality was tested in the regression modeling using a sine and cosine transformation of the sample date in decimal format. The sine and cosine transformation expresses an annual periodic cycle with an unknown phase offset (Helsel and Hirsch, 2002). The expression for this term is represented as $2\pi T$ or 0.0172 (days) when expressed as days. Water-quality parameters and land-use variables were tested, and temperature and urbanization showed some explanatory ability to predict *E. coli* levels. Overall, the improvement gained with additional variables did not support the use of a more complex model over the simplified turbidity, season, and hydrologic condition regression models. Prediction equation diagnostics and plots are shown in table 6 and figure 46*A* and *B*. The five equations for predicting *E. coli* and suspended-sediment concentration were developed for the entire study area and for TUMA and are as follows:

Study area *E. coli* concentration estimation from a measured suspended sediment concentration

$$C_{E.coli} = 50.4(C_{ss})^{0.958286} \times 10^{Flood \times 0.78678}, \quad (5)$$

where

$C_{E.coli}$	is the concentration of *E.coli* in most probable number per 100 milliters and
C_{ss}	is the concentration of suspended sediment in milligrams per liter
Flood	is a binary variable, 1 for sample collected during flooding conditions or 0 for non-flooding conditions, as defined by discharge greater than or equal to 19 ft³/s (long term 25th percentile)

Study area *E. coli* estimation from a turbidity measurement

$$C_{E.coli} = 291(Turb)^{0.580520} \times 10^{Cos\,DT \times -0.495768} \times 10^{Sin\,DT \times -0.134404} \times 10^{Flood \times 1.20396}, \tag{6}$$

where

Turb	is the turbidity in formazin nephelometric units,
CosDT	is the cosine of decimal date computed as, date in decimal days of the year, (cosine (0.0172×decimal days))
SinDT	is the sine of decimal date computed as, date in decimal days of the year, (sine (0.0172×decimal days))

TUMA *E. coli* estimation from a turbidity and streamgage discharge measurement at TUMA or USGS Tubac streamgage (SC14),

$$C_{E.coli} = 113(Turb)^{0.449698} \times 10^{Cos\,DT \times -0.4444630} \times 10^{S\,in\,DT \times -0.164032} \times 10^{Flood \times 1.58324} \times (Q)^{0.289585}, \tag{7}$$

where

Q	is the discharge in cubic feet per second.

Study area suspended sediment concentration estimation from a turbidity measurement at the Park or USGS Tubac streamgage (SC14)

$$C_{SS} = 5.80(Turb)^{1.05319}, \tag{8}$$

TUMA suspended sediment concentration estimation from a turbidity and streamgage discharge measurement

$$C_{SS} = 1.45(Turb)^{0.911992} \times (Q)^{0.570750}. \tag{9}$$

The *E. coli* concentration estimates for the TUMA equation were biased high for concentrations between 10 and 200 MPN/100 mL. Predicting concentrations exceeding the FBC standard may be less reliable than concentrations exceeding the PBC standard. The suspended sediment model had less variability and estimates were closer to the observed values compared to the *E. coli*. The models explained between 80 and 90 percent of the variation in *E. coli* concentration. Turbidity was most influential in the suspended sediment model but also used discharge to explain 90 percent of the variation in suspended sediment concentration.

A

Figure 46. (pages 86–88)   Graphs showing standard linear-regression relations between *Escherichia coli (E. coli)* and water-quality parameters for the Upper Santa Cruz River Watershed, southern Arizona and northern Mexico. *A*, Graphs of linear-regression relations among concentrations of *E. coli,* suspended sediment, and turbidity and associated multiple linear-regression diagnostic plots of *E. coli* and suspended sediment observed values and residuals versus the predicted values for Tumacácori National Historical Park (TUMA) (equations 6 and 8) and the entire study area (equations 7 and 9). *B*, Graphs of the predicted time series of *E. coli* (top) and suspended sediment (bottom) plotted with the observed values and discharge from the Santa Cruz River at Tubac.

A—Continued

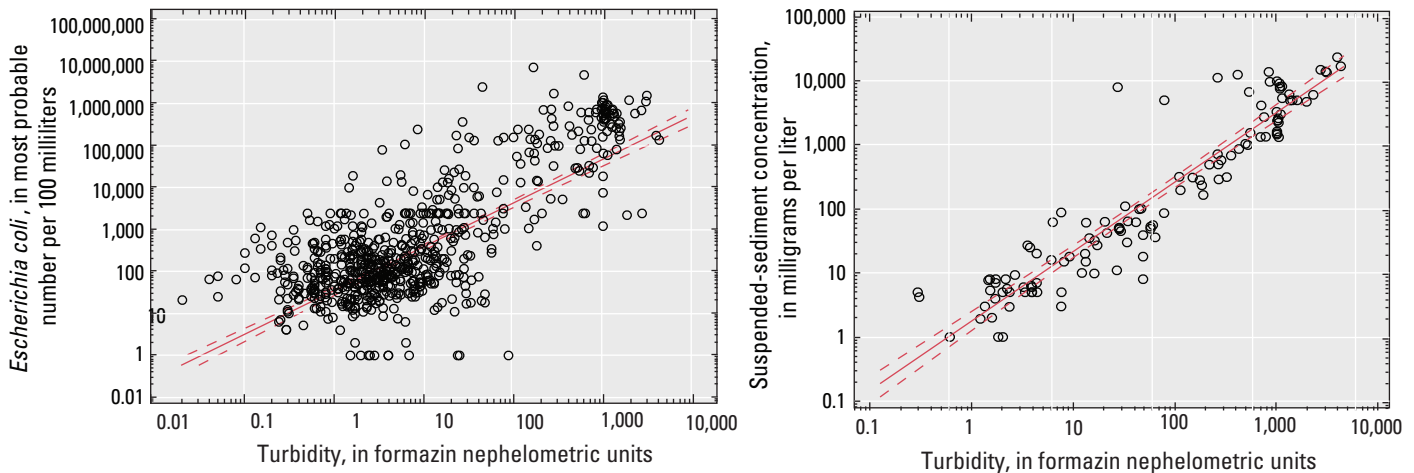**Figure 46. (pages 86–88)** Graphs showing standard linear-regression relations *Escherichia coli (E. coli)* and water-quality parameters for the Upper Santa Cruz River Watershed, southern Arizona and northern Mexico. *A*, Graphs of linear-regression relations among concentrations of *E. coli,* suspended sediment, and turbidity and associated multiple linear-regression diagnostic plots of *E. coli* and suspended sediment observed values and residuals versus the predicted values for Tumacácori National Historical Park (TUMA) (equations 6 and 8) and the entire study area (equations 7 and 9). *B*, Graphs of the predicted time series of *E. coli* (top) and suspended sediment (bottom) plotted with the observed values and discharge from the Santa Cruz River at Tubac.—Continued

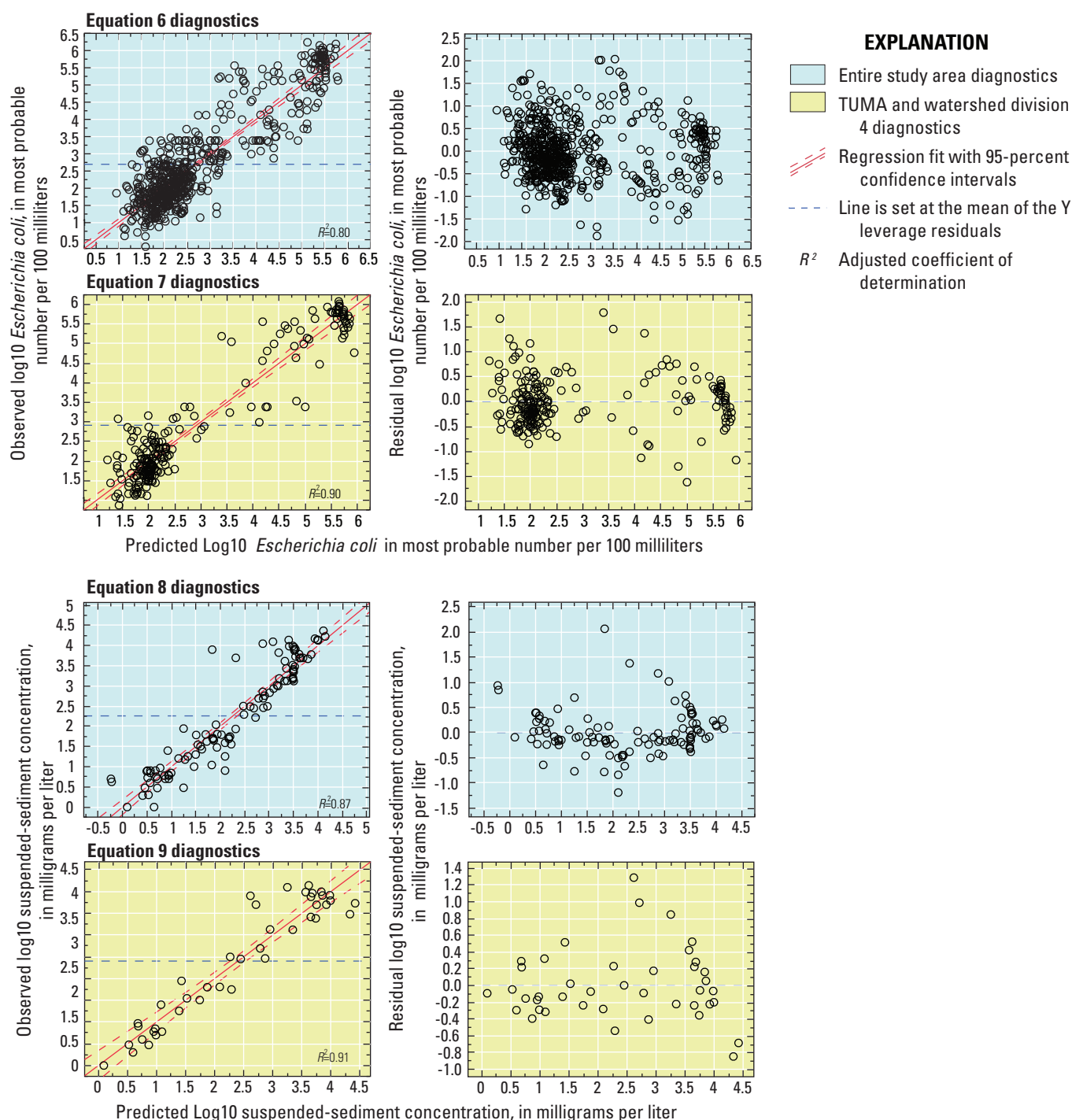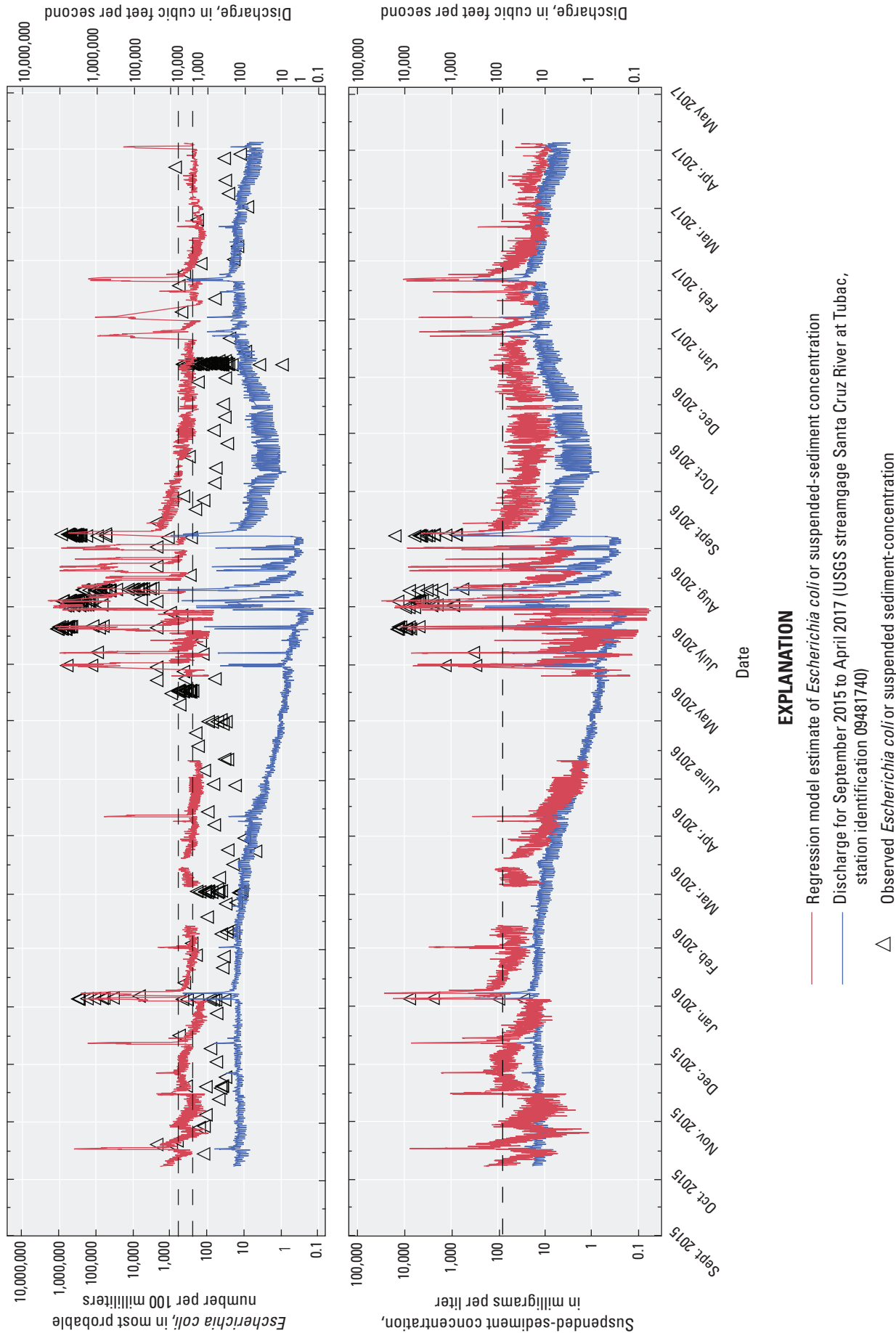**Figure 46. (pages 86–88)** —Continued

Microbial-Source Tracking

The frequency of detection can provide information about the overall contribution of sources affecting each WD. For example, the ruminant (Rum2Bac) MST marker was the most frequently detected marker (greater than 50 percent in all WDs), suggesting cattle and other types of ruminant animals are ubiquitous in the study area and frequently contributing to the *E. coli* levels observed in each WD (fig. 47*A*). Taking both frequency of detection and concentration (fig. 47*B*) into account, ruminant markers showed a pattern of increased contributions with each downstream WD, suggesting additive contributions of sources during flooding events. The percentage of human (HF183) marker was also frequently detected, but mostly in WD2 and WD4, which indicates more of the source originated from WD2 and remained a more constant source from upstream to downstream. The percentage of all marker detections was greatest in WD4 and represented the mixing of *E. coli* sources from upstream to downstream. The GenBac marker was detected in all samples and confirms the general presence and magnitude of fecal contamination. As a result, this marker is very correlated to the measure of total *E. coli* concentration. The median concentration of GenBac is greatest for WD2.

Comparing MST markers to one another showed associations among markers, and similar patterns in the frequency of detection were observed between the HF183 and BacCan MST markers and the CowM2 to the Rum2Bac markers. The concentrations were very correlated between the HF183 and BacCan MST markers (Kendall's tau=0.55, p-value=0.0001) and the CowM2 and Rum2Bac markers (Kendall's tau=0.44, p-value=0.0001). The HF183 marker was also correlated with Rum2Bac but to lower degree of association (Kendall's tau=0.28, p-value=0.0005).

Comparing hydrologic condition distinctly showed that markers in flooding samples were more frequently detected above the method detection limit. Flooding samples had higher concentrations than base-flow samples for all markers, and more often than not base-flow MST marker concentrations were not detected (fig. 47*C*). The only sites above the censoring threshold during base flow were SC8 and SC9 in WD3, which is the WD with the least number of detections overall. The HF183 marker was greatest at NW8 in WD2 but was also high at downstream sites SC9 (WD3), SC10, and SC14 (WD4). The CowM2 marker was greatest at SC10 and SC14, indicating that local cattle sources were contributing to the TUMA river reach during the study (fig. 47*B*). The MST markers were significantly correlated to discharge, suspended-sediment, and turbidity measurements. Suspended sediment was most correlated with ruminant markers (Kendall's tau=0.34, *p*-value=0.003), whereas turbidity showed a stronger correlation to BacCan (Kendall's tau=0.50, *p*-value=0.0001) followed by HF183 (Kendall's tau=0.41, *p*-value=0.001). Seasonal differences were most evident in the winter and spring months sampled (fig. 47*D*). Concentrations of markers were lowest during these months. During months associated with floods, the HF183 marker was an order of magnitude lower in August compared to June/July and September, whereas the Rum2Bac increased

in August. The CowM2 marker was fairly consistent between months, although in the beginning of the monsoon (June/July) the marker was more variable compared to September flooding, possibly a result of less fecal material accumulating on the landscape between runoff events.

One potentially confounding factor to the MST marker results and analysis pertains to the BacCan (canine) marker. Results from analysis of known-source fecal samples showed that the BacCan marker was detected in all cattle fecal samples processed (*n*=4). Methods for these analyses are described in Paretti and others (2018). Although concentrations for BacCan were 2 to 3 orders of magnitude lower than Rum2Bac concentrations in these four cattle samples, they were similar to CowM2 concentrations for the same samples. These results indicate that the specificity of BacCan may have more uncertainty and the elevated BacCan marker concentrations in water-sample analyses have the potential to have been influenced by cattle sources as well as canine. Although the BacCan marker and the HF183 marker were highly correlated, BacCan was inversely correlated with CowM2, suggesting that overall patterns were likely not affected.

The MST multivariate analysis showed a primary gradient of concentration change with flow condition and downstream mixing. A secondary influence of season and MST source was also visually apparent (fig. 48). The nonmetric multidimensional scaling (NMDS) axis 1, from left (quadrants 1 and 3) to right (quadrants 2 and 4), can be described as low concentration, base-flow conditions, and affected by the direct application of chlorine, as shown by the endmember NW8, or influenced by the wastewater treatment plant process, while the right side of the axis is defined by higher concentrations of *E. coli* from human and ruminant sources during flooding conditions. The NIWTP influent had a unique signature and defined the upper threshold of the human-related sources, while samples collected from WD1 and the Santa Cruz River defined an animal-source-related boundary in the NMDS plot. In the middle, tributaries group together, as does a gradient of mixed water samples collected during flooding. This mixing of sources in samples is shown by NW8 samples that mostly plot near the NIWTP influent and as tributary flows and other waters mix downstream, they transition from a more dominantly human source to a mostly cattle-ruminant source.

The MST markers were correlated with axis 2 and caused the upper half of the plot (quadrants 1 and 2) to be defined by human and canine sources and the bottom half (quadrants 3 and 4) to be related to cattle and ruminant sources. This variability or dispersion of samples by location was best shown by Santa Cruz River sites SC9, SC10, and SC14. The dispersion of these samples appeared to be related to timing in the year: June and July samples plotted more with the human and canine source quadrant, and August samples plotted more towards cattle and ruminant sources. This monthly timing of monsoon flow is likely related to the first seasonal flow, or flush (June and July), when there has been accumulation of fecal source material, versus flows later in the season when there is less material available to be transported downstream (August). The lower dispersion of samples and the clustering of tributaries suggests a consistent land-use or watershed-area
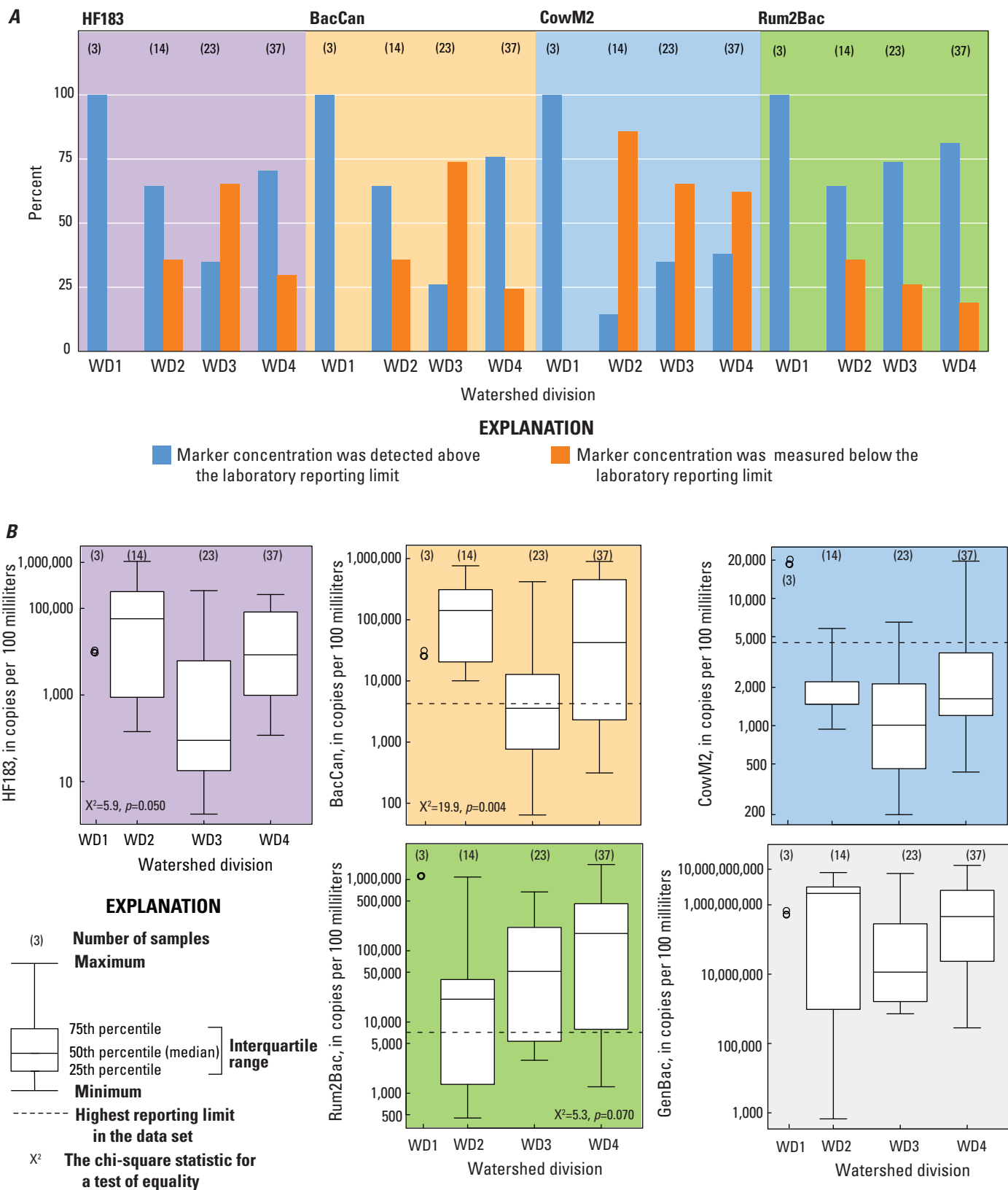
Figure 47. (pages 90–91)   Graph and boxplots of microbial-source-tracking (MST) markers for watershed divisions (WD) in the Upper Santa Cruz River Watershed, southern Arizona and northern Mexico. *A*, Graph showing percent detections of MST markers (HF183, human; Rum2Bac, ruminant animal; CowM2, cattle; BacCan, canine; GenBac, general bacteria). *B*, Censored boxplots (generated using Nondetects and Data Analysis for Censored Environmental Data [NADA; Helsel, 2012] for data below the laboratory method detection limit) of HF183, BacCan, CowM2, and Rum2Bac; GenBac is a regular boxplot. *C*, Censored boxplots of HF183, BacCan, CowM2, and Rum2Bac by hydrologic condition (flooding or base flow); GenBac is a regular boxplot. *D*, Censored boxplots of HF183, CowM2, and Rum2Bac by month(s); GenBac is a regular boxplot. *n*, number of samples.
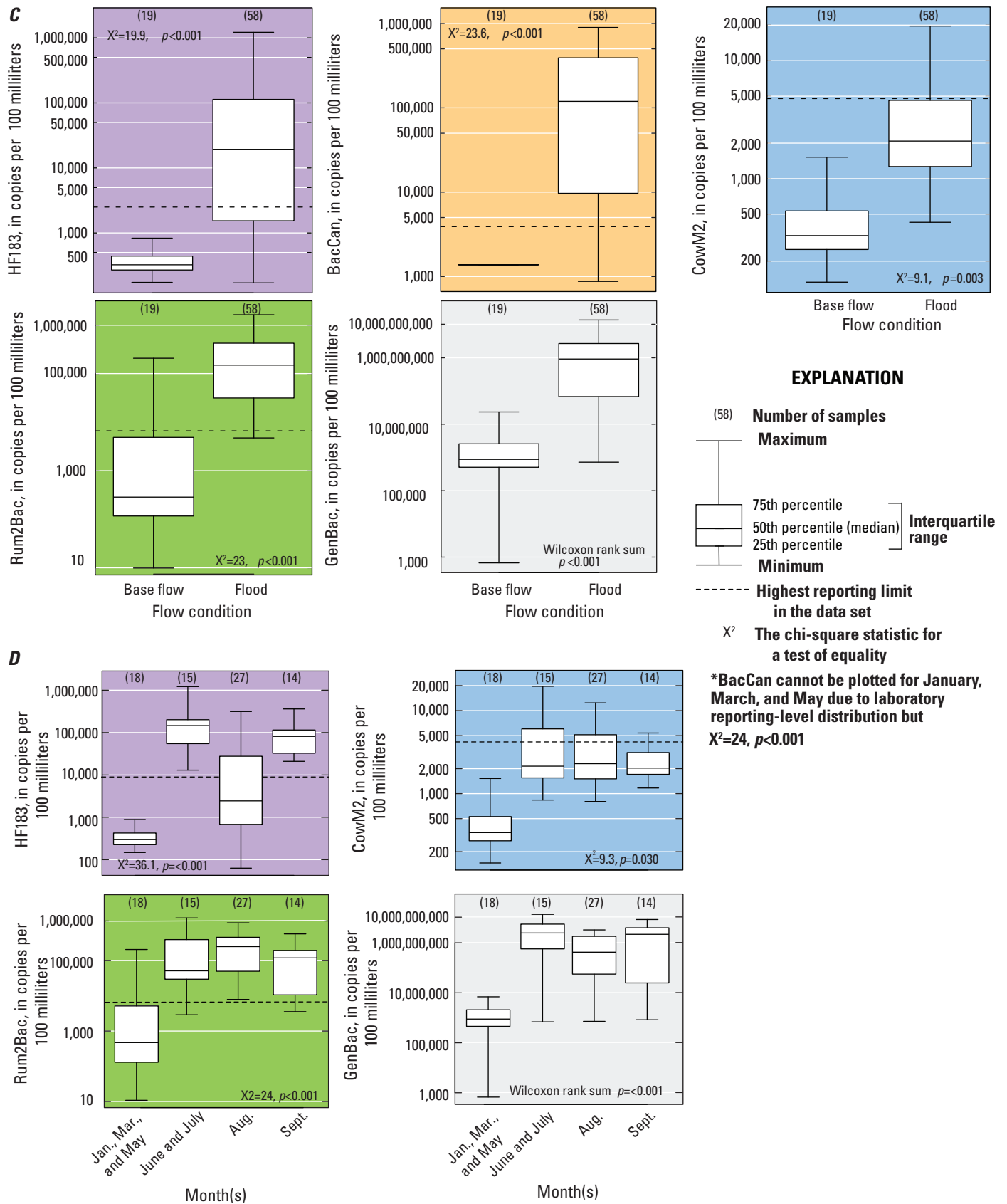
Figure 47. (pages 90–91) —Continued

influence on these ephemeral washes. For example, Peck Canyon Wash samples were more human- and canine-source influenced but plotted consistently near the base-flow samples. Josephine Canyon Wash and Sonoita Creek plotted very closely together, indicating a similar cattle and ruminant signature and with higher concentrations of *E. coli* than Peck Canyon and Agua Fria washes.

The NMDS centroids plot simplifies the representation of MST samples and can be thought of as middle or median of all samples for a site in the multivariate analysis. This helps

to define the boundaries of sources and to better visualize source signatures. These gradients were bounded by marker endpoints defined by SC6, effluent with low human marker only; NIWTP, influent with high human marker; and SC3, with high cattle and ruminant markers. Sites plotting closer to one another or further away in relation to these endpoints will have similar MST signatures. This principle was illustrated by flood samples collected in WD2 that were high in human source markers. As water flowed from Nogales Wash ("NW" sites) down to Santa Cruz River sites in WD3, samples from
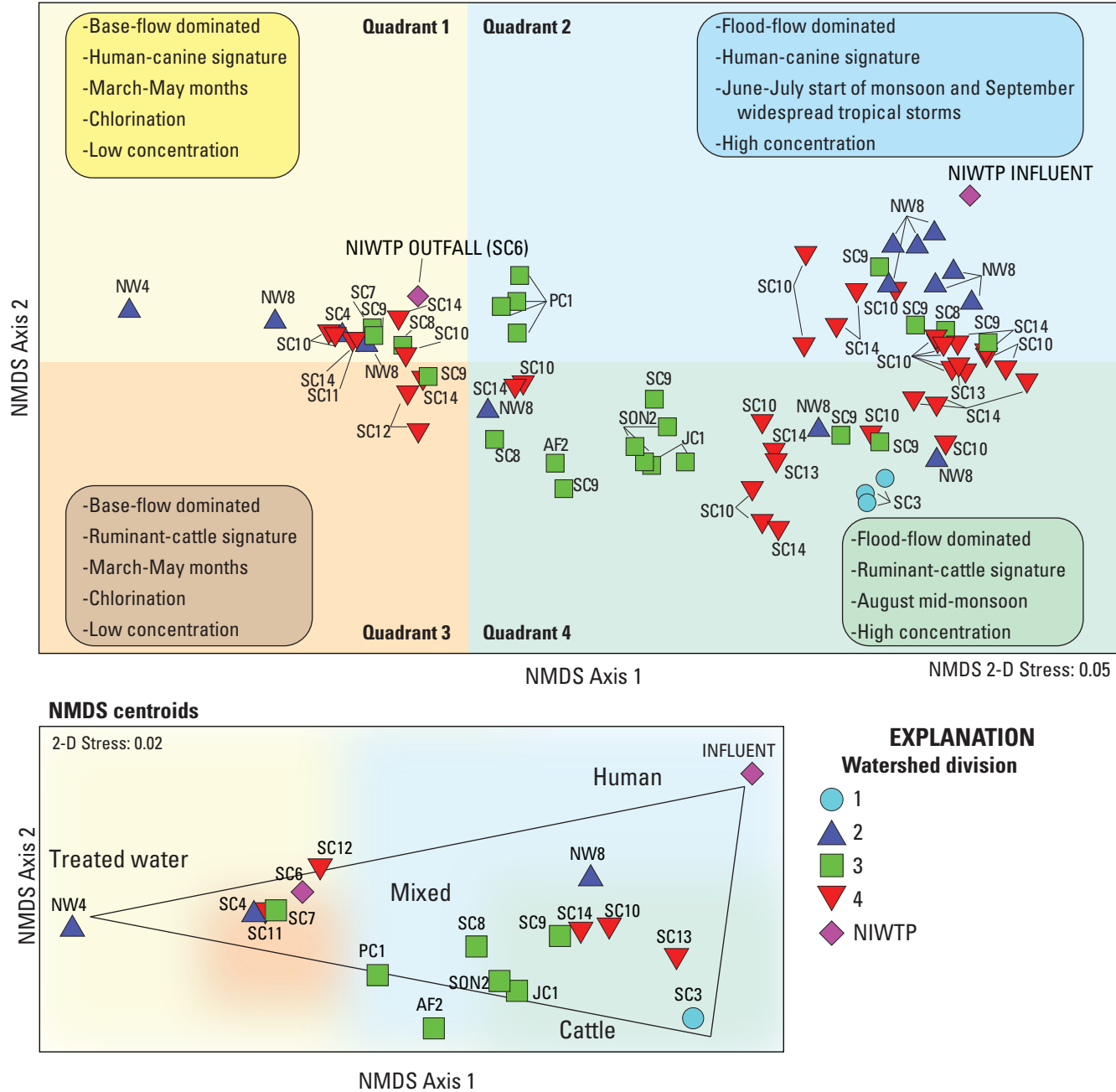
**Figure 48.** Diagram showing nonmetric multidimensional scaling (NMDS) ordination of combined microbial-source tracking (MST) samples color coded by watershed divisions in the Upper Santa Cruz River Watershed, southern Arizona and northern Mexico. The lower NMDS plot is the multivariate centroids for the combined MST marker samples for each station. For detailed explanation of station/sample locations see table 1. Station abbreviations—SC, Santa Cruz River; NW, Nogales Wash; AF, Agua Fria Wash; SON; Sonoita Creek; PC, Peck Canyon Wash; NIWTP, Nogales International Wastewater Treatment Plant. *E. coli, Escherichia coli*; 2-D stress, two-dimensional stress.

sites SC8 and SC9 transitioned to greater levels of ruminant and cattle source markers. Samples from sites SC10 and SC14 contain a mixture of all markers but have a more ruminant and cattle marker influence. Tributaries all carried a similar signature, and human microbial influences appear to not be a major component. Within tributaries, samples at PC1 and AF2 in the western part of the watershed were more like NIWTP-treated water than those at SON2 and JC1 in the east, which carry a greater ruminant and cattle signature. The multivariate analysis provides a representation of commonalties between sites and WDs but also shows different gradients of influence. This type of analysis can help park resource managers and State regulators prioritize potential sources on the basis of the MST signatures of samples. As additional samples are collected, they can be added to the dataset to more clearly define the *E. coli* sources.

Flux and Yields

One of the more important aspects of a comprehensive understanding of *E. coli* and suspended sediment in the Upper Santa Cruz River Watershed is establishing the quantity and scale of the contribution, which requires a quantification of discharge or volume per area from the contributing watershed. Yields were calculated by dividing the constituent daily flux by the area of the contributing watershed at the sample collection site. Concentrations are important when considering recreational exposure and exceedances of WQS, flux is important in the regulatory context of developing total maximum daily loads, and yields can be important when determining locations for remediation efforts (Brown and others, 2004; Bushon and others, 2017; Rasmussen and others, 2008).

The general pattern throughout WDs was that median *E. coli* and suspended-sediment concentrations were roughly similar or were slightly less from upstream to downstream regardless of timing collection. The median *E. coli* and suspended-sediment flux increased slightly between upstream and downstream WDs; however, except for WD1 (significantly lowest flux) the increase was not enough to be significant (figs. 49*A*, *B*). This indicated that, although the volume of water increased downstream, the concentration did not change significantly or the loss of concentration to dilution was replaced by new inputs, ultimately staying unchanged. When flooding conditions were separated, the results showed that much of the suspended sediment delivered downstream was from flooding conditions, and much of it came from WD2. In general, the flux and yield of *E. coli* and suspended sediment was four to six orders greater during flooding compared to baseflow conditions. WD2 had the greatest contribution of suspended sediment per area, which corresponded with the greatest *E. coli* yields of all the WDs.
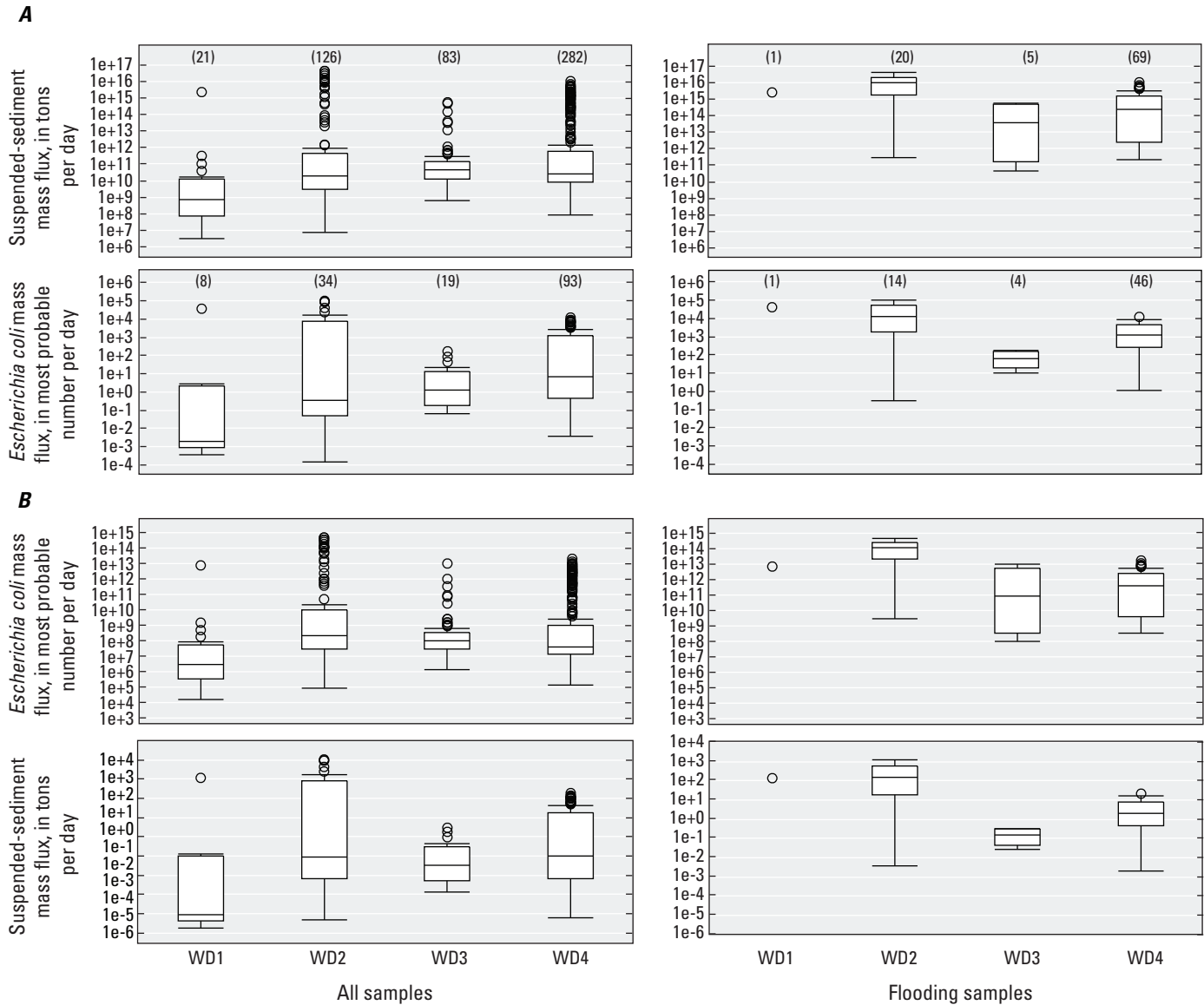
During the study, surface water was connected between WD2 and WD3 about 20 percent of time or roughly 73 days. Including only these days of surface-water connection, the mean annual mass of suspended sediment transported downstream from WD2 was about 20 tons, which was about a quarter ton per square mile. The downstream WD3 averaged less than 0.1 percent of that suspended-sediment transport per square mile, whereas WD4 averaged about 2.05 tons of suspended sediment

transported per square mile. When WD1 flowed to WD3, it contributed more sediment per square mile than WD3 and WD4, but this was for a period on the order of a week or less during the study. WD2 had the greatest suspended-sediment yield, and *E. coli* was about 2.30×10^{13} MPN per square mile, which was two orders of magnitude greater than WD3 and WD4. The similarity in *E. coli* flux and yield between WD3 and WD4, but dissimilarity in suspended sediment, potentially indicates the addition of other sources of *E. coli* that are not associated strictly with runoff-transport mechanisms. For example, inputs from septic fields or *E. coli* hot spots, like those at SC6 where Nogales Wash water flows in the subsurface, concentrate in shallow substrates and increase *E. coli* levels without the proportional increase of suspended fine sediments that would be expected during flooding.

Subsurface-Flow Considerations

Generally, water-quality studies focus on suspended contaminants transported during high flows, and fecal contaminants in bed sediments are typically ignored. However, fecal contaminants in bed sediments need to be considered because of their potential to increase pathogen loadings during high flows that produce bed-load transport (Bradshaw, 2014). Understanding the complexities and dynamic process of *E. coli* loading, persistence, and distribution within the vertical profile of the stream channel was beyond the scope of this study, but some preliminary testing was completed in response to abnormally elevated concentrations observed downstream of NW8 at SC4 where perennial Nogales Wash water meets the dry Santa Cruz River bed and infiltrates into subsurface flow. This section of Santa Cruz River above the NIWTP is a wide sandy channel, and depending on the time of year, water in the form of hyphoreic or subsurface flow can be found at 1 to 2 ft below the dry stream channel. The fine sediments between the sandy substrate interstitial spaces are potentially a large reservoir for *E. coli* and other pathogenic microorganisms. Substrate-attached *E. coli* can survive and persist for months in sediment compared to days in the water column (Garzio-Hadzick and others, 2010; Kiefer and others, 2012; Ishii and others, 2007) and at concentrations typically several fold higher than those overlying in the water column (Anderson and others, 2005; Kiefer and others, 2012). When flooding occurs, the sediments are resuspended and combined with already suspended sediment, and *E. coli* loads are moved downstream.

Mini drive-point piezometers are an effective and rapid approach to monitor groundwater/surface-water exchange processes and sample waters within the hyporheic zone. Mini drive-point piezometers were used to sample waters below the stream channel (about a depth of 2 ft in most cases) at three active stream channel locations—the dry stream channel 2–20 ft from the wetted edge, at the dry-wetted edge interface, and in the middle bed of the stream channel. Sampling details can be found in Paretti and others (2018). Two dry periods were sampled in April and December, each representing a warm and colder period, respectively. The April sampling included the

Figure 49. Boxplots of *Escherichia coli* and suspended sediment for all samples and flooding samples only for all watershed divisions (WD) in the Upper Santa Cruz River Watershed, southern Arizona and northern Mexico. *A*, boxplots of *Escherichia coli* and suspended-sediment mass flux per day; *B*, boxplots of *Escherichia coli* and suspended-sediment yields per square mile.

A. April 2015

B. December 2016

Channel-sample type

EXPLANATION

- Dry-channel sample
- Channel-edge sample
- Mid-channel sample
- Discrete sample

Figure 50. Bar graphs showing hyporheic-zone concentrations of *Escherichia coli* collected at different points along stream cross sections at NW8, SC4, and SC10 in the Upper Santa Cruz River Watershed, southern Arizona and northern Mexico. *A*, April 2015; *B*, December 2016. For detailed explanation of station/sample locations see table 1. SC, Santa Cruz River; NW, Nogales Wash; FBC WQS, full-body-contact water-quality standard; PBC WQS, partial-body-contact water-quality standard; BLS, below land surface; ft, feet.

three locations—NW8, SC4, and SC10 (figs. 50*A*, *B*). NW8 and SC4 were compared to see how Nogales Wash *E. coli* levels were affecting the dry Santa Cruz River stream channel. Concentrations were generally greater at the downstream site SC4 compared to NW8, and concentrations were lowest along the dry stream channel and greatest on the channel wetted edge or within the middle channel bed. The SC4 edge and mid-channel levels were more than two-fold greater than the discrete samples. The SC10 hyporheic levels were much lower than the discrete samples and near the reporting limit. The December samples were only collected at SC4 and SC10 at two depths in the dry channel. Samples were more limited in the December collection, but concentrations were an order of magnitude lower than the April samples. The SC10 location was similar between seasons.

Although the sampling was very limited, there appeared to be a vertical and horizontal gradient with distance from the wetted channel, as well as a seasonal component. The area of the active floodplain is large in the Santa Cruz River near the confluence of Nogales Wash, and depending on the density of *E. coli*, this component of the mass loading in flooding situations may be significant. This could be especially relevant after a breach in the Nogales IOI when loading of *E. coli* into these sediments could be significantly greater. Future studies might best consider examining these sources and to find ways

to monitor them, such as using shallow piezometers. This subsurface source of *E. coli* has the potential to be mobile and enter shallow groundwater systems.

Summary

A 3-year investigation was done by USGS to understand the sources, timing, and distribution of the fecal-indicator bacteria *Escherichia coli* in the Upper Santa Cruz River Watershed as it enters the Tumacácori National Historic Park. The upstream watershed was divided into four watershed divisions based on hydrologic characteristics. Within these four WDs, *E. coli*, microbial-source-tracking markers, suspended sediment, and water-quality parameters were collected at several locations at various temporal scales in order to comprehensively understand the quality of water that flows through the park year-round. Existing data were also compiled and analyzed in relation to the new dataset. The overall findings highlighted the high variability associated with both daily and seasonal *E. coli* levels in the Upper Santa Cruz River Watershed. In addition, hydrology and suspended sediment were found to be the primary determinants of highly variable *E. coli* concentrations and flux. Previous monitoring and studies have been limited

in quantifying these factors when describing *E. coli* in the watershed. This investigation focused efforts on hydrologic-event-based sampling using several water-level stage sensors between streamgages to determine the timing and magnitude of changes in *E. coli* and suspended-sediment concentrations transported downstream. In addition, MST markers were used to understand the sources of the *E. coli* in waters of the Upper Santa Cruz River Watershed. This investigation provides a path forward toward future monitoring and (or) assessments of *E. coli* and a framework for improving collection methods and timing needed to collect data that captures the variability caused by seasonal and hydrologic factors.

For the most part, the section of the Santa Cruz River that flows into Tumacácori National Historic Park is effluent dependent, and base flow is characterized by the water quality of the treated effluent discharged by the Nogales International Wastewater Treatment Plant, plus any additional nonpoint sources such as leaking septic systems or ruminant animals defecating in the stream channel. Watershed divisions WD1 and WD2 streamflow and influences are mostly disconnected from perennial streamflow sustained by the NIWTP discharge. Fifteen to 20 percent of the year, floodwaters or seasonal flow connects with the perennial section of the river, and these waters have highly elevated *E. coli* and suspended sediment concentrations, several orders of magnitude above water-quality standards. Seasonal climate patterns and rainfall runoff were the primary factors that affected the timing, duration, amount, and source of *E. coli* and suspended sediment in floodwaters passing through the park.

Seasonal rainfall events had different temporal and spatial characteristics in runoff processes that resulted in different concentrations and flux from each WD. The Upper Santa Cruz River Watershed receives limited rainfall, mostly during the summer months of July to September, which saturates the sands and clays of the flood plains. The September rainfall produced the longest duration events, with sustained elevated concentrations of both *E. coli* and suspended sediment, partially because of antecedent conditions from previous precipitation. This period is also when the tributaries generally flowed, discharging elevated levels of *E. coli* (above water-quality standards) and suspended sediments into the Santa Cruz River. Because discharge was rarely collected on the tributaries, the yield was not adequately estimated; however, with the frequency and concentrations observed, their impact on the greater hydrologic system is proportionally small in comparison to WD2. Source tracking did show that *E. coli* marker sources from Josephine Canyon Wash and Sonoita Creek tributaries was more likely related to the guts of cattle and ruminants, whereas Nogales Wash had a larger signature from humans and canines, although ruminants were still high. The reason for the human marker sources in WD2 is likely related to breaches at the International Outfall Interceptor, general lack of sewer and infrastructure, and impervious surfaces. The result of those concentrated contaminants was that large pulses of *E. coli* and suspended sediment were transported downstream and eventually flowed through the park any time there

was a precipitation event of multiple inches within a short duration in the upper Nogales Wash Watershed.

Results showed that much of the suspended sediment delivered downstream was from floods, with much of it coming from WD2. In general, the flux and yield of *E. coli* and suspended sediment was four to six orders of magnitude greater during flooding compared to base-flow conditions, and WD2 had the greatest contribution of suspended sediment per area, corresponding with the greatest *E. coli* yields of all the watershed divisions. Regression models were developed to help predict concentrations of *E. coli* and suspended sediment. Understanding the precipitation patterns, resulting rainfall, and eventual runoff and contaminate peak propagation will help in predictive modeling and in determining the timing and amounts *E. coli* moving downstream. Concentration estimation is important when considering exposure related to activities in or near the river and exceedances of water-quality standards. These estimates will help park managers, as well as State agencies and local stakeholders, identify areas where best-management practices and remediation efforts may be most effective.

Unlike approaches used in previous investigations, this investigation holistically described and quantified the distribution, variability, timing, loading, and source of *E. coli* bacteria in the Upper Santa Cruz River Watershed. Furthermore, the hydrologic function and suspended sediment driving the variability of both concentration and source of *E. coli* was analyzed and modeled for future use by Tumacácori National Historical Park managers to determine risk and dispatch safety warnings during conditions of elevated *E. coli*. If new watershed-management activities are implemented in the future, then park resource managers will be able to assess changes using this study as a baseline. Data collection in previous studies has been limited both spatially and temporally and is nonexistent for the contributing ephemeral tributary washes. This investigation sampled hydrologic conditions at many points along the affected waters, as well as multiple points at a single location to characterize rate of change and to quantify the range of variables explaining *E. coli* concentrations, such as season, weather and land-use characteristics. Tributaries have never been monitored for flow frequency or sampled during floods for suspended sediment, *E. coli* concentrations, and source markers. Also, the flow connection between the upper part of the watershed to the perennial section of the Santa Cruz River had never been quantified. With this information, the park will be able to more rapidly respond to the water-quality conditions of waters flowing through the park and this information can be communicated to keep visitors and employees safe.

This dataset, analysis, and interpretation helps to give Tumacácori National Historical Park the ability to discuss management strategies with State and Federal agencies and other stakeholders. Future considerations could involve potential flood mitigation from upstream to slow the rapid pulses of contaminated waters coming from the highly urbanized areas upstream. Other potential possibilities include much needed

repairs to infrastructure, such as the International Outfall Interceptor, and fencing along streambanks to keep cattle out of the stream channel, some of which has already been demonstrated by various groups and agencies working on both sides of the U.S.-Mexico border (Norman, Huth, and others, 2010; U.S. Army Corps of Engineers, 2004), as well as by the park through their local river-restoration management. This study provides a comprehensive understanding of the surface-water hydrology in relation to seasonal precipitation patterns and how those translate into runoff conditions that impact the park with elevated contaminants. The data provided in this investigation provides foundational information that will help the park prioritize and help carry out future best-management actions in order to address these issues.

References Cited

Adams, D.K., and Comrie, A.C., 1997, The North American monsoon: Bulletin of American Meteorological Society, v. 78, no. 10, p. 2197–2214, https://doi.org/10.1175/1520-0477(1997)078<2197:TNAM>2.0.CO;2.

Anderson, C.W., 1998, Turbidity (ver. 2.1, Oct. 2005): U.S. Geological Survey Techniques of Water-Resources Investigations, book 9, chap. A6, sec. 6.7, accessed August 30, 2019, at https://water.usgs.gov/owq/FieldManual/Chapter6/6.7_contents.html.

Anderson, K.L., Whitlock, J.E., and Harwood, V.J., 2005, Persistence and differential survival of fecal indicator bacteria in subtropical waters and sediments: Applied Environmental Microbiology, v. 71, no.6, p. 3041–3048, https://doi.org/10.1128/AEM.71.6.3041-3048.2005.

Anderson, M.J., Gorley, R.N., and Clarke, K.R., 2008, PERMANOVA+ for PRIMER—Guide to Software and Statistical Methods: Plymouth, U.K., PRIMER-E, 214 p.

Anning, D.W., 2003, Assessment of selected inorganic constituents in streams in the Central Arizona Basins study area, Arizona and northern New Mexico, through 1998: U.S. Geological Survey Water-Resources Investigations Report 03–4063, 116 p. [Also available at http://pubs.usgs.gov/wri/wri034063/.]

Arizona Department of Environmental Quality, 2009, Title 18, Environmental quality; chapter 11, Department of Environmental Quality water quality standards; article 1, water quality standards for surface waters: Arizona Department of Environmental Quality, 34 p., accessed November 28, 2018, at http://legacy.azdeq.gov/environ/water/standards/download/SWQ_Standards-1-09-unofficial.pdf.

Arizona Department of Environmental Quality, 2015, 2012/14 Status of water quality—Arizona's integrated 305(b) assessment and 303(d) listing report: Arizona Department of Environmental Quality, 4 p., accessed June 1, 2017, at https://legacy.azdeq.gov/environ/water/assessment/.

Arizona Department of Water Resources, 2017, Statewide groundwater level changes in Arizona—water years 1996 to 2016, 2006 to 2016, and 2015 to 2016: Arizona Department of Water Resources Open-File Report No. 14, June 2017, 30 p. and plates, accessed November 28, 2018, at https://new.azwater.gov/sites/default/files/WL_Change_Report_Final.pdf.

Asociación de Maquiladoras de Sonora, 2013: AMS (Index Nogales): Asociación de Maquiladoras de Sonora website, accessed on July 1, 2018, at http://www.indexnogales.org.mx/.

Aulenbach, B.T., Buxton, H.T., Battaglin, W.A., and Coupe, R.H., 2007, Streamflow and nutrient fluxes of the Mississippi-Atchafalaya River Basin and subbasins for the period of record through 2005: U.S. Geological Survey Open-File Report 2007–1080, accessed November 28, 2018, at https://toxics.usgs.gov/pubs/of-2007-1080/index.html.

Bradley, D.N., 2012, Slope-Area Computation Program Graphical User Interface 1.0—A preprocessing and post-processing tool for estimating peak flood discharge using the slope-area method: U.S. Geological Survey Fact Sheet 2012–3112, 4 p. [Also available at https://pubs.usgs.gov/fs/2012/3112.]

Bradshaw, K., Molina, M., Sullivan, K. and Sidle, R., 2014, Sediment and fecal indicator bacteria loading in a mixed land use watershed: contributions from suspended and bed load transport: American Geophysical Union Fall Meeting, San Francisco, Calif., December 15–19, 2014, accessed July 1, 2018, at https://cfpub.epa.gov/si/si_public_record_report.cfm?dirEntryId=318954.

Broch, M., 2012, NI43-101F1 Technical report feasibility study Sonora, Mexico; El Pilar Project, October 18, 2012: Mercator Minerals, 302 p., accessed on August 1, 2017, at https://secure.kaiserresearch.com/i/jk/tr16/TRML20121018.pdf.

Brown, L.R., Panshin, S.Y., Kratzer, C.R., Zamora, C., and Gronberg, J.M., 2004, Occurrence, distribution, instantaneous loads, and yields of dissolved pesticides in the San Joaquin River Basin, California, during summer conditions, 1994 and 2001: U.S. Geological Survey Scientific Investigations Report 2004–5083, 53 p., [Also available at https://pubs.usgs.gov/sir/2004/5083/.]

Burkham D.E., 1976, Effects of Changes in an Alluvial Channel on the Timing, Magnitude, and Transformation of Flood Waves, Southeastern Arizona, Gila River phreatophyte project: U.S. Geological Survey Professional Paper 655–K, 25 p. [Also available at https://pubs.usgs.gov/pp/0655k/report.pdf.]

Burkham, D.E., 1970, Depletion of streamflow by infiltration in the main channel of the Tucson Basin, southeastern Arizona: U.S. Geological Survey Water-Supply Paper 1939–B, 36 p. [Also available at https://pubs.er.usgs.gov/publication/wsp1939B.]

Bushon, R.N., Brady, A.M.G., Christensen, E.D., and Stelzer, E.A., 2017, Multi-year microbial source tracking study characterizing fecal contamination in an urban watershed: Water Environment Research, v. 89, no. 2, p. 127–143, https://doi.org/10.2175/106143016X14798353399412.

Callegary, J.B., Minjárez Sosa, I., Tapia Villaseñor, E.M., dos Santos, P., Monreal Saavedra, R., Grijalva Noriega, F.J., Huth, A.K., Gray, F., Scott, C.A., Megdal, S.B., Oroz Ramos, L.A., Rangel Medina, M., and Leenhouts, J.M., 2016, San Pedro River Aquifer binational report: International Boundary and Water Commission, 170 p., accessed August 27, 2019, at https://ibwc.gov/Files/San_Pedro_River_Binational%20Report_013116.pdf.

Clarke, K.R., and Gorley, R.N., 2006, Primer v6—User manual/tutorial: Plymouth, United Kingdom, PRIMER-E, Ltd., 190 p.

Coes, A.L., Paretti, N.V., Foreman, W.T., Iverson, J.L, and Alvarez, D.A., 2014, Sampling trace organic compounds in water—A comparison of a continuous active sampler to continuous passive and discrete sampling method: Science of the Total Environment, v. 473–474, p. 731–741, https://doi.org/10.1016/j.scitotenv.2013.12.082.

Condes de la Torre, A., 1970, Streamflow in the upper Santa Cruz River Basin, Santa Cruz and Pima Counties, Arizona: U.S. Geological Survey Water-Supply Paper 1939–A, 26 p. [Also available at https://pubs.usgs.gov/wsp/1939a/report.pdf.]

Constantin de Magny, G., and Colwell, R., 2009, Cholera and climate—A demonstrated relationship: Transactions of the American Clinical and Climatological Association, v. 120, p. 119–28, accessed November 28, 2018, at https://www.researchgate.net/publication/26825605_Cholera_and_Climate_A_Demonstrated_Relationship.

Corkhill, F., and Dubas, L., 2007, Analysis of historic water level data related to proposed assured water supply physical availability criteria for the Santa Cruz Active Management Area—Santa Cruz and Pima Counties, Arizona: Arizona Department of Water Resources Modeling Report No. 18, 48 p., accessed November 28, 2018, at https://new.azwater.gov/hydrology/model-data/analysis-historic-water-level-data-related-proposed-assured-water-supply.

Duan, N., 1983, Smearing estimate—A nonparametric retransformation method: Journal of the American Statistical Association, v. 78, no. 383, p. 605–610.

Durbin, J. and Watson, G. S., 1950, Testing for serial correlation in least squares regression, I, Biometrika, v. 37, no. 3–4, p. 409–428, at http://doi:10.1093/biomet/37.3-4.409.

Garzio-Hadzick, A., Shelton, D.R., Hill, R.L., Pachepsky, Y.A., Guber, A.K., and Rowland, R., 2010, Survival of manure-borne *E. coli* in streambed sediment—Effects of temperature and sediment properties: Water Research, v. 44, no. 9, p. 2753–2762, https://doi.org/10.1016/j.watres.2010.02.011.

Graham, J., 2011, Tumacácori National Historical Park—Geologic resources inventory report: Fort Collins, Colorado, National Park Service, Natural Resource Report NPS/NRSS/GRD/NRR—2011/439, 52 p., accessed November 28, 2018, at https://nature.nps.gov/geology/inventory_embed/publications/reports/tuma_gri_rpt_view.pdf.

Guillen, G., and Wrast, J., 2010, Fishes as sources of *E. coli* bacteria in warm water streams: Houston, Texas, University of Houston Clear Creek, Environmental Institute of Houston, 81 p., accessed November 28, 2018, at https://www.uhcl.edu/environmental-institute/research/publications/documents/10-015guillenetalfishreport.pdf.

Gwilliam, E.L., Filippone, C., and Hubbard, J.A., 2016, Status of climate and water resources at Tumacácori National Historical Park—Water year 2015: Fort Collins, Colorado, National Park Service, Natural Resource Technical Report NPS/SODN/NRR—2016/1293, 30 p., accessed November 28, 2018, at https://science.nature.nps.gov/im/units/sodn/assets/docs/AnnualReports/AR_CW_TUMA_2015.pdf.

Gwilliam, E.L., Raymond, K.L., and Palacios, L., 2014, Streams monitoring at Tumacácori National Historical Park—2011 summary report: Fort Collins, Colorado, National Park Service, Natural Resource Technical Report NPS/SODN/NRDS—2014/743, 15 p., accessed November 28, 2018, at https://science.nature.nps.gov/im/units/sodn/assets/docs/AnnualReports/AR_Streams_TUMA_2011.pdf.

Helsel, D.R., 2012, Statistics for censored environmental data using Minitab® and R (2d ed.): Hoboken, New Jersey, John Wiley & Sons, Inc., 324p.

Helsel, D.R., and Hirsch, R.M., 2002, Statistical methods in water resources—Hydrologic analysis and interpretation: U.S. Geological Survey Techniques of Water-Resources Investigations, book 4, chap. A3, 510 p., accessed November 28, 2018, at https://pubs.usgs.gov/twri/twri4a3/.

Helsel, D., and Lee, L.R., 2006, Analysis of environmental data with nondetects; statistical methods for censored environmental data: Continuing education workshop at the Joint Statistical Meetings American Statistical Association, Seattle, Wash., August 6–10, accessed November 28, 2018, at http://www.practicalstats.com/resources/NADA-resources/NADAforR_Examples.pdf.

Hickin, E.J., 1989, Contemporary Squamish River sediment flux to Howe Sound, British Columbia: Canadian Journal of Earth Sciences, v. 26, no. 10, p. 1953–1963, https://doi.org/10.1139/e89-165.

Hipsey, M.R., Brookes, J.D., Regel, R.H., Antenucci, J.P., and Burch, M.D., 2006, In situ evidence for the association of total coliforms and *Escherichia coli* with suspended inorganic particles in an Australian reservoir: Water, Air, and Soil Pollution, v. 170, no. 1–4, p. 191–209, https://doi.org/10.1007/s11270-006-3010-6.

Hirsch, R.M., and De Cicco, L.A., 2015, User guide to Exploration and Graphics for RivEr Trends (EGRET) and dataRetrieval—R packages for hydrologic data (version 2.0, February 2015): U.S. Geological Survey Techniques and Methods book 4, chap. A10, 93 p., https://dx.doi.org/10.3133/tm4A10.

Hudson Institute of Mineralogy, 2017, Red Mountain Mine (Red Mountain copper prospect; Gem Mine; Carlton property; Ten Grand Mine; Red Mountain project), Red Mountain, Patagonia Mts, Santa Cruz Co., Arizona, USA: Hudson Institute of Mineralogy, mindat.org website, accessed on July 27, 2017, at https://www.mindat.org/loc-53214.html.

Huth, H., 2011, Nogales Wash and International Outfall Interceptor factsheet: Arizona Department of Environmental Quality, Office of Border Environmental Protection, 8 p.

Huth, H., 2015, Border Environment Infrastructure Fund eligibility criteria and management: Arizona Department of Environmental Quality, Office of Border Environmental Protection, 56 p.

Instituto Nacional de Estadística y Geografía, 2010, México—Censo general de población y vivienda 2010: Instituto Nacional de Estadística y Geografía website, accessed November 30, 2018, at http://www3.inegi.org.mx/rnm/index.php/catalog/71/related_materials?idPro=.

Ishii, S., Hansen, D., Hicks, R., and Sadowsky, M., 2007, Beach sand and sediments are temporal sinks and sources of *Escherichia coli* in Lake Superior: Environmental Science and Technology, v. 41, no. 7, p. 2203–2209, https://doi.org/10.1021/es0623156.

Jamieson R., Joy, D.M., Lee, H., Kostaschuk, R., and Gordon, R., 2005, Transport and deposition of sediment-associated *Escherichia coli* in natural streams: Water Reseach, v. 39, no. 12, p. 2665–2675, https://doi.org/10.1016/j.watres.2005.04.040.

Kiefer, L.A., Shelton, D.R., Pachepsky, Y., Blaustein, R., and Santin-Duran, M., 2012, Persistence of *Escherichia Coli* introduced into streambed sediments with goose, deer and bovine animal waste: Letters in Applied Microbiology, v. 55, p. 345–353, https://doi.org/10.1111/j.1472-765X.2012.03296.x.

King, K.A., Zaun, J.Z., and Velasco, L.A., 1999, Contaminants as a limiting factor of fish and wildlife populations in the Santa Cruz River, Arizona: Phoenix, Ariz., U.S. Fish and Wildlife Service, Region 2 Contaminants Program, 66 p., accessed November 28, 2018, at https://catalog.data.gov/dataset/contaminants-as-a-limiting-factor-of-fish-and-wildlife-populations-in-the-santa-cruz-river-ariz.

Konrad, C.P., 2011, Environmental flow allocation and statistics calculator: U.S. Geological Survey Open-File Report 2011–1166, 46 p., accessed November 28, 2018, at https://pubs.usgs.gov/of/2011/1166/.

LaBrie, H., 2016, The potential impacts of the Nogales International Wastewater Treatment Plant on the Santa Cruz River, Arizona: University of Arizona, M.Sc. thesis, 65 p., accessed November 28, 2018, at https://arizona.openrepository.com/arizona/handle/10150/621145.

Lawrence, S.J., 2012, *Escherichia coli* bacteria density in relation to turbidity, streamflow characteristics, and season in the Chattahoochee River near Atlanta, Georgia, October 2000 through September 2008—Description, statistical analysis, and predictive modeling: U.S. Geological Survey Scientific Investigations Report 2012–5037, 81 p., accessed November 28, 2018, at https://pubs.usgs.gov/sir/2012/5037/pdf/sir2012-5037.pdf.

Lee, L., 2015, Package 'NADA'—Nondetects and data analysis for environmental data, version 1.5–6: The Comprehensive R Archive Network website, accessed December 2016, at https://cran.r-project.org/web/packages/NADA/NADA.pdf.

Liang, X., Liao, C., Thompson, M.L., Soupir, M.L., Jarboe, L.R., and Dixon, P.M., 2016, *E. coli* surface properties differ between stream water and sediment environments: Frontiers in Microbiology, v. 7, no. 1732, 10 p., https://doi.org/10.3389/fmicb.2016.01732.

Mayo, J.P., 2017, Supplemental stream-stage, discharge, and *Escherichia coli* datasets used in the assessment of water quality at Tumacácori National Historical Park and the Upper Santa Cruz River, 2009–2017: U.S. Geological Survey data release, https://doi.org/10.5066/F73776ZN.

Mayo, J.P. and Paretti, N.V., 2018, Supplemental regression model data, estimated discharge data, and calculated flux and yields data used in bacterial indicators and microbial source tracking study at Tumacácori National Historical Park and the Upper Santa Cruz River, Arizona (1994-2017): U.S. Geological Survey data release, https://doi.org/10.5066/P93YD8XX.

McAndrew, R.M., 2011, A study of groundwater transport in the effluent-dominated reach of the Santa Cruz River, Arizona: University of Arizona, M.Sc. thesis, 140 p., accessed November 28, 2018, at https://arizona.openrepository.com/arizona/handle/10150/202763.

McOmber, T., 2014, Water quality assessment of the Santa Cruz River in southern Arizona: University of Arizona, Department of Soil, Water, and Environmental Science, Masters thesis, 86 p., accessed November 28, 2018, at https://arizona.openrepository.com/arizona/handle/10150/319998.

Miller, J.R., and Orbock Miller, S.M., 2007, Contaminated rivers—A geomorphological-geochemical approach to site assessment and remediation: London, Springer, Dordrecht, 418 p.

Murphy, J., Farmer, J., and Layton, A., 2016, Water-quality data and *Escherichia coli* predictions for selected karst catchments of the upper Duck River watershed in central Tennessee, 2007–10: U.S. Geological Survey Data Series 1003, 17 p., https://doi.org/10.3133/ds1003.

Myers, D.N., Stoeckel, D.M., Bushon, R.N., Francy, D.S., and Brady, A.M.G., 2007, Fecal indicator bacteria (ver. 2.1, May 2014): U.S. Geological Survey Techniques of Water-Resources Investigations, book 9, chap. A7, sec. 7.1, accessed November 28, 2018, at https://water.usgs.gov/owq/FieldManual/Chapter7/7.1.html.

Nabhan, G.P., and Holdsworth, A.R., 1998, State of the Sonoran Desert biome—Uniqueness, biodiversity, threats and the adequacy of protection in the Sonoran Bioregion: Tucson, Ariz., The Wildlands Project, p. 36–38.

National Invasive Species Council, 2015, Invasive Species Advisory Committee white papers and recommendations 2006–2015: Washington D.C., U.S. Department of the Interior, Office of the Secretary, 52 p., accessed November 28, 2018, at https://www.doi.gov/sites/doi.gov/files/uploads/isac_white_papers_2006-2015.pdf.

National Park Service, 2013, Sonoran Desert Network information brief—The vanishing Santa Cruz River: National Park Service, Intermountain Region Inventory and Monitoring Program, 2 p., accessed October 1, 2017, at https://science.nature.nps.gov/im/units/sodn/assets/docs/briefs/InfoBriefDrySCRiver.pdf.

National Park Service, 2016, Tumacácori's timeline: National Park Service web page, accessed on December 5, 2016, at https://www.nps.gov/tuma/learn/historyculture/timeline.htm.

Nelson, K., and Erwin, G., 2001, Santa Cruz Active Management Area—1997–2001 hydrologic monitoring report: Arizona Department of Water Resources Hydrology Division, 44 p., accessed November 28, 2018, at https://new.azwater.gov/sites/default/files/HMR_SantaCruzAMA_97_01.pdf.

Niraula, R., Norman, L.M., Meixner, T., and Callegary, J.B., 2012, Multi-gauge calibration for modeling the semi-arid Santa Cruz Watershed in Arizona-Mexico border area using SWAT: Air, Soil and Water Research, v. 5, p. 41–57, https://doi.org/10.4137/ASWR.S9410.

Nistor, C.J., and Church, M., 2005, Suspended sediment transport regime in a debris-flow gully on Vancouver Island, British Columbia: Hydrological Processes, v. 19, p. 861–885, also available at https://doi.org/10.1002/hyp.6743.

Norman, L.M., 2007, United States-Mexican border watershed assessment—Modeling nonpoint source pollution in Ambos Nogales: Journal of Borderlands Studies, v. 22, no.1, p. 79–97, https://doi.org/10.1080/08865655.2007.9695670.

Norman, L.M., Caldeira, F., Callegary, J., Gray, F., O' Rourke, M.K., Meranza, V., and Van Rijn, S., 2012, Socio-Environmental health analysis in Nogales, Sonora, Mexico: Water Quality, Exposure, and Health, v. 4, no. 2, p. 79–91, https://doi.org/10.1007/s12403-012-0067-x.

Norman, L.M., Feller, M., and Guertin, D.P., 2009, Forecasting urban growth across the United States-Mexico Border: Computers, Environment and Urban Systems, v. 33, no. 2, p. 150–59, https://doi.org/10.1016/j.compenvurbsys.2008.10.003.

Norman, L., Guertin, D., and Feller, M., 2008, A coupled model approach to reduce nonpoint-source pollution resulting from predicted urban growth—A case study in the Ambos Nogales Watershed: Urban Geography, v. 29, no. 5, p. 496–516, https://doi.org/10.2747/0272-3638.29.5.496.

Norman, L.M, Huth, H., Levick, L., Shea Burns, I., Guertin, D.P., Lara-Valencia, F., and Semmens, D., 2010, Flood hazard awareness and hydrologic modelling at Ambos Nogales, United States–Mexico border: Journal of Flood Risk Management, v. 3, no. 2, p. 151–65, https://doi.org/10.1111/j.1753-318X.2010.01066.x.

Norman, L.M., Villarreal, M.L., Niraula, R., Meixner, T., Frisvold, G., and Labiosa, W., 2013, Framing scenarios of binational water policy with a tool to visualize, quantify and valuate changes in ecosystem services: Water, v. 5, no. 3, p. 852–874, https://doi.org/10.3390/w5030852.

Norman, L.M., Villarreal, M.L., Wallace, C.S.A., Gil Anaya, C.Z., Diaz Arcos, I., and Gray, Floyd, 2010, A high-resolution land-use map—Nogales, Sonora, Mexico: U.S. Geological Survey Open-File Report 2010–1156, 21 p., accessed November 28, 2018, at https://pubs.usgs.gov/of/2010/1156/.

Pandey, P.K., and Soupir, M.L., 2014, Assessing linkages between *E.coli* levels in streambed sediment and overlying water in an agricultural watershed in Iowa during the first heavy rain event of the season: American Society of Agricultural and Biological Engineers, v. 57, no. 6, p. 1571–1581, accessed November 28, 2018, at https://lib.dr.iastate.edu/cgi/viewcontent.cgi?article=1899&context=abe_eng_pubs.

Paretti, N.V., Coes, A.L., Kephart, C.M., and Mayo, J.P., 2018, Collection methods and quality assessment for *Escherichia coli*, water quality, and microbial source tracking data within Tumacácori National Historical Park and the upper Santa Cruz River, Arizona, 2015–16: U.S. Geological Survey Scientific Investigations Report 2017–5139, 30 p., https://doi.org/10.3133/sir20175139.

Paretti, N.V., Kennedy, J.R., Turney, L.A., and Veilleux, A.G., 2014, Methods for estimating magnitude and frequency of floods in Arizona, developed with unregulated and rural peak-flow data through water year 2010: U.S. Geological Survey Scientific Investigations Report 2014–5211, 61 p., https://doi.org/10.3133/sir20145211.

Patz, J.A., Campbell-Lendrum, D., Holloway, T., and Foley, J.A., 2005, Impact of regional climate change on human health: Nature Reviews, v. 438, no. 17, p. 310–317, https://doi.org/10.1038/nature04188.

Powell, B.F., Albrecht, E.W., Halvorson, W.L., Schmidt, C.A., Anning, P., and Docherty, K., 2005, Vascular plant and vertebrate inventory of Tumacácori National Historic Park: U.S. Geological Survey Open-File Report 2005–1142, 126 p., accessed November 28, 2018, at https://pubs.usgs.gov/of/2005/1142/.

Prichard, A.H., and Scott, C.A., 2014, Interbasin water transfers at the US-Mexico border city of Nogales, Sonora—Implications for aquifers and water security: International Journal of Water Resources Development, v. 30, no. 1, p. 135–151, https://doi.org/10.1080/07900627.2012.755597.

Rasmussen, P.P., Gray, J.R., Glysson, G.D., and Ziegler, A.C., 2009, Guidelines and procedures for computing time-series suspended-sediment concentrations and loads from in-stream turbidity-sensor and streamflow data: U.S. Geological Survey Techniques and Methods, book 3, chap. C4, 52 p., accessed November 28, 2018, at https://pubs.usgs.gov/tm/tm3c4/.

Rasmussen, T.J., Ziegler, A.C., and Rasmussen, P.P., 2005, Estimation of constituent concentrations, densities, loads, and yields in lower Kansas River, northeast Kansas, using regression models and continuous water-quality monitoring, January 2000 through December 2003: U.S. Geological Survey Scientific Investigations Report 2005–5165, 117 p., accessed November 28, 2018, at https://pubs.usgs.gov/sir/2005/5165/pdf/SIR20055165.pdf.

Rasmussen, T.J., Lee, C.J., and Ziegler, A.C., 2008, Estimation of constituent concentrations, loads, and yields in streams of Johnson County, northeast Kansas, using continuous water-quality monitoring and regression models, October 2002 through December 2006: U.S. Geological Survey Scientific Investigations Report 2008–5014, 103 p., accessed November 28, 2018, at https://pubs.usgs.gov/sir/2008/5014/.

Runkel, R., Crawford, C., and Cohn, T.A., 2004, Load Estimator (LOADEST)—A FORTRAN program for estimating constituent loads in streams and rivers: U.S. Geological Survey Techniques and Methods, book 4, chap. A5, 69 p., accessed November 28, 2018, at https://pubs.usgs.gov/tm/2005/tm4A5/.

Sanders, E.C., Yuan, Y., and Pitchford, A., 2013, Fecal coliform and *E. coli* concentrations in effluent-dominated streams of the Upper Santa Cruz Watershed: Water, v. 5, no. 1, p. 243–261, https://doi.org/10.3390/w5010243.

SAS Institute, Inc., 2007, JMP statistics and graphics guide, release 7: Cary, North Carolina, SAS Institute, Inc., 1048 p., accessed November 28, 2018, at https://www.jmp.com/support/downloads/pdf/jmp_stat_graph_guide.pdf.

Shamir, E., Megdal, S.B., Carrillo, C., Castro, C.L., Chang, H.I., Chief, K., Corkhill, F.E., Eden, S, Georgakakos, K.P., Nelson, K.M., and Prietto, J., 2015, Climate change and water resources management in the Upper Santa Cruz River, Arizona: Journal of Hydrology, v. 521, p.18–33, https://doi.org/10.1016/j.jhydrol.2014.11.062.

Shamir, E., Sperfslage, J.A., Banks, R.J. and Spencer, C.R., 2016, The water resources climate assessment tool (WARCAT) developed for the Santa Cruz Active Management Area (SCAMA): San Diego, Calif., Hydrologic Research Center Technical Note No. 88, 20 p., accessed on August 20, 2017, at https://warcat.hrcwater.org/SCAMA/resources/HRC_TN_88.pdf.

Schwarz, G.E., 1978, Estimating the dimension of a model: Annals of Statistics, v. 6, p. 461–464, accessed November 28, 2018, at https://projecteuclid.org/download/pdf_1/euclid.aos/1176344136.

Sonoran Institute, 2016, A living river—Charting the health of the upper Santa Cruz River—Changes between 2008 and 2014 water years: Sonoran Institute, 17 p., accessed November 28, 2018, at https://sonoraninstitute.org/resource/living-river-charting-the-health-of-the-upper-santa-cruz-river-2008-2014/.

Sprouse, T., 2005, Water issues on the Arizona-Mexico border—The Santa Cruz, San Pedro and Colorado Rivers: University of Arizona, Water Resources Research Center College of Agriculture Life Sciences, 33 p., accessed November 28, 2018, at https://wrrc.arizona.edu/sites/wrrc.arizona.edu/files/Water%20Issues%20on%20the%20Arizona%20Mexico%20Border.pdf.

Stantec, 2017, Nogales International Wastewater Treatment Plant—Creative solutions for less than 50 percent of the cost of other similar sized facilities: Stantec web page, accessed on May 19, 2017, https://www.stantec.com/en/projects/united-states-projects/n/nogales-international-wastewater-treatment-plant.

Tetra Tech, Inc., 2013, Final—Upper Santa Cruz River Watershed—Data summary and Analysis: Tetra Tech, Inc., prepared July 10, 2013, for EPA Regional 9 Water Division, 53 p.

Tetra Tech, Inc., 2014, Upper Santa Cruz River Watershed implementation plan: Tetra Tech, Inc., prepared April 24, 2014, for EPA Regional 9 Water Division, 29 p.

Treese, S., Meixner, T., Hogan, J.F., 2009, Clogging of an effluent dominated semiarid river—A conceptual model of stream-aquifer interactions: Journal of the American Water Resources Association, v.45, no.4, p. 1047–1062.

U.S. Army Corps of Engineers, 2004, Ambos Nogales special flood damage reduction study Nogales, Sonora, Mexico: U.S. Army Corps of Engineers, Los Angeles District, Arizona area office, report prepared for the International Boundary and Water Commission in association with Tetra Tech, Inc., 56 p., accessed November 28, 2018, at https://www.ibwc.gov/Files/Amb_Nogales_Flood_Reduction_Study_rev_January_2005.pdf.

U.S. Census Bureau, 2012, Data access tools: U.S. Census Bureau web page, accessed November 28, 2018, at https://www.census.gov/geo/maps-data/data/tiger-line.html.

U.S. Department of Agriculture, 2012, Census of agriculture county profile—Santa Cruz County Arizona: U.S. Department of Agriculture National Agricultural Statistics Service, 2 p., accessed on April, 21, 2017, at https://www.nass.usda.gov/Publications/AgCensus/2012/Online_Resources/County_Profiles/Arizona/cp04023.pdf.

U.S. Environmental Protection Agency, 2000, 1998 National water quality inventory report to Congress: U.S. Environmental Protection Agency Report EPA–841–F–00–006, 45 p., accessed November 28, 2018, at https://www.epa.gov/waterdata/1998-national-water-quality-inventory-report-congress.

U.S. Environmental Protection Agency, 2012, Recreational water quality criteria: U.S. Environmental Protection Agency, Office of Water 820-F12-058, 63 p., accessed November 28, 2018, at https://www.epa.gov/sites/production/files/2015-10/documents/rwqc2012.pdf.

U.S. Fish and Wildlife Service, 2011, Biological assessment of the Arizona Game and Fish Department's statewide and urban fisheries stocking program—Chapter 10, Santa Cruz River Watershed: U.S. Fish and Wildlife Service and Arizona Game and Fish Department, 86 p., accessed on April, 21, 2017, at https://www.fws.gov/southwest/federal_assistance/pdfs/chapter%2010%20santa%20cruz%20river%20watershed.pdf.

U.S. Geological Survey, 2006, Collection of water samples (ver. 2.0): U.S. Geological Survey Techniques of Water Resources Investigations, book 9, chap. A4, accessed February 1, 2017, at http://pubs.water.usgs.gov/twri9A4/.

Villarreal, M.L., Norman, L.M., Wallace, C.S.A., and van Riper, Charles, III, 2011, A multitemporal (1979–2009) land-use/land-cover dataset of the binational Santa Cruz Watershed: U.S. Geological Survey Open-File Report 2011–1131, 26 p. and database, accessed November 28, 2018, at https://pubs.usgs.gov/of/2011/1131/.

Wagner, R.J., Boulger, R.W., Jr., Oblinger, C.J., and Smith, B.A., 2006, Guidelines and standard procedures for continuous water-quality monitors—Station operation, record computation, and data reporting: U.S. Geological Survey Techniques and Methods 1–D3, 51 p. + 8 attachments; accessed November, 28, at https://pubs.usgs.gov/tm/2006/tm1D3/pdf/TM1D3.pdf.

Wallace, C.S.A., Villarreal, M.L., and Norman, L.M., 2011, Development of a high-resolution binational vegetation map of the Santa Cruz River riparian corridor and surrounding watershed, southern Arizona and northern Sonora, Mexico: U.S. Geological Survey Open-File Report 2011–1143, 22 p. and data files, accessed November 28, 2018, at https://pubs.usgs.gov/of/2011/1143/.

Westerhoff, P., and Anning, D.W., 2000, Concentrations and characteristics of organic carbon in surface water in Arizona—Influence of urbanization in Journal of Hydrology, v. 236, no. 3–4, p. 202–222, https://doi.org/10.1016/S0022-1694(00)00292-4.

Wilde, F.D., 2003, Guidelines for field-measured water-quality properties (ver. 2.0, October 2008): U.S. Geological Survey Techniques of Water-Resources Investigations, book 9, chap. A6, sec. 6.0, accessed February 1, 2017, at https://water.usgs.gov/owq/FieldManual/Chapter6/6.0_contents.html.

Wilkes, G., Brassard, J., Edge, T.A., Gannon, V., Jokinen, C.C., Jones, T.H., Neumann, N., Pintar, K.D.M., Ruecker, N., Schmidt, P.J., Sunohara, M., Topp, E., and Lapen, D.R., 2013, Bacteria, viruses, and parasites in an intermittent stream protected from and exposed to pasturing cattle—Prevalence, densities, and quantitative microbial risk assessment: Water Research, v. 47, no. 16, p. 6244–6257.

Williams, G.P., 1989, Sediment concentration versus water discharge during single hydrologic events in rivers: Journal of Hydrology, v. 11, p. 89–106, https://doi.org/10.1016/0022-1694(89)90254-0.

Wood, M.L., House, K.P., and Pearthree, P.A., 1999, Historical geomorphology and hydrology of the Santa Cruz River: Arizona Geological Survey Open-File Report 99–13, 98 p., accessed November 28, 2018, at http://repository.azgs.az.gov/sites/default/files/dlio/files/nid824/ofr-99-13_santa_cruz_river.pdf.

Woodhouse, Murphy, 2015, Hunt is on for source of mercury at Peña Blanca Lake, Nogales International: Nogales International online article, accessed August 13, 2015, at https://www.nogalesinternational.com/news/hunt-is-on-for-source-of-mercury-at-pe-a/article_c07d92fa-4215-11e5-b475-43b4af06eb0a.html.

USGS

Paretti and others—**Spatial and Temporal Distribution of Bacterial Indicators and Microbial-Source Tracking within Tumacácori National Historical Park and the Upper Santa Cruz River, Southern Arizona and Northern Mexico, 2015–2016**—Scientific Investigations Report 2019–5108